



Error Detection and Correction Method for Timing Errors in Registers

M.Revathy^{1*}, PN.Sundararajan¹ and M.Kasthuri²

¹Associate Professor, Department of ECE, PSNA College of Engineering and Technology, Dindigul, Tamilnadu, India.

²Assistant Professor Department of ECE, PSNA College of Engineering and Technology, Dindigul, Tamilnadu, India.

Received: 31 Aug 2019

Revised: 02 Oct 2019

Accepted: 04 Nov 2019

* Address for Correspondence

M.Revathy

Associate Professor,
Department of ECE,
PSNA College of Engineering and Technology,
Dindigul, Tamilnadu, India.
Email:revathim@psnacet.edu.in



This is an Open Access Journal / article distributed under the terms of the **Creative Commons Attribution License** (CC BY-NC-ND 3.0) which permits unrestricted use, distribution, and reproduction in any medium, provided the original work is properly cited. All rights reserved.

ABSTRACT

Timing errors are an important concern in nanometer CMOS technologies. A promising way to overcome the timing errors is the development of error detection and correction techniques in registers. Normally timing failures occur in high complexity and high frequency integrated circuits. The reason behind this timing failures are test escapes, environmental conditions, operating conditions and process variations. A local error detection and correction technique is done in this work. It is based on a new bit flipping flip flop. Whenever a timing error is detected, it is corrected by complementing the output of the corresponding flip flop. The addition of a multiplexer and a NOT gate replaces the need of an extra latch and an EX-OR gate in the modified EDC technique. An external OR gate indicates the presence of error in the registers. No extra memory element like latch is required here. This reduction in the elements of the circuit leads to the reduction of silicon area overhead and performance degradation is negligible. No extra circuitry is inserted in the design. Timing errors are identified and corrected within a single cycle and hence design complexity is reduced which results in reduced power consumption and low silicon area. The modified EDC technique is simulated using Modelsim 6.5b and synthesized using Xilinx ISE suite 12.1.

Keywords: Multiplexer, EDC techniques, NOT gate, EX-OR gate, OR gate, registers, Timing errors, Flipflop. Coupling noise, Power supply disturbance, Jitter, Temperature fluctuations.



**Revathy et al.**

INTRODUCTION

Error occurs mainly due to CMOS technology scaling, process variations, various performance degradation mechanism, power supply reduction and increasing complexity that affect the reliability. Various mechanisms like coupling noise, power supply disturbance, jitter and temperature fluctuations are reasons for timing error generation. Transistor aging mechanisms significantly affect the performance of nanometer circuits, which results in the appearance of timing errors continuously. Negative – Positive Bias Temperature Instability (NBTI-PBTI) and hot carrier injection (HCI) degrade transistors' threshold voltage over time increasing signal propagation delays and consequently timing error rate (1). Path delay deviations occurred due to process deviations and manufacturing defects affect the circuit speed also result in timing errors which are not easily detectable in high device count integrated circuits.

EVOLUTION OF TESTING

In the early times of electronics engineering, systems were composed of discrete components, testing of digital systems comprised of three distinct phases. They are:

1. Each discrete component was tested for concordance to its specifications
2. The components were assembled into more complex digital elements (i.e. flip flops etc.), and these are tested for correct functionality Testing and Built in Self Test
3. The higher level system was built up and was tested for functionality.

The first applications of the structural test was discrete components on Printed Circuit Boards (PCBs), which then began to be applied to ICs as the electronics technology developed into higher levels of integration (2). Though the problems of IC testing was not very much different from that of the PCBs, the objective of testing had then changed to discard the faulty units rather than locating the defective components and replace them. In the case of Small Scale Integration (SSI) and Medium Scale Integration (MSI), the problems were relatively as simple as PCB testing, since:

1. Internal nodes of the devices were easily controlled and observed from the primary inputs and outputs of the devices
2. The simplicity of circuit functions permitted the use of exhaustive testing.
3. More complex systems were constructed from basic, thoroughly tested components.

TYPES OF TESTING

Without testing both prior to final installation and once installed onto a circuit board many devices would cease functioning earlier than the expected life spans. There are two main categories of IC testing,

They are:

1. Functional testing.
2. Structural testing.

Functional Testing

The time required to verify anything more than logic functionally is beyond practical limits in terms of ATE time, cost of the chip etc. Also, the quality of test solution (i.e., proper binning of normal and faulty chips) is acceptable for almost all classes of circuits. This is called Functional Testing. Before structural testing was proposed, digital systems were tested to verify their compliance with their intended functionality, i.e. in this philosophy, a multiplier would be tested whether it would multiply and so forth (3). This testing of philosophy is termed as functional testing, which



**Revathy et al.**

can be defined as, applying a series of determined meaningful inputs to check for the correct output responses in terms of the device functionality. Although this methodology imparts a good notion of circuit functionality, under the presence of a definitive fault model, it is very difficult to isolate certain faults in the circuits in order to verify their detection.

Structural Testing

Functional Testing cannot be performed due to extremely high testing time to solve this issue we perform Structural Testing, which takes many fold less time compared Functional Testing yet maintaining the quality of test solution. The Structural testing, introduced by Eldred, verifies the correctness of the specific structure of the circuit in terms of gates and interconnects (4). In other Word Structural testing does not check the functionality of the entire circuit rather verifies if all the structural units (gates) are fault free. So structural testing is a kind of functional testing at unit (gate) level with the proposal of structural testing, which might be defined as, consideration of possible faults that may occur in a digital circuit and applying a set of inputs tailored for detecting these specified faults. As obvious structural testing relies on the fault Testing and Built in Self Test models described for the Device Under Test (DUT), and any result obtained in this manner is unworthy without a proper description of used fault models.

Related Works

Various mechanisms like

1. Coupling noise
2. Power supply disturbance
3. Jitter
4. Temperature fluctuations

are accused for timing error generation. Path delay deviations, due to process variations, and manufacturing defects that affect circuit speed may also result in timing errors that are not easily detectable in high device count ICs.

Detection and Correction of Timing Errors in Registers

Timing errors are an increasing reliability concern in Nanometer technology, high complexity and multi voltage/frequency integrated circuits. A local error detection and correction technique is presented in this work that is based on a new bit flipping flip-flop (5). Whenever a timing error is detected, it is corrected by complementing the output of the corresponding flip-flop. The EDC technique is characterized by very low silicon area and power requirements compared to previous design schemes in the open literature. The new Error Detection / Correction Flip-Flop (EDC Flip-Flop) that is suitable to confront with timing errors. Apart from the original flip flop (Main Flip-Flop), it consists of two XOR gates and a Latch. The first XOR gate compares the input and the F output of the Main Flip-Flop and provides the result to the Latch. The Latch feeds the second XOR gate at the output of the Main Flip-Flop. Depending on the comparison result within a specified time interval, either the F signal of the Main Flip-Flop or its complement is propagated to the output Q of the EDC Flip Flop (6). The Q signal feeds the subsequent logic as shown in the Fig.1.

A clock pulse (Pulse signal) is used to capture the comparison result of the first XOR gate in the Latch (memory state when the Pulse is low) (7). This clock pulse can be generated locally from the CLK signal using a single Pulse Generator per register like the one illustrated in Figure 3.2. Thus, the routing overhead of an extra clock signal is relaxed. The AND gate in Figure 3.2 ensures that a single pulse will be generated only during the first phase of every clock cycle. The pulse width is at least equal to the time required by the Latch to capture the comparison result. The time interval between the triggering edge of CLK and the falling edge of Pulse (minus the Latch set up time and the XOR propagation delay time) determines the maximum detectable signal delay. Every signal transition at the D input of an EDC Flip-Flop within this time interval is considered as a delayed response. So the circuit design must



**Revathy et al.**

guarantee that in the fault free case there are no signal transitions at the inputs of EDC Flip-Flops within this time interval, in order to avoid false alarms.

Circuit Operation

The timing error detection and correction technique operates as shown in the Fig.3. Suppose that a timing error is detected at one or more inputs of the combinational logic stage S_{j+1} , due to a delayed response of the previous stage S_j [8]. Thus, the response of S_{j+1} will be erroneous and must be corrected. To achieve error correction, the output of each flip-flop, at the register between the two stages, where a timing error has been detected is complemented so that valid values feed the S_{j+1} logic stage. Moreover, in case that this stage is not fast enough (not a shallow stage), the evaluation time of the circuit is extended by one clock cycle to guarantee its correct computation (9). Initially, the output Error F of the Latch is reset to zero so that by default the F signal of the Main Flip-Flop propagates to the output Q of the XOR gate and feeds the subsequent logic stage. In the error free case the comparison result is a low value at the CMP output of the first XOR gate after the triggering edge of the clock signal CLK. This value is captured by the Latch. Thus, the Q output signal is identical to the F signal of the Main Flip-Flop, which carries the correct value. This signal feeds the subsequent logic stage S_{j+1} .

However, in the presence of a timing fault in logic stage S_j , a delayed signal arrives at the D input of the main Flip-Flop after the triggering edge of the clock signal CLK. In that case, a timing error is present at the F output of the Main Flip-Flop and erroneous data are provided to the subsequent logic stage S_{j+1} through the Q output (10). In addition, the F signal value differs from the D signal value. The first XOR gate detects this difference and raises its output CMP to high. The Latch captures and holds this response (11). Thus, the second XOR gate provides at its output Q the complement of the F signal. Now the Q output of the EDC Flip-Flop carries the correct value, which feeds the subsequent logic stage S_{j+1} for its computation. Consequently, the error is locally corrected. (12)

PROPOSEDSYSTEM

In modified EDC technique a new soft and timing error detection circuit that delivers fast response times with the use of a MUX and inverter is presented and shown in the Fig.4. The modified EDC technique detects late-arriving data by comparing the input and output of the flip-flop using XOR gate as a comparator. MUX uses the XOR output as a selection line and choose either flip flop normal correct output or inverted output. That is when the xor gate output is "0" then the comparison output is "low" indicating timing error free condition and so the output of the flip flop is given directly to the next stage of combinational circuit through the 2*1 MUX. But when the XOR gate output is "1" then the comparison output is high indicating timing error, hence in this condition the output of the flip flop is inverted using NOT gate and gives the corrected output to the next combinational stage. A main characteristic and an advantage of the proposed circuit is that no circuitry is inserted in the critical path from the D input to the Q output of the Flip-Flop or in the distribution path of the clock signal CLK. The additional MUX is inserted in the path which is not critical. The advantage of the modified EDC technique is that the power consumption and the area is reduced and thereby the speed of the system is increased. The addition of OR gate external to the circuit acts as an indicator of error for registers.

EXPERIMENTAL RESULTS

In the EDC technique *clock, d, reset and f* are the inputs where *y, d1 and compare* the intermediate output, correct is the final output of the flip flop which is given to the next combinational logic stage. Initially clock is given as positive edge triggering where it is the input of the flip flop where it can be given either zero or one here "0" is given first, reset is given "1" for resetting and then "0", fault is initially given as "0" that is fault free condition then checked for



**Revathy et al.**

faulty condition that is "1" the Fig.5 shown is error detection and the next Fig .6 shows the correction of error in the EDC technique in registers.

CONCLUSION

Timing errors are a real concern in modern nanometer CMOS technologies. A promising way to cope with them is the development of error detection and correction techniques. A timing error tolerance technique is presented named modified EDC technique in registers for enhanced reliability in flip-flop based nanometer technology cores. It exploits a new bit flipping flip-flop, which provides the ability to detect and correct timing errors in a circuit with a time penalty of a single clock cycle. The Modified EDC technique has an OR gate that indicates the presence of error in the registers. The modified EDC technique in registers is characterized by low silicon area requirements and reduced design complexity that also result in reduced power consumption with respect to earlier design schemes.

Future Work

The router is characterized by its architecture having four directions (North, South, East, West) suitable for a 2-D mesh NoC. The PEs and IPs can be connected to any side of the router. Therefore there is no specific connection port for a PE or IP. The modified EDC technique can also be applied to NoCs using five port routers with a local port dedicated to an IP. The efficient error detection and correction method is used in router to reduce the timing errors.

REFERENCES

1. Agarwal M., Balakrishnan V., Bhuyan A., Kim K., Paul B. C., Wang W., Yang B., Cao Y., and Mitra S., (2008) 'Optimized circuit failure prediction for aging: Practicality and promise', in Proc. IEEE Int. Test Conf., pp. 1–10.
2. Agarwal M., Paul B.C, Zhang M., and Mitra S., (2007) 'Circuit failure prediction and its application to transistor aging', in Proc. IEEE VLSI Test Symp., 2007, pp. 277–284.
3. Anghel L. and M. Nicolaidis M., (2000) 'Cost reduction and evaluation of temporary faults detecting technique', in Proc. ACM/IEEE Des. Autom. Test Eur. Conf., pp. 591–598.
4. Austin T., Blaauw D., Mudge T. and Flautner K., (Mar. 2004) 'Making typical silicon matter with razor', IEEE Comput., vol. 37, no. 3, pp. 57–65.
5. Bowman K., Tschanz J.W., Kim N.-S., Lee J.C., Wilkerson C. B., Lu S.- L., Karnik T., and De V. K., (Jan. 2009) 'Energy-efficient and metastability- immune resilient circuits for dynamic variation tolerance', IEEE J. Solid- State Circuits, vol. 44, no. 1, pp. 49–63.
6. Das S., Tokunaga C., Pant S., Ma W-H., Kalaiselvan S., Lai K., Bull D. M., and Blaauw D. T., (Jan. 2009) 'Razor II: In situ error detection and correction for PVT and SER tolerance', IEEE J. Solid-State Circuits, vol. 44, no. 1, pp. 32–48.
7. Floros A., Tsiatouhas Y., and Kavousianos X., (2008) 'The time dilation scan architecture for timing error detection and correction', in Proc. IFIP/IEEE Int. Conf. Very Large Scale Integr., pp. 569–574.
8. Kang K., Park S.P., Kim K., and Roy K., (Feb. 2010) 'On-chip variability sensor using phase-locked loop for detecting and correcting parametric timing failures', IEEE Trans. VLSI Syst., vol. 18, no. 2, pp. 270–280.
9. Makris Y., Bayraktaroglu I., and Orailoglou A., (Jun. 2004) 'Enhancing reliability of RTL controller-data path circuits via invariant-based concurrent test', IEEE Trans. Rel., vol. 53, no. 2, pp. 269–278.
10. Matakias S., Tsiatouhas Y., Arapoyanni A., and Haniotakis T.H., (2004) 'A circuit for concurrent detection of soft and timing errors in digital CMOS ICs', J. Electron. Testing: Theory Appl., vol. 20, no. 5, pp. 523–531.
11. McPherson J. W., (2006) 'Reliability challenges for 45 nm and beyond', in Proc. ACM/IEEE Des. Autom. Conf., pp. 176–181.
12. Metra C., Degiampietro R., Favalli M., and Ricco B., 1999 'Concurrent detection and diagnosis scheme for transient, delay and crosstalk faults', in Proc. IEEE Int. On-Line Testing Workshop, pp. 66–70.





Table 1. Comparison of EDC technique and modified EDC technique in registers

S.NO	PARAMETER	EDC Technique in registers	Modified EDC technique in registers
1.	Area (No.LUT + IOB)	26	19
2.	Power	0.027 watts	0.011 watts
3.	Delay	8.166ns	7.798 ns

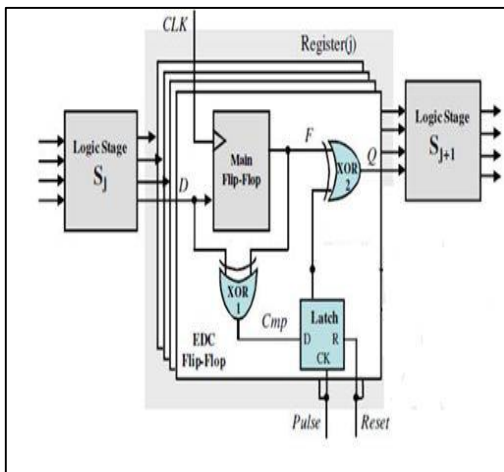


Fig.1.EDC Circuit in registers

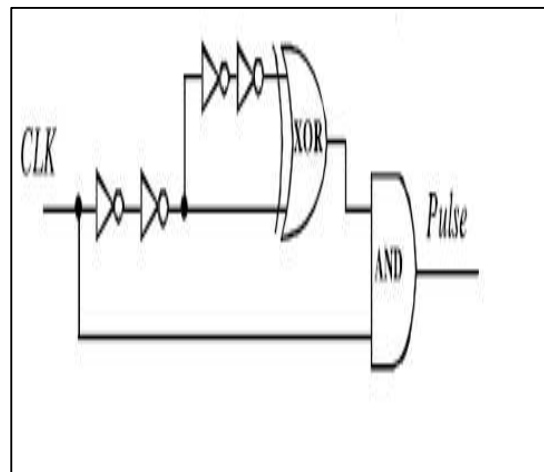


Fig.2. Pulse generator

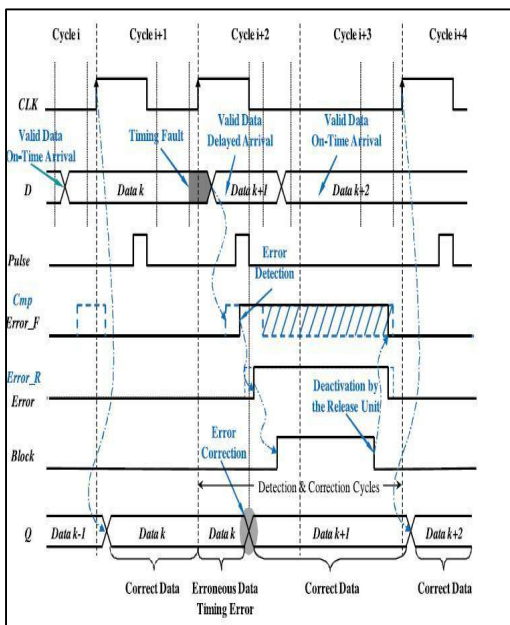


Fig.3. Timing diagram of EDC technique in registers

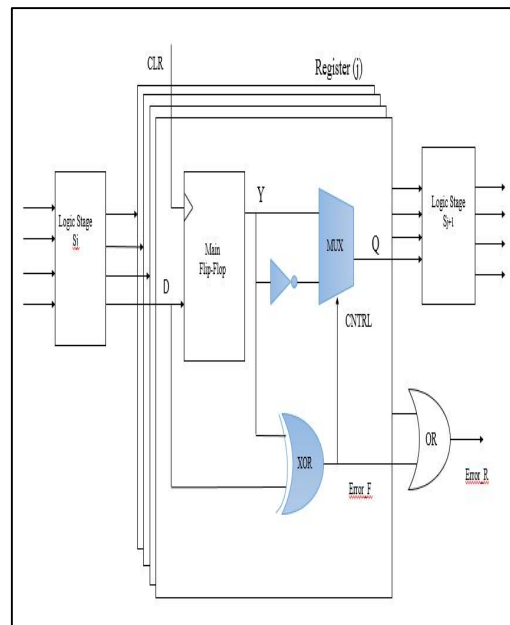


Fig.4. Modified EDC Circuit in registers





Revathy et al.

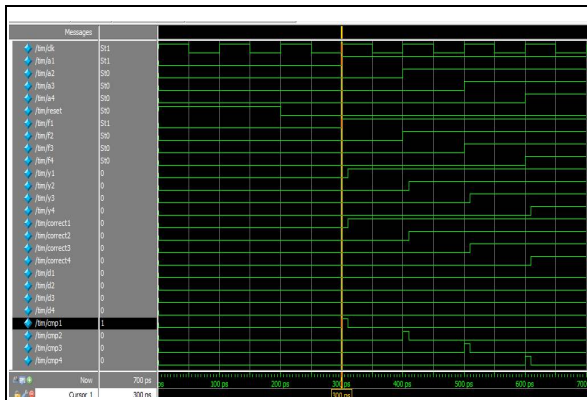


Fig.5. Error detection of EDC technique in registers

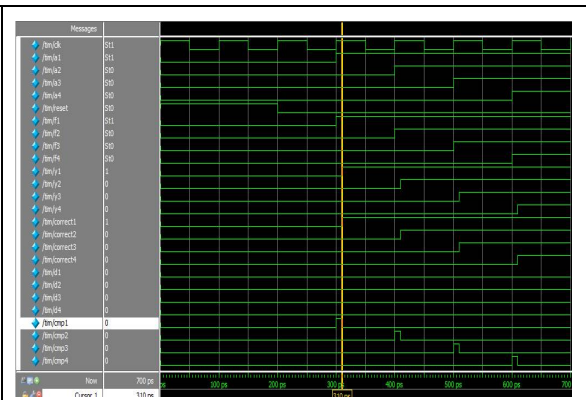


Fig.6. Error correction of EDC technique in registers

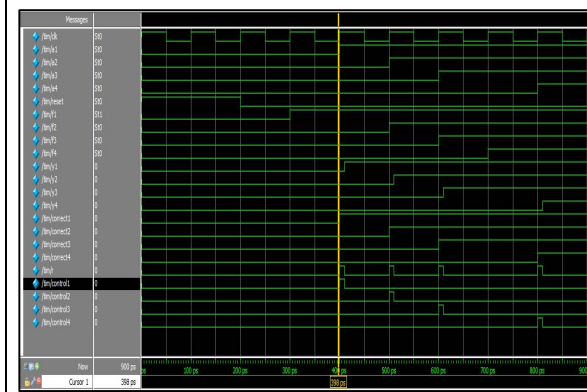


Fig.7. Error detection of modified EDC technique in registers

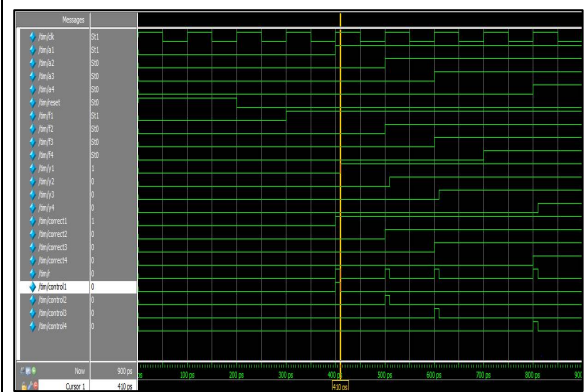


Fig.8. Error correction of modified EDC technique in registers





Interpretation of Grazing Behavior of Cattle in a Semi-Intensive Rearing System

S.K.George^{1,2*}, M.T. Dipu², M. K.Muhammad Aslam² and K. Lalu²

¹Assistant Professor, Base Farm, Kolahalamedu, Idukki, Kerala, India.

²Kerala Veterinary and Animal Sciences University, Pookode, Wayanad, Kerala India.

Received: 03 Sep 2019

Revised: 07 Oct 2019

Accepted: 09 Nov 2019

*Address for Correspondence

S.K.George

Assistant Professor,

Base Farm, Kolahalamedu,

Idukki, Kerala, India.

Email: skgeorge31@gmail.com



This is an Open Access Journal / article distributed under the terms of the **Creative Commons Attribution License** (CC BY-NC-ND 3.0) which permits unrestricted use, distribution, and reproduction in any medium, provided the original work is properly cited. All rights reserved.

ABSTRACT

The present study was conducted to document the grazing pattern of cattle in a semi-intensive system. Study was conducted in a herd comprised of 51 heifers, 43 milch cows, 15 dry cows and 10 pregnant cows belonging to an organised dairy farm. As a management pattern the animals were left out for grazing in pasture for 7 hrs in a day starting at 6.30h in the morning. The study involved thorough observation and recording of various attributes such as grazing time, selection of grazing area, forage preference, forage availability, effect of extra energy supplementation on grazing pattern and the influence of weather on grazing behaviour. It is observed that the cattle are most active during morning in the initial hours of grazing. Cattle always prefer lush immature green leaves and stems. Once it is not available they graze on dry forages. Supplementation of extra feed adversely affected the grazing. During extreme climates cattle spent less time on grazing. Developing skills to observe the grazing behaviour and to relate it with animal performance facilitated better management of dairy farm in a semi intensive system.

Keywords: cattle, dairy, farm, behavior, green leaves, system, management.

INTRODUCTION

Grazing consist of searching and selection of forage by herbivores for grasping it into the mouth. Semi-intensive system of rearing cattle, combines grazing in pastures and stall feeding of concentrates and forages in confinement. Performance of grazing animals is dependent on the quantity and quality of fodder consumed. During grazing the animals eat only a small portion of the forage available and the grazing behaviour of animals gives a rough indication of the forage quality. Building up skills to observe the grazing behaviour and to relate it with animal performance can facilitate development of successful managerial skills in dairy farming were animals are left out for



**George et al.**

grazing. Therefore, the present investigation was carried out to interpret the grazing behaviour of cattle in a semi-intensive system of rearing.

METHODOLOGY

The observational study was conducted in a cattle farm at Kolahalamedu, Vagamon Village, of Idukki District. The area is located at an altitude range of 1100 m above mean sea level. The cattle population of the farm includes mainly crossbreds and a few native breeds such as Gir, Ongole, Sahiwal, Kankrej and Vechur. The population under investigation included 51 heifers, 43 milch cows, 15 dry cows and 10 pregnant cows. The animals are fed concentrates twice daily (5.30 h & 15 h) as per the package of practices recommendations (2016) and with ad libitum fodder while housed inside the shed. Generally they are left out for grazing in pasture found in hilly meadows and valleys for 7 hrs in a day from 6.30 h to 13.30 h. Access to pasture enable the livestock to act out their innate behavior compared to the restrictive in-house situations (Hemsworth et al., 1995). The chief grass found in the hilly meadows is Congo signal and the major grass found in the valleys is setaria. The study involved thorough observation of animals while grazing to enable necessary recording with regard to grazing time, selection of grazing area, forage preference, forage availability, effect of extra energy supplementation on grazing pattern and the influence of weather on grazing behaviour.

RESULTS AND DISCUSSION

Foraging decisions such as when to begin, time spent for grazing, frequency, and how to distribute various grazing events may determine how cattle allocate time to meet their nutritional requirements (Gregorini et al, 2006). It is observed that the cattle are most active during morning in the initial hours of grazing. Their grazing cycle is almost in a constant pattern. Majority of the grazing takes place during the first 4 hrs followed by a resting period of about 1 hr followed by a more selective type of grazing for rest of the time. They do not prefer to remain in a particular location for more than 2 days. Cattle always prefer lush immature green leaves and stems. Once it is not available they graze on dry forage. During summer season when forage availability is less cattle spent more time on grazing. Moreover, cattle prefer to graze in groups when forage is plentiful and they do individual grazing during periods of forage scarcity. Even during forage scarcity cattle prefer to graze rather than to browse on bushes. Most often patches of grazed lands are seen once cattle is left for grazing in a location. This indicates the palatability differences with regard to the forages found. Presence of animal excreta also cause formation of ungrazed patches. Supplemental feeding in the form of broken maize lowered the time spent for initial active grazing as reported in earlier studies (Scaglia et al. 2013). Seasonal changes in pasture biomass and grazing behaviour of cattle is an established fact (Akapali et al., 2018). In the present study, during extreme summer, cattle were grazing only for initial 3 to 4 hrs and later on they were found resting in shades. Cattle with dark coat seeks the shade much earlier than one with lighter coloured coats. During periods of continuous rain it is observed that they prefer to graze on hilly slopes rather than in water logged valleys. Relating the daily grazing behaviour with performance of animals facilitated better management of the farm.

CONCLUSION

In a semi-intensive system of rearing, grazing behaviour of cattle is influenced by various factors such as time of grazing, quality and quantity of available forage, season and climate, supplemental feeding and presence of animal excreta. Developing skills to observe the grazing behaviour and to relate it with animal performance facilitated better management of dairy farm in a semi intensive system





George et al.

REFERENCES

1. Akapali, M., Ansah T., Abdul-Rahman, I. Alenyorage, B. and Baatuuwie. (2018). Seasonal changes in pasture biomass and grazing behaviour of cattle in the Guinea Savanna agroecological zone of Ghana. *African Journal of Range & Forage Science*, 35:2, 101-108.
2. Gregorini P., Tamminga, S. and Gunter S. A. (2006). Review: Behavior and Daily Grazing Patterns of Cattle. *The Prof. Anim. Scientist*. 22:201–209.
3. Hemsworth, P.H., Barnett, J.L., Beveridge, L., Matthews, L.R. (1995). The Welfare of Extensively Managed Dairy-Cattle—A Review. *Appl. Anim. Behav. Sci.* 42:161–182
4. Package of Practices recommendations (2016). Directorate of Entrepreneurship, Kerala Veterinary and Animal Sciences University.
5. Scaglia, G., Williams, C. C. and Dolejsiova, A. H. (2013). Effects of time of supplementation on cattle grazing annual ryegrass. III. Dry matter intake and digesta kinetics. *The Prof. Anim. Scientist*. 29:157-162.





The Effect of Dark and Light Cycle on Immunohistochemical Integrin Protein Expression of Seminiferous Tubules in Adult Mice Testes

Ali Ahmed Naji*, Haider A.Rassoul Jaffer and Husaeen Abaas Ajar alla

College of Medicine, Al-Nahrain University, Baghdad City, Iraq.

Received: 12 Aug 2019

Revised: 15 Sep 2019

Accepted: 18 Oct 2019

*Address for Correspondence

Ali Ahmed Naji

College of Medicine,

Al-Nahrain University,

Baghdad City, Iraq.

Email: Ali_alnaji.aa86@gmail.com



This is an Open Access Journal / article distributed under the terms of the **Creative Commons Attribution License** (CC BY-NC-ND 3.0) which permits unrestricted use, distribution, and reproduction in any medium, provided the original work is properly cited. All rights reserved.

ABSTRACT

Seminiferous tubules of the testis are embedded in interstitial tissue. The tubules are lined by a complex epithelium which is consisted of two very different cell populations, germ cells and Sertoli cells. The sperm cells are produced from germ cells. While the Sertoli cells (SC) are epithelial cells that form the basal lamina of the seminiferous tubules. Sertoli cells extend from the peripheral to the lumen of seminiferous tubule. The spermatogenic lineage cells are associated closely with extended surfaces of sertoli cells along from the base to apex, they are interact directly with developing germ cells throughout spermatogenesis as a supporting cells so called nurse cell. They are arranged together around the inner seminiferous tubules surfaces and between SC are spermatogenic cells assemble in different maturation stage. The Sertoli cell cytoskeleton are linked with many extra cellular matrix protein such as (laminin , collagen, fibronectin) by integrins. Integrins are transmembrane protein consist of alpha and beta sub unit. Upon integrin binding with (ECM) proteins its will activate signal transduction pathways that mediate cellular signals such as the cell cycle regulation, organization of the cytoskeleton, and movement and building of new receptors on cell membrane. In our study thirty adult male mice (albino mice) in age about 9-12 weeks and weight between 25-30 gr divided into three groups are kept in different photoperiod (full light, full dark and control) for 45 days. the testes of each group are extracted and fixed by neutral buffered formalin and applied the hematoxylin and eosin protocol to study the histological changes in seminiferous tubules and Immunohistochemical technique is to evaluation the expression of integrin protein. Aperio Algorithm Program is applied for Immunohistochemical Assessment of this study the sections were captured using a special camera with the program (micro capture Ver 6.9.1) after that, the images were processed by using a program (Aperio Image Scope X64) this system has a set of default input parameters that specialized in estimating the color intensity and brown gradients and classifying them into three types according to the intensity of the color which is weak positive , positive and strong positive were applied.



**Ali Ahmed Najji et al.****Keywords:** seminiferous tubule, Sertoli cells, photoperiod, integrin.

INTRODUCTION

There are two unique types of testis cell junctions are found in the seminiferous epithelium represent by desmosome-like junctions and ectoplasmic specializations (ESs). (B Holthofer, R Windoffer, S Troyanovsky; & R.E Leube., 2007). The desmosome-like junctions are present between Sertoli cells at the blood– testis barrier (BTB) as well as between Sertoli and all germ cells up to, except step 8 spermatids. On the other hand, the basal ES is present between Sertoli cells coexisting with desmosome-like junctions of the BTB, whereas the apical ES is found between Sertoli cells and all elongating / elongated spermatids. The main function of (ES) is to easily germ cell movement, in addition to anchoring function to preserve the germ cells, especially spermatids, in the epithelium until spermiation is taken place. (T. Toyama, M. Maekawa & S. Yuasa. 2003). The name “integrin” was devised because this protein is identified and linked the extracellular matrix to the cytoskeleton. (RO. Hynes. 2004). Integrins function as adhesion receptors for extracellular ligands (RO. Hynes , Q. Zhao. 2000) by attaching the cell cytoskeleton to (ECM). Integrins are complex protein formed through non-covalent association of two types transmembrane glycoproteins beta (β) and alpha (α) subunit. Forming four parts from inside to outside two short cytoplasmic tails, two single-pass transmembrane helices, two multi-domain ‘legs’, extracellular ligand-binding head. (MJ. Humphries, E.J.H. Symonds, & AP. Mould. 2003). In vertebrates there are 18 (α) and 8 (β) subunits that can assemble into 24 different receptors with different binding properties and different tissue distribution (RO. Hynes. 2002) (M. Barczyk, S. Carracedo, D. Gullberg. 2010). The extracellular parts are approximately (α) and (β) subunits contain around 1000 and 750 amino acids, respectively (MA. Amaout, SL Goodman, JP. Xiong . 2007) and form elongated stalks and a globular ligand-binding head region (JP. Xiong *et al.* 2001)

Aims of the study

This study was intended for comparing the expression of integrin protein and evaluate the histological change of seminiferous tubules in different groups of Albino mice that exposure to different photo period in the same circumstances by using Aperio image scope analysis.

MATERIALS & METHODS

The present study was performed on thirty (30) adult male mice (albino mice), were collected from Iraqi center for Cancer and Medical Genetics research, aged about 9-12 weeks, weighing between 25-30 gr. The mouse were apparently healthy and active, were kept under controlled illumination. The animals were placed in plastic cages, easy to clean with free access to fresh tap water and standard pellet food. The cages isolated from each other completely by using larger plastic rooms were kept it under controlled temperature at 23 ± 2 C ° (room temperature) and well ventilated condition. The cages of group A&C illumination by LED white light in intensity 40 watts it's attached with the surface of the cages. (Figure 1) This study was carried out in the Department of anatomy, College of Medicine/ AL-Nahrian University. The duration of work was from December 2018 / to July 2019. The animals divided to three groups each group content ten (10) male mice and were give the animals a period about one week for physiologic, psychologic and nutritional stabilization before their use. Then were kept 2-3 mice in each cages under controlled illumination as the following in (Table 1). The first group (group A) 10 male mice will be expose full daytime (24 hours) in light environment place for 45 days. The second group (group B) 10 male mice will be expose full daytime (24 hours) in darkness place for 45 days. The third group (Control group) 10 male mice will be expose to 14 hours light and 10 hours dark place for 45 days. The cages of group A&C illumination by LED white light in intensity 40 watts it's attach with the surface of the cages. During our experiment time the weight of all three groups been watched weekly and recording the weight in each time then calculate their mean values. The mouse was euthanized by chloroform soaked cotton piece in airtight chamber for 3-5 min. Then the mice were placed on an



**Ali Ahmed Naji et al.**

autopsy platform and fixed through their four limbs as an anatomical position. And median incision was done in chest by using fine scalpel and scissor after then we removed the skin and cut the sternum by scissor and the systematic fixation to all the body by perfusion via the intra-vascular infusion through the heart to have more rapid and uniform fixation, by using neutral buffered formalin (10%) during the 3-5 mints. Then other median incision was done in the lower part of abdomen to remove the skin and peritoneal layer so that to separate the fatty tissues from the testis and take out the testis out from the body by aid the dissection microscope. The specimen is sectioned in cross section, through the whole testis.

The specimen of testes were prepared for histological study by making paraffin wax tissue block in order to be sectioned by microtome, through of following the standard protocol as the following order: Fixation, dehydration, clearing, impregnation, embedding, and sectioning, de-waxing, staining and mounting according to (Baker, F. J., & Silvertan, R. E. 2014.) The specimen of testes was fixed in 10% Neutral Buffered Formalin (NBF). The specimen was fixed in formalin for 48 hour in two steps each step duration (24 hour) at room temperature. Then that the specimen was washed in 70% ethanol alcohol several times for insuring that no fixative still found in specimen to have enough sample dehydration the samples was immersed in series of different concentrations (ascending concentrations) of ethanol alcohol. The specimen was transfer to xylene as a clearing solution in two changes each one takes 20 min to ensure that there is no or lack of alcohol in the sample. Before embedding specimen in paraffin wax the specimen must be applied through Impregnation process. During the Impregnation we made the mixture xylene and paraffin wax in labeled tube in equal amount by using hot air oven in 55-60°C then we was immersion the specimen in it for one hour. Then the absolute paraffin wax is liquefied by applying hot air oven at 60°C in labeled universal tube and transfer the specimen to it and keep it for 2 hour. The hematoxylin and eosin (H&E) stain is the standard method is used for histological microscopic examination of tissues that have been fixed, processed, embedded, and sectioned. This technique is applied to demonstrate the morphometric and histological features of testis in the seminiferous tubules (thickness, diameter, shape nuclear and cytoplasmic changes) of our specimen and so that compare study is done.

Digital Image Analysis Software is applied in this study. The images were taken using Micro Capture Ver 6.9.1 (Figure 2) and taken in many magnification 10X, 40X and 100X. Immunohistochemistry (IHC): the principle of IHC is to detect a specific antibody bound to an antigen (integrin protein) in tissue sections. The specific antibody is located by a secondary antibody polymerized to an enzyme. The specific antibody, secondary antibody enzyme complex is then visualized with an appropriate substrate /chromogen. The advantage is offered by a micro-polymer detection system over an ABC based detection system is that it is biotin free (ideal for studying tissue rich in endogenous biotin e.g. kidney or brain tissue). Anti-Integrin beta 1 antibody (ab183666) is a biotin free immunoenzymatic antigen detection system this technique involves in the sequential incubation of the specimen with an unconjugated rabbit or mouse primary antibody specific to the target antigen, a secondary antibody – Goat anti-rabbit HRP Conjugate and substrate-chromogen. Positive control for Lymph node of human was stained for integrin in the same (IHC) staining steps. While the negative control of testes tissue of adult mice was stained in the same (IHC) staining stapes except add the primary anti body integrin were replaced by PBS. Aperio Algorithm Program is applied for Immunohistochemical Assessment of this study. After the applied the Immunohistochemistry technique on the samples, the sections were captured using a special camera with the program (micro capture Ver 6.9.1) after that, the images were processed by using a program (Aperio Image Scope X64) this system has a set of default input parameters that specialized in estimating the color intensity and brown gradients and classifying them into three types according to the intensity of the color which is weak positive, positive and strong positive were applied.

RESULTS

This study shows many histological and morphometric changes in reproductive structure on experimental animal after they were exposed to different photoperiod these differences varied between increase and decrease based on



**Ali Ahmed Naji et al.**

control group data. The study includes the changes in the size and weight of testes, as well as the diameter and thickness of seminiferous tubules with the expression of integrin protein in seminiferous tubules of mice testis.

Effects of light / darkness on behavior and moods of experimental animals

The experimental mice of light group reveal significant more requirements for food and water consuming with changes in behavior and moods where they become irritable, quarrelling and aggressive in compare to that in the dark group mice which they reveal less requirements for food and water with quiet and calm behavior.

Effects of light / darkness on testis size and weight of experimental animals

The testis in all groups after extraction from experimental animals at the end of the experiment period showed a significant difference in size and weight between light and dark groups, where increased testicular size in the light group animals were evident in compared to that of dark group animals which shows a decrease in testicular size (Figure 6 A&B) and weight in regarding to control group animals (Figure 7 A&B).

Effects of light/darkness on the diameter of seminiferous tubules of experimental animals

After the end of the experiment and the application of the Histological routine stain (Hematotoxylone and eosin) of the samples used in the experiment (testes), observed many various differences in the morphometric analysis of the samples including changes in the diameter of seminiferous tubules and the area between the seminiferous tubules (interstitial spaces) (Figure 8 A&B). In light group showed an increase in seminiferous tubules diameter in comparison to dark group which showed (626.8748 ± 31.4545) for light group mice and (489.6295 ± 41.7693) for dark group mice, respectively. This is achieved in regarding to Control group animals (Table 2).

Effects of light / darkness on the lining epithelium thickness in micrometers of seminiferous tubules of experimental animals

Measuring the thickness of the lining epithelium (sertoli & spermatogonia cells) of seminiferous tubules in light group mice reveals a significant increase in thickness of lining epithelium of seminiferous tubules in comparison to the dark group mice which was recorded (207.8035 ± 10.47166) for light group mice and (142.2035 ± 13.55409) for the dark group mice, respectively. These changes is achieved in regarding to Control group animals (Figure 9 A&B). Histological features show significant difference in the thickness of the lining of epithelium of the seminiferous tubules in different groups as follows by (H&E stain) (Table 3).

Effects of light / darkness on the interstitials space between seminiferous tubules of experimental animals testis

The interstitials space between seminiferous tubules of light group mice reveals a very little space with closely compact together and decrease in its values in comparison to the dark group mice which they have wide interstitials space in between seminiferous tubules. Increased in the diameter of seminiferous tubules in light group in comparison to dark group is due to effect of light on increase of FSH secretion from hypothalamic pituitary axis, lead to increment in spermatogenesis.



**Ali Ahmed Naji et al.****Effects of light / darkness on the marker expression of the integrin protein of seminiferous tubules of experimental animals by applying Aperio program**

After the samples were prepared for each group to perform immunohistochemistry tests and was implemented {Anti-Integrin beta 1 antibody (ab183666)} for detection of the effectiveness and quantity of integrin protein (Figure 10 A&B) (Figure 11 A&B) (Table 4). The marker expression of the integrin protein in the seminiferous tubules of light group mice reveals a significant decrease in values of the wall of seminiferous tubules which was very little in comparison to the dark group mice and this was recorded as (0.1241 ± 0.0090) for light group mice and (0.2314 ± 0.0326) for the dark group mice, respectively. This is achieved in regarding to Control group animals.

DISCUSSION**Changes in behavior and moods**

The experimental mice for light group reveal a significant more requirement for food and water with changes in behavior and moods where they become irritable, quarrelling and aggressive in compare to that of the dark group mice which they reveal less requirements for food and water with quiet and calm behavior. This indicate that light has a stimulant effect on the HPT hunger & thirst center of these animals and this agree with other researchers who found that the hypothalamus play a key role in the regulation of food intake. They concluded that the effects of 4 weeks of short- or long-photoperiod on food intake were related to mRNA expression levels of neuropeptide Y - regulated transcript in the hypothalamus of mouse. There was a significant difference in body fat mass, food intake and neuropeptide Y mRNA expression were seen. The elevation of neuropeptide Y mRNA is a regulated neuropeptide in the hypothalamus that suggests a physiological role of neuroendocrine factors (secreted by HPT) in food intake during the different photoperiods (L Zhang *et al.* 2015).

Furthermore, researchers found that the influence of daylength on copulatory behaviour was assessed by comparing male hamsters exposed to long or short photoperiods (14 or 2 h light/24 h).they concluded that Copulation behavior declined in animals transferred from long to short (photoperiods) days; where most of the hamsters ceased to ejaculate within 9 weeks with sexually receptive female hamsters. This decline in copulation of the hamsters which experiencing short days was associated with atrophy of the gonads. The behavioral changes in these animals were far more gradual than those observed in hamsters after even surgical castration. There was significantly more mating behavior in tests during the subjective night of the hamsters than during their subjective day. There was photoperiodically mediated changes in behaviour, physiology and morphology may each contribute directly to the reproductive quiescence presumed to occur in the field during the short days of autumn and winter as that of dark group animals as in this present study. This indicates that light (photoperiods) has a stimulant effect on the HPT nuclei that leading to change in the mood and behavior activity of mice (Morin & Zucker , 1978). Moreover, this also is agreed with authors who reported that changes in the dark / light circle as in Seasonal affective disorder (SAD) is characterized by depression during specific seasons, generally winter. They showed that laboratory C57BL/6J mice display photoperiodic changes in depression-like behavior and brain serotonin content. The C57BL/6J mice were maintained under short-day conditions, as compared to those under long-day conditions, demonstrated prolonged immobility times in the forced swimming test with lower brain levels of serotonin and its precursor L-tryptophan. These data suggest that the mechanisms underlying SAD involve the brain—peripheral tissue network, and the C57BL/6J mice could serve as a powerful tool for investigating the link between seasons and mood. This indicate that the effect of photoperiod was significantly occur during the light phased and this physical and behavioral activities are related to the length of light in the day time of these animals (Otsuka, *et al.* 2014).



**Ali Ahmed Naji et al.****Increase in size and weight of testicles**

The present study reveals that there are an increase in size and weight of testis of light group animals in comparison to dark group animals. This will agree with researchers who found that experimental rats which were exposed to long photoperiods (LD), they show testicular weights were significantly increased as compared to those in control rats. While, exposure of rats to short photoperiods (SD) (long dark period) resulted in significantly decrease of testicular weights, as compared to those in control group and other group rats which were maintained in long photoperiods. (B. DI, Garyfallou, Urbanski. 2001) (Edmonds, Stetson. 2001) (I .K, Akpolat *et al.* 2003) Moreover, (Shoemaker & Heideman 2002) also agree with this present study who applied the experimental rats which were kept in long photoperiods (L16:D8), adult F344 rats transferred at 4.5 months of age to short photoperiods (L8:D16) had significantly lower testis size, food intake, and body weight. Also they found that the newly weaned F344 rats underwent an initial period of inhibition of reproductive maturation, lower food intake, and lower body weight in short photoperiod or intermediate photoperiod (L12:D12) relative to rats in long photoperiod. In short photoperiod, rats underwent a second period of slight reproductive inhibition between weeks 35 and 48, but there was an effect on body weight and slight inhibition of food intake only in an intermediate photoperiod. While in the present study the albino mice were revealed a significant effect of light on the reproductive activities (behavioural, morphological and immunohistochemical analysis) which is evident even after 4 weeks. (Shoemaker & Heideman. 2002) However, studies on animals with less Photoperiods than 13 hrs would prevent any significant testicular growth in these experimental animals. While more photoperiods of 14 hrs would stimulated testicular growth but the amount of growth was proportional to the photoperiod. The testes of males of 5 weeks of age and exposed to 14 h light/24 h were significantly larger than those of males given 13 h or less but significantly smaller than those of males given 15 h light/24 h. At 6 weeks of age, the testes of males exposed to 14 h light/24 h were significantly heavier than those of males given 12 h or less but significantly smaller than those of males given 15 or 16 h light/24 h. (Anne Grocock, 1981)

Diameter of seminiferous

The present study reveals that there is an increase the diameter of seminiferous tubules of testis of light group animals in comparison to dark group animals. This will agree with researchers who found that in rats exposed to long photoperiods, they found that diameters of seminiferous tubules were significantly increased as compared to those in control rats. While, exposure of these rats to short photoperiods, (SD) (or long dark period) resulted in significantly decrease of diameters of seminiferous tubules, as compared to those in control group rats and other group rats which were maintained in long photoperiods (LD) (B. DI, Garyfallou, Urbanski. 2001) (Edmonds, Stetson. 2001) (I .K, Akpolat *et al.* 2003). (OLAYAKI *et al.* 2010) also found that animals lived in short photoperiod (SP) group were showed that there was a significant decrease in testicular-body-weight ratio from $(0.01 \pm 0.001\text{gr})$ to $(0.004 \pm 0.001\text{gr})$ compared to control, about 60% reduction. While Long photoperiod (LP) did not affect the testicular-body weight ratio. They concluded that SP significantly reduced sperm motility from $(72.60 \pm 8.44 \%)$ in the control group to $(29.00 \pm 5.42 \%)$ in the SP group. Also LP increased sperm motility from $(72.60 \pm 8.44\%)$ in the control group to $(74.00 \pm 6.52 \%)$ in LP group. The SP showed a significant effect on sperm viability, which was reduced from $(57.00 \pm 11.51 \%)$ in the control group to $(23.00 \pm 3.42 \%)$ in the SP group while it was insignificantly increased to $(64.00 \pm 14.36 \%)$ in LP group. Moreover, SP significantly reduced sperm counts from $(41.60 \pm 7.89 \times 10^6 /\text{ml})$ in the control group, to $(17.70 \pm 3.56 \times 10^6 /\text{ml})$ in the SP group. while LP slightly increased the sperm count to $(44.60 \pm 9.86 \times 10^6 /\text{ml})$. This will indicate that light is a stimulant physical factor to the GnRH of the hypothalamus which later on leading to increment in viability, activities and count of spermatozoa and this findings will be the reverse in dark group animals as in this present study (OLAYAKI *et al.* 2010)





Thickness of Seminiferous

In the present study they explain that there is an increase in the thickness of seminiferous tubules of testis in light group animals in comparison to that of dark group animals. This will agree with researchers who found that in hamster exposed to long photoperiods, found that thickness of seminiferous tubules were significantly increased as compared to those in control animals. While, exposure of hamster to short photoperiods (long dark period) resulted in significantly decrease in the thickness of seminiferous tubules, as compared to those in control group animals and other group that maintained in long photoperiods (Meachem SJ, *et al* 2005). This present study will explain the indirect stimulant effect of light on seminiferous tubules via integration of melatonin hormone secretion from pineal gland on the hypothalamic –pituitary testis axis by mean of (FSH) which acts on epithelium of seminiferous tubules, this will later on causing an increase the thickness of this epithelium including sertoli cells. However, certain studies found that the identification of these hormones and other factors will regulate Sertoli cell survival, proliferation, and maturation which is important in testicular cell biology. Moreover, the regulation of Sertoli cell proliferation and differentiation was thought to be controlled by a set of circulating and local hormones (endocrine and paracrine, respectively). The receptors and intracellular signaling pathways activated by androgen, follicle-stimulating hormone, with special emphasis on their receptors has a paracrine activity on epithelium of seminiferous tubules. Androgen receptors activate intracellular signaling pathways that converge on cell cycle and transcription factors that play a role in the regulation of Sertoli cell proliferation and differentiation. Furthermore, (Meachem, *et al.* 2005) concluded that (FSH) stimulates Sertoli cell division at day 9 in rats and differentiation in immature (prepubertal) animals, and these biological responses are correlated with qualitative as well as quantitative differences in FSH receptor signaling activity (Meachem, *et al.* 2005) (Lucas & Nascimento 2014). This present study will clarify that light has a physical stimulant factor that cause the release of gonadotrophic hormones from pituitary gland, which are triggered by hypothalamic nuclei through their releasing hormones, on germinative epithelium of seminiferous tubules of the testis. These hormones will make these epithelial keep cells divisions and become hyperplastic and so this will eventually lead to increase in size and thickness of the epithelium of seminiferous tubules.

Interstitial Leydig cells

In the present study they explain an increase in the thickness of seminiferous tubules causing a diminish in the interstitial space of testis in light group animals with increase in size of cytoplasm of Leydig cells and their nuclei in comparison to dark group which found that there is widening of interstitial space with decrease in size of the cytoplasm of Leydig cells. This findings agree with researchers (Chan WY, *et al* 1994) who found that exposure of hamsters to the 8L:16D short photoperiod (as in dark group) they revealed testicular regression of leydig cells in addition to a reduction in the numbers of spermatids and mature spermatozoa in some animals to an almost complete loss of spermatogenesis in others. This explain that why long photoperiod (as in light group animals) will lead to increase secretion of LH from pituitary gland and that eventually will activate and potentiate the s ER in the cytoplasm of Leydig cells to secrete androgen (that to say increase in the activity of these cells) so this will increase the spermatogenesis. While in short photoperiod animals they reveal a reduce the size of the epithelial cells of seminal vesicles of accessory gland of reproductive system so that they changed their epithelium from a tall columnar to low columnar or cuboidal appearance. The secretory activity of the epithelial cells was also reduce in numbers. (W. Y. Chan & T. B. Ng 1994).

Integrin protein

Integrin protein acts like a receptor protein (modulator protein) for certain hormones in the body, although it reveal a decrease in intensity & quantity of these integrin proteins according to Gonadotrophic hormones (FSH & LH) in male. It was found that integrin activate Focal adhesion kinase (FAK) in the cytoplasm of certain cells and this will potentiate certain activities in these cells to perform certain functions (E. R. Siu *et al* 2009). So that in dark photoperiod





Ali Ahmed Naji et al.

there is increase in melatonin secretion that leads to decrease in (FSH & LH). This furthermore will affect the presence of these modulator protein receptors to be increase in quantity so that to counteract the low hormonal activity leading to increase in sensitivity of these modulator protein receptors in effector cells which is sertoli cell for FSH and leydig cell for LH. (Ch. Molnar and J. Gair 2014). This also agree with researchers who found that serum LH and FSH levels are correlated to respective receptor levels in ovarian tissue in female. They found that high serum gonadotropin levels in peri-menopause have been suggested to the existence of low ovarian gonadotropin receptor levels in the ovary. This is correlating with the increases in gonadotropin levels to corresponding cellular receptors. The action of gonadotropins on gonadal function is mediated through specific binding of the hormones to their receptors located on the surface of certain target cells followed by activation of intracellular second messenger systems (FAK). In the ovary, the target cells for FSH are granulosa cells of ovarian follicles while in male are sertoli cells in seminiferous tubules of testis. The action of LH is mediated through binding of the their receptors in theca, granulosa and luteal cells. while in male the action of LH is mediated through binding of the their receptors in leydig cells (Vihko . 1996). This will also agree with researchers who found that FSH has significant value in Sertoli cell division at day 9 in rats and this are correlated with qualitative as well as quantitative differences in receptor of FSH in these cells³⁹ and in the present study the light group animals showed high activity of sertoli cell due to low melatonin secretion in light group (long photoperiod) which increase activity of the hypothalamic –pituitary testis axis to secrete FSH and LH (Meachem, et al. 2005) (Lucas, et al 2014). The present study reveal that there is increase in integrin protein expression in the seminiferous tubules of mice testis in short photoperiod group animals (dark group) this will postulate that dark period will affect the release of FSH and LH secretion via melatonin hormone secretion from pineal gland. This eventually will lead to decrease in androgen hormone secretion from leydig cells in the testis. This will furthermore increase the integrin protein expression of seminiferous tubules that make integrin protein potentiate FAK and integrin –linked kinase activity. These will enhance the enzymatic pathways in cytoplasm of these cells, to make these cells modulate and regulate the receptor activities of androgen hormone on cell membranes (C-F Yen, H-S Wang, C-L Lee, Sh-K Liao.2014). However, studies illustrated that the number of receptors that respond to a hormone determines the cell's sensitivity to that hormone, and the resulting cellular response. Therefore the number of receptors that are activated to a hormone can change over time, resulting in increased or decreased cell sensitivity. When the number of receptors decreases as in the present study, in response to rising hormone levels, this phenomena is called down-regulation of receptors protein, leading to cellular activity to be reduced. (Charles Molnar & Jane Gair.2012).

REFERENCES

1. Holthofer B., Windoffer R., Troyanovsky S.& Leube R. E.. 2007 Structure and function of desmosomes. *Int. Rev. Cytol.* 264, 65–163.
2. Toyama T, Maekawa M and Yuasa S (2003) Ectoplasmic specializations in the Sertoli cell: new vistas based on genetic defects and testicular toxicology. *Anat Sci Int* 8, 1–16
3. Hynes RO. (2004). The emergence of integrins: A personal and historical perspective. *Matrix Biol* 23: 333–340.
4. Hynes RO, Zhao Q. The evolution of cell adhesion. *J Cell Biol.* 2000;150:F89–F96
5. Humphries MJ, Symonds EJH, and Mould AP. Mapping functional residues onto integrin crystal structures. *Curr. Opin. Struct. Biol.* 2003; 13(2):236–43.
6. Hynes RO. Integrins: bidirectional, allosteric signaling machines. *Cell* 2002; 110(6):673–87.
7. Barczyk M, Carracedo S, Gullberg D. (2010). Integrins. *Cell Tissue Res* 339: 269–280
8. Arnaout MA, Goodman SL, Xiong JP. (2007). Structure and mechanics of integrin-based cell adhesion. *Curr Opin Cell Biol* 19: 495–507
9. Xiong JP, Stehle T, Diefenbach B, Zhang R, Dunker R, Scott DL, Joachimiak A, Goodman SL, Arnaout MA *Science.* 2001 Oct 12; 294(5541):339–45
10. Baker, F. J., & Silverton, R. E. (2014). *Introduction to medical laboratory technology.* Butterworth-Heinemann 7th ed, 299–426)





Ali Ahmed Naji et al.

11. Lin Zhang, Fang Yang, Jinhong Cai, Chunmei Huang, Zhengkun Wang and Wanlong Zhu. The role of photoperiod on the expression of hypothalamic genes regulating appetite in Chevrier's field mouse (*Apodemus chevrieri*)(2015). *Animal Biology* 65 (2015) 45–56
12. L. P. MORIN AND I. ZUCKER, PHOTOPERIODIC REGULATION OF COPULATORY BEHAVIOUR IN THE MALE HAMSTER *J. Endocr.*(1978) . 78,249-258.
13. Tsuyoshi Otsuka, Misato Kawai, Yuki Togo, Ryosei Goda, Takahiro Kawase, Haruka Matsuo, Ayaka Iwamoto, Mao Nagasawa, Mitsuhiro Furuse, Shinobu Yasuo Photoperiodic responses of depression-like behavior, the brain serotonergic system, and peripheral metabolism in laboratory mice(2014). *Psycho neuroendocrinology* 40, 37—47.
14. Brown DI, Garyfallou VT, Urbanski HF. Photoperiodic modulation of GnRH mRNA in the male syrian hamster. *Molecular Brain Res* 2001; 89:119-125
15. Edmonds KE, Stetson MH. Effects of age and photoperiod on reproductive and the spleen in the marsh rice rat (*Oryzomys palustris*). *Am J Physiol Regulatory Integrative Comp Physiol* 2001; 280:1249-1255.
16. Ilter K, Akpolat N , Oner H , Ayar A , H Pekmez, O A Ozen5 & M Sarsilmaz :The effects of photoperiod on testes in rat:A morphometric and immunohistochemical study. *Neuroendocrinology Letters*. 2003: Nos.3/4, Jun-Aug, Vol.24.: 210-214
17. M B Shoemaker and PD Heideman. Reduced body mass, food intake, and testis size in response to short photoperiod in adult F344 rats. *BMC Physiol*. 2002; 2: 11
18. C. Anne Grocock, Effect of different photoperiods on testicular weight changes in the vole, *Microtus agrestis*, Department of Human Anatomy, South Parks Road, Oxford OX1 3QX, U.K.*J.Reprod.Fert.*(1981)62,25-32
19. Brown DI, Garyfallou VT, Urbanski HF. Photoperiodic modulation of GnRH mRNA in the male syrian hamster. *Molecular Brain Res* 2001; 89:119-125
20. Edmonds KE, Stetson MH. Effects of age and photoperiod on reproductive and the spleen in the marsh rice rat (*Oryzomys palustris*). *Am J Physiol Regulatory Integrative Comp Physiol* 2001; 280:1249-1255.
21. Ilter K, Akpolat N , Oner H , Ayar A , H Pekmez, O A Ozen5 & M Sarsilmaz :The effects of photoperiod on testes in rat:A morphometric and immunohistochemical study. *Neuroendocrinology Letters*. 2003: Nos.3/4, Jun-Aug, Vol.24.: 210-214
22. L.A.Olayaki,A.O.Soladoye,T.M.Salman& B.Jorah , Effects of photoperiod on testicular function in male SPRAGUE-DAWLEY rats. *Nigerian Journal of physiological Sciences* (2010).23(1-2):27-30.
23. Meachem SJ, Ruwanpura SM, Ziolkowski J, Ague JM, Skinner MK, Loveland KL. Developmentally distinct in vivo effects of FSH on proliferation and apoptosis during testis maturation. *J Endocrinol*. 2005;186:429–46
24. T F Lucas, A R Nascimento, R Pisolato, M T Pimenta, M F M Lazari, and C S Porto*. Receptors and signaling pathways involved in proliferation and differentiation of Sertoli cells. *Spermatogenesis*. 2014; 4: e28138.
25. W. Y. Chan & T. B. Ng .Effect of Photoperiod on Testicular Histology in Golden Hamsters and C57 and BALB/C Mice, *Archives of Andrology**Journal of Reproductive Systems*,1994.32:2, 101-109
26. Erica R. Siua, Elissa W. P. Wonga, Dolores D. Mruka, Catarina S. Portob, and C. Yan Chenga. Focal adhesion kinase is a blood–testis barrier regulator.2009.*PNAS* June 9, 2009 106 (23) 9298-9303;
27. Vihko KK.Gonadotropins and ovarian gonadotropin receptors during the perimenopausal transition period. *the european menopause journal*.1996 volume23 p 19-22.
28. Chih-Feng Yen, Hsin-Shih Wang, Chyi-Long Lee, Shuen-Kuei Liao. Roles of integrin-linked kinase in cell signaling and its perspectives as a therapeutic target.2014. *Gynecology and Minimally Invasive Therapy* 3 67e72.
29. Charles Molnar and Jane Gair. Unit 4: Animal Structure and Function.18.2 How Hormones Work. 2012.*Concepts of Biology—1st Canadian Edition*.





Ali Ahmed Naji et al.

Table 1.the groups of experimental animal distributed by dark / light cycle

Groups name	Number of animal	(Dark/Light) cycle daily
A (Light)	10	0:24 hr.
B (Darkness)	10	24:0 hr.
C (Control)	10	10:14 hr.

Table 2. The data of diameter measure of seminiferous tubules according to dark / light cycle

	Mean	Std.Deviation	Std.Error	Sig
Full light group	626.8748	31.4545	7.033	0.001
Full dark group	489.6295	41.7693	9.339	
Control group	517.5525	19.50091	4.360	
Total	544.6856	67.60069	8.727	

Table 3. the data of thickness measure of seminiferous tubules

	Mean	Std.Deviation	Std.Error	Sig
Full light group	207.8035	10.47166	2.34153	0.001
Full dark group	142.2035	13.55409	3.03079	
Control group	168.5655	12.00173	2.68367	
Total	172.8575	29.65823	3.82886	

Table 4. the data of expression of integrin in seminiferous tubules by applying Aperio image program

	Mean	Std.Deviation	Std.Error	Sig
Full light group	0.1241	0.0090	0.0020	0.001
Full dark group	0.2314	0.0326	0.0073	
Control group	0.1562	0.0345	0.0077	
Total	0.1705	0.0530	0.0068	



Fig. 1. Animal housing and separated in three different rooms according to illumination time.



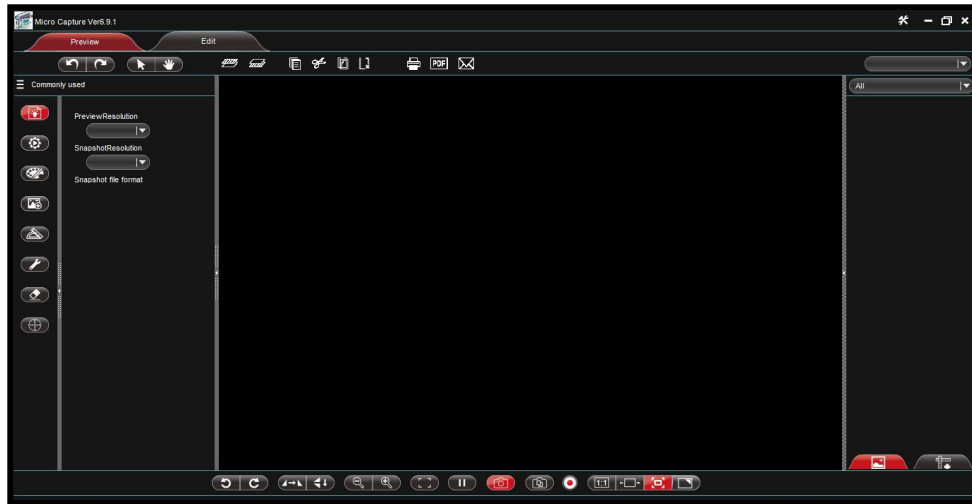


Fig 2. Micro Capture Ver 6.9.1 Application

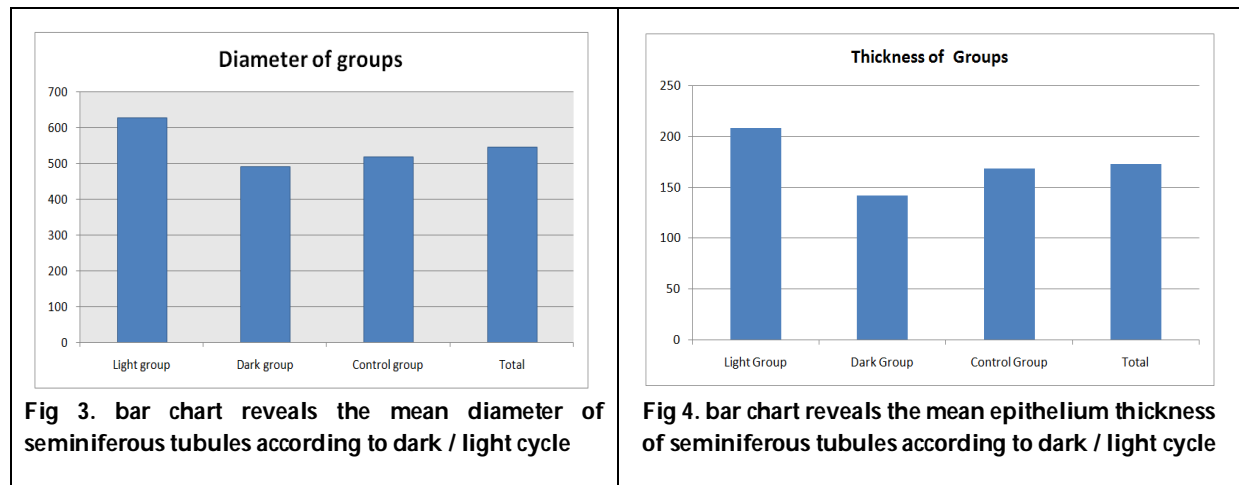


Fig 3. bar chart reveals the mean diameter of seminiferous tubules according to dark / light cycle

Fig 4. bar chart reveals the mean epithelium thickness of seminiferous tubules according to dark / light cycle

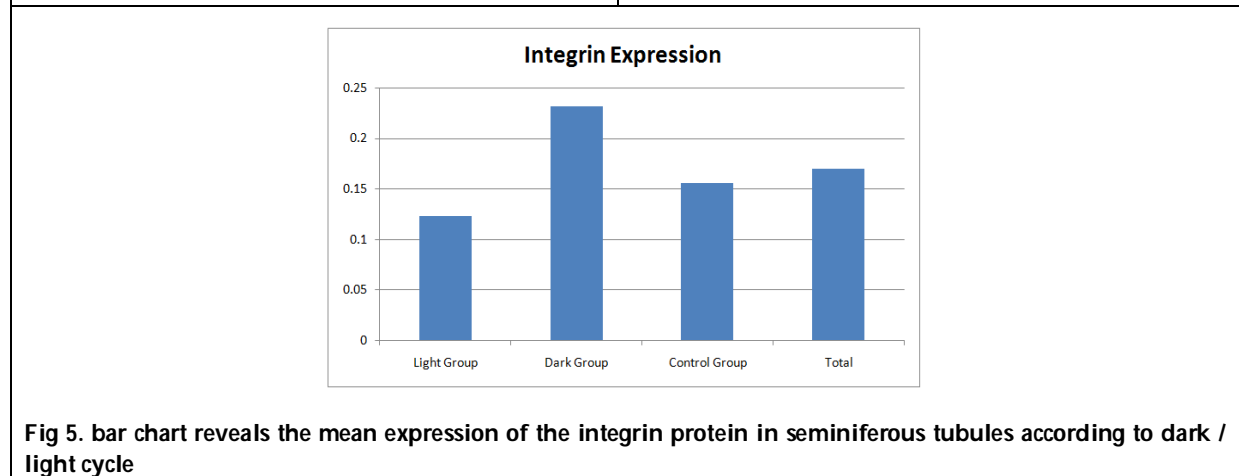


Fig 5. bar chart reveals the mean expression of the integrin protein in seminiferous tubules according to dark / light cycle





Ali Ahmed Naji et al.

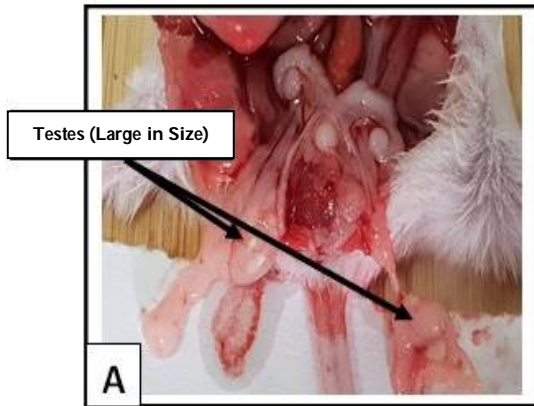
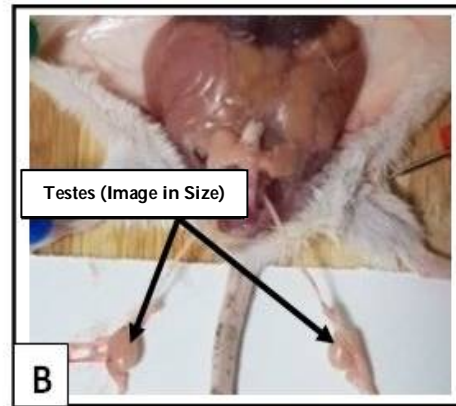


Fig.6 A. Testes of light group,



B. Testes of Dark group

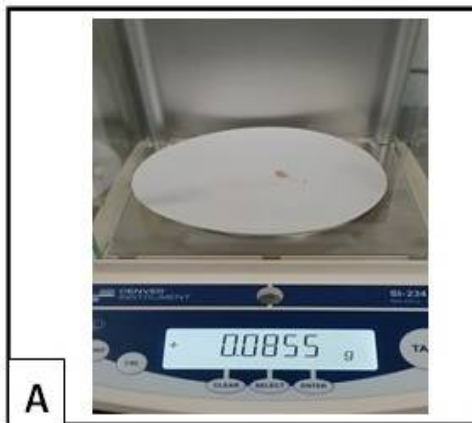
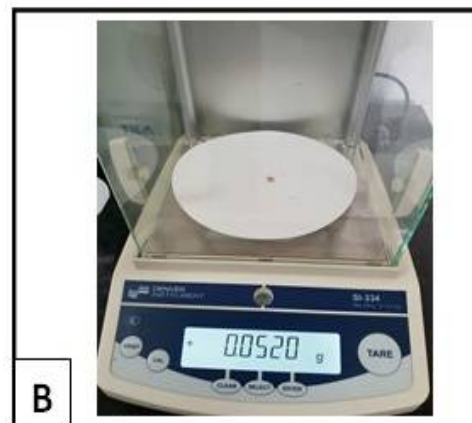


Fig.7 A. Weight of Testes of light group,



B. Weight of Testes of Dark group

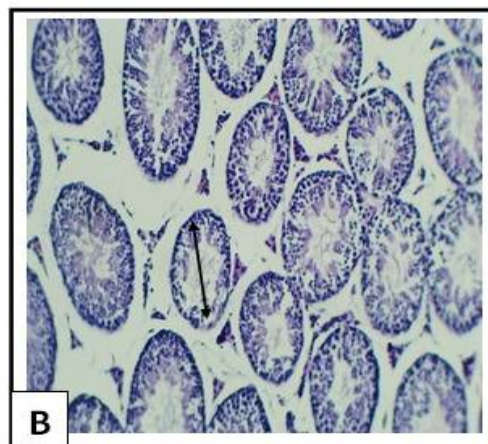
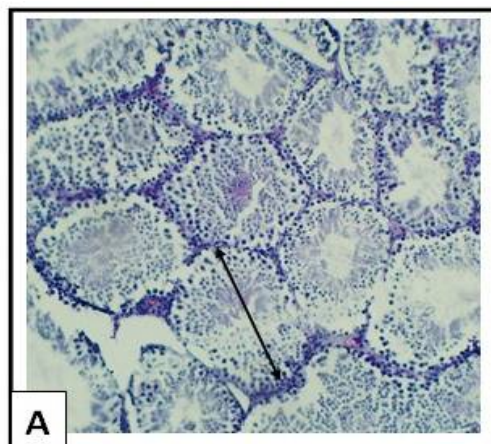


Fig.8. A Increase in the diameter of semiferous tubules of light group, B Decrease in the diameter of semiferous tubules of dark group





Ali Ahmed Naji et al.

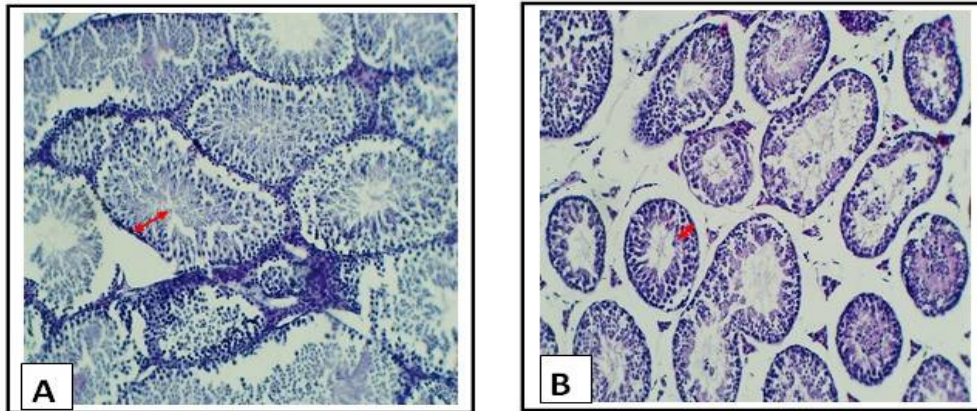


Fig.9. A. Seminiferous Tubules thickness of light group, B Seminiferous Tubules thickness of dark group

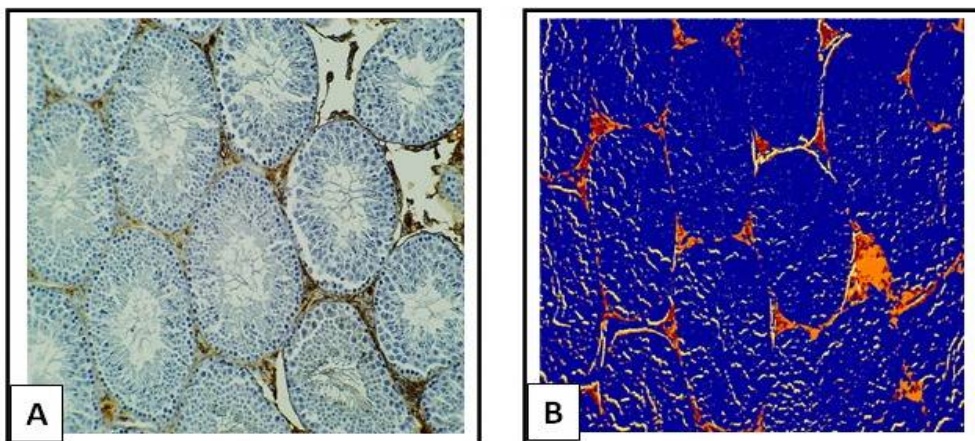


Fig.10. A. Seminiferous tubules Integrin expression of light group, B Seminiferous tubules Integrin expression of light group in analyze view

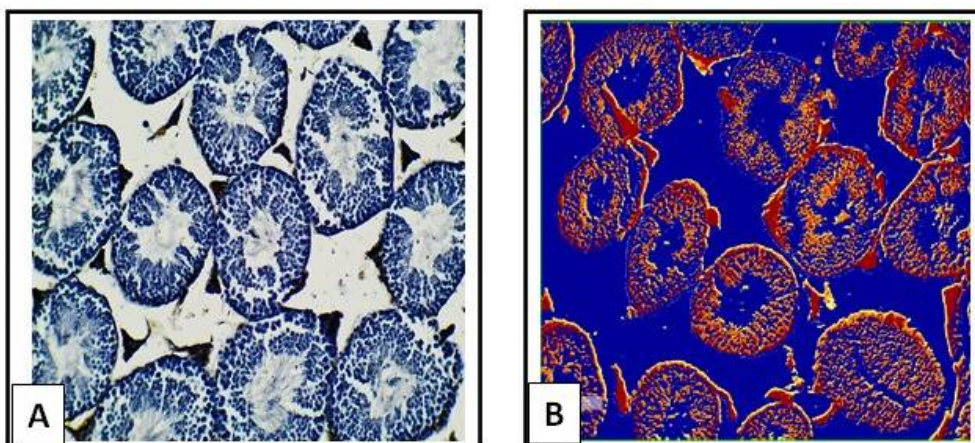


Fig.11. A. Seminiferous tubules Integrin expression of dark group, B Seminiferous tubules Integrin expression of dark group in analyze view





Effect of Different Feldspar Ratios on Thermal Properties of Porcelain Ceramic Foam via Replication Method

H.M.Mahmood* and A.Medeved

YankaKupala State, University of Grodno, Belarus

Received: 14 Aug 2019

Revised: 17 Sep 2019

Accepted: 21 Oct 2019

*Address for Correspondence

H.M.Mahmood

YankaKupala State,
University of Grodno,
Belarus.

Email:hameedmajeed_73@yahoo.com



This is an Open Access Journal / article distributed under the terms of the **Creative Commons Attribution License** (CC BY-NC-ND 3.0) which permits unrestricted use, distribution, and reproduction in any medium, provided the original work is properly cited. All rights reserved.

ABSTRACT

This paper studied, the effect of different feldspar ratios on the thermal properties of porcelain ceramic scaffolds was determined. Polymeric sponge templates were “soaked in ceramic slurry with different feldspar solid loading ranging from 25 to 35 wt. % under vacuum of 10^{-1} Torr and then sintered to 1250°C. Effect of different feldspar solid loadings quantities was based on porosity, density” and thermal properties of the ceramic foam and its ranging between (0.32 to 0.41 K(w/m.°C)).

Keywords: vacuum, microwave drying, polymeric sponge method, porcelain ceramic foam, thermal properties.

INTRODUCTION

Porous ceramic material with porosity ranging between 70% to 90% (1). It has become “increasingly important in industry recently due to their numerous applications (2). Like catalyst carriers, filters for molten metal, water, waste water, hot exhaust gases, insulation, biomedical devices, catalytic converter, membrane absorbents, because of their high surface area, high permeability, good thermal properties, high strength, resistance to chemical attacks (3, 4). Polymeric sponge technique is in fact count as the first method purposefully used for the fabrication of the macroporous ceramics” (5). The procedure demands coating of “open-cell” of replica with “ceramic slurry sponge” out of sintering procedure, which introduce a replica of the ceramic foams that tend to own a “lower mechanical strength, and a higher permeability”. Thermal conductivity is an important factor in manufacturing open-porous materials that used in “heat transfer devices like cross-flow heat exchangers, catalytic converters, electrodes of high-temperature fuel cells or solar collectors (6). Last decade, high-porosity materials have been very attractive because of their low density and high specific strength, showing it possible to improve the thermal execution of devices with the concurrent lowering of their weight and size. Moreover, advantage can be seen in expression of permeability when compared to packed bed, repeatedly used in catalytic converters and thermal energy storage devices”, where it afford



**H.M.Mahmood and A.Medeved**

a large pressure drop throughflow (7-9). The goal of this article is to find out the “effect of different feldspar ratios on the thermal properties of the ceramic foam” (10).

EXPERIMENTAL

Polymeric sponges used each were shaped into a dimension of “70 mm × 30 mm” with the different thicknesses for compression and flexural tests. Mixing feldspar, silica and kaolin in the ratios of 25, 25 and 50 wt. % to produced porcelain powder. “The ceramic slurry was designed in the range of 25 to 35 wt. % of feldspar ratio in constant of kaolin. The mixture was stirred in mechanical stirrer for 15 minute. Prior to the dipping procedure, the viscosity of the ceramic slurry was calculatedutilizing viscometer (model RTV) at spindle speed of 100 rpm. The foamswere squeezed physically and then put in a bell jar and evacuated to 10^{-1} Torrto remove the trapped air and make sure that the sponge saturated with the ceramic slurry. Any excess slurry was removed by squeezing the template through a roller. The templates were dried in a microwave oven for 10 to 12 minute according to the thickness. The sample was sintered at 1250 °C with heating rate 5 °C/min, one hour of soaking time”. The porosity was determined using “Archimedes method” and the particle size was measured by laser particle size analyzer. Thermal properties of the ceramic foams at different thicknesses were determined by Lee discs. The morphological study was doneutilizing “scanning electron microscope”.

RESULTS AND DISCUSSION

Morphology and Physical Properties of Samples

Polymeric foam morphology of is immediatelylinked to the “microstructure” of the polymer foam templates. It was found out that the fineness of ceramic foam is highly affected by the “density of the slurry, and this inverted on porosity Fig. (2). Minimizing the porosity will thus increase the density of ceramic foam from 1.335 to 1.562 g/cm³, it was notice that the slurry density more than 1.562 g/cm³ is unwanteddue to the creation of cavity into the ceramic foam which could be lead to a poor slurry flow and coating. Another factor which could also influence the density and porosity is the microstructure of the polymeric sponge foam which generally consists of open and closed-cell structures. Uncoated polymeric foam will become a cavity”because of the“burn-off process” which later takes part in “low density and weak spot in the foam”.

Microstructural analysis

Fig. (4.a) shows the SEM of ceramic foam. “It is obvious that the degree of porous structure increases with increasing density of slurry, it was also obvious that the cell wall thickness of the ceramics scaffolds microstructure have increased with increasing solid loading”. The cell structure of the foam be composed of “open cell and close cell with a majority of dense portion. Fig. (4.b) revels elemental analysis” of the fired ceramic scaffoldsutilizing EDX technique. Elements like K, Zn, Si, Al, C and O element were seen in the ceramic scaffolds presenting the “organic and inorganic elements” existed in the foam.

Thermal Properties

When feldspar Ratios is increasing the thermal conductivity increases as well due to reduction in porosity and increase in viscosity values also as the sintering temperature increase, thermal conductivity increases too due to the micro pore content reduction due to the densification. This is a good indication that this foam can be used as first layer insulation in furnaces. This agree well with Skibinskiet al. (11) which revealed in their study that “Thermal conductivity is not simply dependent on porosity, andthe increase of pore size distribution leads toimportantdrop of thermal conductivity value”. For “heattransfer devices, where higher thermal conductivity of the material is





H.M.Mahmood and A.Medeved

wanted, open-porous materials with homogeneous pore size differences would be suggested, while for materials used as “isolators”, non-homogeneous pore size differences would be a great candidates.

CONCLUSION

Ceramic scaffolds were successfully synthesized utilizing replication technique and known also as (polymeric sponge technique). It was noticed that the thermal properties of the ceramic foam are largely affected by the preparation under vacuum and microwave drying which reduce the porosity and that leads to an increasing in the thermal properties of the samples. This foam is a good candidates as an insulators due to its homogeneous pore size differences.

REFERENCES

1. Zhang, J.-Y; Fu, Y.-M; Zeng, X.-M Trans. Nonferrous Met. SOC. China 16 453-pp.457, (2000), doi: 10.1016/S1003-6326(06)60232-X
2. J. K. Efavi, Ceram. Int. 36, 673-678, (2010), doi: 10.1016/j.ceramint.2009.10.006.
3. F.F. Lange, K.T. Miller, Adv. Ceram. Mater, 2, pp.827, (1987), doi.:10.1111/j.1551-2916.1987.tb00156.x
4. L. M. Sheppard, Porous Ceramics: Processing and Applications, Ceram. Trans. Vol. 31, pp. 3-23, (1992).
5. Schwartzwalder K., Domers A.V., Method of Making Porous Ceramic Articles, US Pat. No. 3090094, (1963).
6. Han, X.-H.; Wang, Q.; Park, Y.-G.; T'Joen, C.; Sommers, A.; Jacobi, A. A Review of Metal Foam and Metal Matrix Composites for Heat Exchangers and Heat Sinks. Heat Transf. Eng, 33, 991–1009, (2012).
7. Banhart, J. Manufacture, characterisation and application of cellular metals and metal foams. Prog. Mater. Sci, 46, 559–632, (2001).
8. Boomsma, K.; Poulikakos, D.; Zwick, F. Metal foams as compact high performance heat exchangers. Mech. Mater, 35, 1161–1176, (2003).
9. Cwieka, K.; Wejrzanowski, T.; Kurzydowski, K.J. Incorporation of the Pore Size Variation to Modeling of the Elastic Behaviour of Metallic Open-Cell Foams. Arch. Metall. Mater, 62, 269–272, (2017).
10. Aleksandrs Korjajins*, Liga Upeniece**, Diana Bajare, “HIGH EFFICIENCY POROUS CERAMICS WITH CONTROLLABLE POROSITY”, 4th International Conference CIVIL ENGINEERING 13 Proceedings Part II, CONSTRUCTION AND MATERIALS, (2013).
11. Jakub Skibinski, Karol Cwieka, Samih Haj Ibrahim and Tomasz Wejrzanowski, “Influence of Pore Size Variation on Thermal Conductivity of Open-Porous Foams”, Materials, 24 June (2019).



Fig 1. Optical micrograph of the polymeric foam

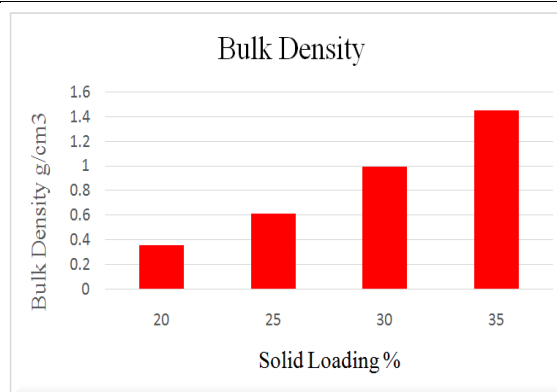


Fig 2: Bulk density of the foam at different feldspar ratios.





H.M.Mahmood and A.Medeved

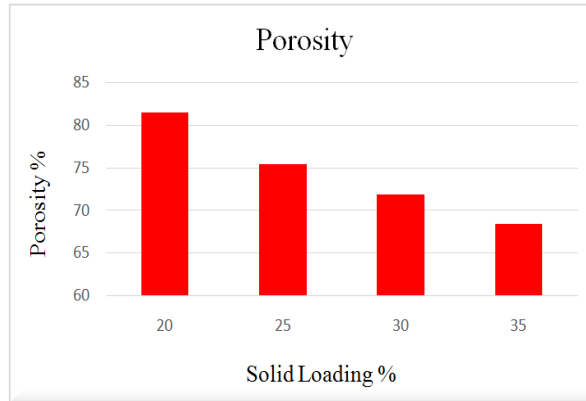


Fig 3. Porosity of the specimens at different feldspar ratios.

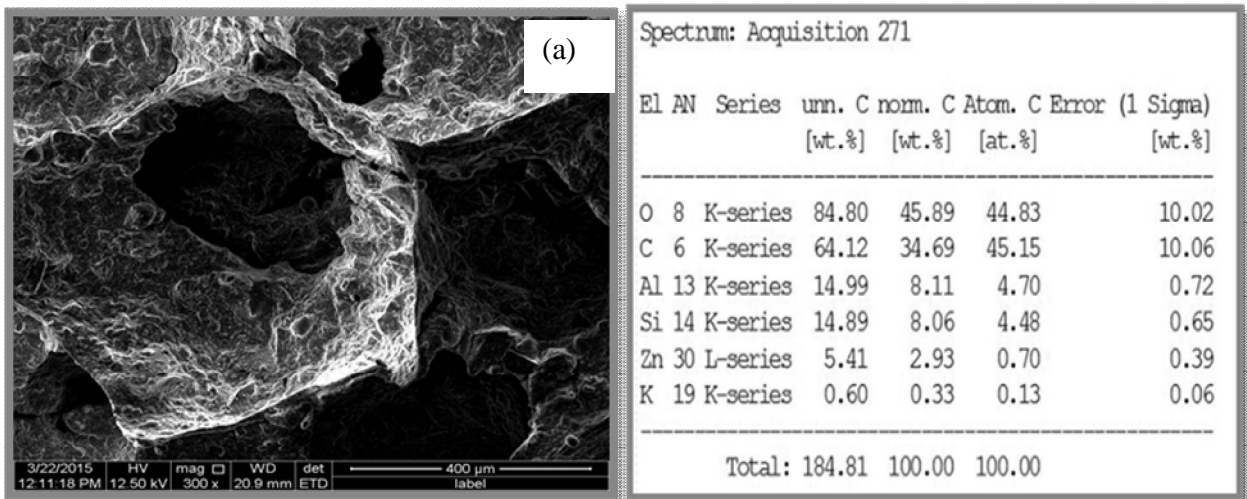


Fig 4: (a) SEM image of sintered ceramic foam, and (b) EDX analysis.





Incidence of Diabetic Retinopathy in Newly Diagnosed Type 2 Diabetes Mellitus Patients

Saleh Muhammad Channa^{1*}, Aijaz Ahmed², Hafiz Muhammad Zeeshan Aslam³, Bashir Ahmed Chandio⁴, Salma Lakho⁵, Abdul Haleem Meerani⁶, Zulfiqar Ali Soomro⁷, Aftab Ahmed Soomro⁸, Zamant Ali⁹ and Fiyaz Hussain¹⁰

¹Professor of Medicine, Ghulam Muhammad Mahar Medical College Teaching Hospital, Sukkur, Pakistan.

²Medical Specialist Indus Hospital Bhung tehsil Sadqabad, Dist Rahimyar Khan, Pakistan.

³Medical officer, Medicine Medical Unit 3 Bahawal Victoria Hospital, Bahawalpur, Pakistan.

⁴Assistant Professor Medicine, Ghulam Muhammad Mahar Medical College Teaching Hospital, Sukkur, Pakistan.

⁵Postgraduate, Medical Unit 1, Ghulam Muhammad Mahar Medical College Teaching Hospital Sukkur, Pakistan.

⁶Assistant Professor, Ophthalmology Department Ghulam Muhammad Mahar Medical College Teaching Hospital, Sukkur, Pakistan.

⁷Consultant Orthopedic & Trauma Surgeon, Ghulam Muhammad Mahar Medical College Teaching Hospital, Sukkur, Pakistan.

⁸Professor of Pathology & Principal of Ghulam Muhammad Mahar Medical College Teaching Hospital, Sukkur, Pakistan.

⁹Postgraduate, Medical Unit 1, Ghulam Muhammad Mahar Medical College Teaching Hospital, Sukkur, Pakistan.

¹⁰Postgraduate, Medical Unit 1, Ghulam Muhammad Mahar Medical College Teaching Hospital, Sukkur, Pakistan.

Received: 17 Aug 2019

Revised: 20 Sep 2019

Accepted: 24 Oct 2019

* Address for Correspondence

Saleh Muhammad Channa

Professor of Medicine,
Ghulam Muhammad Mahar Medical College Teaching Hospital,
Sukkur, Pakistan.

Email: Salehmohammad14@yahoo.com



This is an Open Access Journal / article distributed under the terms of the **Creative Commons Attribution License** (CC BY-NC-ND 3.0) which permits unrestricted use, distribution, and reproduction in any medium, provided the original work is properly cited. All rights reserved.

ABSTRACT

Since type 2 diabetes mellitus may be present well before its clinical diagnosis is made, it is not uncommon to see its micro vascular complications at the time of diagnosis. The longer a person has diabetes, higher the chances of developing diabetic retinopathy. The objective of this study was to determine the incidence of diabetic retinopathy in newly diagnosed type II diabetes patients. Total 113

17790



**Saleh Muhammad Channa et al.**

cases of newly diagnosed type II diabetes mellitus patients with age range from 30-60 years were enrolled in this study at Department of Medicine Department of Medicine, Ghulam Muhammad Mahar Medical Teaching College Sukkur. Patients with type I diabetes, hypertension and with history of previous retinal surgery were excluded. Fundoscopic examination and presence or absence of retinopathy and grades of retinopathy were noted. The observed incidence of diabetic retinopathy was 18 (15.93%) which is relatively high and emphasizes the detailed ophthalmic examination of each patient at the time of diagnosis of diabetes. mean age of the patients was 45.46 ± 7.40 years. Among them 69 (61.06%) were male and 44 (38.94%) were females with male to female ratio of 1.6:1.

Keywords: Type 2 Diabetes Mellitus, newly diagnosed, retinopathy, Incidence.

INTRODUCTION

Diabetes mellitus type 2 (formerly noninsulin-dependent diabetes mellitus (NIDDM) or adult-onset diabetes) is a metabolic disorder that is characterized by high blood glucose in the context of insulin resistance and relative insulin deficiency(1). This is in contrast to diabetes mellitus type 1, in which there is an absolute insulin deficiency due to destruction of islet cells in the pancreas (2). While the Incidence of diabetes mellitus is 10-14% worldwide (3).The classic symptoms are excess thirst, frequent urination, and constant hunger. Type II diabetes makes up about 90% of cases of diabetes with the other 10% due primarily to diabetes mellitus type 1 and gestational diabetes (4).Long-term complications from high blood sugar can include heart disease, strokes, diabetic retinopathy where eyesight is affected, kidney failure which may require dialysis, and poor circulation in the limbs leading to amputations (5). Rates of diabetes are increasing worldwide. The International Diabetes Federation predicts that the number of people living with diabetes will to rise from 366 million in 2011 to 552 million by 2030 (6).In the United States, the prevalence of diagnosed diabetes has more than doubled in the last 3 decades, largely because of the increase in obesity.

Diabetic retinopathy is the leading cause of new blindness in persons aged 25-74 years. The exact mechanism by which diabetes causes retinopathy remains unclear, but several theories have been postulated to explain the typical course and history of the disease (7). Hyperglycemia affects blood vessel formation in the retina of the eye, can lead to visual symptoms, reduced vision, and potentially blindness (8).The longer a person has diabetes, the higher is the chances of developing diabetic retinopathy (9).Reported prevalence of diabetic retinopathy at the time of diagnosis of type 2 diabetes varies from 5-35% (10). Blindness due to diabetic retinopathy can be delayed with timely detection and appropriate therapy.Hussain F et al in a study hasfound frequency of diabetic retinopathy in newly diagnosed type II diabetes mellitus patients as 12% (8). In another study, Wahab S et al hasshown the frequency of diabetic retinopathy in newly diagnosed type II diabetes mellitus patients as 15% (11). In a study by Khanzada MA et al the prevalence of diabetic retinopathy was found very high i.e. 40.64%³. This high prevalence of diabetic retinopathy was also found in the study from Egypt, that reported its frequency 42.0% and a study from Oman that reported 42.4% (12,13). As there was controversy in previous results andalso the type II diabetes mellitus goes on increasing in our population with majority of them are uneducated, belong to poor socioeconomic status and remain unaware of their diabetes due to unavailability of easily approachable health care facilities which result in their late presentation with its long term micro vascular complications, so the purpose of this study was to determine incidence of diabetic retinopathy in newly diagnosed type II diabetes patients visiting Department of Medicine, Department of Medicine Ghulam Muhammad Mahar Medical Teaching Colloge Sukkur Pakistan.

MATERIALS AND METHODS

A Cross-sectional study was conducted (From 24th August 201 to 23rd February 2019) at Department of Medicine, Department of Medicine Ghulam Muhammad Mahar Medical Teaching College Sukkur after obtaining the ethics



**Saleh Muhammad Channa et al.**

committee approval. Non-probability, consecutive sampling method was used and Sample size of 113 cases has been calculated with 95% confidence level, 6% margin of error and taking expected frequency of diabetic retinopathy in newly diagnosed type II DM patients as 12.0% (8) by using following formula. Informed consent was obtained from each subject prior to enrolment in the study. Patients having age > 30 years with diagnosed diabetes mellitus < 6 months and HbA1c levels ≥ 6.5 was deemed as positive or newly diagnosed Type II diabetes mellitus were included in the study. While patients with type I diabetes mellitus, hypertension, any retinal surgery were excluded from the study. Fundoscopic examination was conducted by consultant ophthalmologist. In each patient diabetic retinopathy (present/absent) was noted. Presence of any one of the following on fundus examination was deemed as positive for Diabetic retinopathy.

- a. Grade I (Background Diabetic Retinopathy): presence of microaneurysms and retinal hemorrhage \pm any exudates.
- b. Grade II (Diabetic Maculopathy): presence of focal/diffuse maculopathy and macular oedema.
- c. Grade III (Pre-proliferative Diabetic Retinopathy): presence of venous beading, venous reduplication, intraretinal microvascular abnormality and blot hemorrhage.
- d. Grade IV (Proliferative Diabetic Retinopathy): presence of new vessels on disc (NVD), pre-retinal/vitreous hemorrhage and pre-retinal fibrosis \pm tractional retinal detachment.

Results were presented as mean and standard deviation for quantitative variables i.e. age and duration of disease. Frequency and percentage were calculated for qualitative variables like gender, educational status, family monthly income and diabetic retinopathy (present/absent) and Statistical analysis was performed using SPSS version 20.0.

RESULTS

Age range in this study was from 30 to 60 years with mean age of 45.46 ± 7.40 years. Majority of the patients i.e. 56 (49.56%) were between 41 to 50 years of age. Out of these 113 patients, 69 (61.06%) were male and 44 (38.94%) were females with male to female ratio of 1.6:1. (Table 1). Mean duration of disease was 4.46 ± 1.40 months. fundoscopic examination for presence or absence of diabetic retinopathy shows that retinopathy was present in 18 (15.93%) while 95 (84.07%) patients have shown no retinopathy. (Figure 1)

DISCUSSION

The longer a person has diabetes, the higher the risk of developing some ocular problem. Between 40 to 45 percent of Americans diagnosed with diabetes have some stage of diabetic retinopathy (14). Research indicates that at least 90% of these new cases could be reduced if there was a proper and vigilant treatment and monitoring of the eyes. This study was conducted to determine the incidence of diabetic retinopathy in newly diagnosed type 2 diabetes mellitus patients. In a pilot study conducted at Karachi on 3000 diabetic patients, it was observed that 26% of the patients suffered with retinopathy. However, a European study by Kohner EM et al has reported 35% prevalence rate of retinopathy for women in United Kingdom Prospective Diabetes Study (15). In Europeans, the prevalence of retinopathy at the time of diagnosis of type 2 diabetes varies and in the United Kingdom Prospective Diabetes study (UKPDS), 35% of type 2 diabetic subjects were reported to have retinopathy at diagnosis (16). This is considerably higher than that reported in our study. It, therefore, appears that prevalence of retinopathy at the time of diagnosis of type 2 diabetics in our patients is lower than that reported in UK and USA but similar to that reported from Australia and India (17). This difference in prevalence of retinopathy in newly diagnosed type 2 diabetics might be due to variable time interval between onset and detection of the disease. It can be a result of socio-economic factors which mainly determine the access to and availability of medical care and variation in defining the presence of diabetes mellitus.



**Saleh Muhammad Channa et al.**

Patient's age in this study was from 30 to 60 years with mean age of 45.46 ± 7.40 years. Majority of the patients i.e. 56 (49.56%) were between 41 to 50 years of age. This was very much comparable to the study of Iqbal T et al (18) and Khanzada MA et al (3) who had also observed the mean age of 47 and 45 years respectively. In this study, out of these 113 patients, 69 (61.06%) were male and 44 (38.94%) were females with male to female ratio of 1.6:1. Many previous studies have also found higher incidence of type II diabetes in male than female patients (19-21). While Memon WU et al (20) and Mahar PS et al (19) have shown female predominance in his studies. Hussain F et al (8) in a study has found frequency of diabetic retinopathy in newly diagnosed type II diabetes mellitus patients as 12%. In another study, Wahab S et al has shown the frequency of diabetic retinopathy in newly diagnosed type II diabetes mellitus patients as 15% (11). In a study by Khanzada MA et al the prevalence of diabetic retinopathy was found very high i.e. 40.64% (3). This high prevalence of diabetic retinopathy was also found in the study from Egypt, that reported its frequency 42.0% and a study from Oman that reported 42.4% (12,13).

There are many clinic based studies on newly diagnosed type 2 diabetic patients which have shown similar results for prevalence of retinopathy to our study i.e. Abdollahi A et al (21) reported 13.8%, Agarwal S et al (22) reported 11.7%, while Nathan (23) has reported 12.6% prevalence of retinopathy in newly diagnosed diabetics in a Diabetes Prevention Programme. Amir et al conducted a study on admitted diabetes mellitus patients in various units of Hayatabad Medical Complex, Peshawar and evaluated 202 patients for the evidence of microvascular complications due to longstanding diabetes mellitus including diabetic retinopathy (24). They reported a staggering figure of 58% incidence of diabetic retinopathy in admitted patients. Pakistan National Blindness and Visual Impairment Survey data was analyzed by Sheikh et al and found diabetic retinopathy in 15.3% subjects recruited in the survey from the general population across Pakistan (25).

CONCLUSION

High incidence of diabetic retinopathy was observed in newly diagnosed type II diabetes mellitus with male predominance. Longitudinal studies are required to observe the prevalence of this disease. We recommend that there should be public awareness and intensive periodic educational programs on national and regional levels for all newly diagnosed type 2 diabetic patients to spread awareness and education of disease, its complications, detailed ophthalmic examination at the time of diagnosis of diabetes and periodic screening to detect retinopathy early so that early therapeutic measures could be taken to prevent its further complications.

Conflicts of Interest

None.

ACKNOWLEDGEMENTS

The authors are thankful to the Medical Affairs department, Getz Pharma.

Funding Source

None.

REFERENCES

1. Vijan S. Type 2 diabetes. Ann Intl Med. 2010;152(5):31–15.
2. Ludwig J, Sanbonmatsu L, Gennetian L, Adam E, Duncan GJ, Katz LF, Kessler RC, Kling JR, Lindau ST, Whitaker RC, McDevitt TW. Neighborhoods, obesity, and diabetes--a randomized social experiment. N Engl J Med. 2011;365(16):1509-1519.



**Saleh Muhammad Channa et al.**

3. Khanzada MA, Siyal NA, Mirza SA, Memon A, El-Muttaqi A, Mirza AA. Frequency and types of diabetic maculopathy in type II diabetes. *Pak J Surg.* 2013;29(2):139-142.
4. Hectors TL, Vanparys C, van der Ven K, Martens GA, Jorens PG, Van Gaal LF, et al. Environmental pollutants and type 2 diabetes: a review of mechanisms that can disrupt beta cell function. *Diabetologia.* 2011;54(6):1273-1290.
5. Boussageon R, Bejan-Angoulvant T, Saadatian-Elahi M, Lafont S, Bergeonneau C, Kassai B, Erpeldinger S, Wright JM, Gueyffier F, Cornu C. Effect of intensive glucose lowering treatment on all cause mortality, cardiovascular death, and microvascular events in type 2 diabetes: meta-analysis of randomised controlled trials. *Bmj.* 2011;343:d4169.
6. One adult in ten will have diabetes by 2030. International Diabetes Federation. November 14, 2011. Available at <http://www.idf.org/media-events/press-releases/2011/diabetes-atlas-5th-edition>.
7. Bragge P, Gruen RL, Chau M, Forbes A, Taylor HR. Screening for Presence or Absence of Diabetic Retinopathy: A Meta-analysis. *Arch Ophthalmol.* 2011;129(4):435-444.
8. Hussain F, Arif M, Ahmad M. The prevalence of diabetic retinopathy in Faisalabad, Pakistan: a population-based study. *Turk J Med Sci.* 2011;41(4):735-742.
9. Barchetta I, Riccieri V, Vasile M. High prevalence of capillary abnormalities in patients with diabetes and association with retinopathy. *Diabet Med.* 2011;28(9):1039-1044.
10. Massin P, Lange C, Tichet J, Vol S, Erginay A, Cailleau M, et al. Hemoglobin A1c and fasting plasma glucose levels as predictors of retinopathy at 10 years: the French DESIR study. *Arch Ophthalmol.* 2011;129(2):188-195.
11. Wahab S, Mehmood N, Shaikh Z, Kazmi H. Frequency of retinopathy in adults with newly discovered and retinopathy in newly diagnosed type 2 diabetes patient. *J Pak Med Assoc.* 2008;58(10):557.
12. Santos K.G, Tschiedel B, Schneider JR, Souto KEP, Roisenberg I. Prevalence of retinopathy in Caucasian type 2 diabetic patients from the South of Brazil and relationship with clinical and metabolic factors. *Braz J Med Biol Res.* 2005;38(2):221-225.
13. Herman WH, Aubert RE, Engelgau MM. Diabetes mellitus in Egypt glycaemic control and microvascular and neuropathic complications. *Diab Med.* 1998;15(12):1045-51.
14. Causes and Risk Factors". Diabetic Retinopathy. United States National Library of Medicine. 15 September 2009.
15. Kohner EM, Aldington SJ, Stratton IM, Manley SE, Holman RR, Mathews DR. United Kingdom Prospective Diabetes Study, 30: diabetic retinopathy at diagnosis of non-insulin-dependent diabetes mellitus and associated risk factors. *Arch Ophthalmol* 1998;116(3):297–303.
16. Owens DR, Volund E, Jones D. Retinopathy in newly presenting non-insulindependent type 2 diabetic patients. *Diabetes Res Clin Pract.* 1988;9(2):59-65.
17. Klein R, Knudtson MD, Lee KE, Gangnon R, Klein BE. The Wisconsin Epidemiologic Study of Diabetic Retinopathy XXIII: the twenty-five-year incidence of macular edema in persons with type 1 diabetes. *Ophthalmology.* 2009;116(3):497-503.
18. Iqbal T. Frequency of Retinopathy in newly diagnosed type 2 diabetes mellitus. *Rawal Med J.* 2009;34(2):167-169.
19. Mahar PS, Awan MZ, Manzar N, Memon MS. Prevalence of Type-II Diabetes Mellitus and Diabetic Retinopathy: The Gaddap Study. *J Coll Physicians Surg Pak.* 2010;20(8):528-532.
20. Memon WU, Jadoon Z, Qidwai U, Naz S, Dawar S, Hasan T. Prevalence of Diabetic Retinopathy in Patients of Age Group 30 Years and Above Attending Multicentre Diabetic Clinics in Karachi. *Pak J Ophthalmol.* 2012;28(2):99-104.
21. Abdollahi A, Malekmdani MH, Mansoori MR, Bostak A, Abbaszadeh MR, Mirshahi A. Prevalence of diabetic retinopathy in patients with newly diagnosed type II diabetes mellitus. *Acta MedicalIranica.* 2006;44(6):415–419.
22. Agarwal S, Raman R, Kumari RP, Deshmukh H, Paul PG, Gnanamoorthy P. Diabetic retinopathy in type II diabetics detected by targeted screening versus newly diagnosed in general practice. *Ann Acad Med Singapore.* 2006;35(8):531–535.
23. Diabetes Prevention Program Research Group. The prevalence of retinopathy in impaired glucose tolerance and recent-onset diabetes in the Diabetes Prevention Program. *Diabetic Med.* 2007;24(2):137–144.
24. Amir AH, Rehman S, Ali SS, Jadoon MZ. Pattern of microvascular complications and associated comorbidities among Diabetic patients at a tertiary care hospital. *J Postgrad Med Inst* 2005;19(4):400-406.





Saleh Muhammad Channa et al.

25. Shaikh A, Shaikh F, Shaikh ZA, Ahmed J. Prevalence of diabetic retinopathy and influence factors among newly diagnosed diabetics in rural and urban areas of Pakistan. Data analysis from the Pakistan Blindness & Visual Impairment Survey 2003. Pak J Med Sci 2008;24(6):774-779

Table I: Characteristic of study participants

Characteristics		n	%
Gender	Male	69	61.06
	Female	44	39.94
Age (in years)	30-40	27	23.89
	41-50	56	49.56
	51-60	30	26.55
Duration of diabetes (months)	≤3 months	44	38.94
	>3 months	69	61.06
Educational status	Uneducated	15	13.27
	School	22	19.47
	College	27	23.89
	University	49	43.36
Family monthly income	<5000	23	20.35
	5000-10000	26	23.01
	>10000	64	56.64

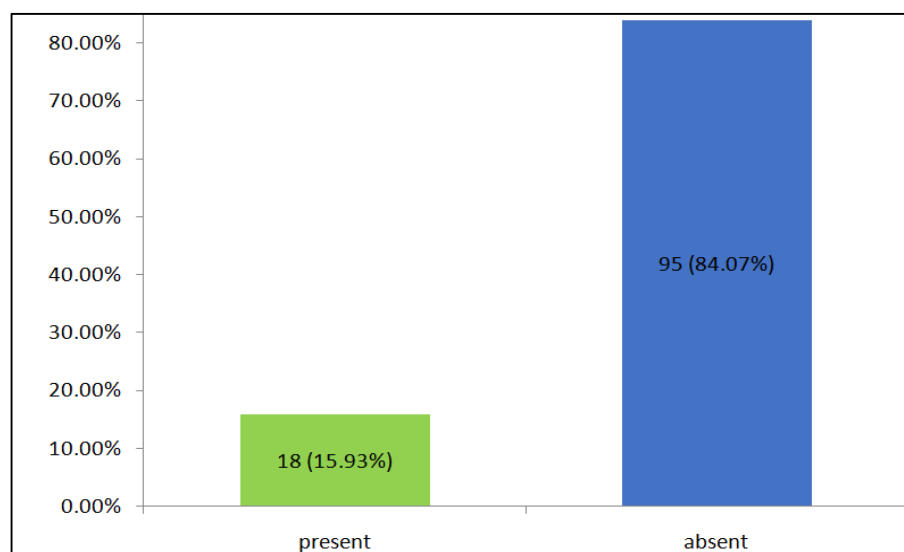


Figure 1. Incidence of diabetic retinopathy





Response of Broiler to Supplementation of Human Oral Rehydration Salt during Pre-Slaughter Fasting

Albino Namoc Taer* and E. Catipan Taer

Surigao State College of Technology, Pongtud, 8425 Alegria, Surigao del Norte, Philippines

Received: 17 Aug 2019

Revised: 20 Sep 2019

Accepted: 25 Oct 2019

*Address for Correspondence

Albino Namoc Taer

Pongtud, 8425 Alegria,

Surigao del Norte, Philippines

Email: albinotaer74@gmail.com



This is an Open Access Journal / article distributed under the terms of the **Creative Commons Attribution License** (CC BY-NC-ND 3.0) which permits unrestricted use, distribution, and reproduction in any medium, provided the original work is properly cited. All rights reserved.

ABSTRACT

Mitigation measures are means to remunerate the losses by pre-slaughter feed withdrawal practices of broiler chicken. The therapeutic effect of drinking with oral rehydration salt solution (ORSS) versus tap water (TW) during fasting (0-h versus 24-h versus 48-h) period was investigated in this trial. Data on water intake, meat quality, carcass traits and sensory of broiler chicken were subjected to a two-way ANOVA in a complete randomized design. The water intake of broiler was significantly higher before fasting while highly significantly lower after feed removal. Water with ORSS was consumed by broilers significantly higher over TW after feed withdrawal. Live weight loss was significantly higher in ORSS group while consistent significant higher live weight loss in 48-hr fasted chicken in all tested periods of fasting $P < 0.05$. Slaughter weight, hot carcass, liver weight, and gut (full, empty, and residual) were significantly affected by the fasting period while similar average values in dressing percentage. Mean values of meat pH and cooking loss were statistically significant by fasting while comparable in effect of water. Both drinking water and the fasting period did not alter the meat sensory profile. All parameters tested, drinking water did not interact ($P > 0.05$) with fasting periods except on texture and overall acceptability of meat sensory. Broilers fasted within 48 hours significantly lost live weight while pH and cooking loss responded positively and moderate acceptability on sensory of meat. ORS therapy significantly induced water intake but negatively affect live weights.

Keywords: Feed Withdrawal, Oral rehydration, Water Intake, Carcass Characteristics, and Meat Quality.

INTRODUCTION

Commercial broilers are exposed to several stressors before slaughter, including feed deprivation, crowding density, and transportation (Delezie, Swennen, Buyse, & Decuyper, 2007). Feed consumed by broilers is only of economic value if it is converted to saleable pounds of meat (Smidt, Formica, & Fritz, 1964). Since the early days of commercial

17796



**Albino Namoc Taer and E. Catipan Taer**

poultry production, preparing broilers for processing included a time of feed withdrawal from the birds so that all of the feed consumed before processing was converted to edible tissue. However, the no tolerance for ingesta or fecal contamination policy from FSIS, (1996) increased the importance of proper FW periods before slaughter. Although the concern for converting feed to muscle was still important, preventing ingesta or fecal contamination of broiler carcasses was a significant concern and required a longer FW period than for just converting feed to edible tissue.

Usually, before slaughtering of birds, while they are still on the poultry cages, their feed is removed and they undergo fasting that aims to minimize the contents of gastrointestinal tracts, and subsequent contamination of the carcasses by fecal matter during transport and evisceration (Contreras-Castillo *et al.*, 2007). But, concern about body weight losses reducing the economic value of the carcass is the main reason why feed fasting was not practiced by many poultry raisers. The effect of an extended FW time was recognized as having a negative effect on BW and carcass yield. May and Brunson, (1955) were the first to report a significant reduction in eviscerated carcass yield in both males and females after a feed withdrawal period of 24 hours but little effect on yield with shorter FW periods. An effective feed withdrawal program should provide adequate clearance of the digestive tract while controlling shrink and yield losses (Smidt, *et al.*, 1964; Veerkamp, 1978; Lyon, *et al.*, 1991; Papa, 1991; Moran Jr and Bilgili, 1995). A mitigation action may be effective to lessen the adverse effect of pre-slaughter feed deprivation.

Oral Rehydration Salt solution was found to help correct the acidosis in children with acute diarrhea (Ghishan, 1990), these formulations included glucose more as a source of nutrition than as the major driving force for fluid absorption. The key to the success of ORT is that it replaces the fluid being lost, circumventing the need for intravenous replacement in 80 to 90% of the cases of mild-moderate diarrhea and is lifesaving in acute diarrheal diseases (Rao, 2004). Some of the symptoms seen in humans experiencing gastrointestinal disturbance are similar to those experienced by broilers deprived of feed and heat stress, normally water and electrolyte loss (Sayed and Downing, 2011). However, basic information about the influence of ORS treatment on the performance of broiler undergoing pre-slaughter fasting is poorly documented. Consequently, this trial was initiated to determine the alleviatory factor of ORS during pre-slaughter feed withdrawal on the live weight losses, meat and carcass traits, and sensory characteristics of broiler chicken.

MATERIALS AND METHODS

Subject animal

A total of ninety (90) heads of 28-30 days old marketable sized broiler of almost similar body weight were acquired from a backyard farm. The birds were randomly selected and divided into two groups (group 1: ORSS; group 2: Tap water). In every group, the birds were further divided into three sub-groups (sub-group 1: 0-h fasting; sub-group 2: 24-h fasting; sub-group 3: 48-h fasting) replicated three times having five birds each and started the six-day trial conducted at Surigao State College of Technology-Mainit Campus (SSCT-Mainit) Poultry House.

Treatment

The human ORS (Hydrite by Amherst Lab. Inc.) was dissolved in water at a ratio of one pack (4.1 g) per 300 ml water. The solution contains 5.00 mmol Sodium, 1.33 mmol Potassium, 4.33 mmol Chloride, 0.76 Citrate, and 5.00 mmol Glucose per liter of water which was given to the ORSS treatment group starting in three days before fasting. Feeds were removed totally during fasting while drinking water (ORSS and TW) remained until slaughter time. Water in a plastic container was securely tied via a plastic cord attached to every cage wall.



**Albino Namoc Taer and E. Catipan Taer****Slaughtering and processing**

To make the slaughtering simultaneous, the birds under 48-h fasting from each group were treated with ORSS on day-1 and fasted on day-4, followed by 24-h fasting treated on day 2 fasted on day-5, while 0-h fasting treated on day-3 until day-6. All birds were simultaneously slaughtered and processed for analysis on day-6. Before slaughtering, the birds were assessed for the final weight at slaughter. Two chickens close to average per cage were slaughtered simultaneously. The head was dislocated, eviscerated, and evaluated the warm carcass weight and intestinal tract before they were transported to SSCT-Mainit Campus Food Laboratory and chilled for two hours at 0.5 °C before the preparation of meat samples for analysis.

The following parameters were calculated using the formula:

Water intake = Water offered – Water remained

Live weight loss = Pre-fasting weight – Post-fasting weight

% live weight loss = Pre-fasting weight/Post-Fasting weight x 100

Dressing percentage = hot carcass weight/Post-withdrawal weight x 100

Residual gut fill = Digestive tract full – Digestive tract full empty

Determination of pH and cooking loss of meat

The pH of meat from broiler chicken breast in each sample was measured in duplicate by a Digital pH Meter (PH-108). Beforehand, the pH-meter was calibrated using standardized buffers of pH 4.0, 6.9 as mentioned by (Siekman et al., 1985). Approximately 10 g of ground meat was mixed with 100 ml distilled water and blended for 30 seconds at a high speed. The pH meter electrode was immediately inserted after the blended sample was poured into a clear glass. Cooking loss percentage determination was done by oven-cooking of meat samples. The 10 g meat was subjected to a maximum oven temperature of 150 °C for one (1) hour and was let to cool for 30 minutes until the temperature normalizes. The weight of raw and cooked samples was recorded. The following equations were used to determine the percentage cooking loss:

Cooking loss % = Weight of raw meat – Weight of cooked meat / Weight of raw meat x 100

Sensory testing

Meat sensory attributes viz. odor/aroma, appearance, texture, taste, juiciness, and overall acceptability were scored by panel evaluators (untrained) using the five-point hedonic scale. Approximately 10 g of meat samples were steamed for 30 minutes (no seasoning and spices). Each sample was coded and randomized according to Kwanchai & Arturo, (1984) methods and placed in disposable plastic cups ready for evaluation by 10 panelists composed of faculty, staff, and students of SSCT-Mainit Campus done in the college food laboratory. Before testing, the panel evaluators have oriented and provided score sheets for the basis of scoring using the five-point scale namely: 5- extremely acceptable, 4- moderately acceptable, 3- acceptable, 2- moderately unacceptable, and 1- unacceptable. The panelists cleansed the palate by drinking water after every sample.

Statistical analysis

Data gathered was subjected to statistical analyses using two-way ANOVA in CRD using SPSS version 20 to determine the statistical difference of main effects and interactions between drinking water and fasting periods on the water intake, meat quality, carcass traits, and sensory attributes of broiler chicken. To determine homogeneity, Tukey HSD was used at a 5% level of significance.



**Albino Namoc Taer and E. Catipan Taer****RESULTS****Water intake**

Effects of drinking water (ORSS vs. TW) and fasting periods (0, 24, and 48 hours) on water intake of broiler chickens before and after feed withdrawal are presented in (Table 1). Neither before nor after feed withdrawal, the water intake of broiler was significantly affected by fasting but not significantly different by the main effect of drinking water and interaction of drinking water*fasting periods ($P > 0.05$). In the study, the water intake of the chickens was measured from the amount of water given less the water remained daily. Based on the results, the daily water intake increment before fasting were all highest in 0-h fasted followed by 24-h fasted while lowest total water consumption in 48-h fasted chickens in three days before feed withdrawal (Table 2). The average value differences among 0-h, 24-h, and 48-h fasting were all significant to each other. Meanwhile, water intake by broiler after feed removal was significantly lesser than water intake before fasting. The 48-h fasted chickens consumed significantly higher total values over the 24-hour fasting chickens during fasting regime. No water consumption was noted in 0-h fasted chickens.

Live weight loss

Total weight losses during fasting are presented in (Table 3). The total live weight loss and % total live weight loss significantly higher in 48-h fasted over the 24-h fast. No live weight losses observed in 0-h fasting chickens. While data on drinking water treatments showed significantly higher total live weight loss and % total live weight loss in ORSS treated over the TW group.

Carcass characteristics

The mean summary of the effects of ORSS and TW during feed withdrawal on carcass characteristics of broiler chicken is shown in (Table 4). All of the parameters of carcass characteristics except dressing percentage were significantly influenced the fasting period while ORSS treatments failed to show statistical differences on carcass parameters. No hour fasting*drinking water interactions were noted. Slaughter weight is the final weight of birds after feed fasting, showed the highest final weight on the non-fasted chickens compared to the lowest 48-h fasted. The mean value of 24-h fasting did not significantly differ to either 0-h or 48-h fasted chicken groups. The resulting significant different values of warm carcasses, as well as the weight of birds at slaughter data, were homogenous in the pattern. The percentage of the live animal weight that becomes the carcass weight at slaughter as dressing percentage of broiler in drinking water and period of fasting with Drinking water vs. fasting period interaction showed no differences ($P > 0.05$). The liver was separately weighted after the evisceration. The heaviest liver was observed in 0-h fasted chickens while in the 0-h fasted chickens, the liver weight did not vary from the other two groups. The group which had the lowest liver weight was observed in the 48-h fasted chickens. Alimentary tract or digestive tract of broiler chicken, the 0-h fasting were all highest among digestive tracts (full, empty, and residual gut fill) parameters and 48-h fasted chickens were lowest in the foregoing. The digestive tracts (full) of 24-h fasted was statistically different to both 0-h and 48-h fasted, while the digestive tract (empty) was comparable to 0-h and significant to 48-h fasted chickens. Moreover, the residual gut fill of 24-h fasted chickens was statistically significant to 0-hr but comparable to 48-h fasted chickens.

Meat quality

As shown in Table 4, an analysis of the pH of broiler chicken breast meat means revealed no statistical difference between the means for ORSS and tap water groups. The pH means of the fasting periods were significantly different ($P < 0.05$) with the mean for 48-h being the highest and the mean for 0-h has the lowest while the mean of 24-hr fasting is intermediate and not significant to either 48-hr or 0-hr fasted chickens. The data of cooked meat and cooking loss of



**Albino Namoc Taer and E. Catipan Taer**

broiler chicken meat are likewise shown in Table 4. The weight of cooked meat and percent cooking loss have significant ($P < 0.05$) effects found for the main effect of fasting. But the main effect of drinking water falls short of statistical significance, and Drinking water x Hour fasting interaction, ($P > 0.05$) on the weight of cooked meat and % cooking loss. Meanwhile, the two parameters were exactly contrasting in the mean values pattern. As shown in Table 4, the weight of cooked meat is significantly highest in 48-h fasted followed by 24-h fasted and the lowest is 0-h fasted compared to the percentage cooking loss, the highest is in 0-hr fasted followed by 24-h fasted while the lowest is 48-h fasted.

Sensory of meat

The summary of different organoleptic characteristics as affected by the drinking water treatment fasting period is shown in Table 5. All attributes viz. odor/aroma, appearance, texture, taste, juiciness, and overall acceptability have no significant differences by the main effects of drinking water and feed withdrawal period ($P > 0.05$), but drinking water interacts to the meat texture and overall acceptability in levels of hour fasting ($P < 0.05$).

DISCUSSION

Consumption of water by broiler was significantly different before and after feed fasting. The intake of water was significantly higher before the feed was removed when compared to the intake of water during fasting Table 1. The result manifested that feed deprivation declines water consumption activity. Drinking water activity and feed intake are positively correlated, such that if the feed is not available will surely affect water intake. The demand for water is dependent on the amount of dry matter taken. In previous literature, the ratio of water consumption and dry-matter intake (DMI) is relatively constant at approximately 2:3 for turkey Degen, Kam, Rosenstrauch, & Plavnik, (1991). Fairchild and Ritz, (2009) reported, the recent water consumption for chicken normally ranges from 1.6 to 2.0 times that of feed intake. In the study, significant higher water intake before feed fasting was consistent with 0-h fasted chickens from day 1-3, followed by 24-h fasted while the 48-h fasted chickens were lowest Table 2. The significant differences in water consumption before fasting among the group fasted may be explained by the disparity of chicken sizes. The 48-h fasted were slightly smaller in sizes since they were treated and fasted ahead from the other two groups. This confirms that the amount of water intake is relatively proportional to the size of the animal wherein the larger the size of an animal the higher is the demand for dry matter intake.

Similarly, the water intake behavior in the drinking water group of chickens was higher before feed withdrawal while lower at fasting. The ORS group received more water over tap water (2051.83 vs. 1837.89) respectively before fasting, but the value differences were not significant. (Borges et al., 2000) observed an increased intake of water in broilers chicken supplemented with 1.0 percent KCl from day 21 onwards. However, the effect of ORSS on water intake after feed removal was limited but the total value of the averages showed higher in ORS treated over the pure tap water (971.61 vs. 807.38). It is established that supplementation of drinking water or in diet form with electrolytes improved the intake of water in birds reared in heat stress surroundings (Ahmad et al., 2008; Fairchild and Ritz, 2009). Live weight loss refers to the weight shrinkage by broilers during feed withdrawal. A significant higher live weight loss and % live weight loss was noticed in 48-h fasting chickens when compared to 24-h fasting while 0-h or unfasted chicken groups recorded no weight loss. A clear evidence that the longer the animal has withdrawn from feeds the more weight loss is observed due to excretion of fecal matter in digestive tract (Wabeck, 1972; Veerkemp, 1886) and because of the removal of water from the body due to the metabolic process of body tissues for energy maintenance (Salmon, 1979). Broilers' weight loss after the first 6 hours fasting is largely due to the decrease in the content of the digestive tract (Veerkemp, 1986).

Beyond 6 hours of fasting, moisture and nutrients are drawn from reserved nutrients and body tissues. For our study, it showed 108.33 g live weight loss with 8.18 % live weight loss on the first 24 hours versus 65.00 g live weight



**Albino Namoc Taer and E. Catipan Taer**

and 5.40 % live weight loss respectively after 48 hours of feed deprivation (Table 3). The electrolyte component of human ORS in water during pre-slaughter fasting failed to regulate the negative effects on the live weights of broiler chickens. Rahi, Afrin, Howlider, & Ali, (2015) KCl in drinking water during hot and humid summer had no effect ($P>0.05$) on growth and meat quality characteristics of broilers except feed conversion ($P<0.05$) at different target weights; however, other studies have shown drinking water supplemented with 0.6% potassium reduced panting-phase blood pH to 7.31 and significantly increased live weight gain by 14.5 ($P<0.05$) and 7.9% ($P<0.05$) at 28 and 42 days of age (Ahmad *et al.*, 2008). Our findings showed higher total live weight loss and % total live weight loss in ORSS group compared to tap water, however, comparing their average value differences it showed no significant. This discrepancy in the results can be explained by different types of stressed imposed on chicken between the studies. Pre-slaughter feed withdrawal stress induces rapid potassium and sodium excretion along with the emptying of digestive tract contents. The potassium excretion is rapid during the early part of fasting and then tapers off to a constant level of about 10 to 15 mEq/day. Similarly, excretion of sodium is also triggered early in feed withdrawal, continuously decline to between 1 and 15 mEq/day, losses that remain even through extended withholding caloric intake (Weinsier, 1971).

Higher carcass weight was noted on 0-hr fasting compared to 24-h fasted and 48-h fasted chickens which were anticipated due to apparent higher slaughter weight because 0-hr chickens were not fasted (Table 4). However, dressing percentage as the relationship between the carcass weight and its live weight before slaughter was not affected by fasting periods. The recent findings supported the study of Saffle & Cole (1960) that dressing percentage was not significantly affected by fasting when using off-feed weights. In the first 24 h of fasting, the pig can losses up to 5% of its live weight, at an approximate rate of 0.2% per hour, or 0.25 kg/h, resulting in a live weight loss of approximately 5 kg after 24 h of fasting (Faucitano, Chevillon, & Ellis, 2010). However, the live weight losses are more linked to the defecation of urine and feces rather than to body tissues and consequently carcass weight is not affected (Beattie, Burrows, Moss, & Weatherup, 2002). While the not significant effect of drinking water with electrolyte in this trial was probably following the earlier findings of Rahi, Afrin, Howlider, & Ali, (2015) KCl in water during hot and humid summer was not significant ($P>0.05$) on growth and characteristics of meat yield broilers excluding feed conversion ($P<0.05$) at different target weights. Similarly, (Souza *et al.*, 2002) did not mention any effect of potassium chloride supplementation on carcass response or abdominal fat. Our case, though comparable in between water groups, it was observed the ORSS treated chickens had slightly lower dressing percentage than tap water which can be explained by rapid excretion of sodium and potassium during fasting before it was absorbed in the muscle tissues that will form part of the carcass.

The liver may almost be depleted of glycogen if they have fasted for more than 24 hours or longer. A remarkable lowest liver weight values in 48-hours fasted in this trial probably due to the relatively smaller sizes of the liver in proportion to their body weight plus the massive glycogen depletion by feed withdrawal and post-partum glycolytic activities. The decline in liver weight is mainly attributed to a loss of water and glycogen (Jones, Rompala, & Haworth, 1985); the weight of liver, glycogen reserve, and concentration of circulating glucose significantly reduced after long feed fasting (Warriss, *et al.*, 1993). The electrolyte component of ORS did not counter the effect of fasting on liver weight shrinks in this trial. This report upheld the claims of Koreleski, Świątkiewicz, & Arczewska, (2010) that levels of K and Na not significant on breast meat yield, abdominal fat content in the carcass quality and relative weights of liver and heart. The result showed the ORSS treated chicken group had a slightly higher weight of the liver over the tap water group (Table 4).

Remarkable highest digestive tracts (full) was observed from non-fasted chickens while lower in the fasted group because of the presence of fecal matter and undigested food. Castroverde, Olarve, & Cruzana, (2010) observed that higher weight of intestinal tract and residual gut fill were found in chicken with zero fasting hour compared to fasted broilers due to gastrointestinal content that is still intact since they have not fasted. ORSS supplementation in drinking water before and after fasting together with interactions showed no significant effect on digestive tracts (full, empty, and residual gut fill). Earlier reports emphasized that glucose and Na salts in ORT solutions might have



**Albino Namoc Taer and E. Catipan Taer**

increase water absorption in the intestine, and therefore enhanced water retention consequently affects gut-weight. Recent studies showed that water absorption in the gut is related to solute uptake and that glucose remarkably enhances both salt and water absorption (Gagnon, Bissonnette, Deslandes, Wallendorff, & Lapointe, 2004). The contrasting results of the study can be explained by the rapid excretion of fluids along with the emptying of the digestive tract during fasting. The rate and levels of pH reduction are the main determining factors of meat quality Van Laack, (2000). Table 4 shows a higher pH of meat is detected in 48-hr fasted followed by 24-hr and 0-hr fasting chickens. Ngoka & Froning, (1982) indicated that feed withdrawal has a significantly altered meat final pH, water retention capacity, live weight and moisture content of turkey breast muscle when compared to the fed group. After slaughter, when the muscle is transformed into the meat, anaerobic glycolysis results in a pH decline. Our study found a significant pH decline in non-fasted chicken resulted from high glycogen levels at slaughter because they are unfasted. If the glycogen reserves are depleted before slaughter, the ultimate pH does not fall to 5.3-5.6. It remains high at 6.8, (Greaser, 1986). Fasting or inadequate feeding in the period of pre-slaughter lowers glycogen reserves. Ultimate pH is determined largely by levels of muscle glycogen at death. They stressed that the formation of lactate declines pH (Greaser, 1986).

Cooking loss and pH of meat values are positively correlated. As the pH decreased, the quality of the final produce increased because the cooking losses were less (Contreras-Castillo, 2007). Moreover, loss of weight during cooking of meat is a result of water and fat loss. After heating the muscle fiber protoplasm coalesces which results in contraction of fiber and muscle cell (Price, 1971). In comparison to our findings, the higher percentage of cooking loss was in 0-hr fasted chicken because they had lots of water and fats since they have not fasted. Furthermore, pre-harvest fasting for 24-hr would result in cooking yield increase of 1.6% compared to 18-hr, which confirms the correlation ($r=0.7$ to 0.8) between ultimate meat pH and technological yield of cooked hams (Monin, 1988). A higher ultimate pH (pHu) is related to a darker color, reduced drip loss (higher WHC and WBC) and tougher meat (Warner, 1994; Pearson & Young, 1989). Pale breast meat of broiler has a lower water-holding capacity, causing in 8-10% reduction in cooking yields (van Laack *et al.*, 2000). Pale colored meat and low WHC correlate with a lower in ultimate pH. Ultimate pH of pale broiler breast meat approximately 5.70 versus 5.96 in normal-colored breast meat (van Laack, 2000). Apple, Unruh, Minton, & Bartlett, (1993) observed the administration of electrolytes did not affect lamb carcass quality. Contrary to (Babji, Froning, & Ngoka, 1982) under the conditions of this study, pre-slaughter administering of electrolytes did not prevent changes in muscle characteristics after exposure to pre-slaughter stress. Holding birds at a maximum temperature (38 C) before slaughter produced meat with a lower water holding capacity, pH, cooking yield, and a higher shear value. In our case, the pH of meat from ORSS treated chickens gained slightly higher pH and lower in cooking loss values over the plain water groups, however, differences in values between ORSS and tap water was not statistically significant ($P > 0.05$).

The sensory attributes like odor/aroma, appearance, texture, taste, juiciness, and overall acceptability of steamed broiler meat samples were rated by consumer and untrained sensory panel using the 5-point hedonic scale. Husson & Pagès, (2003), the analyses of variance show that the two types of juries (trained and untrained) give similar sensory profiles and the few differences are mainly due to different ways of using the scale. Comparing the differences among the averages of the scores of different attributes it shows no significant effects by all levels of hour fasting (Table 5) having scores ranging from 3.53 to 4.33. However, the 0-h fasted has found highest in odor, appearance, and overall acceptability, while lowest in texture, taste, and juiciness equivalent to Contreras-Castillo, (2007) no differences in juiciness for the different FW periods, so this attribute did not interfere with the tenderness scores. Lyon, Smith, Lyon, & Savage, (2004), noticed that fasting did not alter the flavor attribute; nonetheless, meat from birds at 0 h fasting was darker and redder. The flavor was not tested in the entire study but it was observed darker and redder in appearance in 0-h fasting. Smith, Lyon, & Lyon, (2002) found that feed withdrawal produced lighter and less red broiler breast meat. Further, fillets from 8-h FWD birds had significantly higher L^* values (lighter) whether cooked or uncooked and continued the trend of lighter fillets resulting from feed withdrawal stress.

The meat texture, taste, and juiciness of 48-h fasted chickens are of a similar trend wherein the better texture the samples are, the juicier and tastier they become. Diet and fasting significantly altered sensory texture (Lyon, Smith,



**Albino Namoc Taer and E. Catipan Taer**

Lyon, & Savage, (2004). Having scores average ranging from 3.53 to 4.02, the presence of ORS did not manifest significant effects on all sensory attributes of broiler chicken meat over the tap water group in conformity with the findings of Schaefer, Murray, Tong, Jones, & Sather, (1993), both oral potassium and intramuscular magnesium aggravated subjective pork structure and texture scores but was found to improve muscle brightness and hue (higher b^* value). The result reflected that ORSS treatment was brighter in color as it was scored higher values on appearance (3.80) over TW (3.75) Table 5. Testing on the interactions of these factors, the different levels of hour fasting versus drinking water showed significant interactions in terms of texture and overall acceptability. This then implies that the effect of levels hour fasting on texture and overall acceptability of steamed broiler meat is dependent on treatment in drinking water and vice versa. Figures 1 and 2 show the graphs of these interactions respectively. It can be argued that the comparability of all sensory profile scores may be attributed to the failure of untrained testers to use the scale correctly. Further study should be made on sensory of meat to be done by a trained panelist probably using the 9-point hedonic scale to clearly distinguish differences between sensations.

Overall findings in this proceedings disclosed that the ORSS treatment in pre-slaughter fasting did not alleviate or inhibit the adverse effect of feed withdrawal which aligned to the conclusions of Schaefer, Murray, Tong, Jones, & Sather, (1993), that oral potassium and intramuscular magnesium, as provided in the present study, had no advantageous impacts on pork quality but that the beneficial effects of Magnesium Aspartate on meat color and drip loss may warrant further investigation. In conclusion, the treatment of human Oral Rehydration Salt in during pre-slaughter fasting were all comparable to the effect of tap water except in water intake after feed fasting therefore not recommended. The study found the optimum feed withdrawal period of broiler whether in ORS or tap water before the slaughter could go as far as 48 hours with beneficial effects to the consumers but of monetary loss to poultry growers. Fasting within 24 hours or longer, the bird loses more live weight, liver, and empty gut-weight which are economically unfavorable to broiler raisers. Parameters on cooking loss and meat pH revealed that as the number of hours fasting increases, meat pH normalizes and cooking loss decreases which is an indicator of good quality meat sought after by broiler meat buyers. The comparable results of sensory and consumer's acceptability from acceptable to moderately acceptable levels of meat from broiler revealed that the odor, appearance, texture, taste, juiciness and overall acceptability from zero to 48 hours fasting in drinking water with ORS remain stable and acceptable to the consumers.

ACKNOWLEDGEMENTS

This work was supported by Surigao State College of Technology research division headed by DR. GIDEON A. EBARSABAL and the college president DR. GREGORIO Z. GAMBOA JR. This paper was written as part of the college program to enhance faculties on paper publications with mentors Professors Virgilio B. Ratunil Jr., Emanuel Masuhay, Mr. Ludy G. Alsong and Armand M. Bermon.

REFERENCES

1. Delezie, E., Swennen, Q., Buyse, J., & Decuyper, E. (2007). The effect of feed withdrawal and crating density in transit on metabolism and meat quality of broilers at slaughter weight. *Poultry Science*, 86(7), 1414-1423.
2. Smidt, M. J., Formica, S. D., & Fritz, J. C. (1964). Effect of fasting prior to slaughter on yield of broilers. *Poultry Science*, 43(4), 931-934.
3. FSIS, U. (1996). Pathogen reduction: hazard analysis and critical control point (HACCP) systems; final rule. *Federal Register*, 61, 38806-38989.
4. Contreras-Castillo, C., Pinto, A. A., Souza, G. L., Beraquet, N. J., Aguiar, A. P., Cipolli, K. M. V. A. B., & Ortega, E. M. (2007). Effects of feed withdrawal periods on carcass yield and breast meat quality of chickens reared using an alternative system. *Journal of Applied Poultry Research*, 16(4), 613-622.




Albino Namoc Taer and E. Catipan Taer

5. May, K. N., & Brunson, C. C. (1955, January). Effect of length of starvation period on eviscerated yield of broilers. In *Poultry Science* (Vol. 34, No. 5, pp. 1210-1210). 1111 NORTH DUNLAP AVE, SAVOY, IL 61874: POULTRY SCIENCE ASSOC INC.
6. Veerkamp, C. H. (1978). The influence of fasting and transport on yields of broilers. *Poult. Sci.*, 57(3), 634-638.
7. Lyon, C. E., Papa, C. M., & Wilson Jr, R. L. (1991). Effect of feed withdrawal on yields, muscle pH, and texture of broiler breast meat. *Poultry Science*, 70(4), 1020-1025.
8. Papa, C.M., 1991. Lower gut contents of broiler chickens withdrawn from feed and held in cages. *Poultry Sci.* 70:375-380.
9. Moran Jr, E. T., & Bilgili, S. F. (1995). Influence of broiler livehaul on carcass quality and further-processing yields. *Journal of Applied Poultry Research*, 4(1), 13-22.
10. Rao, M. C. (2004). Oral rehydration therapy: new explanations for an old remedy. *Annu. Rev. Physiol.*, 66, 385-417.
11. Sayed, M. A. M., & Downing, J. (2011). The effects of water replacement by oral rehydration fluids with or without betaine supplementation on performance, acid-base balance, and water retention of heat-stressed broiler chickens. *Poultry science*, 90(1), 157-167.
12. Siekmann, L. (1985). Determination of creatinine in human serum by isotope dilution-mass spectrometry. *Definitive methods in clinical chemistry, IV. Clinical Chemistry and Laboratory Medicine*, 23(3), 137-144.
13. Kwanchai, A. G., & Arturo, A. G. (1984). *Statistical procedures for agricultural research*. John Wiley et Sons: New York.
14. Degen, A. A., Kam, M., Rosenstrauch, A., & Plavnik, I. (1991). Growth rate, total body water volume, dry-matter intake and water consumption of domesticated ostriches (*Struthio camelus*). *Animal Science*, 52(1), 225-232.
15. Fairchild, B. D., & Ritz, C. W. (2009). *Poultry drinking water primer*.
16. Borges, S. A., Ariki, J., de Moraes, V. M. B., Pedroso, A. A., Salvador, D., & Martins, C. L. (2000). Potassium chloride supplementation in broilers diets during summer. *Ars Veterinaria*, 16(1), 64-70.
17. Ahmad, T., Khalid, T., Mushtaq, T., Mirza, M. A., Nadeem, A., Babar, M. E., & Ahmad, G. (2008). Effect of potassium chloride supplementation in drinking water on broiler performance under heat stress conditions. *Poultry science*, 87(7), 1276-1280.
18. Wabeck, C. J. (1972). Feed and water withdrawal time relationship to processing yield and potential fecal contamination of broilers. *Poultry Science*, 51(4), 1119-1121
19. Salmon, R. E. (1979). Effect of food and water deprivation on live-weight shrinkage, eviscerated carcass yield and water absorption during chilling of Turkey carcasses. *British Poultry Science*, 20(3), 303-306.
20. Greaser, M. L. (1986). Conversion of muscle to meat. *Muscle as food*, 37-102.
21. Rahi, R. A., Afrin, S., Howlader, M. A. R., & Ali, M. S. (2015). Response of broiler to supplementation of potassium chloride during summer. *Asian Journal of Medical and Biological Research*, 1(1), 103-108.
22. Weinsier, R. L. (1971). Fasting—a review with emphasis on the electrolytes. *The American journal of medicine*, 50(2), 233-240.
23. Saffle, R. L., & Cole, J. W. (1960). Fasting effects on dressed yields, shrinkage, and pH of contractile tissue in swine. *Journal of Animal Science*, 19(1), 242-248.
24. Faucitano, L., Chevillon, P., & Ellis, M. (2010). Effects of feed withdrawal prior to slaughter and nutrition on stomach weight, and carcass and meat quality in pigs. *Livestock Science*, 127(2-3), 110-114.
25. Beattie, V. E., Burrows, M. S., Moss, B. W., & Weatherup, R. N. (2002). The effect of food deprivation prior to slaughter on performance, behaviour and meat quality. *Meat science*, 62(4), 413-418.
26. Souza, B. B., Bertechini, A. G., Teixeira, A. S., Lima, J. A. F., Pereira, S. L., & Fassani, E. J. (2002). The effects of potassium and ammonium chlorides on the performance and deposition of abdominal fat in carcass of broilers diets raised in summer. *Brazilian Journal of Poultry Science*, 4(3), 209-218
27. Jones, S. D. M., Rompala, R. E., & Haworth, C. R. (1985). Effects of fasting and water restriction on carcass shrink and pork quality. *Canadian Journal of Animal Science*, 65(3), 613-618.




Albino Namoc Taer and E. Catipan Taer

28. Warriss, P. D., Kestin, S. C., Brown, S. N., Knowles, T. G., Wilkins, L. J., Edwards, J. E., ... & Nicol, C. J. (1993). The depletion of glycogen stores and indices of dehydration in transported broilers. *British Veterinary Journal*, 149(4), 391-398.
29. Koreleski, J., Świątkiewicz, S., & Arczewska, A. (2010). The effect of dietary potassium and sodium on performance, carcass traits, and nitrogen balance and excreta moisture in broiler chicken. *Journal of Animal and Feed Sciences*, 19(2), 244-256.
30. Castroverde, K. B. V., Olarve, J. P., & Cruzana, B. C. (2010). Effects of feed withdrawal prior to slaughter on broiler's carcass characteristics and meat quality. *Philippine Journal of Veterinary Medicine*, 47(2), 98-102.
31. Gagnon, M. P., Bissonnette, P., Deslandes, L. M., Wallendorff, B., & Lapointe, J. Y. (2004). Glucose accumulation can account for the initial water flux triggered by Na⁺/glucose cotransport. *Biophysical journal*, 86(1), 125-133.
32. Van Laack, R. L. J. M. (2000). Determinants of ultimate pH of meat and poultry. In 53 rd Annual Reciprocal Meat Conference (pp. 74-75).
33. Ngoka, D. A., & Froning, G. W. (1982). Effect of free struggle and pre-slaughter excitement on color of turkey breast muscles. *Poultry Science*, 61(11), 2291-2293.
34. Price, J. (1971). *The science of meat and meat products*. American Meat Institute Foundation.
35. Monin, G. (1988). Post-mortem evolution of muscle tissue and consequences on the quality of pork.
36. Warner, R. D. (1994). Physical properties of porcine musculature in relation to postmortem biochemical changes in muscle proteins. University of Wisconsin--Madison.
37. Pearson, A. M., & Young, R. B. (1989). Proteins of the thick filament. *Muscle and meat biochemistry*, 66-97
38. Apple, J. K., Minton, J. E., Parsons, K. M., & Unruh, J. A. (1993). Influence of repeated restraint and isolation stress and electrolyte administration on pituitary-adrenal secretions, electrolytes, and other blood constituents of sheep. *Journal of animal science*, 71(1), 71-77.
39. Babji, A. S., Froning, G. W., & Ngoka, D. A. (1982). The effect of preslaughter environmental temperature in the presence of electrolyte treatment on turkey meat quality. *Poultry science*, 61(12), 2385-2389.
40. Husson, F., & Pagès, J. (2003). Comparison of sensory profiles done by trained and untrained juries: methodology and results. *Journal of Sensory Studies*, 18(6), 453-464.
41. Lyon, B. G., Smith, D. P., Lyon, C. E., & Savage, E. M. (2004). Effects of diet and feed withdrawal on the sensory descriptive and instrumental profiles of broiler breast fillets. *Poultry science*, 83(2), 275-281.
42. Smith, D. P., Lyon, C. E., & Lyon, B. G. (2002). The effect of age, dietary carbohydrate source, and feed withdrawal on broiler breast fillet color. *Poultry Science*, 81(10), 1584-1588.
43. Schaefer, A. L., Murray, A. C., Tong, A. K. W., Jones, S. D. M., & Sather, A. P. (1993). The effect of ante mortem electrolyte therapy on animal physiology and meat quality in pigs segregating at the halothane gene. *Canadian Journal of Animal Science*, 73(2), 231-240.

Table 1. Total water intake before and after fasting

Treatment	Water Intake ^a	Water Intake ^b
Drinking water		
ORS	2051.83 ^{ns}	971.61 ^b
TW	1837.89 ^{ns}	807.38 ^a
Hour fasting		
0 hour	2450.25 ^b	0.00 ^a
24 Hours	1880.00 ^a	1676.16 ^c
48 Hours	1504.33 ^a	992.33 ^b

Legend: ^aWater intake before feed withdrawal, ^bWater intake after feed withdrawal

Values within the same column with the same superscript are not significantly different ($P > 0.05$)

^{ns} Not significant





Albino Namoc Taer and E. Catipan Taer

Table 2. Daily water intake increment over 3 days before fasting and 48 hours after fasting

Treatment	Intake of Water				
	Daily Increment BFW			Daily reduction AFW	
	Day 1	Day 2	Day 3	24 -hr	48 - hr
Drinking water					
ORS	540.78 ^{ns}	732.94 ^{ns}	778.11 ^{ns}	209.00 ^{ns}	41.44 ^{ns}
TW	481.83 ^{ns}	636.27 ^{ns}	719.78 ^{ns}	196.11 ^{ns}	30.67 ^{ns}
Hour fasting					
0 hour	703.08 ^b	899.00 ^b	848.17 ^b	0.00 ^a	0.00 ^a
24 Hours	439.16 ^a	659.83 ^a	781.00 ^b	203.83 ^b	0.00 ^a
48 Hours	391.66 ^a	495.00 ^a	617.67 ^a	403.83 ^c	108.17 ^b

Values within the same column with the same superscript are not significantly different

^{ns} Not significant

Table 3. Live weight loss of broiler chicken

Treatment	Initial BW	Weight loss (g)		Weight loss (%)		Final weight
		24-hr	48-hr	24-hr	48-hr	
Drinking water						
ORS	1380.55 ^{ns}	77.77 ^{ns}	23.88 ^b	5.71 ^b	1.92 ^{ns}	1278.88 ^{ns}
Tap water	1378.33 ^{ns}	63.33 ^{ns}	19.44 ^a	4.78 ^a	1.67 ^{ns}	1295.55 ^{ns}
Hour fasting						
0 hour	1455.00 ^{ns}	0.00 ^a	0.00 ^a	0.00 ^a	0.00 ^a	1455.00 ^b
24 Hours	1369.16 ^{ns}	103.33 ^b	0.00 ^a	7.56 ^b	0.00 ^a	1265.83 ^b
48 Hours	1314.16 ^{ns}	108.33 ^b	65.00 ^b	8.18 ^b	5.40 ^b	1140.83 ^a

Values within the same column with the same superscript are not significantly different

^{ns} Not significant

Table 4. Meat quality and carcass characteristics of broiler chicken breast meat

Parameters	Drinking water		Hour fasting		
	ORS	Tap water	0hr	24hr	48hr
Slaughter weight	1278.89 ^{ns}	1295.56 ^{ns}	1455.00 ^b	1265.83 ^{ba}	1140.83 ^a
Warm carcass weight	868.33 ^{ns}	898.05 ^{ns}	989.16 ^b	865.83 ^{ba}	794.58 ^a
Dressing percentage	55.49 ^{ns}	56.39 ^{ns}	55.54 ^{ns}	55.77 ^{ns}	56.52 ^{ns}
Liver weight	28.11 ^{ns}	26.00 ^{ns}	30.83 ^b	26.41 ^a	23.91 ^a
Gut weight (full)	157.62 ^{ns}	151.88 ^{ns}	185.58 ^c	154.50 ^b	124.16 ^a
Gut weight (empty)	136.55 ^{ns}	130.05 ^{ns}	152.08 ^b	136.25 ^b	111.58 ^a
Residual gut fill	21.05 ^{ns}	21.83 ^{ns}	33.50 ^b	18.25 ^a	12.58 ^a
Meat pH	6.16 ^{ns}	6.02 ^{ns}	5.94 ^a	6.09 ^{ab}	6.23 ^b
Cooking loss	47.35 ^{ns}	47.51 ^{ns}	49.38 ^b	47.38 ^{ba}	45.53 ^a

Values within the same row within the same group with the same superscript are not significantly different

^{ns} Not significant



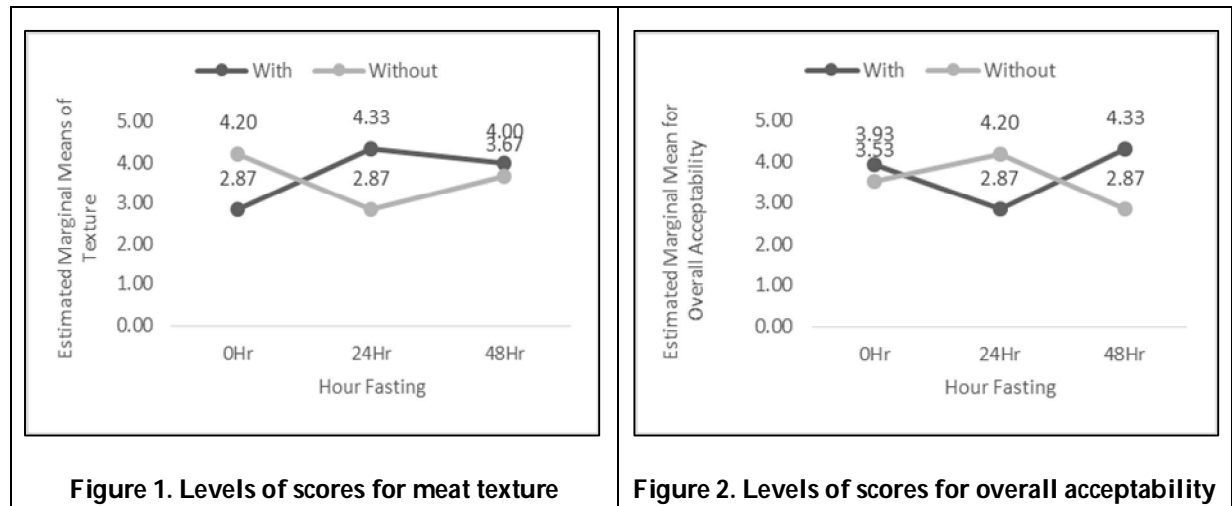


Albino Namoc Taer and E. Catipan Taer

Table 5. Summary of mean for sensory attributes of broiler chicken breast meat

Treatment	Odor	Appearance	Texture	Taste	Juiciness	Overall Acceptability
Drinking water						
ORS	4.02 ^{ns}	3.80 ^{ns}	3.73 ^{ns}	3.97 ^{ns}	3.83 ^{ns}	3.70 ^{ns}
Tap water	3.82 ^{ns}	3.75 ^{ns}	3.75 ^{ns}	3.56 ^{ns}	3.71 ^{ns}	3.53 ^{ns}
Hour fasting						
0-h	4.33 ^{ns}	3.83 ^{ns}	3.53 ^{ns}	3.76 ^{ns}	3.80 ^{ns}	3.73 ^{ns}
24-h	3.93 ^{ns}	3.83 ^{ns}	3.60 ^{ns}	4.02 ^{ns}	3.83 ^{ns}	3.53 ^{ns}
48-h	3.80 ^{ns}	3.73 ^{ns}	3.83 ^{ns}	4.20 ^{ns}	3.93 ^{ns}	3.60 ^{ns}

^{ns} Not significant





Assessment of Water Quality of Gulf of Aqaba along the Haql Coast, Saudi Arabia

Mazen A. Alsolami

Department of Biology, Environmental Research Unit, College of Haql, University of Tabuk, Tabuk 71491, Saudi Arabia.

Received: 14 Aug 2019

Revised: 17 Sep 2019

Accepted: 21 Oct 2019

*Address for Correspondence

Mazen A. Alsolami

Department of Biology,
Environmental Research Unit,
College of Haql, University of Tabuk,
Tabuk 71491, Saudi Arabia.
Email: m.alsolami@ut.edu.sa



This is an Open Access Journal / article distributed under the terms of the **Creative Commons Attribution License** (CC BY-NC-ND 3.0) which permits unrestricted use, distribution, and reproduction in any medium, provided the original work is properly cited. All rights reserved.

ABSTRACT

The present investigation was carried out to evaluate the quality of water of Gulf of Aqaba along the Haql coast of Saudi Arabia. Water quality was evaluated by measuring physico-chemical properties such as turbidity, pH, total dissolved solids (TDS), biochemical oxygen demand (BOD) and chemical oxygen demand (COD). Inorganic chemical components were measured in terms of total Kjeldahl nitrogen (TKN), ammonia (NH₃), nitrate (NO₃⁻), total phosphorus (P), fluoride (F⁻), total chlorine residual, and Fe. Heavy metals (HMs) composition was tested by assessing the level of As, Cd, Se, Cu, Hg, Pb, Ba, and Zn. The results show that the turbidity and pH of tested water samples were under the permissible limit as recommended by Royal Commission for Environmental Regulations (RCER), Saudi Arabia. However, the levels of TDS, BOD, and COD were higher than the recommended values. Regarding nitrogen forms; TKN, NH₃, and NO₃⁻ were at higher level along with the P and F⁻ which were slightly higher than the threshold level. However, total chlorine residual was found below the permissible limit. Although, the studied HMs were below to their recommended limit but Pb ranked the highest while Cd the least. The HMs were in the order of Pb > Ba > As > Hg > Se > Zn > Cu > Cd. Thus, based on the assessment of results it can be concluded that the collected water samples contain higher level of inorganic chemical compounds including nitrogen and P and higher TDS, BOD and COD levels which indicates that the water is contaminated by organic and inorganic pollutants. However, the level of HMs was under the permissible limits.

Keywords: Heavy metals, marine ecosystem, nitrogen, phosphorus, pollutants, Red Sea.



**Mazen A. Alsolami**

INTRODUCTION

Increasing population and their ever-increasing demand has led to exploitation of natural resources to such an extent that made the pristine atmosphere unsuitable for human health. Adverse effects of anthropogenic activities are reflected in the form of sudden climatic changes, flood, temperature fluctuations etc. that lead to losses of human lives (1/4). Water is elixir of life, however, its quality is degrading day by day through a number of factors which include natural and anthropogenic factors (2-4/1-3). Anthropogenic factors are considered as the worst culprits of degraded quality of waters. Such deterioration of water adversely affects aquatic ecosystem and availability of safe water for human consumption. Pollutants deposited in water lead to very serious changes that directly or indirectly influence the ecological balance of the environment that cause extensive damage to aquatic organisms which results in mass deaths and cessation of activities due to their high poisoning and bioaccumulation effects (5).

Marine ecosystem is the reservoir of a variety of natural resources and primary production on the planet earth. However, our marine ecosystem could not remain unaffected by human activities. Excessive, discharge from industries, sewage, agricultural runoff, construction sites and urban areas add loads of pollutants that changes physical as well as chemical components of aquatic ecosystem. Excessive accumulation of nutrients particularly N and P from various point and non-point sources cause eutrophication which induces excessive growth of algae leading to algal blooms (6, 7). These algae need a lot of oxygen to decompose after their death and decay which causes depletion of oxygen in the water that results in death of various aquatic animals. Biochemical oxygen demand (BOD) is the amount of oxygen used by organisms to consume oxidizable organic matter in a given time (8). Higher level of BOD indicates organic pollution and reduced availability of oxygen that degrades aquatic ecosystem and impair water use (9, 10). Marine ecosystem is also get polluted by changes in the composition of organic and inorganic chemicals. Moreover, addition of heavy metals (HMs) causes their accumulation in aquatic ecosystem. Higher concentration of HMs affects entire aquatic system from where these HMs enter the food chain and adversely affect human life.

Coastal areas of Red Sea are more prone to pollution because in addition to natural factors (temperature, precipitation, bedrock, soil, terrain etc.) they are also exposed to anthropogenic activities (oil spills, industrial wastewater and sewage, heated effluents of desalination plants, explosives, building activities along the seashore, hypersaline water rejection, navigation and shipping operations, mining and raw material grinding, shipyards, landfilling, domestic wastes etc.) which impose stresses on the coastal areas of Red Sea. Increased human activities add HMs, organic matter (11), hydrocarbons which adversely affect marine ecosystem. To test water quality index various criteria have been proposed by different workers and agencies which include estimation of dissolved oxygen, nitrates and nitrites, total phosphates, total suspended solids, biological oxygen demand, fecal coliforms and pH, to study the impact of domestic contamination in marine waters (12). Where as, according to Torres et al. (13) in determining water quality index, dissolved oxygen and pH are the two most common parameters, BOD, nitrates, fecal coliforms, temperature, turbidity and total suspended solids are in the second place. The HMs are usually associated with the chemical risks of contamination of surface waters. In addition, sewage oil and grease have been identified as a major causative agents of beach pollution (14). Presence of oil and greases in marine ecosystem leads to devastating impact on aquatic life such as coating animals and plants with oil and suffocating them by oxygen depletion (Eljaiek-Urzola et al. 2019), and the presence of even the thinnest layer will affect aquatic life by decreasing both the penetration of light and the oxygen transfer between air and water (15).

Haqlis located along the coast of Gulf of Aqaba (The northern tip of Red Sea) in the north-east region of Saudi Arabia and is the main attraction point for tourists of the region. Therefore, it is highly desirable to check the quality of water along the Haql coast of Red Sea so that the plans for saving marine ecosystem could be drafted. The present investigation was carried out to test the quality parameters of the coastal water of Gulf of Aqaba along the Haql coast.



**Mazen A. Alsolami**

MATERIALS AND METHODS

Sample Collection

Water samples were collected near the water surface at a distance of about 6 meters from the shore line from five points of gulf of Aqaba along the Haql coastal area of Red Sea, Saudi Arabia. Water quality was assessed using the mean values of five sampling data sets.

Analyses of water samples

Collected water samples were used for the estimation of following quality parameters: turbidity was measured using nephelometer, and pH using portable pH meter. Total dissolved solids (TDS) were estimated using conductivity meter. Biochemical oxygen demand (BOD) and chemical oxygen demand (COD) were measured by the volumetric titration method (16). Total Kjeldahl nitrogen (TKN) was estimated by colorimetric method (17), ammonia (NH₃) was estimated by Nessler method as described by Koch and T McMeekin (18), nitrate (NO₃⁻) was determined according to Rodger et al. (19) using cadmium reduction method (20). Fluoride was estimated by SPADNS method adapted from standard methods for the examination of water and wastewater (21). Total phosphorus (P) and total chlorine residual, and iron (Fe) were analyzed using standard methods (21) as described in method 8048-Hach, 8167-Hach, and 8008-Hach, respectively. Heavy metals (HMs) were estimated by inductively coupled plasma-atomic emission spectrometry as described in EPA-200.7 (22). Concentration of following HMs was tested: Arsenic (As), Cadmium (Cd), Copper (Cu), Mercury (Hg), Lead (Pb), Selenium (Se), Barium (Ba), and Zinc (Zn). The collected data were compared with permissible limits as recommended by Royal commission for environmental regulations (RCER), Saudi Arabia (23).

Statistical analysis

The data were analyzed statistically using SPSS-20 statistical software (SPSS Inc., Chicago, IL, USA). Means of five independent replicates were statistically compared by Duncan's multiple range test (DMRT) at $p < 0.05\%$ level.

RESULTS AND DISCUSSION

The data of Table 1 show that the turbidity level (0.25 NTU) was far less than the permissible limit (5 NTU) as recommended by RCER, Kingdom of Saudi Arabia (23). Turbidity is the reduction in water clarity caused by particles suspended or dissolved in water that scatter light making the water appear cloudy or murky. Elevated turbidity is a kind of pollution and is consequence of nutrient supply, transport of dissolved organic materials, macrophytes, and periphyton. High turbidity can significantly reduce the aesthetic quality of water and can harm fish and other aquatic life by reducing food supplies, degrading spawning beds, and affecting gill function (24). Phosphorus, through improving algal growth, is also considered as the key player in enhancing turbidity of water. In the present investigation increased value of P coupled with a slight increase in BOD was observed but a lower level of turbidity was recorded. It indicates that the water is under oligotrophic phase. In addition, the pH level (8.6) of collected water sample (Table 1) was almost closer to the threshold value (7.8 – 8.5) as recommended by RCER (23). It shows that the pH may cross the limit if preventive measures will not be taken. The pH of water is positively correlated with alkalinity and negatively correlated with CO₂ concentration, therefore, higher the pH, higher the alkalinity and lower the level of free CO₂ (25). The value for TDS exceeded the limit and BOD was also higher than the limit recommended by RCER (Table 1). The TDS are the inorganic salts, organic matter, and other dissolved materials in water. Higher level of TDS was also reported by Ahmed et al. (26) and Siddiqui et al. (27). Moreover, higher TDS values have been reported in arid or desert areas than in tropical areas that receive ample rainfall (28). The value of BOD indicates impact of effluents discharged into the receiving water bodies, and the amount of organic matter present in the

17810



**Mazen A. Alsolami**

waterbody (29). Therefore, a low BOD indicates good quality of water, while a high BOD indicates contaminated water (30). The increase in BOD indicates that there is an increase in organic pollution that may be due to untreated domestic sewage, agriculture runoff, and residual fertilizers (31). The data show that the level of COD was much higher as compared with the limit recommended by RCER. Higher values of these parameters indicate adverse impact of human activities in the coastal waters of Red Sea in Haql region.

In the present investigation inorganic nitrogen was estimated in the form of TKN, ammonia and NO_3^- . The data shows that TKN was less than 1 which was almost closer to the permissible limit (Figure 1). However, the levels of ammonia and NO_3^- were much higher than the limit recommended by RCER. Regarding, total phosphorous content, it was about 2.5 times higher than the value recommended by RCER (Figure 1). Excessive input of N and P is the key factor of water impairment. Fertilizers are the most significant sources of N contamination of ground and surface waters (7). A portion of N lost through evaporation enters water bodies through atmospheric deposition. Of the various N forms, NO_3^- , the highly mobile species, is mainly responsible for N losses from soils through leaching (32). However, P tightly binds with soil particles, therefore, increase in soil erosion accelerates P runoff (33, 34) to streams, rivers, lakes, and coastal regions. Phosphorus is considered as the primary limiting nutrient in eutrophication (35) and concentrations as low as between 10 and 20 $\mu\text{g P L}^{-1}$ are enough to support luxurious growth of phytoplankton, aquatic plants, and algal blooms (36). In the present investigation 0.06 mg L^{-1} of P was recorded in the water samples which is much higher than the above-mentioned level of P (10 and 20 $\mu\text{g P L}^{-1}$) that can support eutrophication (Figure 1). Eutrophication is followed by the uncontrolled growth of phytoplankton and algal blooms which deplete oxygen owing to decomposition of organic matter that adversely affects aquatic lives (37). The results of the study showed that fluoride value (1.78 mg/L) was slightly higher than the recommended value (1.5 mg/L). On the contrary, the level of residual chlorine and Fe was less than the permissible limit recommended by RCER (Figure 2).

Industrial growth has galvanized the discharge of waste and accumulation of HMs in the marine ecosystem which severely damages aquatic flora and fauna across the world. These HMs can transfer to fishes from where they may enter the food chain and thus adversely affect human health (38). Although, some HMs are needed by humans for various physiological and biochemical activities but others such as Hg, Cd, Pb, As etc. are toxic that can lead to serious health problems (39-41). HMs-induced toxicity and health risks include kidney and skeletal damages, neurological disorders, endocrine disruption, cardiovascular dysfunction, and carcinogenic effects (39). In the present investigation the values of all the studied HMs (As, Cd, Cu, Hg, Pb, Se, Ba, and Zn) were lower (Figure 3) than the permissible limit as recommended by RCER. In the analyzed water samples HMs were found in the following order: $\text{Pb} > \text{Ba} > \text{As} > \text{Hg} > \text{Se} > \text{Zn} > \text{Cu} > \text{Cd}$. Lower level of HMs in Red Sea was also reported by Siddiqui et al. (27) and Fahmy et al. (42).

CONCLUSIONS

On the basis of results obtained in the present investigation, it can be concluded that the turbidity and pH of water were under normal limit where as, TDS, BOD and COD were above the permissible limit as recommended by RCER. The results show that the level of N and P was higher which may lead to algal blooms and eutrophication. However, HMs were below the permissible limit.

REFERENCES

1. Lelieveld J, Klingmüller K, Pozzer A, Burnett RT, Haines A, Ramanathan V. Effects of fossil fuel and total anthropogenic emission removal on public health and climate. *PNAS* 2019; 116: 7192–7197.
2. Baker A. Land use and water quality. *Hydrol Process* 2003; 17:2499–2501.
3. Smith AJ, Thomas RL, Nolan JK, Velinsky DJ, Klein S, Duffy BT. Regional nutrient thresholds in wadeable streams of New York State protective of aquatic life. *Ecol Indic* 2013; 29:455–467.



**Mazen A. Alsolami**

4. Li SY, Xia XL, Tan X, Zhang QF. Effects of catchment and riparian landscape setting on water quality chemistry and seasonal evolution of water quality in the upper Han River Basin, China. PLoS ONE 2013; e53163.
5. Inyinbor AA, Adebisin BO, Oluyori AP, Adelani-Akande TA, Dada AO, Oreofe TA. Water pollution: Effects prevention and climatic impact. In: Glavan M, editor. Water Challenges of an Urbanizing World. Intech Open;2018. doi: 10.5772/intechopen.72018.
6. KhanMN, Mohammad F. Eutrophication: Challenges and Solutions. In: Eutrophication: Causes, Consequences and Control, Vol. 2, Abid A. Ansari and S. S. Gill (Eds.). Springer International Publishing, New York; 2013
7. Khan MN, Mobin M, Abbas ZK, Alamri SA. Fertilizers and their contaminants in soils, surface and groundwater. In: Dominick A. DellaSala, and Michael I. Goldstein, editros. The Encyclopedia of the Anthropocene, Oxford: Elsevier; 2018 vol. 5, p. 225-240.
8. European Environment Agency (EEA), 2015. Oxygen consuming substances in rivers. Indicators assessment, data and maps. Available at: <https://www.eea.europa.eu/dataand-maps/indicators/oxygen-consuming-substances-in-rivers/oxygen-consuming-substances-in-rivers-7> (19 pp.).
9. Ferreira ARL, Sanches Fernandes LF, Cortes RMV, Pacheco FAL. Assessing anthropogenic impacts on riverine ecosystems using nested partial least square regression. Sci Total Environ 2017; 583, 466–477. <https://doi.org/10.1016/j.scitotenv.2017.01.106>.
10. Vigiak O, Grizzetti B, Udias-Moinelo A, Zanni M, Dorati C, Bouraoui F et al. Predicting biochemical oxygen demand in European freshwater bodies. SciTotal Environ2019; 666:1089–1105.
11. Madkour HA, Dar MA. The anthropogenic effluents of the human activities on the red seacoast at Hurghada harbour (case study).Egypt JAquat Res 2007; 33: 43-58.
12. INVEMAR. Informe del Estado de los Ambientes y Recursos Marinos y Costeros de Colombia; Serie de Publicaciones Periódicas No. 3.; INVEMAR: Santa Marta, Colombia, 2017.
13. Torres BF, González Márquez LC, Díaz Solano B, Espinosa Torregroza AC, Cantero Rodelo R. Effects of beach tourists on bathing water and sand quality at Puerto Velero, Colombia. Environ Dev Sustain 2016; 20: 255–269.
14. Schulz TJ, Marczan PJ, Fane AG. Behavior of sewage effluent oil and grease in the ocean. Water Environ Res 1994; 66:800–804.
15. Pinto AMA, VilarVJP, Botelho CMS, Boaventura RAR. Oil and grease removal from wastewaters: Sorption treatment as an alternative to state-of-the-art technologies. A critical Rev Chem Eng J 2016; 297: 229–255.
16. APHA (American Public Health Association) Standard Methods for Analysis, America Public Health Association, 1995.
17. United States environmental protection agency (EPA) Method 351.1: Nitrogen, Kjeldahl, Total (Colorimetric, Automated Phenate) by Autoanalyzer, 1978.
18. Koch FC, McMeekin TL. "A new direct nesslerization micro-kjeldahl method and a modification of the nessler-folin reagent for ammonia." JAm Chem Soc 1924; 46: 2066–2069.
19. Rodger BB, Andrew DE, Eugene WR Standard Methods for the Examination of Water and Wastewater. APHA, Washington, DC, 23rd Edition; 2017.
20. Hach Company, (2014) Nitrate. Cadmium reduction method, Method 8039 (DOC316.53.01066), Water Analysis Handbook, Hach Company, Loveland, CO, Edition 9.
21. Standard Methods for the Examination of Water and Wastewater, 20th edition, APHA (American Public Health Association), Washington; 1998.
22. United States environmental protection agency (EPA) Method 200.7, Revision 4.4: Determination of Metals and Trace Elements in Water and Wastes by Inductively Coupled Plasma-Atomic Emission Spectrometry
23. Royal Commission Environmental Regulations, Vol. 1; 2004
24. Minnesota Pollution Control Agency, 2008.
25. Mackereth FJH, Heron J, Talling JF Water analysis. Fresh Water Biological Association, UK; 1989.
26. Ahmed SM, Hussain M, Abderrahman W. Using multivariate factor analysis to assess surface/logged water quality and source of contamination at a large irrigation project at Al-Fadhli, Eastern Province, Saudi Arabia. Bull Eng Geol Environ 2005; 64: 319–327.





Mazen A. Alsolami

27. Siddiqi ZM, Saleem M, Basheer C. Surface water quality in a water run-off canal system: A case study in Jubail Industrial City, Kingdom of Saudi Arabia; 2016.
28. Uhl VW, Baron JA, Davis WW, Warner DB, Seremet CC. Groundwater development: basic concepts for expanding CRS water programs. Catholic Relief Services, United States Conference of Catholic Bishops, 73; 2009
29. Sawyer C, Parkin G, McCarty P. Chemistry for Environmental Engineering; Mc Graw-Hill Book Company: New York, NY, USA, 2003.
30. Eljaiek-Urzola M, Romero-Sierra N, Segrera-Cabarcas L, Valdelamar-Martínez D, Quiñones-BolañosÉ. Oil and Grease as a Water Quality Index Parameter for the Conservation of Marine Biota. Water 2019; 11: 856; doi:10.3390/w11040856.
31. Maurya PK, Malik DS, Yadav KK, Kumar A, Kumar S, Kamy H. Bioaccumulation and potential sources of heavy metal contamination in fish species in River Ganga basin: Possible human health risks evaluation. Toxicol Rep 2019; 6: 472–481.
32. Tesoriero A, Liescher H, Cox S. Mechanism and rate of denitrification in an agricultural watershed: electron and mass balance along ground water flow paths. Water Resour Res 2000; 36: 1545–1559.
33. Eghball B, Gilley JE. Phosphorus risk assessment index evaluation using runoff measurements. J Soil Water Conserv 2001; 56: 202–206.
34. Uusitalo R, Yli-Halla M, and Turtola E. Suspended soil as a source of potentially bioavailable phosphorus in surface runoff waters from clay soils. Water Research 2000; 34: 2477–2482.
35. Correll DL. The role of phosphorus in the eutrophication of receiving waters: a review. J Environ Quality 1998; 27: 261–266. <https://doi.org/10.2134/jeq1998.00472425002700020004x>.
36. Powlson DS. Phosphorus, agriculture and water quality. Soil Use Manag 1998; 14: 123. <https://doi.org/10.1111/j.1475-2743.1998.tb00629.x>.
37. Pickney JL, Paerl HW, Tester P, and Richardson TL. The role of nutrient loading and eutrophication in estuarine ecology. Environ Health Perspect 2001; 109: 699–706.
38. Ashraf W, Seddigi Z, Abukibash A, Khalidi K. Level of selected metals in canned fish Consumed in Kingdom of Saudi Arabia. Environ Monit Assess 2006; 117: 271–279.
39. Renieri EA, Safenkova IV, Alegakis AK, Slutskaya ES, Kokaraki V, Kentouri M et al. Cadmium, lead and mercury in muscle tissue of gilthead seabream and seabass: risk evaluation for consumers. Food Chem Toxicol 2019; 124: 439–449.
40. Yadav KK, Gupta N, Kumar V, Singh JK. Bioremediation of heavy metals from contaminated sites using potential species: a review. Indian J Environ Prot 2017; 37: 65–84.
41. Renieri EA, Alegakis AK, Kiriakakis M, Vinceti M, Ozcagli E, Wilks MF et al. Cd, Pb and Hg biomonitoring in fish of the Mediterranean region and risk estimations on fish consumption, Toxics 2014; 2: 417–442.
42. Fahmy MA, Fattah LMA, Abdel-Halim AM, Aly-Eldeen MA, Abo-El-Khair EM, Ahdy HH et al. Evaluation of the Quality for the Egyptian Red Sea Coastal Waters during 2011-2013. Journal of Environ Protec 2016; 7: 1810-1834. <http://dx.doi.org/10.4236/jep.2016.712145>.

Table 1. Physicochemical properties of water of Gulf of Aqaba

Physicochemical characteristics				
Turbidity (NTU)	pH	TDS (mg/L)	BOD (mg/L)	COD (mg/L)
0.25 ± 0.019	8.6 ± 0.79	38100 ± 8.52	28 ± 1.63	3040 ± 21.47

Values are average ± SE of five independent replicates. TDS: total dissolved solids; BOD: biochemical oxygen demand; COD: chemical oxygen demand





Mazen A. Alsolami

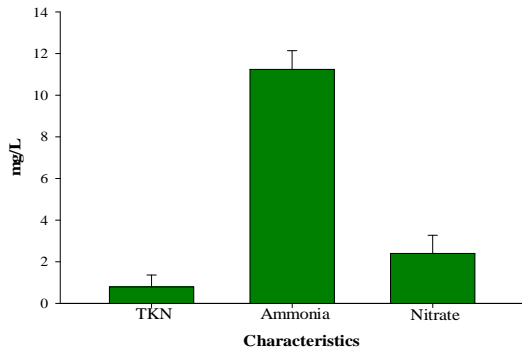


Figure 1. Total Kjeldahl nitrogen (TKN), ammonia and nitrate in the water of Gulf of Aqaba. An average of five determinations is presented, with bars indicating SE

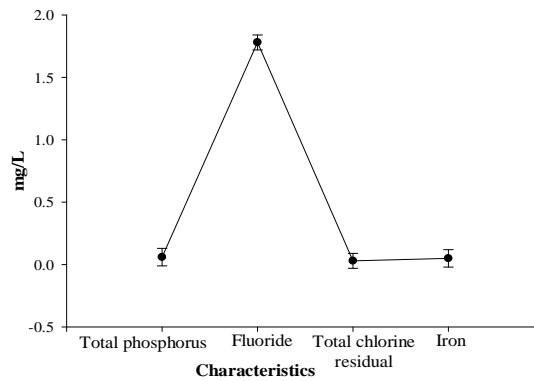


Figure 2. Total phosphorous, fluoride, total chlorine residual and iron in the water of Gulf of Aqaba. An average of five determinations is presented, with bars indicating SE

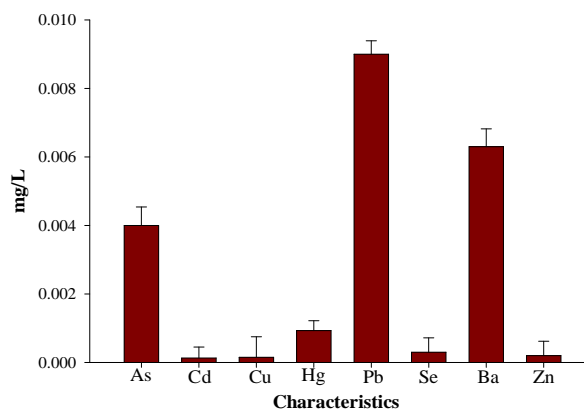


Figure 3. Heavy metal composition of the water of Gulf of Aqaba. An average of five determinations is presented, with bars indicating SE





Histoarchitecture and Histochemical Study of the Duodenum in Adult Guinea Pigs (*Cavia porcellus*)

F.J. Al-Saffar^{1*} and Riyadh Hameed Nasif²

¹Department of Anatomy, College of Veterinary Medicine, University of Baghdad, Baghdad, Iraq

²College of Science, University of Diyala, Diyala, Iraq

Received: 09 Sep 2019

Revised: 12 Oct 2019

Accepted: 11 Nov 2019

*Address for Correspondence

F.J. Al-Saffar

Department of Anatomy,
College of Veterinary Medicine,
University of Baghdad,
Baghdad, Iraq.
Email: fayak1955@gmail.com



This is an Open Access Journal / article distributed under the terms of the **Creative Commons Attribution License** (CC BY-NC-ND 3.0) which permits unrestricted use, distribution, and reproduction in any medium, provided the original work is properly cited. All rights reserved.

ABSTRACT

The present study was conducted to investigate the histological and histochemical structures of the duodenum in the adult males and females guinea pigs. Eight animals of each sex were used to carry out this research. Histological sections prepared from the specimens collected from different parts of duodenum and fixed by 10% neutral buffered formalin and others by Bouin's solution. Next step was application of routine histological procedure on specimens; different stains were used such as hematoxylin and eosin, Masson's Trichrome, Periodic acid Schiff, Alcian blue and combined of the last two stains to stain the sections. Histologically, the wall of duodenum possessed thick tunica mucosa, thin tunica muscularis (of two inner circular and outer longitudinal layers) and thinnest submucosa. Characteristically goblet cells were existed in the villi and lining epithelium of the intestinal glands. Histochemically goblet cells were stained with Periodic acid Schiff (PAS), Alcian blue (AB) stains. Paneth cells were detected in the duodenal crypts all over the mucosa of the duodenum. Muscularis mucosa was present continuously all over the duodenal mucosa. Brunner's glands were found also all over the wall of the duodenum. The submucosa showed only Henle's nerve plexuses and lack of Meissner's one. Tunica muscularis was formed of thicker inner circular layer and thinner outer longitudinal layer. Auerbach's nerve plexuses were existed all over the tunica muscularis as rosary and continuous between the internal and external layers of this tunic as well as in small discontinuous groups between these two muscular layers. Definitely, this tunic was thickest at the entrance of minor pancreatic duct.

Keywords: duodenum, guinea pig, histochemistry, goblet cells, Brunner's glands..





INTRODUCTION

Frequently, duodenum is considered the initial segment of the small intestine and it was grossly characterized in the mammalian species by typical U-shaped morphology of two arms generally designated as descending and ascending limbs where they close the pancreas between them (1). It was well known that the small intestine had three segments i.e. duodenum, jejunum and ileum. These segments had many common histological features such as the villi with some minor structural differences. The duodenum had intestinal villi (leaf-like) which were seen in the mucosa. Intestinal glands (Brunner's glands) were seen in the submucosa and were the major distinguishing features observed in the duodenum (2). The epithelium of the small intestine is made up of enterocytes, goblet cells, paneth cells and enteroendocrine cells. Paneth cells usually located in Lieberkühn crypts, originate from the same crypt stem cells that generate all intestinal epithelial cell lineages (3).

Histochemically, goblets cells in the duodenum of human, Rhesus macaque, rats, white-tailed deer, cat, domestic rabbits and raccoon are stained positively with PAS and Alcian blue (pH 2.5) (4). In combined staining procedures using both of the above stains, goblet cells stained dark blue, a brilliant red or a combination of the two colors. These remarks suggested that goblets contain neutral and / or acidic mucin. Generally, goblet cells in within the crypts of duodenum appear to contain neutral and / or acidic mucin and the more mature goblet cells located on villi acidic mucin (5). Up to date there is no research in the current literatures conducted to compare the morphology and histology of the duodenum of the adult guinea pigs and there is paucity of work focused only on the pathological aspect and concerned diseases of these organs in rabbit and other species. The current study is realized that the data which may be obtained will provides basic scientific information to conduct physiological and pharmaceutical researches that are related to the diseases of pancreas and duodenum mentioned in the above. Certainly the obtained data will provide good animal model for both veterinary field in animals and public health in human.

MATERIALS AND METHODS

Animal Collection and Study Design

Clinically healthy sixteen adult guinea pigs (eight of both males and females) were bought from local farms at Diyala province and they were caged in the animal house till their euthanasia and dissection to obtain their duodenum. Each chosen animal was euthanized prior to its dissection by intra-venous injection of over dose of 140 mg/kg of sodium phenobarbital [6]. After that, the animal was dissected on a dissecting board and the abdominal wall was opened to view the abdominal viscera, then representative specimens were cut for histological approach. They were cut from proximal, middle and distal portions of the descending duodenum. Similarly, specimens were cut from proximal, middle and distal portions of the ascending duodenum. Specimens were immersed in 10% neutral buffered formalin for 72 hrs and some specimens in Bouin's solution for 16 hrs. Specimens were dehydrated through ascending series of ethanol and then cleared with xylene. Processed specimens were infiltrated with paraffin wax on 58 °C then embedded with paraffin wax to obtain blocks of paraffin. Sections of six micrometers were prepared by using rotary microtome. The sections were stained with either one of the following stains: Hematoxylin and Eosin, Masson trichrome stain, PAS, AB stains. The latter stains used to stain goblet cells in the duodenum lining epithelium. The tissue sections were examined using Olympus light microscope. Sections were photographed and analyzed by Dino-eye piece camera provided with Image software.

RESULTS

Descending duodenum

In general, the wall of the duodenum was made up of 4 layers of tissue that were identical to the other layers of the gastrointestinal tract. From innermost to the outermost layer, these were the mucosa, submucosa, muscularis and



**F.J. Al-Saffar and Riyadh Hameed Nasif**

serosa layers. Wall in the proximal portion of the descending duodenum showed thick tunica mucosa compared to thinner tunica muscularis and thinnest submucosa. It was constructed from epithelial cells, lamina propria and muscularis mucosa (Fig. 1). The mucosa showed numerous projections that were finger like structures called intestinal villi and invaginations formed intestinal glands or called crypts of Lieberkühn. Both were lined with typical simple columnar cells with goblet unicellular cells. Core of each villus was composed of aerolar connective tissue, rich in blood vessels. The goblet cells were characteristically numerous spread among the other cells of the villi. Their shapes appeared circular and they were filled with a mucous secretion which pushed the nucleus and associated cytoplasm into the base. Their mucous stained blue in color with Alcian blue stain whereas, stained pink with periodic acid Schiff stain (Fig. 2, 3).

The lining epithelium was invaginated downward into the subepithelial lamina propria forming crypts of Lieberkühn. They were very well developed oval or spherical structures closely related to the bases of the villi as they were located in the inter-villi spaces. These glands were similarly covered with the same epithelial lining of the villi (Fig. 4). Prominently, intestinal glands showed the presence of many Paneth cells in their bases. These cells were large and pyramidal in shape characterized by basal nuclei and apical cytoplasm filled with coarse reddish granules post staining with Masson's trichrome stain. In fact, these cells were detected all over the duodenal wall (Fig. 5). The next structure of the mucosa was the muscularis mucosa. It was constructed from a thin layer of smooth muscle fibers that were circularly arranged. The muscularis mucosa separated the connective tissue lamina propria and the different sized intestinal glands from the connective tissue of the underlying submucosa (Fig. 4, 5). Tunica submucosa appeared prominently thin layer formed of loose connective tissue fibers abundantly supplied with blood vessels. It included many glands that can be called submucosal glands or Brunner's glands (Fig. 1). These glands were surrounded with scanty loose connective tissue. They were aggregated as mucous secretory units invested in scanty loose connective tissue as 3 to 8 aggregates (Fig. 4). Their mucous was stained blue with AB whereas, moderately stained pinkish with PAS stain (Fig. 6, 7). Submucosal nerve plexuses were present in the deep part of submucosa adjacent to the internal layer of the tunica muscularis. These were called Henle's nerve plexuses (Fig. 8). They were present in all parts of the duodenum.

Tunica muscularis found obviously thicker than the submucosa (Fig. 1). It was made of two layers that were thicker inner circular and thinner outer longitudinal layers of smooth muscle bundles. Loose connective tissue fibers were interspersed within the bundles of each layer and among the two layers that were sites of many nerve plexuses i. e. Auerbach's nerve plexuses (myenteric plexuses) associated with rich blood vessels (Fig. 9). Nerve plexuses called Auerbach's structures have different sizes and shapes (spherical or elongated). They resemble rosary structures distributed linearly in the connective tissue along the length all of the duodenum wall with same density. These nerve plexuses were constructed neurons and enteric glial cells. Most of the neurons were characterized by a pale basophilic cytoplasm with nuclei darkly blue stained have prominently one or two nucleoli, while a few other neurons possessed darkly basophilic stained cytoplasm. Most of the neurons possessed central nuclei, while a few cells showed eccentrically situated nuclei. The shape of glial cells was polygonal or elongated ovoid with different sizes and dark-colored. The number of neurons in the Auerbach's plexuses was little compared to those of glial cells which were stained with Hematoxylin and eosin (Fig. 9).

Tunica serosa, which was the outer layer of the wall of intestine, was composed of thin layer of loose connective tissue enclosed by a single sheet of mesothelial cells with the presence of nerves and a lot of blood vessels (Fig. 1). The second part of the descending limb of duodenum showed slight changes was detected such as thinner mucosa, submucosa and muscularis layer compared to the described first part. Moreover, the mucosal villi were decreased in length. Number of goblet cells was distinctly larger in both lining epithelium and intestinal crypts compared to those of the first part. Intestinal submucosal glands were decreased in density because of thinner submucosa. No changes in the muscularis mucosa thickness. No changes in the appearance Auerbach's nerve plexuses (Fig. 10). In the third part of the descending duodenum, slight changes were observed such as decrease in heights of the villi. Distinctly,



**F.J. Al-Saffar and Riyadh Hameed Nasif**

the number of goblet cells was increased in the lining epithelium and intestinal crypts compared to the first part of the descending duodenum.

Ascending duodenum

Generally, the histological structure of the duodenal wall of the ascending limb was similar to that described in the wall of the descending duodenum with a few detected differences. Characteristically it showed thinner mucosa, submucosa and tunica muscularis compared to those described parts of the descending duodenum (Fig. 11, 12). The length of mucosal villi of the first part was decreased. The submucosa appeared thinner due to the fewer scattered number of submucosal or Brunner's glands at this part of the duodenal submucosa. Auerbach's plexuses were smaller in size but numerous occurred between inner and outer layers of tunica muscularis in this part of the wall of ascending duodenum compared to those described in the structure of the descending duodenum wall (Fig. 11, 12). In the second part of the ascending duodenum slight changes were appeared compared to the previous part. Characteristically it showed thin mucosa, submucosa and muscularis mucosa. It showed decreased number of submucosal glands than those described in the wall structure of the descending duodenum. The third part of the ascending duodenum showed prominent changes. It showed thicker mucosa, submucosa and muscularis mucosa compared to those of the previously mentioned parts of the ascending duodenum where the minor pancreatic duct was opened between the external and internal layers of tunica muscularis. The length of mucosal villi was decreased (Fig.13). Distinctly, higher proportion of the goblet unicellular cells was recorded in the intestinal villi of the ascending duodenal wall compared with their percentage in the descending duodenal wall.

DISCUSSION

Microscopic findings recorded four tunicae that were tunica mucosa, tunica submucosa, tunica muscularis, and tunica serosa in the wall of the duodenum. Similar findings to the guinea pigs were recorded in previous studies such as in domestic cats (1), humans (7) and indigenous Gazelle (8). Current findings showed the presence of goblet cells scattered among other epithelial cells of the villi and crypts of Lieberkühn. They were prominently circular in shape with spacious free apical part and their nuclei imposed toward the bases of these unicellular glandular cells. Their cytoplasmic mucin substance positively reacted strongly with both Periodic acid Schiff (PAS) (indicate the presence of neutral mucin) and Alcian blue (AB) stains (indicate the presence of acidic mucin). These findings were comparable with those recently observed by (15) and (16) in the New Zealand and white Italian rabbits, respectively. Also, these findings were in agreement with those recorded by (4) in several mammalian species such as humans, white-tailed deer, cat, opossum and rats.

Markedly, the wall of the duodenum in guinea pig showed the presence of Brunner's glands existed in all parts of the organ. In fact, the present and quantity of Brunner's glands was greater in the submucosa of the first part of the descending duodenum. Subsequent gradual diminish in the number of these glands in both second and third parts. Continued decrease of the number of the Brunner's glands in the submucosa of the ascending duodenum toward the jejunum was in agreement with those observed in the duodenal submucosa of human beings (19), Angora rabbits (20) and indigenous rabbits (14). Also in small and large animals such as one Humped Camel (18), bovine (21), pony (22) and sheep (23). The percentage of goblet cells to the whole number of the duodenum columnar lining cells (Enterocytes) was increased in the direction from the pylorus to the jejunum. That is to say the increasing number of the goblet cells took place on the expense of enterocytes number. In other speaking, the enterocytes number was decreased in contrary to the number of the goblet cells. Enterocytes present in the beginning part of the duodenum may act to neutralize the acidity of the stomach because previous reference (24) mentioned that enterocytes secrete bicarbonate to inhibit the excessive quantity of gastric acidity. Moreover, the Brunner's glands previously described their role in neutralized gastric acidity (25). This role of Brunner's glands may decrease with their decreased number in the wall of duodenum because of the decrease of the submucosa thickness recorded in the present studied guinea



**F.J. Al-Saffar and Riyadh Hameed Nasif**

pigs. The important feature of Bruner's glands and their existence all over the wall of duodenum referred to their important functions. These findings came in parallel with the explanation of (28) who supposed that these glands secrete epidermal growth factors a powerful gastric inhibitor against gastric acidity. Current observations indicated that the characteristic feature of the duodenal submucosal glands observed in all mammals. They are a tubuloalveolar compound type with the main excretory duct that opened into the base of the duodenal crypts. They formed from mucous secretory units only densely packed within the duodenal submucosa at various parts along the duodenum. These results disagreed with those mentioned in Angora rabbits (20) horse (29), African Giant Rats (2), camels (32), indigenous Gazelle (8) and Goat (33) who observed that the Brunner's glands were composed of two kinds of cells that were mucous and serous cells. In another hand, previous findings in other animals showed mucous, serous and mixed acini or demilune such as white rabbits (34), indigenous rabbits (14).

Histochemical aspect of the current study revealed that the Brunner's glands were reacted positively with both PAS and AB stains. These positive reactions came in agreement to previous findings in different animal species such as white-tailed deer, domestic rabbits and cotton-tailed rabbits (4). Inconstantly, in bat (35), humans, Japanese macaques, opossums, raccoons and rats (4) referred to positive reaction with PAS only. The wall of the duodenum in the adult guinea pigs showed well-developed Auerbach's nerve plexuses. They appeared in between the bundles of internal layer of tunica muscularis as well as between both layers of this tunic. It appeared continuous resemble rosary structures positioned in the connective tissue among the two muscular layers of tunica muscularis throughout the whole parts of the duodenum. The presence of Auerbach's nerve plexuses were in a good agreement with previously records in the intestinal wall of humans (36) and different animal species such as rats (37), opossums (4), cats (11) and indigenous rabbits (14). Current microscopic examination showed different picture of nerve plexuses in the submucosa of the duodenum of the guinea pigs to other species. In the current animals only deep submucosal nerve plexus called Henle's nerve plexuses. In other species, present superficially located and adjacent to the mucosa nerve plexus called Meissner's nerve plexuses in addition to the deep Henle's nerve plexuses such as in humans (36), mouse (42), indigenous rabbits (14) and cats (11).

CONCLUSIONS

Distinctly, the Brunner's glands were distributed in the submucosa all over the wall of the duodenum. Microscopically, numerous Paneth cells were recorded in the intestinal crypts all over the duodenal mucosal. Henle's nerve plexus were identified in the deep part of the submucosa starting from pylorus till the end of the duodenum. Moreover, Auerbach's nerve plexuses present all over the wall of duodenum between the two layers of muscularis and even between the bundles of the internal layer of this tunica.

REFERENCES

1. Isitor, G. N.; Rao, S.; Nayak, S. B. and Sundaram, V. (2009). Autofluorescent vesicular structures in hematoxylin and eosin stained duodenal mucosa of the domestic cat. *West Indian Veterinary Journal*, 9 (2): 27-32
2. Nazlak, J. O. (2010). Anatomical and histochemical studies of the digestive system of the African giant Rat (*Cricetomys gambianus*-Water house). PhD Thesis, A.B.U. Zaria Univ, Northern, Nigeria
3. Garabedian, E. M., Roberts, L. J. J., Mcnevin, M. S. and Gordon, J. I. (1997). Examining the role of Paneth cells in the small intestine by lineage ablation in transgenic mice. *J. Biol. Chem.*, 272: 23729-23740
4. Schumacher, U.; Duku, M.; Katoh, M.; Joëns, J. and Krause, W. J. (2004). Histochemical similarities of mucins produced by Brunner's glands and pyloric glands: a comparative study. *Anat. Rec.*, 278: 540-550
5. Krause, W. J. (2000). Brunner's glands: a structural, histochemical. and pathologic profile. *Progress in Histochemistry and Cytochemistry*, 35(4): 259-367





F.J. Al-Saffar and Riyadh Hameed Nasif

6. Eifler, A. C.; Lewandowski, R. J.; Virmani, S.; Chung, J. C.; Wang, D.; Tang, R. L.; Kowalska, B. S.; Woloschak, G. E.; Yang, G. Y.; Robert, K.; Ryu, R. K.; Salem, R.; Larson, A. C.; Cheon, E.; Strouch, M.; Bentrem, D. J. and Omary, R. A. (2009). Development of the VX2 pancreatic cancer model in rabbits: A platform to test future interventional radiology therapies. *J. Vasc. Interv. Radiol.*, 20(8): 1075–1082
7. Rao, J. N. and Wang, J. Y. (2010). Regulation of gastrointestinal mucosal growth. *Integrated Systems Physiology: From Molecule to Function*, 3(2): 111-114
8. Hamza, L. O. and Al-Mansor, N. A. (2017). Histological and histochemical observations of the small Intestine in the indigenous Gazelle (*Gazella subgutturosa*). *J. Entomol. Zool. Studies*, 5(6): 948-956
9. Zanuzzi, C. N.; Barbeito, C. G.; Ortíz, M. L.; Lozza, F. A.; Fontana, P. A.; Portiansky, E. L. and Gimeno, E. J. (2010). Glycoconjugate histochemistry in the small and large intestine of normal and Solanum glaucophyllum-intoxicated rabbits. *Res. Vet. Sci.*, 89: 214–222
10. Desantis, S.; Zizza, S.; Accogli, G.; Tufarelli, V. and Laudadio, V. (2011). Morphometric features and glycoconjugate pattern of rabbit intestine are affected by particle size of pelleted diets. *Anat. Rec.*, 294: 1875–1889
11. Macéa, M. I. M.; Macéa, J. R. and Fregnani, J. H. T. G. (2006). Quantitative study of Brunner's glands in the human duodenal submucosa. *Int. J. Morphol.*, 24(1): 7-12
12. Ergün, E.; Ergun, L.; Asti, R. N. and Kurum, A. (2003). Light and electron microscopic morphology of Paneth cells in the sheep small intestine. *Rev. Méd. Vét.*, 154(5): 351- 355
13. Al-Saffar, F. J. and Al-Haak, A. G. (2016). Histomorphological relationship of Paneth cells with stem cells in the small intestine of indigenous rabbit at different postnatal ages. *Singapore J. Chem. Biol.*, 5: 11-19
14. Kadhim, Kh. H.; AL-Mehanna, N. H. and AL-Baghdadi, E. F. (2012). The Distribution of the Goblet cells, Paneth cells and Brunner's glands in duodenum of adult one Humped Camels (*Camelus dromedarius*). *AL-Qadisiya J. Vet. Med. Sci.*, 11 (2): 46-52
15. Takehana, K.; Abe, M.; Iwasa, K.; Hiraga, T. and Miyata, H. (1991a). Carbohydrate histochemistry of bovine duodenal glands. *J. Vet. Med. Sci.*, 53: 699-706
16. Takehana, K.; Masty, J.; Abe, M. and Yamaguchi, M. (1991b). duodenal glands of the pony (*Equus caballus*). *Anat. Histo. Embryol.*, 20: 1-9
17. Carvalho, A. D. V.; Magalhaes, M. J. and Ribeiro, J. E. (1988). Histochemistry of mucins of duodenal glands and goblet cells of sheep. *Arq. Bras. Med. Vet. Zool.*, 40: 369-376
18. Underwood, J. C. (1996). *General and Systematic Pathology*. 2nd ed. London, Churchill Livingstone
19. Morikawa, Y.; Miyamoto, M. and Okada, T. (1993). Perinatal development of Brunner's glands in the rat: Morphometrical study. *Biol. Neonate.*, 63(4): 258-67
20. Farkas, I. E. and Gero, G. (1989). The role of Brunner's glands in the mucosal protection of the proximal part of duodenum. *Acta Physiol. Hung.*, 73(2-3): 257-60
21. Oduor-Okelo, D. (1976). Histochemistry of the duodenal glands of the cat and horse. *Acta Anat.*, 94(3): 449-456
22. Takehana, K.; Eerdunchaolu, U.; Kobayashi, H.; Iwasa, A. and Sou, K. (2000). A histochemical study of the camel (*Camelus bactrianus*) duodenal glands. *J. Vet. Med.Sci.*, 62: 449-452
23. Hassan, A. S. and Moussa, E. A. (2015). Light and scanning electron microscopy of the small intestine of goat (*Capra hircus*). *J. cell anim. Biol.*, 9(1): 1-8
24. Elnasharty, M. A.; Abou-Ghanema, I. I.; Sayed-Ahmed, A. and Abo Elnour, A. (2013). Mucosal-Submucosal changes in rabbit duodenum during development. *World Academy of Science, Engineering and Technology*, 1: 7-14-24
25. Scillitani, G.; Zizza, S.; Liquori, G. E. and Ferri, D. (2007). Lectin histochemistry of gastrointestinal glycoconjugates in the greater horseshoe bat *Rhinolophus ferrumequinum* (Schreber,1774). *Acta Histochem.*, 109: 347–57
26. Castelucci, P.; De Souza, R. R.; De Angelis, R. C.; Furness, J. B. and Liberti, E. A. (2002). Effects of pre- and postnatal protein deprivation and postnatal refeeding on myenteric neurons of the rat large intestine: a quantitative morphological study. *Cell Tissue Res.*, 310: 1-7
27. Al-Saffar, F. J. and Al-Zuhairy, M. F. (2016). Postnatal developmental histomorphological and histochemical study of the duodenum in the domestic cat. *Int. J. Curr. Res.*, 8: 43681-43690





F.J. Al-Saffar and Riyadh Hameed Nasif

28. Fekete, É.; Bagyánszki, M. and Béla, A. (2000). Prenatal development of the myenteric plexus in the human fetal small intestine. *Acta Biologica Szegediensis*, 44(1-4): 3-19
29. Furness, J. B.; Clerc, N.; Lomax, A. E. G.; Bornstein, J. C.; Kunze, W. A. A. and June, E.(2006). Shapes and projections of tertiary plexus neurons of the guinea-pig small intestine. *Cell & Tissue Research*, 300 (3): 383

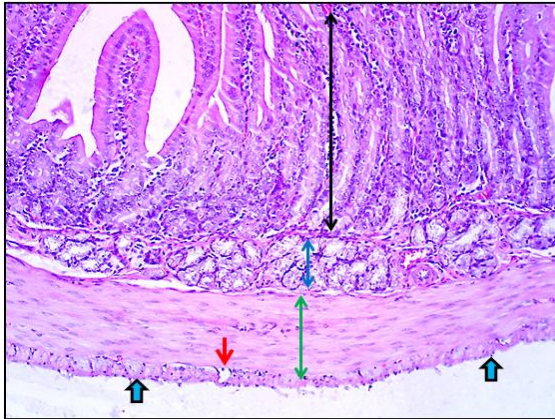


Fig. 1. Wall of the first part of descending duodenum in adult female guinea pig. It showed tunica mucosa (double heads black arrows), submucosa (double heads blue arrows), tunica muscularis (double heads green arrows), Auerbach's plexuses (red arrow) and serosa (blue arrows). H&E, X10

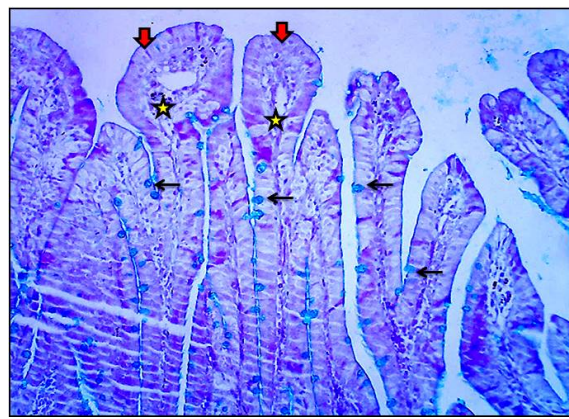


Fig. 2. Positively stained bluish colored mucous by AB stain in the goblet cells (black arrows) present in mucosal villi (red arrows) of the first part of descending duodenum in adult female guinea pigs. AB, X10

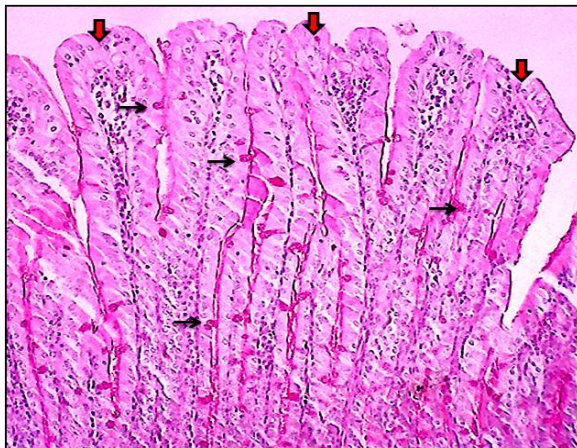


Fig. 3. Positively stained pinkish colored mucous by PAS stain in the goblet cells (black arrows) present in mucosal villi (red arrows) of the first part of descending duodenum in adult male guinea pigs. PAS, X10

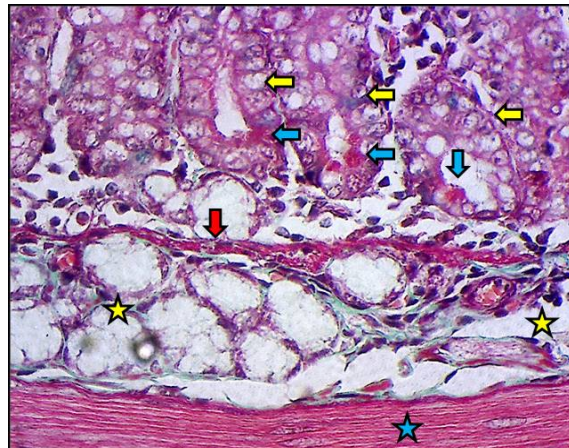


Fig. 4. First part of descending duodenum in adult female guinea pig showed Paneth cells (blue arrows) in the bases of intestinal glands (yellow arrows). The figure also showed muscularis mucosa (red arrow), Brunner's glands (yellow stars) in the submucosa, internal layer of tunica muscularis (blue star). Masson's trichrome, X40



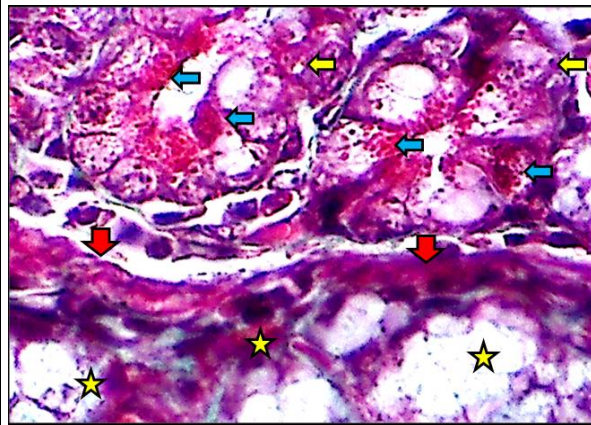


Fig. 5. First part of descending duodenum in adult male guinea pig showed Paneth cells (blue arrows) in the bases of intestinal glands (yellow arrows). The figure also showed muscularis mucosa (red arrow), Brunner's glands (yellow stars) in the submucosa. Masson's trichrome, X100

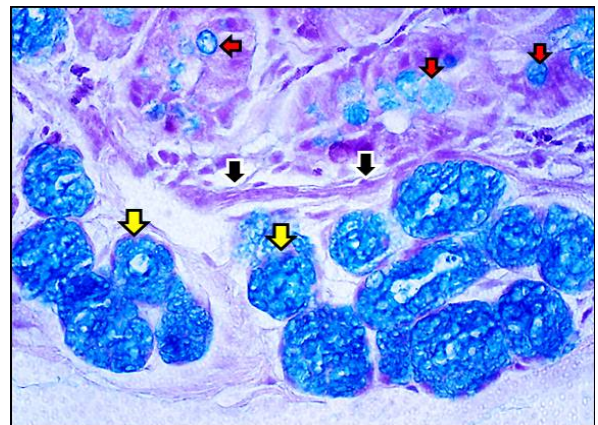


Fig.6. Positive reaction of mucous toward AB stain in both goblet cells of intestinal glands (red arrows) and Brunner's glands (yellow arrows) . Section at mucosa & submucosa of the first part of descending duodenum in adult female guinea pig. Muscularis mucosa present in between (black arrows). Alcian Blue, X40

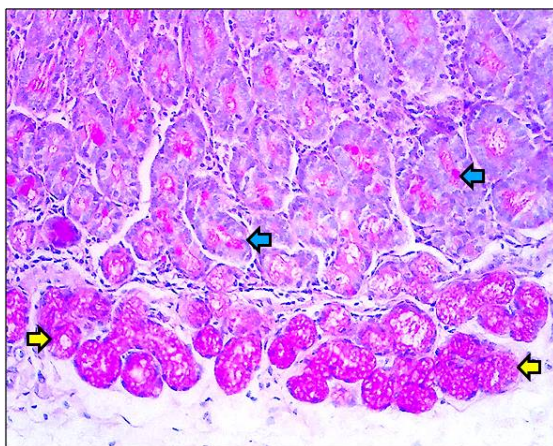


Fig. 7. Positive reaction of mucous of the goblet's cells of intestinal glands (blue arrows) and Brunner's glands (yellow arrows) toward the PAS stain in the mucosa & submucosa of the first part of descending duodenum in adult male guinea pig. PAS, X20

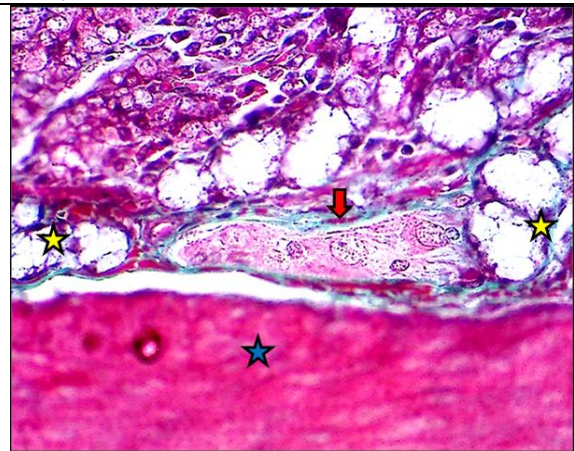


Fig. 8. First part of descending duodenum in adult female guinea pig showed in the submucosa (yellow stars) the Henle's nerve plexus (red arrow) adjacently located to internal layer of tunica muscularis (blue star). Masson's trichrome, X40





F.J. Al-Saffar and Riyadh Hameed Nasif

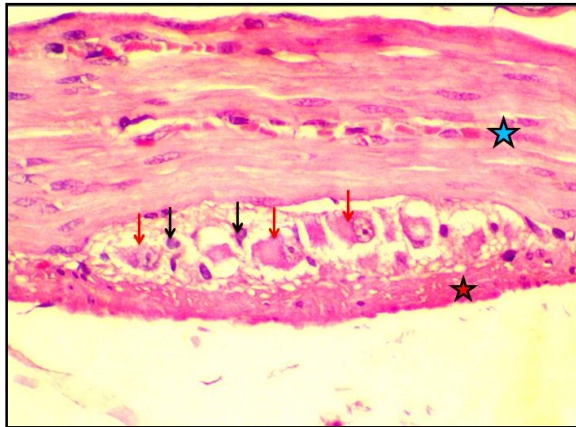


Fig. 9. Auerbach's plexuses in the wall of the first part of descending duodenum of adult male guinea pig. showed neurons (red arrows) characterized by eccentric nucleus with one nucleoli and glial cells (black arrows), present between inner layer (blue star) and the outer layer (red star) of tunica muscularis. H&E, X40

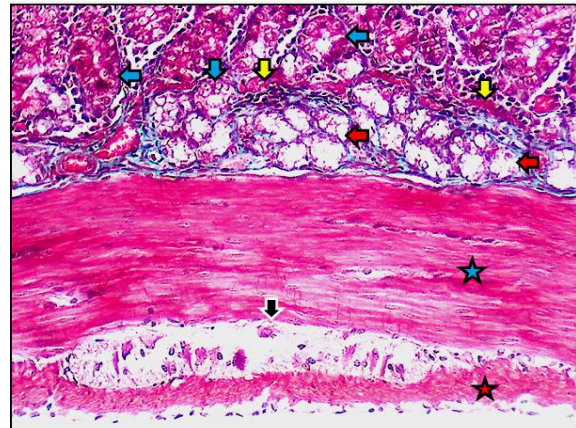


Fig. 10. Wall of the second part of descending duodenum in adult female guinea pig showed muscularis mucosa (yellow arrows), intestinal glands (blue arrows), (Brunner's glands (red arrows) in the submucosa surrounded by thin connective tissue, Auerbach's plexuses (black arrows) present between inner layer (blue stars) and outer layer (red star) of tunica muscularis. Masson's trichrome, X20

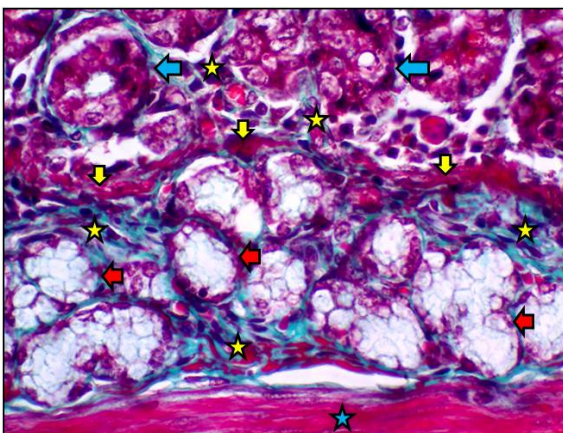


Fig. 11. Wall of the first part of ascending duodenum in adult female guinea pig showed muscularis mucosa (yellow arrow), intestinal glands (blue arrow), Brunner's glands (red arrows), scanty connective tissue around these glands (yellow stars), inner layer of tunica muscularis (blue star). Masson's trichrome, X20

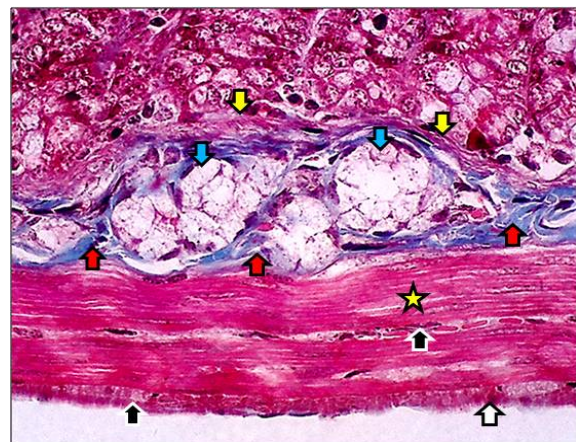


Fig. 12. Wall of the first part of ascending duodenum in adult male guinea pig showed muscularis mucosa (yellow arrows), Brunner's glands (blue arrows) surrounded by the submucosal connective tissue (red arrows), inner layer (yellow star) and outer layer (white arrow) of tunica muscularis and Auerbach's plexuses (black arrows), Masson's trichrome, X40





F.J. Al-Saffar and Riyadh Hameed Nasif

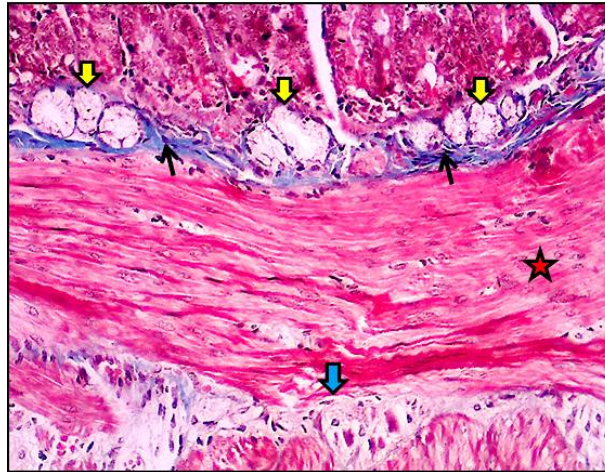


Fig. 13. Third part of ascending duodenum in adult female guinea pig. It showed Brunner's glands surrounded by thin connective tissues (black arrows), thick inner circular muscle bundles of tunica muscularis (red star), prominent Auerbach's plexuses (blue arrow). Masson's trichrome, X40





Neem in Endodontics

Smita D Dutta^{1*}, Rahul Maria² and Prashik Parvekar³

¹Assistant Professor, Department of Endodontics, College of Dentistry, Qassim University, Kingdom of Saudi Arabia.

²Professor and Head, Department of Endodontics, BCDS, Bhopal, Madhya Pradesh, India

³Ph.D Scholar, PAHER, Udaipur, Rajasthan, India

Received: 13 Sep 2019

Revised: 15 Oct 2019

Accepted: 20 Nov 2019

* Address for Correspondence

Smita D Dutta

Assistant Professor,
Department of Endodontics,
College of Dental Medicine,
Qassim University,
Kingdom of Saudi Arabia.
Email: smita_d_dutta@yahoo.com



This is an Open Access Journal / article distributed under the terms of the **Creative Commons Attribution License** (CC BY-NC-ND 3.0) which permits unrestricted use, distribution, and reproduction in any medium, provided the original work is properly cited. All rights reserved.

ABSTRACT

Simulated biofilm was created and the effect of calcium hydroxide and Neem oil was compared against E. fecalis. It was observed in the study the combination of Neem oil and calcium hydroxide was superior to calcium hydroxide alone hence encouraging the use of ayurvedic medicines in dentistry.

Keywords: biofilm, calcium hydroxide, Neem oil.

INTRODUCTION

The word "Neem" is an emotion in India. It is just not a plant type because of its medicinal uses and solutions to many routine minor ailments it has aptly been designated as green dispensary. For rural India it is the first choice even before the doctor. This plant has proved over and over its importance. Every part of the plant is useful, beside the obvious ecological benefits, the medicinal benefits are undeniable. Roots, twigs, bark, leaves, fruits, flowers not a single part of plant can be denied of its medicinal properties. The common being tooth cleaning, anti insect, anti fever, anti mosquito, anti septic, digestion, joint ailments, hair loss, the count is vast. The tooth brush of Neem encourage us to use its oil as an antibacterial media for root canal infection. Root canal treated teeth fails at times and the major causative stubborn bacteria is E. fecalis which is found. Though gold standard Calcium hydroxide paste is used as intra canal medicament to kill the bacteria, E. fecalis is significantly resistant to calcium hydroxide. The microbial resistance is an alarming issue. Hence this study was taken to evaluate the antimicrobial activity of calcium hydroxide when Neem oil is used as a delivery vehicle.





Smita D Dutta et al.

METHODOLOGY

40 Recently extracted intact single rooted human single rooted single canal teeth were selected and sterilized Access opening was done, working length determined and All canals sequentially prepared using step-back technique up to size # 35K master apical file under irrigation with saline. Irrigation protocol included NaOCl and EDTA wash with intermediate saline flush .nail varnish was applied on the root of all the teeth. Teeth placed in a closed container containing 4 ml of brain heart infusion (BHI) broth, sterilized by autoclaving at 121 °C for 20 min and incubated for 24 h at 37 °C to confirm sterility by absence of turbidity. A suspension of micro organisms was prepared in sterile containers. 2 ml of the sterile BHI broth from each tube were replaced by 2 ml of the prepared mixed microbial suspension, and then the test tubes were closed and incubated at 37 °C for 24 hours.

After contamination period, each specimen was removed from its test tube under aseptic conditions in the laminar air flow chamber and irrigated with 5 ml of sterile saline and dried with sterile paper points # 35. The specimens were divided randomly into equal groups I (Calcium hydroxide and saline) and group II (Calcium hydroxide and Neem oil) according to the intra-canal medications used. Intra canal medicament was introduced in the root canal system using lentulo spirals and hand file .the orifice was sealed with cavit not less than 3 mm in thickness. After incubation period, the intra-canal medications were removed. The root canals were irrigated using sterile saline solution and then dried with sterile paper points # 35K left in the root canal for 1 min to absorb the canal fluid and placed in sterile Eppendorf test tube containing 0.5 ml of sterile saline, vortexed for 30 s, and this suspension was represent the specimen taken from the main canal lumen. Sterile loops were standardized to carry 1µL of the microbial suspension to be seeded on the three media specific for the growth of the tested microorganisms. BHI blood agar for counting of *E. Faecalis* colonies The plates were incubated at 37 °C for 7 days . Growing colonies were counted and recorded as colony forming units CFU All the collected, tabulated and statistically analyzed. Analysis of variance ANOVA was performed according to the computer program SPSS Version 17for Windows.

RESULTS

Antimicrobial activity of study samples against *E. faecalis* (Table 1 and Figure 1), Group I (Calcium Hydroxide and Neem Oil) (Figure 2), Group II (Calcium Hydroxide and saline) (Figure 3).

DISCUSSION

In the present study it was found that the combination of calcium hydroxide with Neem oil was more effective than calcium hydroxide alone as shown in Table 1.Figure 1. There was statistically difference between the antimicrobial properties of both .group I was superior to group II . Calcium hydroxide alone was inferior in anti microbial property .the variation was too much in terms of colony forming units .In fact studies have quotes ineffectiveness of calcium hydroxide against *E Fecalis* by many authors (1-5). As the rates of root canal treatments is increasing so are the cases of endodontic failure *Fecalis* is the most stubborn bacteria to be eliminated from the root canal ,which is found in cases of failed RCT. calcium hydroxide is on the gold standard material for intracanal medicament. Various vehicles are used to deliver calcium hydroxide in canal that are broadly categorized as aqueous ,viscous ,oil based.²amongst all the used delivery vehicles the antimicrobial property of any is not proven, in fact the antimicrobial activity of calcium hydroxide vehicles is less explored so far.

Various pharmacological properties of Neem such as Antidiabetic Antihyperlipaemic, Antibacterial Activity: Antifungal Activity, Anticarcinogenic Activity: Antimalarial Activity: Antiulcer Activity: Wound Healing Activity have been proved by studies yet the use of herbal products is still less in dentistry .there is scarcity of literature regarding the use of Neem oil as a vehicle for calcium hydroxide. In fact this study is one of its kinds that studies the effect of Neem oil and calcium hydroxide in a simulated environment.(6-12). This studies proves the hypothesis that





Smita D Dutta et al.

Neem oil has an additive effect on the antimicrobial property of calcium hydroxide against *E. faecalis*. Further investigations such as effect of the combination on dentine strength, sealer adhesion, physical property of the dentine is warranted. The promising result encourages to unfold the use of ayurvedic agents in dentistry. The biggest advantage will be to overcome the resistance that the microbes have developed over the time and secondly there are apparently no side effects of Neem oil when used in such small amount.

REFERENCES

1. Ohara P, Torabinejad M, Kettering JD. Antibacterial effects of various endodontic irrigants on selected anaerobic bacteria. *Endod Dent Traumatol* 1993;9:95- 100.
2. Turk BT, Sen BH, Ozturk T. In vitro antimicrobial activity of calcium hydroxide mixed with different vehicles against *Enterococcus faecalis* and *Candida albicans*. *Oral Surg Oral Med Oral Pathol Endod* 2009;108: 297-301.
3. Pacios MG, Silva C, López ME, Cecilia M. Antibacterial action of calcium hydroxide vehicles and calcium hydroxide pastes. *J Investig Clin Dent* 2012;3:264-270.
4. Gomes BP, Ferraz CC, Vianna ME, Rosalen PL, Zaia AA, Teixeira FB, Souza-Filho FJ. *In vitro antimicrobial activity of calcium hydroxide pastes and their vehicles against selected microorganisms. Braz Dent J* 2002;13: 155-161.
5. Siqueira JF Jr, de Uzeda M. Intracanal medicaments: evaluation of the antibacterial effects of chlorhexidine, metronidazole, and calcium hydroxide associated with three vehicles. *J Endod* 1997;23:167-169
6. Maan P, Yadav KS and Yadav NP: Wound Healing Activity of *Azadirachta indica* A. Juss Stem Bark in Mice. *Pharmacognosy Magazine*.2017; 13(S-2): S316-S320. doi:10.4103/0973-1296.21016
7. David and Mediscope SN: Anti-pyretic of neem oil and its constituents. 1969; 12: 25-27
8. Bhajoni PS, Meshram GG and Lahkar M: Evaluation of the antiulcer activity of the leaves of *Azadirachta indica*: An experimental study. *Integr Med Int*. 2016; 3: 10-16.
9. Balasenthil S, Arivazhagan S, Ramachandran CR and Nagini S: J. *Ethnopharmacol*. 1999; 67: 189-195.
10. Surabhilal W, Charan AA and Bind A: *International J of Medicine and Pharma Sci (IJMPS)*. 2013; 3(2): 79-86.
11. Aslam F, Khalil-Ur-rehman, Asghar M and Sarwar M: *Pak. J Agri. Sci*. 2009; 46(3).
12. Bopanna KN, Kannan J, Gadgil S, Balaraman R and Rathod SP: Antidiabetic and antihyperlipaemic effects of neem seed kernel powder on alloxan diabetic rabbits. *Ind J Pharmacy*. 1997; 29: 162-167

Table 1. Antimicrobial activity of study samples against *E. faecalis*

Study Sample	Number of Colonies (Mean ± S.D.)
Group E (Calcium Hydroxide and Neem Oil)	38.3±3.86
Group I A(Calcium Hydroxide)	185.8±3.01

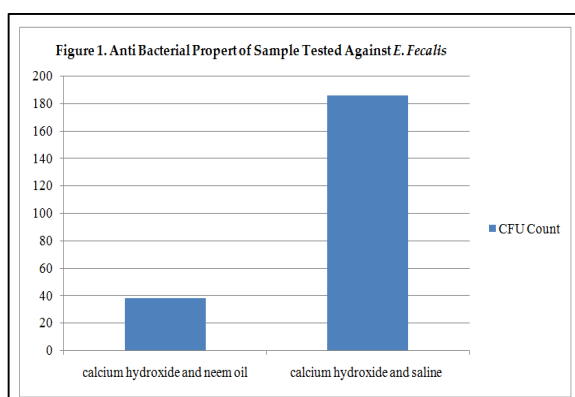


Figure 1. Anti Bacterial Propert of Sample Tested Against *E. Fecalis*





Smita D Dutta et al.



Figure. 2. Group I (Calcium Hydroxide and Neem Oil)



Figure. 3. Group II (Calcium Hydroxide and saline)





The Effect of Carbon Dioxide Perturbation Experiment on Growth Rate, Physico-Chemical, Biochemical Composition and Chlorophyll II Pigments of the Marine Pennate Diatom *Amphora subtropica*

Rajeswari Balakrishnan¹, Anand Muthusamy^{1*}, Santhanam Perumal², Rangesh Kannan¹, Divya Meril², Sasirekha Rajendran², Jeeva priya Radhakrishnan¹, Muthuchamy Maruthupandy¹ and Jayalakshmi Thillainayagam²

¹Department of Marine and Coastal Studies, School of Energy, Environment and Natural Resources, Madurai Kamaraj University, Madurai-625021, Tamil Nadu, India.

²Marine Planktonology & Aquaculture Laboratory, Department of Marine Science, School of Marine Sciences, Bharathidasan University, Tiruchirappalli - 620024, Tamil Nadu, India.

Received: 13 Sep 2019

Revised: 15 Oct 2019

Accepted: 18 Nov 2019

*Address for Correspondence

Anand Muthusamy

Department of Marine and Coastal Studies,
School of Energy, Environment and Natural Resources,
Madurai Kamaraj University, Madurai-625021,
Tamil Nadu, India.

Email: anandm21@yahoo.com



This is an Open Access Journal / article distributed under the terms of the **Creative Commons Attribution License** (CC BY-NC-ND 3.0) which permits unrestricted use, distribution, and reproduction in any medium, provided the original work is properly cited. All rights reserved.

ABSTRACT

This contemporary microcosm experiment was aimed to deduce the response of *Amphora subtropica* for carbon-di-oxide (CO₂) perturbation. *Amphora subtropica* exposed to carbon-di-oxide (CO₂) perturbation experiment for fifteen days in different pH concentrations viz., pH 7.0, pH 7.5, pH 8.0 and 8.1 (Control), to the projected corresponding atmospheric pCO₂ concentrations in the scenario of Business – as usual emission. The cell density rapidly increased in pH 7.5 (853333cells/ml) compared to pH 7 (506666.6 cells/ml) and control (163333 cells/ml). Nevertheless, the chlorophyll pigments viz., chl 'a' (p < 0.003), chl 'b' (p < 0.046) and chl 'c' (p < 0.107) were increased in pH 7 more than the other elevated pH conditions and control. The nutrients, phosphate (PO₄³⁻) and ammonia (NH₃) were gradually reduced, however the nitrite (NO₂) and nitrate (NO₃) were increased throughout the experiment in all pH conditions, simultaneously the silicate (SiO₂) was reduced till the 10th day but subsequently increased up to 15th day of the experiment in all pH conditions. The calcium (Ca⁺) concentration was gradually elevated until the 10th day and drastically reduced further till 15th day. The protein, carbohydrate and lipid composition of the diatom showed significant differences (p < 0.05) in various carbon dioxide concentrations throughout the experimental period. Scanning Electron Microscopy image of *A. subtropica* showed broadening of the cell at a higher pCO₂ concentration. Finally the results revealed that increasing CO₂ exerted a positive



**Rajeswari Balakrishnan et al.**

influence on *A. subtropica* culture in terms of cell density, photosynthetic process and the biochemical composition.

Keywords: *Amphora subtropica*, Atmospheric CO₂, Cell density, Chlorophyll pigments, Diatom, ions, Ocean acidification (OA) and nutrient.

INTRODUCTION

The industrial revolution and need for energy demand exhaustive burning of fossil fuel where consequently increased CO₂ concentration in the atmosphere. The excessive CO₂ in the atmosphere dissociate into seawater and inturn affect the carbonate system and thereby reduce ocean pH, termed as Ocean acidification (1,2). The atmospheric pCO₂ levels will reach approximately 500 μatm by end of the year 2050 compared to the preindustrial era of 280 μatm (3). Rising CO₂ levels in seawater could potentially influence the marine phytoplankton populations (4,6). For fast industrialization activities and 'natural CO₂ emission scenario', oceanic uptake of CO₂ can alter the ocean surface pH in 0.3-0.4 units by end of this century (7). The elevated pCO₂ can decrease the particulate organic production (POC) and particulate inorganic production (PIC) (8). Coastal waters experience variations in CO₂ and pH, and hence coastal phytoplankton populations may be intermittently susceptible to seawater acidification. The availability of CO₂ may be beneficial for marine phytoplankton (9). The pH changes are influencing the marine phytoplankton in different ways, positively for *Prochlorococcus* (Cyanobacteria) and in some cases, negatively for *Coccolithophore Emiliana huxleyi* (Prymnesiophyte) (10).

Diatoms are widely recognized as indicator species for environmental changes (11-13). Diatoms are the dominant group of phytoplankton protected with silica cell wall called frustules, which is the highest class of silicifying organisms on the sphere, also the major contributor to biogeochemical processes. Diatoms concentrate CO₂ (CO₂ Concentrating Mechanisms, CCMs) inside the cell (14). Diatoms-resolve export creation and can tolerate the climate change through both utilization and atmospheric CO₂ sequestration (15). A few diatom species are strong to lower pH whilst, others are susceptible to the acidified environment (16). Carbon stability fixed by microalgae is combined into carbohydrates and lipids, thus that energy, elements or food could be produced from biomass of algal (17,18). Accordingly, the rising CO₂ enhance the microalgae growth and photosynthetic process especially in carbon fixation (19). An Equatorial Pacific and Southern Ocean field study revealed that changing CO₂ move the diatom assemblage to aggregates (20, 21).

According to the (22) report in higher pH the *Skeletonema costatum* had enhanced growth rate, CO₂ uptake and amino acid content. The addition of carbon dioxide had increased the protein content in diatom *Phaeodactylum tricoratum* (23). The carbohydrates, protein and lipids contents were changed in diatom *Chaetoceros wighamii* under various CO₂ conditions (24). Very limited studies were conducted on the morphology changes of non-calcifying algae as an effect of ocean acidification. The ultrastructure of fresh water green algae *C. reinhardtii* and *Scenedesmus obliquus* were not affected under elevated CO₂ concentrations (25). Hypothetically, growth and pigmentation of diatom species (19¹) and oceanic photosynthetic activity increased by the excess of atmospheric CO₂ (26) Several diatoms are positively responding to pH changes (27), and a few marine diatoms exhibited moderate to low response over CO₂ induced pH variations (28 and 14¹).

Diatom exhibits varying response to OA, due to their phenotype and species variation. The biogenic silica content can be reduced by Ocean acidification in diatoms, though this impact by high CO₂ is not common in all diatoms (29-33). In a Mesocosm study through elevated partial pressure of CO₂ the diatoms dominated in over all primary production in coastal eutrophic water (34). Under acidified conditions, coastal diatom *Thalassiosira weissflogii* exhibited rapid particulate carbon production rate, compared to *Thalassiosira oceanica* the pelagic species which revealed slow growth rate during the diel pH fluctuations, the coastal diatom is tolerant to the reduced of pH



**Rajeswari Balakrishnan et al.**

conditions compared to pelagic species (35). The elevated CO₂ concentrations led to an increase in phytoplankton growth particularly in colony forming diatom, *Asterionellopsis glacialis* (36). Optimum growth conditions, the acclimatization capacity were found in a diatom species *Thalassiosira weissflogii* showed that statistically noticeable response in cell growth and photosynthesis regarding pigment concentration (37).

A. subtropica is most common distributed and available in the coast of Tamil Nadu (38). The distribution and structural characterization, molecular identification was carried out in Marine diatom *A. subtropica* (39). The focus of this present study is to deduce the influence of CO₂ and rising ocean acidity on growth, morphological changes, nutrient availability, chlorophyll, carbohydrate, protein and lipid contents in non-calcifying diatom *A. subtropica*. As per the IPCC predictions the anthropogenic emission of CO₂ in the “Business as usual scenario” projects the pH reduction to a magnitude of 2050-8.0, 2100-7.8, 2150-7.6. Hence it is evident that the oceans water is in the high risk of increasing acidity. There exists a large gap in finding mitigation for this increasing acidity. Phytoplankton is the potential source to sequester the excess CO₂ in ocean water. Among the three type of phytoplankton namely diatoms, dianoflagellates and coccolithophores. Diatoms depend on siliceous material for their cell wall, whereas the other two variety of phytoplankton depends on calcium mineral. Hence it is hypothesized that the siliceous diatom *A. subtropica* exhibit a potentially positive response to CO₂ perturbed ocean pH, an ideal solution for CO₂ mitigation and increasing ocean acidity. There is a limited finding for CO₂ perturbation experiment on non-calcifying diatoms therefore the present study is the first of its kind that *A. subtropica* - a silicifying diatom was elucidated to understand the CO₂ perturbed experiment on its growth rate, physico-chemical, biochemical composition and chlorophyll pigments.

MATERIALS AND METHODS

To find the overall response of *A. subtropica* to ocean acidification four different pH viz., 7.0, 7.5, 8.0 and 8.1 (control) were maintained. The lowest CO₂ treatment was meant to be at approximately atmospheric levels (408 ppm) pH 8.1. The most elevated CO₂ treatment was bubbled with CO₂-enriched air (1000 ppm) of approximately pH 7. CO₂ adjustment through bubbling method is logistically simple and relatively cheap way of maintaining constant carbonate chemistry. On the other hand, by cause of the potential damage to fragile cells, bubbling speed, i.e. the volume of CO₂ – enriched air delivered per minute, cannot be increased substantially to accommodate large culture vessels. Experimental bottles were continually bubbled with three different pCO₂ through air stones (408ppm, 560 ppm, 793 ppm and 1000 ppm), representing from lower ambient concentration to (LC) and higher future atmospheric partial pressures (HC). The pH was fluctuated, regular adjustments of the volume of CO₂ added through air bubbling to the culture flask for twice in everyday (9¹).

Isolation and Identification

The diatoms *A. subtropica* were isolated and identified based on its morphological structures (40). During the experiment period the unialgal *A. subtropica* was captured by inverted phase contrast microscope (made in Austria) (Fig. 1).

Culture Media

Unialgal *Amphora subtropica* stock culture was procured from aquaculture and planktonology laboratory, Bharathidasan University, Trichy (stock cultures were incubated with TMRL medium). Sample was illuminated with white florescence lamps at intervals of 12:12 h of light/ dark regime. The temperature and salinity were maintained between the range of 23 °C to 36 °C and from 25 to 28 ppt respectively. *A. subtropica* was cultured in a sterile conical flask with TMRL medium.



**Rajeswari Balakrishnan et al.**

Experimental Design

Culture was incubated in triplicate autoclaved 2 L conical flasks containing TMRL enriched seawater medium with initial cell count of 5×10^4 cells ml^{-1} from the stock culture. Experimental vessels were maintained for four different pCO_2 conditions viz., 1000 ppm, 793 ppm, 560 ppm and 408 ppm approximately to their respective ocean pH scenario pH 7.0, pH 7.5, pH 8.0, pH 8.1 (control) with the standard deviation of ± 0.02 . The culture was irradiated using white fluorescence lamps with intervals of 12:12 h of light/ dark regime by CO_2 mixing and the cultures incubated at 23°C - 36°C temperature culture was maintained (Fig. 2) (9²).

Algal Growth Measurements

During the entire 15 day study period, the cells were counted in an interval of 5 days. 0.5ml of sample was taken from experimental stock and assessed for growth of the species by simple counting numbers using a haemocytometer (neubauer chamber) under the light microscope (Magnus MLX – DX, OLYMPUS made in India). The morphological structure was also observed by scanning electron microscope.

Physico - Chemical Analysis of Culture Media

The pH was monitored every day during the experimental period using an ELICO grip pH meter. Salinity and Temperature were calculated by using Standard Celsius thermometer and ERMA, Hand Refractometer respectively. A 50 ml of samples were used to determine the NH_3 , NO_2 , NO_3 , SiO_2 and PO_4^{3-} concentrations. Total alkalinity, Ca^+ , Mg^+ , NH_3 , NO_2 , NO_3 , SiO_2 and PO_4^{3-} were determined as per the standard procedure (41). Chlorophyll - a, b and c concentration were estimated by pigment extraction procedure using 90% acetone. Chlorophyll pigments obtained samples were placed in refrigerator for incubation (24 h) under dark condition. Pigment absorption was attained through Spectrophotometer (Spectro 20D PLUS, made in U.S.A) using 5 ml sample at 630 nm, 645 nm, and 665 nm (42). CO_2 adjustment in conical culture flask was achieved by CO_2 gas mixing (9⁴).

Biochemical Analysis

Three culture flasks were grown with pCO_2 concentration and control were sampled while exponential growth phase on day 15 to estimate the algal carbohydrate, protein, lipid and cell's ultrastructure. The carbohydrate was tested using the Phenol-sulfuric acid method followed by Dubois *et al.* (43) with glucose as the standard. The protein was determined using Folin-phenol method followed by Lowery *et al.* (44). Lipid contents were tested by the chloroform-methanol (2:1) using Folch method with modified by Bligh and Dyer (45). For Scanning Electron Microscopy analysis the experimental cells were cleaned with 30% H_2SO_4 and KMnO_4 method. The samples were smeared with gold sputtering and the digital images were taken by VEGA-3 Tescan model.

Statistical Analysis

The results were analyzed using SPSS statistical program for Correlation, two-way analysis of variance (ANOVA) with significant "p value ≤ 0.05 " mean and standard error evaluation.

RESULTS

Cell Count

During the study period, the cell count was continuously increased in pH 7.5 and 8.0, while a gradual decrease was noticed in the control (Fig. 3). In pH 7.0 the cell count was reduced on 10th day of the experiment and increased

17832



**Rajeswari Balakrishnan et al.**

further which signify the fact that CO₂ perturbation influence the lag and exponential phase of *A. subtropica* cell culture at pH 7. The consequence of CO₂ on *A. subtropica* growth was significant over a time of exposure ($p < 0.05$) whereas, not significant across pH ($p > 0.05$). The current results indicate that the higher pCO₂ enhances the growth of *A. subtropica*. At the same time gradual decrease was noted in control (Fig. 3). The ANOVA test confirmed that cell counts were highly significant ($p < 0.05$) at time of exposure (Table 5). Correlation result shown that the growth of *A. subtropica* represented in the cell number at pH 7.5 concentrations was positively correlated with NO₂.

Physico-chemical analysis of nutrients

Silicate (e), calcium (f), magnesium (g) and salinity (h) with different pH concentrations. The nutrients level viz., NH₃, PO₄³⁻ and Mg⁺ ("p value ≤ 0.05 ") in culture media (Fig. 4 a, d and g) were rapidly decreased in all pH treatment which denotes that the phytoplankton consumed the nutrients for its growth. Similarly, the SiO₂ was initially taken up by the cells till the 10th day of the experimental period, whereas at pH 7 and 7.5 a remarkable increase in SiO₂ (Fig. 4 e) and Ca⁺ (Fig. 4 f) was observed in medium, which signify its dissolution from the cells into the media, these were confirmed by highly significant statistical value of $p < 0.05$. Fig. 4 b and c illustrate that the nitrification process exhibited a negative impact over reduced pH which was evidenced by the level of nitrite increase in the medium compared to nitrate. In all pH concentrations the level of ammonia was reduced drastically, which shows that NH₃ was the initial source of vital nitrogen for the cell growth shown in Fig. 4 a. Nitrate is a stable form of inorganic nitrogen in water. In our present study, nitrite and nitrate attained a maximum level of 24.58 and 6.35 $\mu\text{mol/l}$ during the last day of experiment in pH 7. These findings proved a inverse relationship between the NH₃ with NO₃ and NO₂ by nitrification process as well as a positive relationship between NO₃, NO₂ and cell count. The results which is in confirmation to earlier reports (46-49). Table 5 confirmed that the nutrient parameters were significant both across pH and time of exposure at $p < 0.05$.

The role of phosphate was considered as a vital source for the growth and frustules formation of diatom (50). At the initial stage of experiment the phosphate (6.48 $\mu\text{mol/l}$) was maximum and the minimum (0.94 $\mu\text{mol/l}$) during the 15th day of experiment at pH 7 (Fig. 4 d) where confirmed the weak positive linear relationship ($r = 0.29$) between the cell count and phosphate in the study (Table 1). The low level of silicate indicates that was utilized as a nutrient for its frustules development (Fig. 4 e) (51). The flourishing growth of diatoms revealed a moderate to strong positive linear relationship between silicate and cell counts in pH 7 ($r = 0.47$), pH 7.5 ($r = 0.62$) and pH 8 ($r = 0.82$) in table 1, 2 and 3 respectively. Calcium plays a major part in the motility and adhesion of *Amphora* cells (52). Ca⁺ was increased up to 10th day in all elevated pCO₂ chambers (Fig. 4 f). The initial level of calcium (400 mg l⁻¹) was gradually increased (1220 mg l⁻¹) at pH 7 and exhibited a positive linear relationship with nitrite. The obtained "r" value in all treatment chambers, including control were 0.82, 0.60, 0.88 and 0.42 for pH 7.0, 7.5, 8.0 and 8.1 respectively. The intracellular signals of calcium and nitric oxide influence the succession of phytoplankton groups (53). Magnesium is another essential element to make the diatom shell (frustules). These frustules constructed with magnesium and silicon or carbon. In this result the lower level of Mg⁺ denotes that diatom had taken Mg⁺ from the culture media (Fig. 4 g). This requirement of Mg⁺ confirmed in *A. Subtropica* had a positive linear relationship with PO₄³⁻ and in all pH 7.0 ($r = 0.95$), 7.5 ($r = 0.99$), 8.0 ($r = 0.97$), 8.1 ($r = 0.85$).

Biochemical Analysis

The effect of different pH concentrations on biochemical compositions of the *A. subtropica* throughout the experimental phase is shown in Fig. 5. The biochemical test results pointed out that, the total protein and lipid had significant differences ($p < 0.05$) except carbohydrate composition ($p > 0.05$) in exposed different pH concentrations. The biochemical results revealed that, a higher protein concentration was observed even in excess carbon-dioxide concentrations (pH 7). The correlation data represented the significant positive correlation between physico-chemical parameter ($r = 0.99$) and protein carbohydrate and lipid composition. The carbohydrate content was decreased with



**Rajeswari Balakrishnan et al.**

rising pCO₂, attains the maximum value at higher pH only (pH 8 and 8.16). Finally, this finding was confirmed by the negative correlation with pCO₂, PO₄³⁻ (r = -0.56) and mg (r = -0.79). Together, the lipid content rapidly increased with higher pCO₂ (Fig. 5). This also confirmed by a high significant positive correlation with pCO₂ (r = 0.99), NO₃ (r = 0.92), NO₂ (r = 0.98) and cell count (r = 0.99). Correlations with NH₃ (r = -0.85) and PO₄³⁻ (r = -0.74) were highly significant negative.

Pigment Analysis

Compared to other elevated pH conditions and control the chlorophyll pigment concentrations viz., chl 'a' (p < 0.00), chl 'b' (p < 0.04) and chl 'c' (p < 0.10) were increased in pH 7 (Fig. 5 a –c). The chl 'a' exhibited moderate to strong correlation whereas chl 'b' and chl 'c' revealed a strong correlation with reference to cell count. The concentration of chlorophyll was significant over a time of exposure (p value 0.00) whereas, not significant across pH (p value 0.17). Correlation coefficients of physico-chemical parameters and pigment analysis of diatom *A. subtropica* in different pH viz., 7.0, 7.5, 8.0 and 8.1 was given in Table 1 – 4, respectively.

Analysis of Variance

Two way ANOVA of nutrient and chlorophyll pigment data across various pH revealed highly significant changes (p < 0.05) in all parameters like NH₃, NO₂, NO₃, SiO₂, PO₄³⁻, Ca⁺, Mg⁺ and TA except chl 'a', chl 'b', chl 'c' and cell count (Table 5). Whereas, the results were highly significant (p < 0.05) over time of exposure for all parameters except NH₃, NO₃, SiO₂, PO₄³⁻, chl 'c', Ca⁺ and Mg⁺ in *A. subtropica*. However, time of exposure over different pH indicated no significant variation in salinity. The overall results recommended that the CO₂ microcosm environment varied significantly across the nominal pH regimes and also across the exposure time.

Scanning Electron Microscope

The results of scanning electron microscope revealed to significant changes for the diatom shell across various pH concentrations. The image captured at various magnification (µm) viz., 10, 5 and 2 were presented in Fig. 7, 8 and 9 respectively.

DISCUSSION

The rising atmospheric CO₂ level leads to reduced ocean pH which affects the physico-chemical parameters (e.g., nutrients) of diatom and exhibited positive effects on chlorophyll concentrations and growth. A few phytoplankton species use the CO₂ as the carbon source for their growth (54). Fleshly algae and some of diatom are benefited or less influenced by the impact of ocean acidification (55). *Euglena gracilis* is one of the greatest CO₂ tolerant algal species (56). *Isochrysis affinis galbana* was a highly sensitive micro algae, the growth is limited by excess CO₂ availability (57). 10% CO₂ could be optimal conditions for *Chlorella* sp. UK001 successful growth (58). The elevated pCO₂ significantly inducing the growth of *Thalassiosira pseudonana* in a sub-saturating growth light (59).

Some species like diatom or phytoplankton showed the different preferences to CO₂ or HCO₃, especially *Nitzschia* sp can live without their cell walls (frustules) even in the CO₂ acidified water (60). Hanan *et al.* results showed that increasing carbon level and ocean acidification (1050µatm), decrease the *Chaetoceros gracilis* growth (61). The total alkalinity (AT) may be influenced by dissolved organic matter liberated from the algal cultures (62). Our study has shown that ocean acidification influenced the growth of *A. subtropica* towards decreased pH. The present CO₂ perturbation results exhibited an increased cell numbers at pH 7.5 confirmed the positive influence of reduced ocean pH on diatom *A. subtropica*. The "r" values for *A. subtropica* increased for chl 'a' and cell count at pH 7 (0.52) and pH 7.5 (0.89). NH₃ uptake significantly influenced the diatom's growth in reduced pH conditions. This results revealed



**Rajeswari Balakrishnan et al.**

that CO₂ enriched seawater enhanced the utilization of nutrients especially NH₃ for its growth. In marine phytoplankton nitrogen was one of the major factors to inhibit their growth (63). The phytoplankton and a few microorganisms carry out the nitrification process (nitrogen cycle) in an ocean environment, the existence of nitrate and nitrite increased through oxidation of ammonia in its normal bio-geochemical cyclic process (64). Our findings forecast the point that as the anthropogenic CO₂ affect the ocean pH, ammonia oxidation rates could alter the nitrogen cycle and convention process in the sea. Silicate is the essential factor to engage the phytoplankton growth especially diatoms (65) The presence of silicate is crucial to enhance the silicifying diatom species for its sole dependence to build their structural conformity which is good agreement with the present study, initially the silicate level was gradually decreased till 10th day. The lower values of silicate indicate the uptake of silicates by diatom for their biological activity. After 10th day the SiO₂ level was raised, which signifies the dissolution of silicate from its structural component frustules. Our findings were in confirmation with the oceanic diatoms *Thalassiosira weissflogii* and *Thalassiosira oceanic* which evince that Si: O ratios of both the species were affected under elevated pCO₂ condition (35¹). Similarly, under increased ocean acidity the biogenic silicate decreased in few diatoms (66, 67, 30¹). Global warming, exposure to UV radiation, nutrient limitation and changing ocean pH are the most common stressors for the silicate mineralization process in marine plankton (68,69).

In general, the existence of phosphorus favours phytoplankton growth while in excess level leads to abnormal proliferation of cells (70). In the current observation, the PO₄³⁻ concentrations was reduced in all pH conditions; whereas, compared to treatment chambers in control the PO₄³⁻ level was drastically reduced on the 5th day of the culture period. This denotes that the addition of CO₂ in the treatment chambers interfere with the transformation of PO₄³⁻ to particulate phosphorus in the plankton growth. Similar to our observations in a mesocosm experiment PO₄³⁻ concentrations were significantly diminished in CO₂ treatment chambers than in control (71). The phosphorus necessity is considerably differing among species to species for optimum algal growth (72). This decline may be for the stimulation of phytoplankton production, higher salinity and which shows that increase in chl 'a' concentration. Under three pCO₂ conditions (350 μatm, 700 μatm and 1050 μatm) phosphate depletion in the medium affect the specific alkaline phosphatase activity (APA) phosphate affinity in phytoplankton and bacterial community (73, 74). The diatom frustule was composed by magnesium silicon nitride and nano crystalline silicon. In our experimental period, the initial (85.12 mg l⁻¹) Mg⁺ level was after 5th day drastically declined (0 mg l⁻¹) in all pH concentrations which denotes that Mg⁺ was one of the crucial sources to build the frustules in diatom shell (75).

Very limited studies were available on biogenic silica and ocean acidification impacts. Calcium minerals help to build and strengthen the biogenic silica frustules (76). The diatoms use clay and calcium carbonate as a source of biogenic silica synthesis (77). It evidenced with similar study Badger *et al.* (78) That diatom release the calcium carbonate in acidified conditions, the *Calcariana* (Foraminifera) gets energy from its symbiotic diatom to primary process of calcification. The biodiversity of phytoplankton is strongly influenced by variations of water quality parameters (79). Many authors have reported that the increasing atmospheric CO₂ decrease the ocean pH but well promote phytoplankton productivity and in the related diatom species in particular by stimulating their growth rate (80 and 19²,81-84 , 9⁵) Similar to these findings in the present experiment results showed that the reduced pH conditions viz., 7.0 and 7.5 favoured the *A. subtropica* for its growth and chlorophyll pigment concentration and hence proved the hypothesis that this species can adapt its photosynthetic activity and also quickly react to the changing pH/pCO₂ parameters in marine environment.

The highest protein value was observed in pH 7, and positively significant with total alkalinity (r = 0.92) and cell count (r = 0.98). Protein result indicated a significant positive correlation with nitrate (r= 0.99). Carbon utilized by microalgae is combined into carbohydrates and lipids, thus the energy and food could be formed through algal biomass (17¹, 18¹). Generally, the algae utilized CO₂ along with water and convert them into carbohydrates and some other valuable products. The present results specified that, the highest carbohydrate composition was recorded in high pH and control (pH 8.1) which is in confirmation with Thornton (85) in *Chaetoceros muelleri* was grown at lower pH (6.8), the amount of carbohydrates are stowed within the cells then decreased and further dissolved into the





Rajeswari Balakrishnan et al.

surrounding medium. The lipid test showed that maximum level present in rising pCO₂. The lipid content was high in elevated pCO₂ concentrations of *A. subtropica* exposure. The lipid results exhibited a highly significant positive correlation with SiO₂ (r = 0.90), NO₂ (r = 0.98) and NO₃ (r = 0.99) whereas highly negative correlations with NH₃ (r = - 0.99), PO₄³⁻ (r = - 0.78) and Magnesium (r = - 0.80). The increased protein and decreased carbohydrate contents in diatom *Chaetoceros wighamii* cultured under high CO₂ conditions, but no significant impacts obtained on lipid content (24¹).

The results of scanning electron microscope displayed clear frustules, the enlargement of the cell volume and no cell lyses was observed in *A. subtropica* across various pH exposures. Contrary to the present findings is lower pCO₂ concentration (280 µatm) caused enlargement of *Chaetoceros gracilis* cell further increase in pCO₂ from 550 to 1050 µatm exhibited disorder malformations, chloroplast damage, thylakoid membranes disintegration and cell lyses, these are the impact of slower growth rate of the cell (85¹). The impact of CO₂ enhancement to 186 µmol.l⁻¹ was insignificant for the size and shape of *Chlamydomonas reinhardtii*, but substantial in reduced the cell volume of *Scenedesmus obliquus* (25¹). The additional energy of the diatom species exerted to maintain their physiology is of great concern in increasing ocean acidity conditions of the ocean system to balance their population and ecosystem services.

CONCLUSIONS

Diatoms play a vital role in marine ecosystem and governing the biogeo carbon cycle. The present work deduces a positive influence on *A. subtropica* in terms of cell size above 13.5 µm in all pH and chlorophyll pigment concentration towards increasing atmospheric CO₂ level. This study evidenced that there is no damage in *A. subtropica* frustules to different pH exposure for their primary need on silica rather than calcium for shell formation. In contrary, the negative response was observed among various taxa for increasing ocean acidity, especially for the marine calcifiers. Here, a diatom *A. subtropica* is benefitted morphologically and biochemically during the exposure to the predicted ocean acidification scenarios. This study can help to understand the effect of ocean acidification on non-calcifying phytoplankton.

ABBREVIATIONS

<i>A. subtropica</i>	-	<i>Amphora subtropica</i>
APA	-	Alkaline phosphatase activity
Ca ⁺	-	Calcium ion
Chl	-	Chlorophyll
CO ₂	-	Carbon dioxide
Mg ⁺	-	Magnesium ion
NH ₃	-	Ammonia
NO ₂	-	Nitrogen dioxide
NO ₃	-	Nitrate
pCO ₂	-	Partial carbon dioxide
PO ₄ ³⁻	-	Phosphate
SiO ₂	-	Silicon dioxide

Ethical approval and informed consent

"All applicable international, national, and/or institutional guidelines for the care and use of animals were followed." "This article does not contain any studies with animals performed by any of the authors."



**Rajeswari Balakrishnan et al.****Authors' Contributions**

B. Rajeswari, M. Anand, and P. Santhanam contributed actively lead in manuscript writing, correction and discussion part. K. Rangesh, M. Divya, R. Sasirekha contributed in editing the manuscript. R. Jeeva priya, M. Maruthupandy and T. Jayalakshmi contributed in the beginning for designed the study and gave suggestions for this work. All authors have been personally and actively involved in substantive work leading to the manuscript, and will hold themselves jointly and individually responsible for its content. All authors read and approved the final manuscript.

ACKNOWLEDGEMENTS

Authors are acknowledging the authorities of Madurai Kamaraj University, Madurai, India for the facilities provided. The first author is thankful to the Aadhi Dravidar Welfare Department (ADW SCHOLARHIP) for their financial support to carry out this work and DST PURSE Madurai Kamaraj University, Madurai for providing the instrumentation facility to complete this study.

The potential conflict of interest disclosure form(s)

The authors declare that they have no conflict of interest.

REFERENCES

1. IPCC, Climate change: The physical science basis. Contribution of Working Group I to the fourth assessment report of the intergovernmental panel on climate change, 996 p. Cambridge University Press, New York. 2007.
2. Doney SC, Fabry VJ, Feely RA, Kleyvas JA. Ocean acidification: The other CO₂ problem. Annual Review of Marine Science. 1: 169–192.010908.163834.
3. IPCC. 2000. Special Report on Emissions Scenarios, Working Group III, Intergovernmental Panel on Climate Change, edited by N. Nakicenovic *et al.*, 595 pp., Cambridge University Press, New York. 2009.
4. Beardall J, Stojkovic S, Larsen S. Living in a high CO₂ world, impacts of global climate change on marine phytoplankton. Plant Ecology and Diversity. 2009; 2(2): 191–205.
5. Boyd PW, Strzepek R, Fu F, Hutchins DA. Environmental control of open-ocean phytoplankton groups, now and in the future. Limnology Oceanography 2010; 55(3): 1353–1376.
6. Collins S, Rost B, Rynearson TA. Evolutionary potential of marine phytoplankton under ocean acidification. Evolutionary Applications 2014; doi: 10.1111/eva.12120.
7. Caldeira K, Wickett ME. Anthropogenic carbon and ocean pH. Nature 2003; 425: 365–365.
8. Zondervan I, Zeebe R E, Rost B, Riebesell U. Decreasing marine biogenic calcification: A negative feedback on rising atmospheric pCO₂, Global Biogeochemical Cycles 2003 ; 15: 507–516.
9. Wu Y, Gao K, Riebesell U. CO₂ -induced seawater acidification affects physiological performance of the marine diatom *Phaeodactylum tricorutum*, Biogeosciences, 2010; 7: 2915–2923.
10. Biswas H, Jie J, Li Y, Zhang G, Zhu ZY, Wu Y. Response of a natural phytoplankton community from the Qingdao coast (Yellow Sea, China) to variable CO₂ levels over a short-term incubation experiment. Current Science. 2015; 108:1901–1909.
11. Huvane, J. K. & Cooper, S. R. Diatoms as indicators of environmental change in sediment cores from Northeastern Florida Bay. Bulletins of American Paleontology 2001; 361: 145-1 58.
12. Ross MS, Gaiser EE, Meeder JF, Lewin MT. Multi-taxon Analysis of the "White Zone", a Common Ecotonal Feature of South Florida Coastal Wetlands. In: Everglades, Florida Bay, and Coral Reefs of the Florida Keys: An Ecosystem Sourcebook, (J.W. Porter & K.G. Porter, eds), CRC Press, Boca Raton, Florida. 2002.



**Rajeswari Balakrishnan et al.**

13. Gaiser EE, Brooks MJ, Kenney WF, Schelske CL, Taylor BE. Interpreting the hydrological history of a temporary pond from chemical and microscopic characterization of siliceous microfossils. *Journal of Paleozoology* 2004; 31: 63-76.
14. Tortell PD, Reinfelder JR, Morel FM. Active uptake of bicarbonate by diatoms. *Nature* 1997; 390: 243-244.
15. Granum E, Raven JA, Leegood RC. How do marine diatoms fix 10 billion tonnes of inorganic carbon per year? *Canadian Journal of Botany -Rev. Can. Botanique* 2005; 83: 898-908.
16. Dupont S, Portner H. Marine science: get ready for ocean acidification. *Nature* 2013; 498: 429-429.
17. Lee JS, Kim DG, Lee JP, Park SC, Koh JH, Ohh SJ. CO₂ fixation by *Chlorella* sp. KR-1 using flue gas and its utilization as a feed stuff for chicks. *J. Microbiol. Biotechnol.* 2001; 11: 772-775.
18. Olaizola M, Commercial development of microalgal biotechnology: from test tube to marketplace. *Biomolecular engineering* 2003; 4-6: 459-466.
19. Riebesell U, Wolf-Gladrow DA, Smetacek VS. Carbon dioxide limitation of marine phytoplankton growth rates, *Nature* 1993; 361: 249-251.
20. Tortell PD, Morel, FMM. Sources of inorganic carbon for phytoplankton in the eastern subtropical and equatorial Pacific Ocean. *Limnology Oceanography* 2002; 47:1012-1022.
21. Tortell PD, Payne CD, Li Y, Trimbom S. The CO₂ response of Southern Ocean phytoplankton. *Geophysical Research Letters* 2008; 35: L04605, doi: 10.1029/2007GL032583.
22. Taraldsvik M, Mykkestad SM. The effect of pH on growth rate, biochemical composition and extracellular carbohydrate production of the marine diatom *Skeletonema costatum*. *European Journal of Phycology* 2000; 2: 189-194.
23. Chrismadha T, Borowitzka M, Effect of cell-density and irradiance on growth, proximate composition and eicosapentaenoic acid production of *Phaeodactylum tricornutum* grown in a tubular photobioreactor. *Journal of Applied Phycology.* 1994; 6: 67-74.
24. Araujo SC, Garcia VMT, Growth and biochemical composition of the diatom *Chaetoceros cf. wighamii* Brightwell under different temperatures, salinity and carbon dioxide levels I. Protein, carbohydrates and lipids. *Aquaculture* 2005; 246: 405-412.
25. Jian-Rong XIA, Kun-shan GAO. Effects of enrichment on microstructure and ultrastructure of two species of fresh water green algae. *Acta Botanica Sinica.* 2002; 44 (5): 527-531.
26. Hein M, Sand-Jensen K. CO₂ increases oceanic primary production. *Nature* 1997; 388: 526- 527.
27. Hinga KR. Effects of pH on coastal marine phytoplankton. *Marine Ecology Progress Series.* 2002; Vol. 238: 281-300.
28. Burkhardt S, Amoroso G, Riebesell U, Sultemeyer D. CO₂ and HCO₃-uptake in marine diatoms acclimated to different CO₂ concentrations. *Limnology Oceanography* 2001; 46:1378 - 1391.
29. Milligan AJ, Varela DE, Brzezinski MA, Morel FM. Dynamics of silicon metabolism and silicon isotopic discrimination in a marine diatom as a function of p CO₂. *Limnology Oceanography* 2004; 49: 322-329.
30. Tatters AO, Fu FX, Hutchins DA. High CO₂ & Silicate Limitation Synergistically Increase the Toxicity of *Pseudo-nitzschia fraudulenta*. *Public Library of Science, ONE* 2012; 7(2): e32116.
31. Xu K, Fu FX, Hutchins DA. Comparative responses of two dominant Antarctic phytoplankton taxa to interactions between ocean acidification, warming, irradiance, and iron availability. *Limnology Oceanography* 2014; 59: 1919-1931.
32. Qu P, Fu, FX, Hutchins DA. Responses of the large centric diatom *Coscinodiscus* sp. to interactions between warming, elevated CO₂, and nitrate availability. *Limnology Oceanography.* 2018; 63: 1407-1424.
33. Li W, Ding J, Li F, Wang T, Yang Y, L, Y. Functional responses of smaller and larger diatoms to gradual CO₂ rise. *Science of the Total Environment.* 2019; 680: 79-90.
34. Huang Y, Liu X, Laws EA, Bingzhang C, Li Y, Xie Y. Effects of increasing atmospheric CO₂ on the marine phytoplankton and bacterial metabolism during a bloom: a coastal mesocosm study. *Science of the Total Environment* 2018; 633: 618-629.



**Rajeswari Balakrishnan et al.**

35. Li F, Wu Y, Hutchins DA, Fu F, Gao K. Physiological responses of coastal and oceanic diatoms to diurnal fluctuations in seawater carbonate chemistry under two CO₂ concentrations, *Biogeosciences*, 2016; 13: 6247–6259, 2016.
36. Ramos, BJ, Schulz KG, Brownlee C, Sett S, B. Azevedo E. Effects of increasing sea water carbon 308 dioxide concentrations on chain formation of the diatom *Asterionellopsis glacialis*, *PLoS ONE*, 2014; 9(3): e90749. 309.
37. Passow U, Laws EA. Ocean acidification as one of multiple stressors: growth response of *Thalassiosira weissflogii* (diatom) under temperature and light stress, *Marine Ecology Progress Series* 2015; Vol. 541: 75–90.
38. Wachnicka AH, Gaiser EE. Characterization of *Amphora* and *Seminavis* from South Florida, U.S.A, *Diatom Research*, 2007; 22(2): 387- 455, 240 figs, 4 tables.
39. Sasirekha R, Santhanam P. Isolation, molecular identification and structural characterization of Marine diatom, *Amphora subtropica*, Conference: National Conference on Perspectives and Prospects in Aquatic Research At: Kongunadu Arts and Science College, Coimbatore. 2016.
40. Subrahmanyam R. A systematic account of the marine plankton diatoms of the Madras Coast. *Proceedings of the Indian National Science Academy*, 1946; 24: 85-197.
41. APHA, Standard methods for the examination of water and wastewater, 22nd edition edited by Rice EW, Baird RB, Eaton AD, Clesceri LS. American Public Health Association (APHA), American Water Works Association (AWWA) and Water Environment Federation (WEF), Washington, D.C., USA. 2012.
42. Strickland JDH, Parsons TR. A practical handbook of seawater analysis, *Journal of the Fisheries Research Board of Canada* 1972; 167(2): 310.
43. Dubois M, Gilles KA, Hamilton JK, Rebers PA, Smith F. Colorimetric method for determination of sugars and related substances. *Analytical Chemistry* 1956; 28 (3): 350–356.
44. Lowery OH, Roseborough NJ, Farr AL, Randall RJ. Protein measurement with the Folin phenol reagent. *Journal of Biological Chemistry* 1951; 193: 265–275.
45. Bligh EG, Dyer WJ. A rapid method of total lipid extraction and purification. *Canadian Journal of Biochemistry and Physiology* 1959; 37: 911–917.
46. El-Naggar AH, Osman MEH, El-Sherif ZM, Nassar MZ. Phytoplankton and seaweeds of the western coast of Suez Gulf (from Red Sea) in relation to some physico-chemical factors, oil and sewage pollution. *Bulletin of the Faculty of Science. Assiut University* 2002; 31 (1): 77–104.
47. Nassar MZ, Hamed MA. Phytoplankton standing crop and species diversity in relation to some water characteristic of Suez Bay (Red Sea). *Egyptian journal of aquatic biology and fisheries* 2003; 7 (3): 25 – 48.
48. Nassar MZ. Nutrients and phytoplankton distribution in the coastal waters of Aqaba Gulf, Red Sea. *Egyptian Journal of Aquatic Research* 2007; 33 (2): 133–151.
49. Madkour FF, El-Sherbiny MM, Aamer MA. Phytoplankton population along certain Egyptian coastal regions of the Red Sea. *Egyptian journal of aquatic biology and fisheries* 2010; 14 (2): 95–109.
50. Mackey MRK, Labiosa GR, Street H, Post J, Paytan A. Taxon - specific phosphorus status in the Gulf of Aqaba, Red Sea *Limnology Oceanography* 2007; 52: 873–885.
51. Wu JT, Chou TL. Silicate as the limiting nutrient for phytoplankton in a subtropical eutrophic estuary of Taiwan. *Estuarine, Coastal and Shelf Science* 2003; 58: 155–162.
52. Geesey GG, Cooksey BW, Cooksey KE. Influence of calcium and other cations on surface adhesion of bacteria and diatoms: A review, *Biofouling* 2000; 15:1-3, 195-205,
53. Vardi A, Formiggini F, Casotti R, de Martino A, Ribalet F. A stress surveillance system based on calcium and nitric oxide in marine diatoms. *Public Library of Science* 2006; 4(3)1-9.
54. Elzenga JTM, Prins HBA, Stefels J. The role of extracellular carbonic anhydrase activity in inorganic carbon utilization of *Phaeocystis globosa* (Prymnesiophyceae): a comparison with other marine algae using the isotopic disequilibrium technique. *Limnology Oceanography* 2000; 45 (2): 372–380.
55. Koch M, Bowes G, Ross C, Zhang XH. Marine macro-autotrophs and climate change. *Global Change Biology* 2013; 19:103–132.



**Rajeswari Balakrishnan et al.**

56. Miyatake K, Okuno H, Hamazaki K, Takenaka S, Honami N, Kiyota M, Aiga I, Kondo J. Growth of photosynthetic algae *Euglena* in high CO₂ conditions and its photosynthetic characteristics. *Acta Hort.* (ISHS) 1996; 440: 49–54.
57. Marchetti J, Bougaran G, Le Dean L, Megrier C, Lukomska E, Kaas R, Olivo E, Baron R, Robert RR, Cadoret JP. Optimizing conditions for the continuous culture of *Isochrysis affinis galbana* relevant to commercial hatcheries. *Aquaculture* 2012; 326– 329, 106–115.
58. Hirata S, Taya M, Tone S. Characterization of *Chlorella* cell cultures in batch and continuous operations under a photoautotrophic condition. *Journal of Chemical Engineering of Japan* 1996; 29: 953–959.
59. Li G, Douglas AC. Rising CO₂ interacts with growth light and growth rate to alter photosystem ii photo inactivation of the coastal diatom *Thalassiosira pseudonana*. *Public Library of Science One J.* 2013; 8: 1–13.
60. Jeyanthi S, Santhanam P, Shenbaga Devi A, Balamurugan A, Dinesh kumar S, Balaji Prasath B. Laboratory mesocosm studies on the response and potential effects of marine diatom *Nitzschia* sp. To ocean acidification, *Indian Journal of Geo- Marine Science* 2015; PP 1559-1567.
61. Hanan MK, Shaltout NA, El-Naggar MF, El-Naggar NA. Impact of elevated CO₂ concentrations on the growth and ultrastructure of non-calcifying marine diatom (*Chaetoceros gracilis* F.Schutt), *Egyptian Journal of Aquatic Research* 2014; 40: 243–250.
62. Koeve W, Oschli A. Potential impact of DOM accumulation on fCO₂ and carbonate ion computations in ocean acidification experiments. *Biogeosciences* 2012; 9: 3787–3798
63. Ryther JH, Dunstan WM. Nitrogen, Phosphorus, and Eutrophication in the Coastal Marine Environment, *Science.* 1971; 12 Mar. Vol. 171: 1008-1013.
64. Beman J, Chow CW, King AL, Feng Y, Fuhrman JA, Anderson A, Bates NR, Popp BN, Hutchins DA. Global declines in oceanic nitrification rates as a consequence of ocean acidification, *Proceedings of National Academy of Sciences.* 2011; vol. 108. no. 1. 208–213.
65. Panigrahi SN, Acharya BC, Das SN. Distribution of diatoms and dinoflagellates in tropical waters of Orissa and West Bengal with emphasis on neritic assemblages. In: *Proc Natn. Sem. New Frontiers in Marine Bioscience Res* 2004; 535-543.
66. Herve V, Derr J, Douady S, Quinet M, Moisan L, Lopez PJ. Multiparametric analyses reveal the pH-dependence of silicon biomineralization in diatoms. *Public Library of Science, ONE* 7, 2012; Doi: 10.1371/journal.pone.0046722.
67. Mejia LM, Isensee K, Mendez-Vicente A, Pisonero J, Shimizu N, Gonzalez C, Monteleone B, Stoll H. B content and Si/C ratios from cultured diatoms (*Thalassiosira pseudonana* and *Thalassiosira weissflogii*): relationship to seawater pH and diatom carbon acquisition. *Acta.* 2013; 123: 322–337.
68. Flynn KJ, Blackford JC, Baird ME. Changes in pH at the exterior surface of plankton with ocean acidification, *Nature Climate Change* 2012; 2: 510–513.
69. Morel F, Cox E, Kraepiel A, Lane T, Milligan A. Acquisition of inorganic carbon by the marine diatom *Thalassiosira weissflogii*. *Functional plant biology* 2002; 29: 301–308.
70. Varadharajan D, Soundarapandian P. Effect of Physico-chemical Parameters on species biodiversity with special Reference to the Phytoplankton from Muthupettai, South East Coast of India, *Journal of Earth Science and Climatic Change* 2014; 5:5,10.417/2157-7617.1000200.
71. Nausch M, Bach LT, Czerny J, Goldstein J, Grossart HP, Hellemann D, Hornick T, Achterberg EP, Schulz KG, Riebesell U. Effects of CO₂ perturbation on phosphorus pool sizes and uptake in a mesocosm experiment during a low productive summer season in the northern Baltic Sea, *Biogeosciences* 2016; Doi: 10.5194/bg-13-3035-2016.
72. Kuhl A. Phosphorus. In: Stewart, W.D.P. (Ed.), *Algal Physiology and Biochemistry.* Univ. of California Press, California 1974; pp. 636–654.
73. Tanaka T, Henriksen P, Lignell R, Olli K, Seppala J, Tamminen T, Thingstad TF. Specific affinity for phosphate uptake and specific alkaline phosphatase activity as diagnostic tools for detecting P-limited phytoplankton and bacteria, *Estuaries and Coasts* 2006; 29: 1226–1241.





Rajeswari Balakrishnan et al.

74. Tanaka T, Thingstad TF, Løvdal T, Grossart HP et al. Availability of phosphate for phytoplankton and bacteria and of glucose for bacteria at different pCO₂ levels in a mesocosm study. *Biogeosciences* 2008; 5:669–678
75. Degard IA, Romann J, Fossdal A, Royset A, Tranell G. Synthesis and properties of silicon/magnesium silicon nitride diatom frustule replicas, *Journal of Materials Chemistry A*, 2014; 2: 16410–16415, Doi: 10.1039/c4ta03750b.
76. Hunter GK. Interfacial aspects of biomineralization. *Current Opinion in Solid State and Materials Science*. 1:30-35 Iler RK 1979. *The chemistry of silica*. Wiley, New York. 1996.
77. Passow U, Christina L, Rocha DL. Accumulation of mineral ballast on organic aggregates, *Global Biogeochemical Cycles* 2006; Vol. 20: GB1013, Doi: 10.1029/2005GB002579.
78. Badger MR, Andrews TJ, Whitney SM, Ludwig M, Yellow lees DC, Leggat W, Price GD. The diversity and coevolution of Rubisco, plastids, pyrenoids, and chloroplast-based CO₂-concentrating mechanisms in algae, *Canadian Journal of Botany*; 1998: 76, 1052–1071.
79. Vengadesh PN, Rajkumar M, Perumal P, Thillai Rajasekar K. Seasonal variations of plankton diversity in the Kaduviyar estuary, Nagapattinam, southeast coast of India. *Journal of Environmental Biology*; 2009: 30 (6) pp. 1035-1046.
80. Rost B, Riebesell U. *Coccolithophores* and the biological pump: responses to environmental changes In: *Coccolithophores – From molecular processes to global impact*. Springer 2004; pp76–99.
81. Schippers P, Lurling M, Scheffer M. Increase of atmospheric CO₂ promotes phytoplankton productivity. *Ecology Letters* 2004; 7: 446–451.
82. Anderson RA. *Algal culturing techniques*, Elsevier Inc., San Diego, USA 2005; pp.35-64.
83. Hu H, Gao K. Response of growth and fatty acid compositions of *Nannochloropsis sp.* to environmental factors under elevated CO₂ concentration, *Biotechnology Letters* 2006; 28: 987 – 992.
84. Sobrino C, Ward ML, Neale PJ. Acclimation to elevated carbon dioxide and ultraviolet radiation in the diatom *Thalassiosira pseudonana*: effects on growth, photosynthesis, and spectral sensitivity of photoinhibition. *Limnology Oceanography* 2008; 53: 494–505.
85. Thornton DCO. Effect of low pH on carbohydrate production by a marine planktonic diatom (*Chaetoceros muelleri*). *Research Letters in Ecology* 2009; 5: 1–4.

Table 1 The experimental pH 7 correlation coefficients between physico-chemical parameters and chlorophyll pigment in *A. subtropica*

pH-7	NH ₃	NO ₃	NO ₂	PO ₄ ³⁻	SiO ₂	Calcium	Mg ⁺	Cell Count	Salinity	TA	Chl 'a'	Chl 'b'	Chl 'c'
NH ₃	1												
NO ₃	-0.431	1											
NO ₂	-0.667	0.937	1										
PO ₄ ³⁻	0.776	-0.773	-0.792	1									
SiO ₂	0.129	0.798	0.651	-0.241	1								
Calcium	-0.717	0.834	0.825	-0.993	0.346	1							
Mg ⁺	0.932	-0.664	-0.790	0.951	-0.091	-0.920	1						
Cell Count	-0.007	0.180	0.332	0.291	0.474	-0.255	0.146	1					
Salinity	-0.773	0.777	0.795	-0.999	0.248	0.994	-0.949	-0.288	1				
TA	-0.306	-0.392	-0.356	-0.257	-0.812	0.169	-0.279	-0.850	0.251	1			
Chl 'a'	-0.354	0.931	0.926	-0.551	0.877	0.620	-0.504	0.524	0.556	-0.663	1		
Chl 'b'	-0.426	0.832	0.906	-0.460	0.787	0.514	-0.488	0.682	0.464	-0.700	0.968	1	
Chl 'c'	-0.432	0.734	0.852	-0.363	0.715	0.409	-0.436	0.775	0.367	-0.722	0.916	0.986	1

The data in table 1 and 2 represented a strong positive linear relationship for salinity with calcium ($r = 0.99$) and magnesium with phosphate ($r = 0.99$) respectively. The result is in accordance to the proportional increase of *A. subtropica* cell numbers by rapidly utilizing these nutrients at pH 7.5 (853333Cells/ml) and pH 7.0 (506666.6 Cells/ml) with reference to the control (163333.3) and the concentration of chlorophyll pigments (chl 'a' ($p < 0.003$), chl 'b' ($p < 0.05$)) was highly significant in lower pH conditions. Concurrently a strong negative linear relationship ($r = -0.99$) was observed between Salinity and phosphate in all pH conditions viz., 7.0, 7.5 and 8.0 except control (8.1). This decreasing





Rajeswari Balakrishnan et al.

level of PO₄³⁻ confirmed that uptake of phosphate in the culture medium for the diatom flourishing growth. The pH 7 results confirmed strong positive linear relationship between the chl 'a' and NO₃ (r = 0.93) and chl 'a' and NO₂ (r = 0.92). In same pH the strong positive linear relationship between the chl 'b' and NO₃ (r = 0.83) and chl 'b' and NO₂ (r = 0.90) was found in this study.

Table 2. The experimental pH 7.5 correlation coefficients between physico- chemical parameters and chlorophyll pigment in *A. subtropica*

pH-7	NH ₃	NO ₃	NO ₂	PO ₄ ³⁻	SiO ₂	Calcium	Mg ⁺	Cell Count	Salinity	TA	Chl 'a'	Chl b	Chl 'c'
NH ₃	1												
NO ₃	-0.382	1											
NO ₂	-0.577	0.926	1										
PO ₄ ³⁻	0.902	-0.491	-0.757	1									
SiO ₂	-0.113	0.961	0.820	-0.255	1								
Calcium	-0.655	0.256	0.601	-0.894	0.071	1							
Mg ⁺	0.950	-0.464	-0.716	0.991	-0.212	-0.843	1						
Cell Count	-0.791	0.805	0.952	-0.912	0.626	0.732	-0.892	1					
Salinity	-0.788	0.562	0.828	-0.975	0.363	0.931	-0.939	0.929	1				
TA	-0.400	0.280	0.099	-0.602	-0.430	0.853	-0.559	0.280	0.613	1			
Chl 'a'	-0.682	0.925	0.905	-0.677	0.793	0.353	-0.689	0.895	0.669	-0.166	1		
Chl 'b'	-0.548	-0.030	-0.110	-0.135	-0.185	-0.242	-0.261	0.072	-0.074	-0.283	0.291	1	
Chl 'c'	-0.550	-0.167	-0.205	-0.139	-0.335	-0.192	-0.265	0.011	-0.079	-0.159	0.176	0.986	1

The pH 7.5 results confirmed that strong positive linear relationship between the chl 'a' with cell count (r = 0.89), NO₃ (r = 0.92) and NO₂ (r = 0.90) respectively.

Table 3 The experimental pH 8 correlation coefficients between physico- chemical parameters and chlorophyll pigment in *A. subtropica*

pH-7	NH ₃	NO ₃	NO ₂	PO ₄ ³⁻	SiO ₂	Calcium	Mg ⁺	Cell Count	Salinity	TA	Chl 'a'	Chl b	Chl 'c'
NH ₃	1												
NO ₃	-0.568	1											
NO ₂	-0.676	0.984	1										
PO ₄ ³⁻	0.849	-0.875	-0.899	1									
SiO ₂	-0.218	0.587	0.638	-0.274	1								
Calcium	-0.729	0.893	0.881	-0.978	0.200	1							
Mg ⁺	0.935	-0.811	-0.870	0.979	-0.315	-0.915	1						
Cell Count	-0.532	0.941	0.960	-0.747	0.821	0.720	-0.728	1					
Salinity	-0.794	0.943	0.963	-0.983	0.427	0.965	-0.956	0.852	1				
TA	-0.392	0.556	0.477	-0.712	-0.343	0.818	-0.587	0.246	0.640	1			
Chl 'a'	-0.583	0.857	0.911	-0.688	0.886	0.618	-0.712	0.975	0.793	0.075	1		
Chl 'b'	-0.450	0.501	0.607	-0.335	0.937	0.200	-0.437	0.754	0.448	-0.397	0.874	1	
Chl 'c'	-0.278	-0.574	-0.425	0.269	-0.153	-0.444	0.078	-0.422	-0.348	-0.549	-0.226	0.162	1

The pH 8 results confirmed that strong positive linear relationship between the chl 'a' with cell count (r = 0.97), NO₃ (r = 0.85) and NO₂ (r = 0.91) respectively. In same pH the moderate positive linear relationship between the chl 'b' with cell count (r = 0.75), NO₃ (r = 0.50) and NO₂ (r = 0.60) respectively.





Rajeswari Balakrishnan et al.

Table 4 The experimental control correlation coefficients between physico- chemical parameters and chlorophyll Pigment in *A. subtropica*

Control	NH ₃	NO ₃	NO ₂	PO ₄ ³⁻	SiO ₂	Calcium	Mg ⁺	Cell count	Salinity	TA	Chl 'a'	Chl 'b'	Chl 'c'
NH ₃	1												
NO ₃	-0.585	1											
NO ₂	-0.556	0.936	1										
PO ₄ ³⁻	0.999	-0.553	-0.527	1									
SiO ₂	-0.117	0.685	0.862	-0.088	1								
Calcium	-0.838	0.643	0.428	-0.828	-0.085	1							
Mg ⁺	0.875	-0.886	-0.782	0.856	-0.359	-0.895	1						
Cell count	0.655	-0.965	-0.987	0.627	-0.772	-0.564	0.870	1					
Salinity	-0.837	0.912	0.799	-0.816	0.387	0.885	-0.997	-0.883	1				
TA	-0.347	0.322	-0.020	-0.339	-0.438	0.792	-0.507	-0.115	0.522	1			
Chl 'a'	-0.561	0.499	0.751	-0.555	0.736	0.100	-0.471	-0.707	0.445	-0.514	1		
Chl 'b'	-0.422	-0.374	-0.173	-0.452	-0.225	-0.038	0.054	0.159	-0.126	-0.413	0.463	1	
Chl 'c'	0.338	-0.914	-0.742	0.302	-0.507	-0.614	0.750	0.780	-0.796	-0.545	-0.118	0.690	1

In table 4 at Control the highly positive correlation 0.99 was observed between phosphate and ammonia. At the same time the highly negative correlation -0.98 was observed between Cell count and Nitrite. The amount of net nutrient uptake was calculated by subtracting the final concentrations from their initial values and has been presented in Table: 1, 2, 3 and 4.

Table 5 Probability values for changes in all nutrients and chlorophyll concentration of the *A. Subtropica*

ANOVA (P Value)		
Parameters	Across pH	Time of exposure
Ammonia	0.000	0.406
Nitrate	0.000	0.295
Nitrite	0.000	0.054
Silicate	0.000	0.440
Phosphate	0.000	0.165
Chlorophyll 'a'	0.171	0.003
Chlorophyll 'b'	0.354	0.046
Chlorophyll 'c'	0.690	0.107
Calcium	0.000	0.974
Magnesium	0.000	0.436
Cell count	0.807	0.042
Total Alkalinity	0.000	0.393
Salinity	No variation	No variation





Rajeswari Balakrishnan et al.

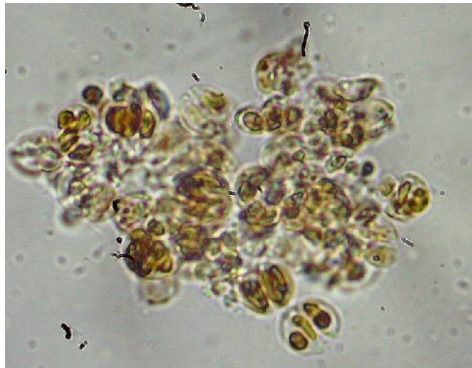


Fig. 1. The structure of *A. subtropica* (scale bar =10 μ m)



Fig. 2. Experimental set up of *A. subtropica*

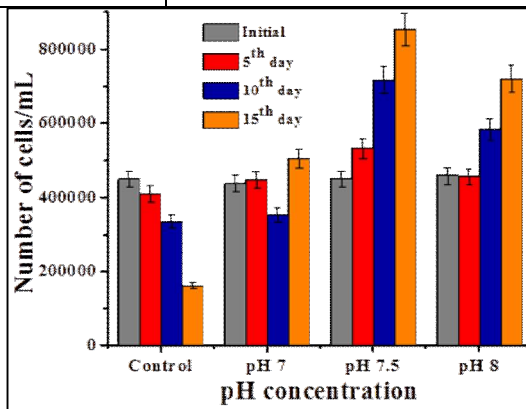
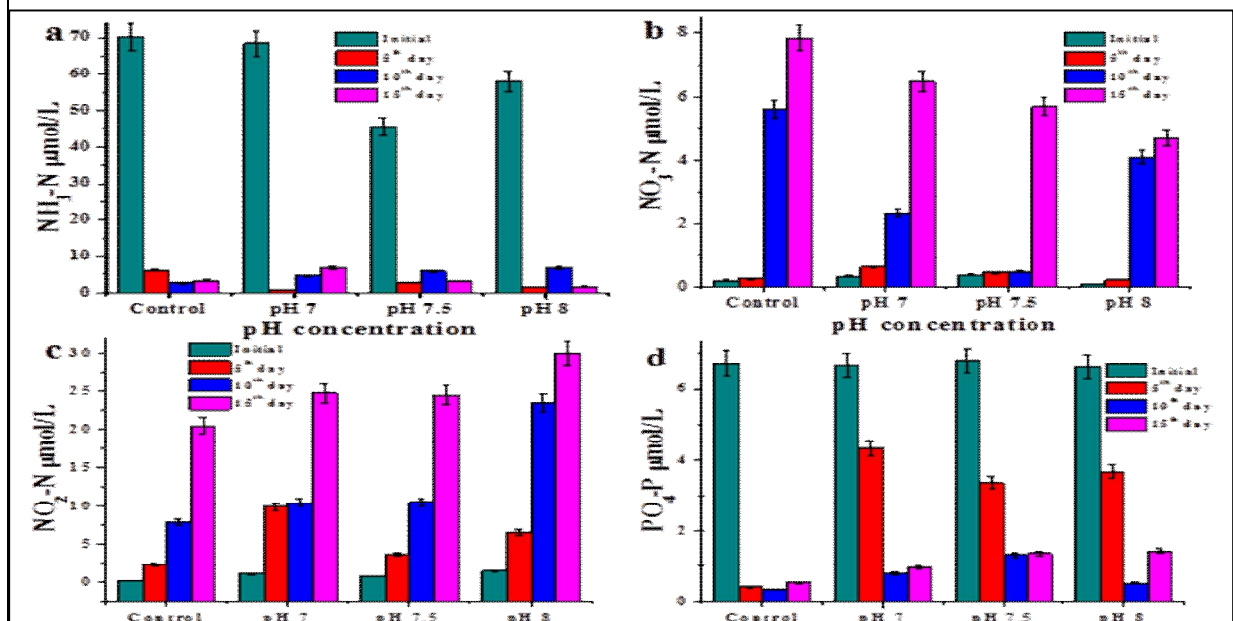


Fig. 3. Growth of marine diatom *A. subtropica* with different pH concentration.





Rajeswari Balakrishnan et al.

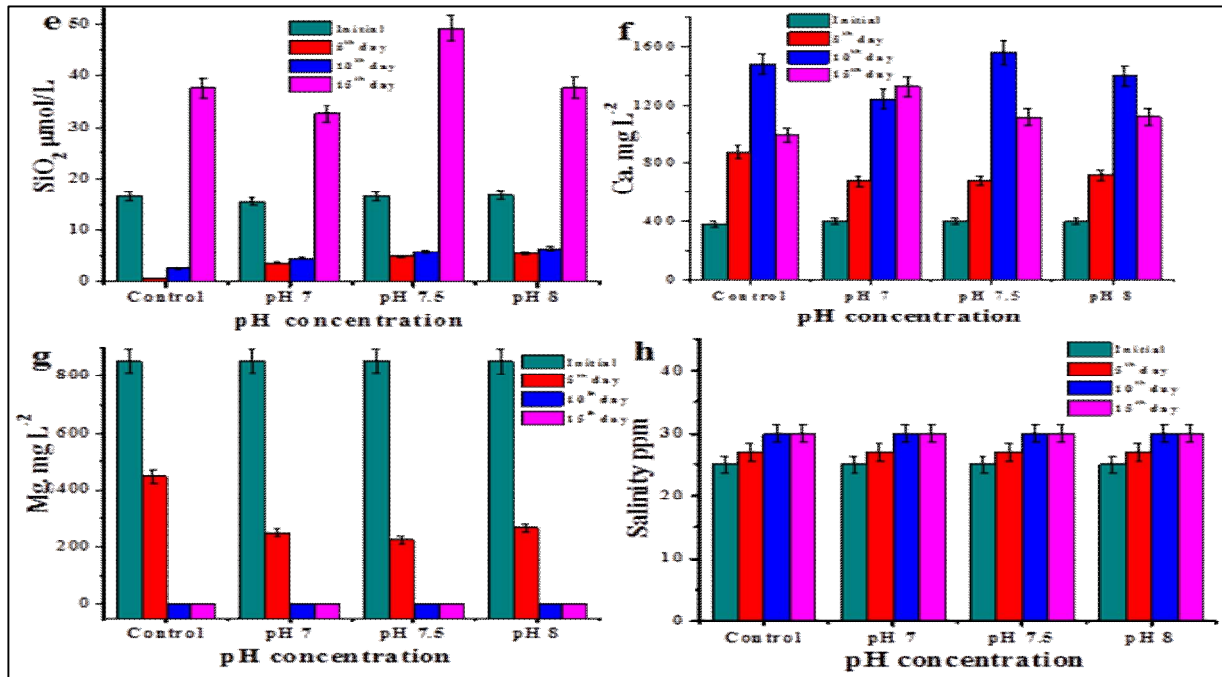


Fig. 4. Physico-chemical parameters of ammonia (a), nitrate (b), nitrite (c), phosphate (d), silicate (e), calcium (f), magnesium (g) and salinity (h) with different pH concentrations

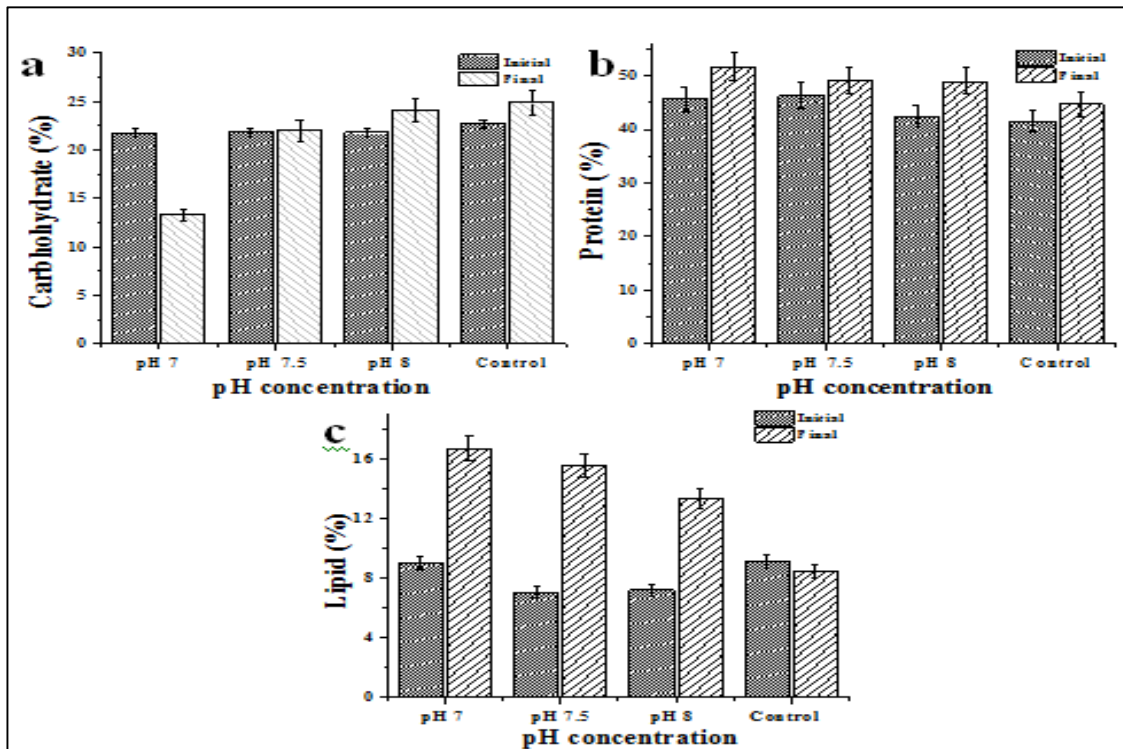


Fig. 5. Carbohydrate (a), protein (b) and lipid (c) in *A. subtropica* under different CO₂ concentrations during the experimental period (From 1st to 15 day).





Rajeswari Balakrishnan et al.

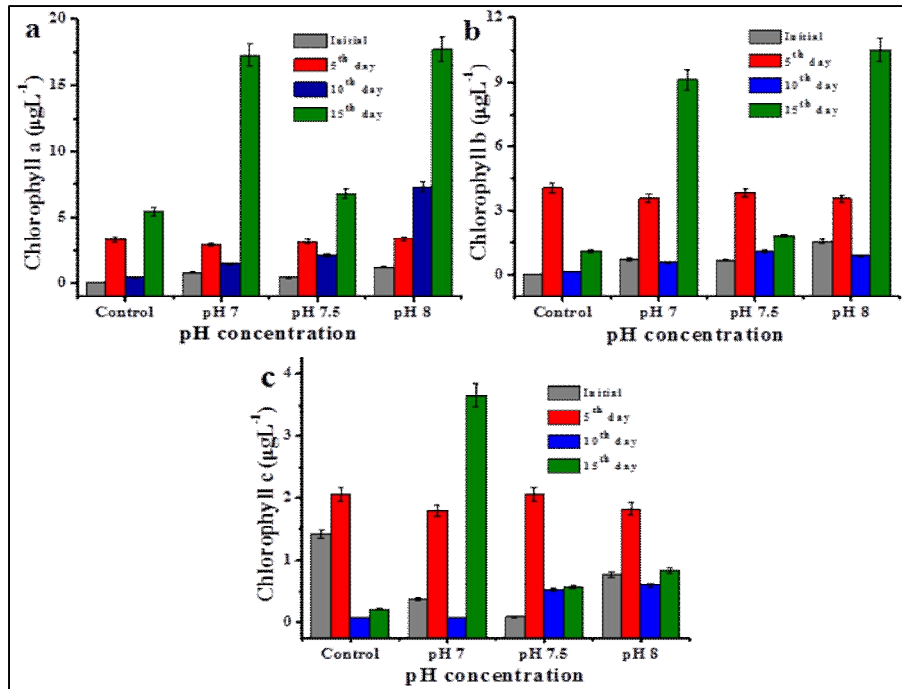


Fig. 6. Chlorophyll contents: chl 'a' (a), chl 'b' (b) and chl 'c' (c) with different pH concentrations

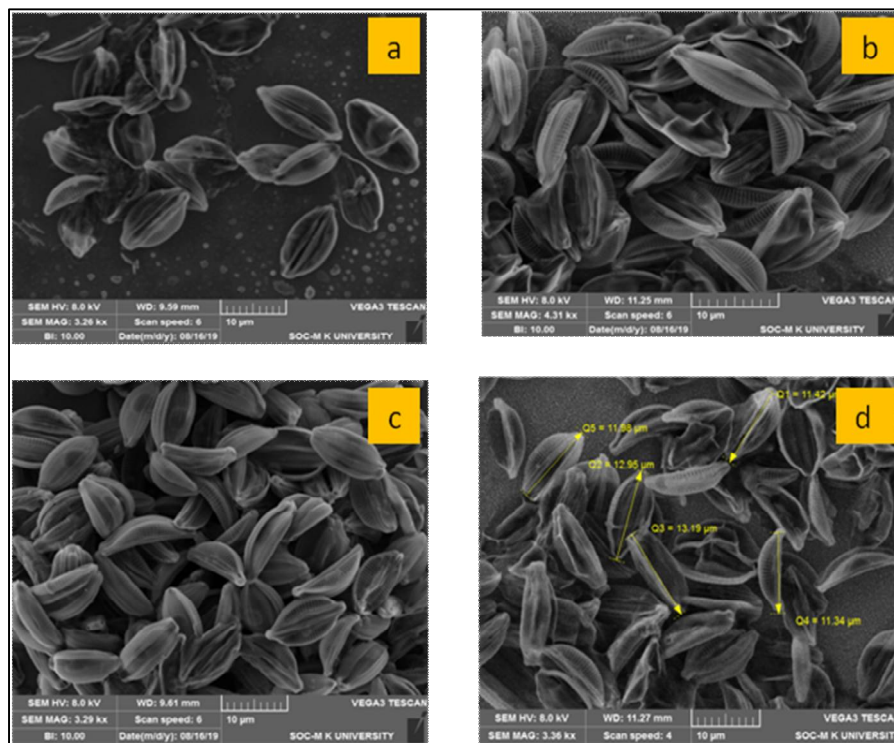


Fig. 7 Scanning electron microscope images: Control (a) pH 8 (b), pH 7.5 (c), pH7 (d) of *A. subtropica* in 10µm





Rajeswari Balakrishnan et al.

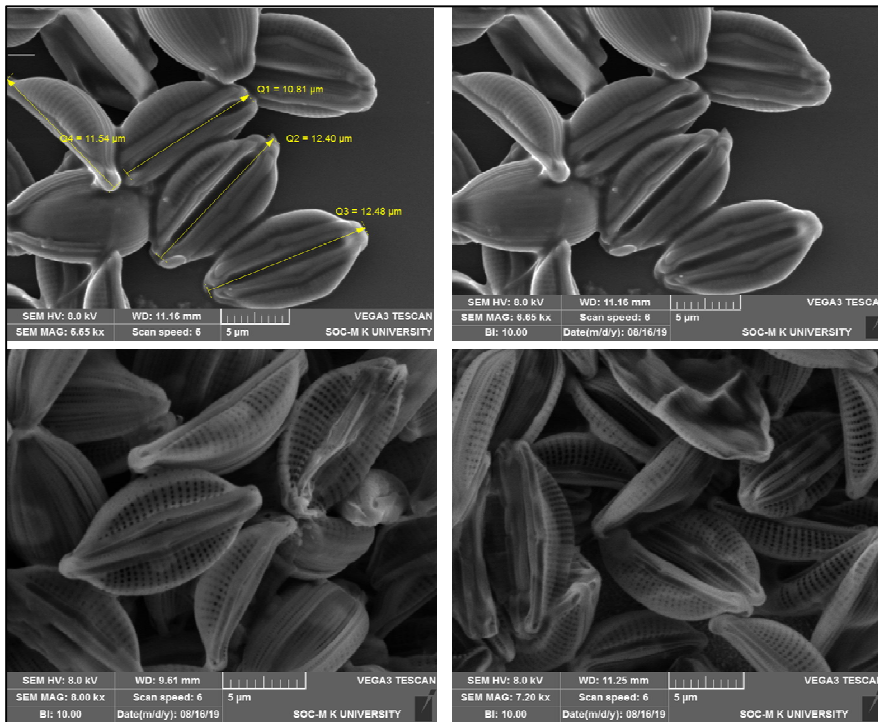


Fig. 8 Scanning electron microscope images: Control (a) pH 8 (b), pH 7.5 (c), pH7 (d) of *A. subtropica* in 5μm

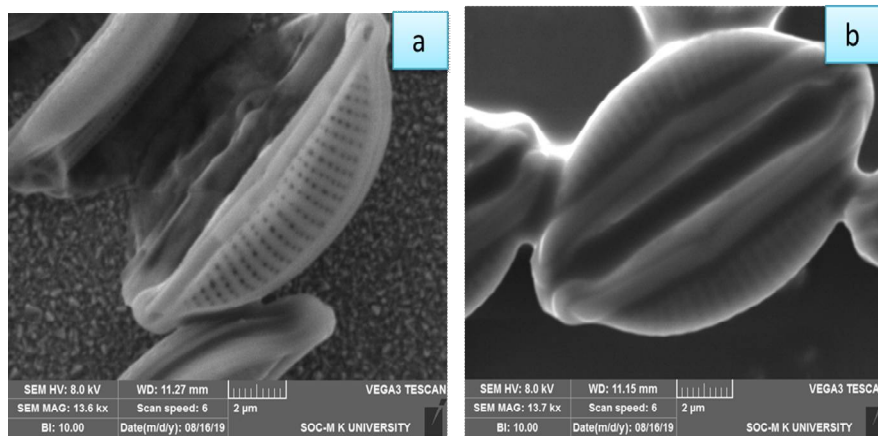


Fig. 9 Scanning electron microscope image: Control (a) pH7 (b) of *A. subtropica* in 2μm





Teacher's Philosophies and Logic: Indeed, Earned Students' Highest Trust and Confidence

Edilmar P. Masuhay^{1*}, Rosemarie C. Arcaya² and Gil M. Alegre²

¹Surigao State College of Technology, Magpayang, Mainit, Surigao del Norte, Philippines.

²Surigao State College of Technology, Surigao City, Philippines.

Received: 20 Aug 2019

Revised: 25 Sep 2019

Accepted: 29 Oct 2019

*Address for Correspondence

Edilmar P. Masuhay

Surigao State College of Technology,

Magpayang, Mainit,

Surigao del Norte, Philippines.

Email:yahusamedilmar@gmail.com



This is an Open Access Journal / article distributed under the terms of the **Creative Commons Attribution License** (CC BY-NC-ND 3.0) which permits unrestricted use, distribution, and reproduction in any medium, provided the original work is properly cited. All rights reserved.

ABSTRACT

Mathematics is one of among the funniest subjects ever taught in the curriculum however it depends on how teachers performs his duty to satisfies this means. This study showed that Teachers has rumbled personalities, wrangled philosophies and acted their logic differently. This paper served asan exploratory survey about the pulse of mathematics by all possible ways in one of the prestigious State Universities and Colleges (SUC's) of the Philippines. Collated data thru investigation, evaluated the frequencies of faculty potentials on how this faculty upholds their duty to put the university in the level of excellence and competence. Results displayed teacher's performance on how he earned the students' highest trust and confidence.

Keywords: Mathematics, Potential teachers, Weaknesses of teachers, Agonies of students in mathematics, Student's reflection on mathematics.

INTRODUCTION

Plato said, "God is a geometer." Jacobi changed this to, "God is an arithmetician." The came Kronecker and fashioned the memorable expression, "God created the natural numbers, and all the rest is the work of men." by Felix Klein (Kuo, 2010). Recent reforms probably focus much in upgrading the educational system with inclination to professional growth of the faculty, and technological advances that provides first hand opportunities for both the teacher and the learners (pupils and students). However, issues focused on the level of the learners' conceptions are quietly behind and the readiness of the teachers is mainly based on their skills and qualifications (Okpala, & Ellis, 2005); (Guo, Connor, Yang, Roehrig, & Morrison, 2012).On the other hand, strategic teaching in the classroom on "how to teach" were preferably to produce competent graduates with excellence performance that well make known





Edilmar P. Masuhay et al.

and recognized by their field of expertise. And this simply adds-on merit for the university's prestige. Whereas, this case surely predestine the students to sojourn this platform may be true to all of the educational level..., both in rural and urban categories most precisely in remote areas, and noticed also that the country's educational system highly regarded on standard-based strategies in teaching (Borkowski, & Muthukrishna, 1992); (Murdoch, & Wilson, 2008); (Lawrence-Brown, 2004). However, above idealism were misinterpreted by some educators they pretend to be more competent in their field of expertise, and wishing to enhance their students qualities based on their expectations and somehow prejudged the learners that leads to frustrations and depressions and impacted the philosophies of the students that made him gloomy, and this burdens those mediocre students (in average intelligent quotient level) and take a hard time or even doubled their time to struggle just to cop up his teacher's anticipation and the worst is it infected the other subjects taught in the curriculum, because his time management has been ruined at all. But then, a Microteaching is hereby introduced as other means of teaching at any age level, as an effective learning technique for effective teaching. Whereby, it describes that learning is a change of behavior, which is brought about by activity, training, or experiencing at any age.

This method also increased teacher's self-confidence in an atmosphere of friendliness and equanimity (Masuhay, 2018). Then, considering also this shared quotation of Bale Gates that "Technology is just a tool. In terms of getting the kids working together and motivating them, the teacher is most important" that Teacher is the key figure in school. The success of the school and of the students in terms of each educational progress rests on the active awareness and leadership of the teacher in carrying out its programs. The Teacher are expected to initiate techniques and strategies that create meaningful and favorable atmosphere in which educational process is successfully took place. He should help set the goals for the school in allotting resources needed to arrive at the desirable teaching-learning situation. These cited literatures, are more precisely concerned on the teacher's development and stratification of curriculum standards that plotted to incur technological advances in order to level up the quality standards of education and to be globally competitive, but then how about the issues referring on the learners' conceptions which involves the behavioral pedagogy that understood the weakness and strengths of the students (Rilles, 2019). This study discovered teacher's desirable virtues and appropriate methodology that may able to transform his students' resemblance to the desired outcomes. He is one of a kind, a teacher and a good leader, that keeps always a good ideas for his students to do something better. The scenario has inspired the author and decided to draw a conclusive perspective by *prima-facie* evidence. So, as far as teacher-educator-researcher is concern, and in the pursuit to national development and progress. Hereafter, the study on the Learners' perspective on their teacher's instructional techniques in Mathematical investigation and modeling of graduate studies at CSU has been explored to justify the means (Chauvot, 2009); (Giles, 2007); (Goodchild, 2008); (Wilson, 2006); (Tack, & Vanderlinde, 2014).

Objectives of the Study

The study investigated and *measured the perspective views* of students on their teacher's philosophies and logic and indeed, this study showed results on how teacher earned his students' highest trust and confidence. Thereby, the following the following hypotheses were considered: H₁: Students personal and socio-demographic has no significance to their attitudes and habits in the Classroom; H₂: Teacher instructional techniques has significance to motivate, conveyed the learners and learnt the topics; H₃: Teacher virtues has significance in transforming their students; H₄: Technology has significance in communication; and H₅: There is no significance relationship between the teacher's instructional techniques across the learners' personal and the related socio-demographic records of the students.

Theoretical / Conceptual Framework

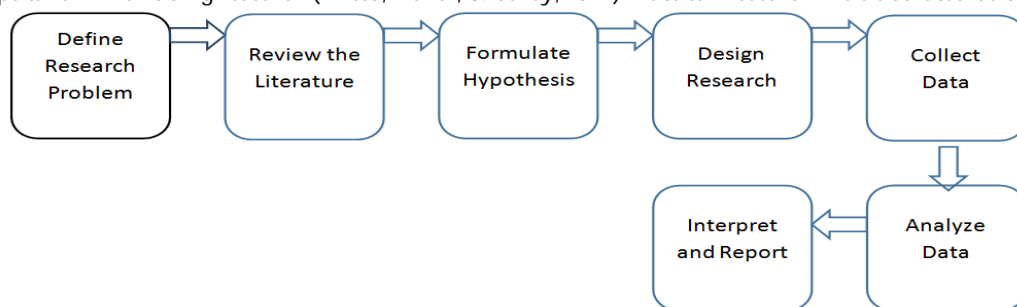
In formulating a questions, the theory of Flick (2002) should be applied. The flow: formulation of the overall question, formulation of specific research question, formulation of sensitizing concepts, selection of research groups with which to study the question, selection of appropriate designs and methods, evaluation and reformation of the specific





Edilmar P. Masuhay et al.

questions, collection of data, analyzing of data, generalization and evaluation of the analyses and formulation of the findings (Prado, Penaso, Cimene, Aves, & Simbulas, 2011). The research process followed diagrammatic presentation of the steps taken when doing research (Prieto, Naval, & Carey, 2017). Practical Research. As elaborated below:



Depicts by Prado, et.al. (2011), that the hypotheses are formulated before the study is conducted because they provide direction for data collection, analysis and interpretation. Hence, the hypothesis flow from the problem statement, literature review, and theoretical framework (Prado, et.al., 2011). This is illustrated below:



Source: Wood & Haber (1998)

MATERIALS AND METHODS

The study has utilized the following instruments: First, the Judge’s Items Rating Form for determining the Content Validity, (Prado, et.al. (2011). Methods of Research, page 134, Source: Martuza, Hambleton, and Bausell, as cited by Gregory (1996), applied to pre-determine the validity of the questionnaire with the principles of Comery (1973) rated orthogonal factor loadings as follows: 0.73 and above is excellent; 0.63 – 0.70 is very good; 0.55 – 0.62 is good; 0.45 – 0.54 is Fair; and 0.32 – 0.44 is Poor. Second, the Semantic Differential Scale and Likert Scale, Prado (1995) used as a tool during the conduct of face-to-face questioning and interview, answered questions/hypotheses relevant to learner’s perspective on their teacher’s instructional techniques and the attitudes of the learners in the Classroom, in the scale specified from 1 to 5. Wherein 1, is equated to Strongly Disagree (SD); 2, is Disagree (D); 3, is Neutral (N); 4, is Agree (A); and 5, is Strongly Agree (SA). Third, Descriptive statistics, were utilized in computing the mean values of the learners’ perspective on their teacher’s instructional techniques that includes: frequency and percentages and standard deviation, with criterion for mean values as follows: Very Low 1.0 – 1.80; Low 1.81 – 2.60; Average 2.61 – 3.40; High 3.41 – 4.20; and Very High 4.21 – 5.0 interpreted the data gathered. Fourth, Statistical Package for Social Sciences (SPSS) processor were done through described the data for presentation purposes as emphasized by Masuhay, (2018).

Technically, the study undergo the following activities: the validity of questionnaire tried by ten (10) selected experts of which evidently reflected that the instrument is valid with an average rating score of 0.85, accumulated from all of the areas, with an average factor loading score of Part I, 0.8, Part II, 0.68, Part III, 0.93, and Part IV is 1.0; determining the number of contributors thru purposive sampling considering 20 respondents; the conduct of face-to-face questioning and interview every Saturday classes schedules only during their free time and leisure; tallied and tabulated group of data in order to account the number of distribution; answered questions and hypotheses by frequency counts and percentages by using a frequency table introduced by Prado, Penaso, Climente, Aves, and



**Edilmar P. Masuhay et al.**

Simbulan (2011); and calculated the frequency counts and percentages of those enumerated variables thru SPSS for presentation

RESULTS AND DISCUSSION

Respondents' personal records and socio-demographic information used as pointers to measure the frequencies and percentages of distributions as basis of analyzing the data, this can be seen in Table 1a. While, Tables from 1b-1h, shows the distribution of respondents by all of the variables specified therein. Table 1a and Tables from 1b-1h, indicates results on Frequency counts and percentages of the graduate students in Mathematics investigation and modeling in CSU, that majority are female (12 or 60%) and minority are male (8 or 40%), their ages were ranging from 20 to 50 years old of which majority of the age level full under the age of twenties (55%) with frequency counts of 11 out of 20, while, the marital status mostly were single in a percentage of 65:35, acquired Mathematics Bachelor's degree in BSEd, BSE and other related courses in a ratio of 13:5:2, Majority has its tenure of appointment in a count of 16, while the rest is under contractual or probationary status, 7 from these respondents has more than "5 siblings", 1 respondent has "five siblings" 2 respondents has "4 siblings", 3 respondents has "3 siblings", 3 respondents has "2 siblings" and 4 respondents has "1 sibling", most of these respondents where geographically beyond the boundaries of Butuan City with percentile records of 60:40.

Table 2, showcase a results during the conduct of face-to-face questioning and interview that would particularly answers questions/hypotheses relevant to learner's perspective on their teacher's instructional techniques and the attitudes of the learners in the Classroom, in the scale specified from 1 to 5. Wherein 1, is equated to Strongly Disagree (SD); 2, is Disagree (D); 3, is Neutral (N); 4, is Agree (A); and 5, is Strongly Agree (SA). Wherein it can be seen that most of the items has reflected that there were bigger proportions of students who agree or strongly agree. This implies that majority of those learners has positive perspective in respect to their teacher's instructional techniques. Based on *frequency and percentage counts*, majority of the learners has described that their teacher utilized *Student focused* as means of instructional techniques in the classroom, indicated in Table 3. And it can be seen that most of the respondents preferred to study alone, and feeling comfortable once their teacher used student focused strategies in teaching. Although, students has complex ideas on feed backing but rest assured all of them needs their teacher's feedback.

Table 4, this prescribed the Teacher's Teaching Methods in the Classroom. In conformity 85% among the respondents were proportionally motivated and self-disciplined, 100% with confidence to learn the subject, and 100% liked their teacher's feed backing. While on the other views, 6 out of 20 respondents thought to believed that learning can take place without having a face-to-face interaction with the teacher, 2 out of 20 respondents felt uncomfortable with their teacher's methodology, 3 are not comfortable communicating in writing, 3 has no reading habits, 2 accepted that they were not self-motivated, 2 confessed that they are not comfortable with their teacher's methodology and 1 doesn't need the teacher's motivation

CONCLUSION AND RECOMMENDATION

Study reflected that teacher's motivational strategies and virtues ignites his students' interest in participating and be more progressive. Eventually, students felt comfortable with their teacher motivational strategies, students wanted to have their teacher's feedback and preferred to be with their teacher or classmates. Teacher simplified the situations under complexities though mostly students has no internet access at their home, they still believed that computer can help them in learning, take place without having a face-to-face interaction with their teacher, and they were comfortable communicating in writing and enjoyed reading. By evidence, the factors that affects the teacher's instructional techniques to be more effective were due to the fact that the teacher itself has desirable virtues, and students are self-motivated with self-disciplined, and with confidence to learn the subject. Finally, this study answers





Edilmar P. Masuhay et al.

all the hypotheses therein from H_1 to H_6 . Such that the Teacher's instructional techniques has significance in transmitting educations indeed to target students with positive virtues but delimit to students with behavioral problems. But rather, this study tells that there is no significant relationship between the teacher's instructional techniques across the learners' personal and the related socio-demographic records of the students. So, the study clearly stressed that transmitting education to students with positive attitudes is not a problem, but sojourn to students with behavioral problems. The study contemplated that Students personal and socio-demographic has no significance to their attitudes and habits in the Classroom, that Teacher instructional techniques has its significance to motivate, conveyed the learners and learnt the topics, that Teacher virtues has significance in transforming their students, that Technology has the significance in communication and that there is no significance relationship between the teacher's instructional techniques across the learners' personal and the related socio-demographic records of the students.

REFERENCES

1. Okpala, C. O., & Ellis, R. (2005). The Perceptions of College Students on Teacher Quality: A Focus on Teacher Qualifications. *Education*, 126(2).
2. Guo, Y., Connor, C. M., Yang, Y., Roehrig, A. D., & Morrison, F. J. (2012). The effects of teacher qualification, teacher self-efficacy, and classroom practices on fifth graders' literacy outcomes. *The Elementary School Journal*, 113(1), 3-24.
3. Borkowski, J., & Muthukrishna, N. (1992). Moving metacognition into the classroom: "Working models" and effective strategy teaching.
4. Murdoch, K., & Wilson, J. (2008). *Creating a Learner-centred Primary Classroom: Learner-centered Strategic Teaching*. David Fulton Publishers.
5. Lawrence-Brown, D. (2004). Differentiated instruction: Inclusive strategies for standards-based learning that benefit the whole class. *American secondary education*, 34-62.
6. Masuhay, E. P. (2018). A Teacher's Will Nor His Strategies, Guides Itself to Motivate the Learners' Desires. *Int'l J. Soc. Sci. Stud.*, 6, 1.
7. Rilles, G. M. (2019). WHY TEACHERS STILL MATTER MOST IN THE DIGITAL AGE?. *PROCEEDING IAIN Batusangkar*, 3(1), 13-16.
8. Chauvot, J. B. (2009). Grounding practice in scholarship, grounding scholarship in practice: Knowledge of a mathematics teacher educator–researcher. *Teaching and Teacher Education*, 25(2), 357-370.
9. Giles, D. (2007). Humanising the researcher: The influence of phenomenological research on a teacher educator. *International Journal of Pedagogies and Learning*, 3(1), 6-12.
10. Goodchild, S. (2008). A quest for 'good' research: The mathematics teacher educator as practitioner researcher in a community of inquiry. In *The Handbook of Mathematics Teacher Education: Volume 4* (pp. 201-220). Brill Sense.
11. [Wilson, S. M. (2006). Finding a canon and core: Meditations on the preparation of teacher educator-researchers. *Journal of Teacher Education*, 57(3), 315-325.
12. Tack, H., & Vanderlinde, R. (2014). Teacher educators' professional development: Towards a typology of teacher educators' researchly disposition. *British journal of educational studies*, 62(3), 297-315.
13. Prado, N.L., Penaso, A.M., Cimene, F.T., Aves, L.S., & Simbulas, S.G. (2011). *Methods of Research*, page 68, page 147.
14. Prieto, N.G., Naval, V.C., & Carey, T.G. (2017). *Practical Research*
15. Prado, N.L. et al., (2011). *Methods of Research*, page 184.
16. Campus Map and Virtual Tour | Caraga State University. (n.d.). Retrieved July 17, 2018, from <http://www.carsu.edu.ph/?q=about-csu/campus-map-and-virtual-tour>.
17. Kuo, Stephen (2010). *Successful and Satisfied for Teachers*, pages 6-7.





Effect of Dark / Light Daytime Cycle on Integrin Protein Expression in Retina of Adult Mice

Ali Abdul sattar*, H.A.Jafer and H.Abaas Ajar alla

Alnahrain University, Medical College, Baghdad, Iraq.

Received: 20 Sep 2019

Revised: 22 Oct 2019

Accepted: 20 Nov 2019

*Address for Correspondence

Ali Abdul sattar

Alnahrain University,
Medical College,
Baghdad, Iraq.



This is an Open Access Journal / article distributed under the terms of the **Creative Commons Attribution License** (CC BY-NC-ND 3.0) which permits unrestricted use, distribution, and reproduction in any medium, provided the original work is properly cited. All rights reserved.

ABSTRACT

The retina is a thin, delicate, transparent sheet of tissue derived from the neuroectoderm. It comprises the sensory neurons that begin the visual pathway. Light must traverse these many layers before initiating signal transduction in the rods and cones. Integrins are a family of heterodimer plasma membrane proteins important for cell-cell and cell-extracellular matrix of retina. They consist of variable α and β subunits. It provides a link between their extracellular ligand and the cytoskeleton of sensory neurons and helps modulate various signaling pathways including, cell adhesion, migration, differentiation, angiogenesis. Aim of this study is to evaluate the morphological and histological changes of retina in response to dark and light cycle. To assess the IHC reactivity of integrin protein marker in retina in response to dark and light cycle by applying Aperio image scope analysis software. A forty (40) adult healthy male mice (albino mice), weighing between 25-30 g were divided into four groups (each with 10 mice): A, B, C & D according to dark/ light day periods. Animals in group A were kept in normal diurnal variance, 10hr dark and 14 hr light. Group B animals were kept in full time light. Group C animals were kept in full dark. Group D animals were kept in inverse state (10hr of full dark during daylight and 14hr light during the night). All animals were euthanized at 45 days by inhalation of chloroform in soaked cotton piece. The whole eye ball was dissected and fixed in 10% natural buffered formalin, processed for paraffin blocks and stained for H&E and IHC for integrin (monoclonal antibodies Ab183666). Histological slides were assessed by image J software version (1.47p) for histomorphometric analysis of thickness of retina, rods and cones, and bipolar cells. Immunohistochemical analysis done by Aperio positive pixel count algorithm (V11) for assessment of total positivity of integrin. Histomorphometric analysis revealed that the highest thickness of retina was recorded in dark group ($139.02 \pm 2.53 \mu\text{m}$), while control group had the least thickness ($116.86 \pm 6.67 \mu\text{m}$) with significant differences. Mean bipolar cells thickness ranged from $70.71 \pm 4.81 \mu\text{m}$ in control group to $97.21 \pm 8.17 \mu\text{m}$ in dark group. In between, lies bipolar cell thickness of inverse and light group with significant differences. The highest and least thickness of rods and cones were reported in dark group and control group respectively ($80.33 \pm 5.06 \mu\text{m}$ and $43.46 \mu\text{m}$

17853



**Ali Abdul sattar et al.**

respectively). A significant variation in integrin expression was seen, with light group showed the highest expression (0.295 ± 0.04), while the dark group had the lowest expression (0.158 ± 0.014). There is marked effect of light on decrease in thickness of retina as a whole as well as each of bipolar cells, rods and cones indicating an apoptotic mechanism that responsible for death of photoreceptors and bipolar cells. Increased integrin expression in light group animals compared to other groups is due to receptor effect of integrin on the retinal pigment epithelium (RPE)-photoreceptor interface which promotes RPE phagocytic signaling in response to circadian photoreceptor shedding. Thus, the normal diurnal cycle of light and dark seems to be the essential factor in controlling visual cell viability and susceptibility.

Key words: retina, integrin, photoreceptors.

INTRODUCTION

The mouse eye is similar to other vertebrate animals, which has a cornea and lens that refract light to form an image on the light sensitive retina. (Remtulla and Hallett, 1985; Lyckman *et al.*, 2008), and they have a large lens accounting for 60% of the axial length (Remtulla and Hallett, 1985). The lens transmits ultraviolet light, essential for the ultraviolet sensitive photoreceptors found in the mouse retina (Douglas and Jeffery, 2014). The retina is about 0.5 mm thick and lays the back of the eye. The optic nerve contains the ganglion cell axons running to the brain and, furthermore, incoming blood vessels that open into the retina to vascularize the retinal layers and neurons. Integrin's are the main cell-ECM adhesion receptor that links the internal signaling components of the cytoskeleton to the extracellular proteinaceous microenvironment. There are 18 and 8 β subunits, comprising 24 unique integrin receptor heterodimers with various affinities for binding different extracellular matrix (ECM) proteins. (Hynes RO. 2002).

Integrin's are capable of mediating signal transduction through the cell membrane in both directions: binding of integrin's to ECM ligands results in cell signals that have effects on proliferation, survival, migration and gene expression (termed outside-in signaling) and signals from within the cell, as a result of, for example growth factor stimulation, can act to regulate integrin ligand-binding affinity and cell adhesion (termed inside out signaling). Expression of some of the integrin receptor has been studied using cultured or in situ RBE previously (Andresonet *al.*, 1990; Meitinger *et al.*, 2001). Aim of this study is to evaluate the morphological and histological changes of retina in response to dark and light cycle. To assess the IHC reactivity of integrin protein marker in retina in response to dark and light cycle by applying Aperio image scope analysis software.

MATERIALS AND METHODS

A forty (40) adult healthy male mice (albino mice), were collected from technical biological institute, aged about 8 weeks (Nakamura1 *et al.*, 2018) weighing between 25-30 g . These were kept at room temperature (20 ± 2 C °)(Nakamura1 *et al.*, 2018) in a clean and well ventilated room and The cages of group A&C illumination by LED white light in intensity 40 watts

Sample collections

The animals were divided into four groups according to daily illumination times (dark /light cycle). Each group has 10 male mice and were kept in different illuminated room. The 40 male young adult mice are applied in the study. They were classified into group A, B, C & D according to dark/ light day periods in which the animals were kept. The group A 10 animals were kept in normal diurnal variance, 10 hrs. Dark and 14 hrs. Light for period of one month. The Group B 10 animals were kept in room with full time light for period of 45 day. The Group C 10 animals were kept in room with full time of darkness for period of 45day. The Group D 10 animals were kept in inverse state

17854



**Ali Abdul sattar et al.**

for normal diurnal variance (10hr of full darkness during daylight and 14hr light during the night) for 45day Immediately after removal the specimens of eye bull were fixed in 10% Neutral Buffered Formalin (NBF). Then the tissue staining of Hematoxylin and eosin (H & E) is method used for histological microscopic examination of tissue that have been fixed, processed, embedded, and sectioned. The principle of IHC detection kit is to detect a specific antibody bound to an antigen in tissue sections. The specific antibody is located by a secondary antibody polymerized to an enzyme. The specific antibody, secondary antibody enzyme complex is then visualized with an appropriate substrate/chromogenic. The advantage offered by a micro-polymer detection system over an ABC based detection system is that its biotin free (ideal for studying tissue rich in endogenous biotin e.g. kidney or brain tissue). In addition, the use of a micro-polymer detection system is advantageous over a polymer detection system as a smaller detection complex is formed rather than a polymer backbone aiding better tissue penetration.

The primary antibody (Anti-Integrin beta 1 antibody) (Ab183666) is a biotin free immunoenzymatic antigen detection system this technique involves the sequential incubation of the specimen with an unconjugated rabbit or mouse primary antibody specific to the target antigen , a secondary antibody – Goat anti-rabbit HRP Conjugate and substrate-chromogenic. Staining protocol for Anti-Integrin beta1 antibody (ab183666) was applied in this study. The positive control: epithelial tissue of testes was stained for integrin in the same staining steps and the negative control for retina of mice was stained in the same staining steps except the primary antibody EPCAM & MDA were replaced by PBS.

Digital Image Analysis Software

Image J was used the software Image J (Java-based image processing program developed at National Institutes of Health, USA) version 1.47p; which already installing of personal computer. Image J software is keystone in the morphometric study by which different processing and procedures can be performed. It can read many image formats including TIFF, GIF, JPEG, and BMP. It can calculate area and pixel value statistical of user- defined selection, it use for scale bar application in image J as follow (Abramoff *et al.*, 2004).

Immunohistochemical Assessment (Aperio Algorithm Program)

Gene light microscope in Histology Department, Medical College, University of Al-Nahrain with its camera were used to capture the fields and by using Aperio Image Scope V11 count algorithms program to quantify the amount of a specific color in a tissue section, this system has a set of default input parameters which have been configured for brown color quantification in the three intensity ranges (degrees) which are either weak positive, positive and strong positive were applied. In the current study we assess the immunohistochemical reactivity using the positivity. Then using the Image J software (Java –based image processing program developed at the National Institutes of Health, USA), version 1.47p, which already installed in a personal computer. Image J software is the keystone in the morphometric study by which different processing and procedures can be performed.

RESULTS

The retina thickness according to dark/ light life cycle by applying Hematoxylin and Eosin staining reveals increase in thickness of retina in dark group animals in contrast to light group which had a marked decrease in values: $139.02 \pm 11.31 \mu\text{m}$ and $133.22 \pm 11.89 \mu\text{m}$ respectively. This is achieved by applying image J program. The variation in retina thickness between the four groups was relatively low; however, this variation reached a significant level (Table 1), with the highest mean thickness was recorded in dark group ($139.02 \pm 2.53 \mu\text{m}$) in comparison to light group animals, while control group had the least mean thickness ($116.86 \pm 6.67 \mu\text{m}$) as shown in figure 1. Dark group differed significantly from all the other groups. Light group came second and differed significantly from control group only, while there was no significant difference between inverse group and control group (Table 2). The retina





Ali Abdul sattar et al.

of experimental groups reveals increase in thickness of photoreceptors (rods & cone layer) retina in dark group which records $80.33 \pm 16.8 \mu\text{m}$ while light group reveal a marked decrease in values which record $76.1 \pm 34.57 \mu\text{m}$. This is achieved by applying image j program. Table 3 and figure 2 illustrates respectively the descriptive statistics and mean rods and cones thickness in different groups. The highest thickness were recorded in dark group animals in comparison to light group animals and least in values in control group and they record $80.33 \pm 5.06 \mu\text{m}$, 76.1 ± 34.57 and $43.46 \mu\text{m}$, respectively). Overall, there was a highly significant difference between the four groups. Multiple comparison divided the study groups into two categories: control group and inverse group on one hand which had comparable values with no significant difference between them, while dark group and light group on the other hand also had comparable values with no significant difference between them, but differ significantly from the first category (control group and inverse group) as shown in table 3-4.

The retina of experimental groups reveals increase in thickness of bipolar cells layer retina in dark group while in light group they reveal a marked decrease in values which record $97.21 \pm 30.6 \mu\text{m}$ & $94.57 \pm 16.44 \mu\text{m}$, respectively. The mean bipolar cells layer thickness ranged from $70.71 \pm 4.81 \mu\text{m}$ in control group to high value $97.21 \pm 8.17 \mu\text{m}$ in dark group. While the intermediate results is seen in inverse and light group. The p-value showed significant differences between the four groups (Table 3-7, figure 3-4). Mean bipolar cells thickness of retina reveals high values in dark group in comparison to light, reverse and control groups which are recorded 97.21 ± 8.17 , 94.57 ± 16.44 , and 74.95 ± 18.71 & $70.71 \pm 4.81 \mu\text{m}$, respectively. Although this showed that there was no significant difference between dark and light groups. A multiple comparison between the groups showed that there was no significant difference between dark and light groups, while both of them differed significantly from each of inverse and control groups, which did not differ significantly from each other's (Table 3-8).

Immunohistochemical reactivity of integrin

Integrin alpha2 and 3 is dimerize with beta 1 to form receptor for collagen, laminin and fibronectin protein in the retina. These made them detectable in the photoreceptor (outer segment of outer nuclear layer in the retina), in addition to vascular endothelium near retinal pigmented epithelium of the retina. It has protective functions (by linking protein to rod and cone layer) and a receptor activity for ECM in the retina. So that it is also present at area between the retinal pigment epithelium and neural part of retina, at the apical surface of RBE, making attachment between them and prevent from separation and detachment during the light diurnal cycle. The expression of integrin beta 1 in retinal pigment epithelium was studied immunohistochemically by applying monoclonal primary antibody against to integrin beta 1. In the light group animals they reveal a marked high expression of integrin beta 1 at retinal pigmented epithelium which evaluated as (0.295 ± 0.13) in comparison to other group animals (control, reverse, & dark) which recorded 0.197 ± 0.03 , 0.196 ± 0.05 and 0.158 ± 0.05 , respectively. In dark group animals they reveal very low expression of integrin, which estimate as (0.158 ± 0.05) .

Moreover, in reverse group animals they reveal also weak expression of integrin beta 1 at RBE, which estimate as (0.196 ± 0.05) , in comparison to control group, In control group animals they reveal expression of integrin beta 1 at RBE, which estimate as (0.197 ± 0.03) , which is higher in comparison to dark & reverse group which was 0.158 ± 0.05 & 0.196 ± 0.05 , respectively, Descriptive statistic and mean integrin Aperio score are shown in table(7) and figure (9). Generally, there were highly significant differences between different groups regarding integrin score, with light group had the highest mean score (0.295 ± 0.01) , while the inverse group had the lowest mean score (0.196 ± 0.016) . Multiple comparison between different groups (Table 8) revealed that light group differed significantly from all the other groups while there were no significant differences between dark, inverse and control groups



**Ali Abdul sattar et al.**

DISCUSSION

Effect of illumination variance on histological, morphometric features of mice retina

This present study found that there is an increase in thickness of whole retina in contrast to light group which had a marked decrease in their values that agrees with authors who found that the effect of light and unilateral visual deprivation (achieved by lid-suturing) on the retina of albino rats by lid-sutured and un-operated animals were illuminated daily for 8, 11, or 16 hrs. Also they found that increasing time of illumination would reveal a progressive decrease in thickness of the outer retinal layers that observed in un-deprived animals and in the open eye of the monocular deprived rats (E. FIFKOVA.1972). Furthermore, authors found that the applied mouse-derived cells have been used to demonstrate light-induced retinal damage model in vitro (Santos A M, 2012; Yang L P et al.,2007). also other researcher, concluded that retinal damages are induced by light depend on radiation intensity, radiation wavelength and time of exposure (Noell W K et al.,1966; Organisciak D T et al.1999).

Light-induced retinal lesions are characterized by a degeneration of photoreceptors outer segments leading to their death by apoptosis (Reme, C. E, et al.2000). moreover, reports suggested that the blue (high energy) light causes more severe damage to retinal photoreceptor cells than green (low energy) light in rats (Grimm C, 2001). The present study is applied 400 Lux as LED light as an illumination source that lead to marked decrease in the thickness of whole retina and rod and cone layer and this the same as other researchers who applied 500 lux-cold white light LED in albino rat in short term (acute) exposure with other animal that applied Long term exposure to LED at 500 lux in cycle light and dark condition (light /dark) so that will lead to induce retinal damage in experimental mice (Krigel A,2016). However, authors found that LED light caused a state of suffering of the retina with oxidative damage and retinal injury. It was observed a loss of photoreceptors and the activation of caspase independent apoptosis and necrosis. Other authors found that A wavelength dependence for the effects of light was observed according to energy of applied light more light less energy and visa versa . (Imene Jaadane,2015)

Effect of illumination variance on histological, morphometric features of mice photoreceptors in the retina.

The retina of experimental groups reveals increase in thickness of photoreceptors (rods & cone layer) of retina in dark group while in light group they reveal a marked decrease in its value this is agreed with researchers who found that the effect of Light applied continuously to the animals which live in lack of light stimuli (as in dark field) on the retina, they found that the severity of the damage to retina was related to the duration of continuous light exposure. They concluded that after exposing rats reared in dark to daylight would lead to shrinkage of the receptor endings which was observed by (Crag B.1996) other researchers found that a diurnal variation in the susceptibility of neurons to light induced cell death in the outer nuclear layer. The cells are susceptible to damage during dark period and the early light period and less susceptibility during the middle and at the end of the light period. This pattern of sensitivity to high intensity illumination is linked to light/ dark cycle and to the clock time suggesting that an underlying circadian rhythm (Duncan TE, and Osteen WK 1984).

Light applied to albino rats continuously led to a degeneration of the outer retinal layer that is photoreceptors (rods & cone) layer (O'Steen, W. K., and K. V. Anderson.1971) moreover, researchers illustrated that the loss of receptors seems to be due to effect of the length of illumination time. The decrease in thickness of the outer retinal layers in the open eye of the un-deprived animals was greater than in the deprived ones suggesting that there was more light enters the former eye. It was assumed that receptors of retina had developed a degeneration in an animal which has only one eye available keeps it open for longer periods of time than when both eyes are used. (E. FIFKOVA. 1972). These findings concluded that light has a stimulant physical factor affecting the photoreceptors activities in the retina which later on lead to degeneration, apoptosis and decrease in thickness of these cells in the outer layer of the retina.



**Ali Abdul sattar et al.**

Certain researchers (Y-M Shang *et al* 2014) found that white LED group which was exposed to 750 lux white LED light for 28 days exhibited pyknotic photo receptor nuclei, swelling of the inner segment, and a disorganized outer segment. They found that the ONL thickness was significantly decreased at day 9 and day 28 in the white and blue LED groups. Furthermore, other reporters found that the light-induced photoreceptor damage in albino mice is a widely used model. The pattern of the photoreceptor degeneration resembles the changes that occur in non-exudative degeneration of macula in retina (Izawa *et al.*, 2015; Narimatsuet *al.*, 2013). Further study showed that exposure of mice to 7000 lux of white fluorescent light for 50h followed by 70h of darkness caused retinal damage (Bai *et al.*, 2013).while Other studies recorded that there was no retinal damage was observed when mice were less exposed to the light 1200 to 1600 lux of white fluorescent light for 24h only (Chen *et al.*, 1999). The retinal damage was seen but not severe when pigmented rat stains, were exposed to a bright luminous environment of less than 10,000 lux (12h light/12h dark) for 6 consecutive days (Polosaet *al.*, 2016).

Certain studies found that there had no light-induced retinal damage model for pigmented black mice. But retinal damage model was done as an earlier study after exposure of albino mice to blue LED-light of lower intensity than those used with fluorescent light which would induce severe retinal damage(Nakamura *et al.*, 2018). This indicates that pigmented epithelium make a protective layer for the retina.Further studies concluded that the Frogs maintained on a diurnal photoperiod of light-dark cycle (14 hours light and 10 hours darkness) they reveal shedding in their rod photoreceptor outer segment tips after the onset of light. The shedding is occurred about 25 percent of the rod photoreceptors in each day while prolonged exposure to total darkness decreases the amount of shedding, then after which exposure to light will results in a large burst of synchronous shedding. However, the synchronous shedding of rod outer segment tips in the frog retina is shown to be directly related to light stimulation effect. So that they agree with present study which they concluded that the light induce rod photoreceptor shedding with decrease in thickness in frogs was previously adapted for at least 2 months to a diurnal cycle of 14 hours light and 10 hours dark.(S Basinger *et al.*, 2017).

The effect of light on retinal pigmented epithelium

The photoreceptors and retinal pigment epithelial (RPE) cells of the retina considered as the main sites of light energy absorption (Tso, M.O. 1973) It has been found that lights with shorter wavelengths (high energy light-blue) induce more retinal damage than those with longer wavelengths (low energy light-red)(Ham, W.T *et al.*, 1976; Young, R.W. 1988). In particular, LED-induced retinal RPE cell damage have been observed in several experimental animal studies (Jaadane, *et al.*, 2015) even at domestic (ordinary) lighting levels (Shang, Y.M, 2014). Furthermore, they showed that light-damaged cells of the retinal pigment epithelium (RPE) also die by apoptosis (Remeet *al.*, 1995).

Immunohistochemical reactivity of Integrin

Integrin beta 1 has protective functions and a receptor activity in the retina. So that it is also present at area between the outer retinal pigmented epithelium and inner neural part of retina. The expression of integrin beta1 in retinal pigment epithelium was studied and assessed in this present study immunohistochemically (IHC) through applying monoclonal primary antibody against integrin beta 1 protein which is present in the retina. it was found that there was more increase in integrin expression for the light group animals in comparison to other groups and that agree with researchers who found that integrin has its sole receptor at the retinal pigment epithelium (RPE)-photoreceptor interface and promotes RPE phagocytic signaling to the tyrosine kinase (TK) once a day in response to circadian photoreceptor shedding (Emeline F *et al.*, 2006). Earlier studies found that integrin alpha 2 and 3 is dimerize with beta 1 to form dimer receptor for ECM like collagen, laminin and fibronectin protein by adhering them with the pigmented epithelium in the retina. These made them detectable in the photoreceptor (outer segment of outer nuclear layer in the retina), in addition to vascular endothelium near retinal pigmented epithelium of the retina by applying IHC technique (Integrin antibody B1) (Brem RB *et al* 1994). This made integrin protein has protective functions (by linking protein to rod and cone layer) and receptor activity for ECM in the choroid (vascular) part of retina by





Ali Abdul sattar *et al.*

binding them with RPE of inner neural retina. So that making attachment between them between the retinal pigment epithelium and neural part of retina, at the apical surface of RBE, and prevent from separation and detachment during the light/ dark diurnal cycle changes.

The effect of light on integrin expression of retina

They identify a novel role for v5-integrin in permanent RPE-photoreceptor adhesion they found that retinal adhesion by the integrin protein in mice, which made mechanically attachment of RPE with neural retina. So that the lack of integrin with normal expression of other RPE integrin greatly weakened retinal adhesion in young mice and accelerated its agedependent decline. Unexpectedly, the strength of retinal adhesion varied with a diurnal rhythm that peaked 3.5 h after light onset, after the completion of phagocytosis, when integrin signaling to TK is minimal. Permanent v5 integrin receptor deficiency attenuated the diurnal peak of retinal adhesion in 5-integrin protein in mice. These results concluded that v5-integrin is the first RPE receptor that contributes to retinal adhesion, a vital mechanism for long-term photoreceptor function and viability (Emeline F *et al.*, 2006).

The effect of integrin on endothelial choroid cell

They found that it has indicated that a major function of this integrin *in vivo* is to promote TGF β activation (proliferation) of epithelium of retina. They show that α V β 8- mRNA is strongly expressed in murine Müller glia and retinal ganglion cells. Furthermore researchers found that endothelial choroidal cells (ECs) secrete factors that remodel RPE basement membrane, and integrin receptors sense these changes triggering GTPase signals that modulate RPE tight junctions and enhance RPE barrier and adhesion function in the retina (Benedicto I *et al* 2017).

The role of integrin in integrity of RPE

This present study is agreed with authors who concluded that integrin/cell matrix interactions have a significant role between the RPE and the basement membrane in retinal maintenance and its function. They found that the functional importance of α 1 β 1 integrin for retinal pigment epithelial cell homeostasis and retinal health could be assessed by comparing α 1 integrin knockout mice with strain- and age-matched wild-type mice. They also recorded that Integrin α 1 β 1 localizes to the basal aspect of retinal pigment epithelial cells co-localizing with the basal lamina of the RPE. Furthermore, authors found that Integrin α 1 -null mice have delayed-onset progressive retinal degeneration associated with thickening of the basement membrane, defect in morphology of basal processes and fundoscopic abnormalities. This means it affect the dynamic activity of integrin protein in the development and maintenance of retina. They concluded finally that Integrin α 1-null mice display marked delays in transduction translocation compared with dark-adapted wild-type mice after exposure to light. This study indicates the significant role of integrin in the integrity of RPE of the retina. This is agreeing with Y-Wei Peng *et al* who found that there was an essential role for α 1 β 1 integrin -basement membrane interactions of the RPE in basement membrane metabolism and translocation of transduction in photoreceptors of rods and cones. This will give evidence for the essential role of Integrin / basement membrane interaction in the RPE.

CONCLUSIONS

The severity of the damage to retina through decrease in retinal morphometric values was related to the duration of continuous light exposure. The increase in integrin expression of the light group animals in comparison to other groups is due to receptor effect of integrin at the retinal pigment epithelium (RPE)-photoreceptor interface and promotes RPE phagocytic signaling once a day in response to circadian photoreceptor shedding. Integrin is the a receptor protein that contributes to retinal adhesion, a vital function in the photoreceptor layer viability integrin is the





Ali Abdul sattar et al.

first RPE receptor that contributes to retinal adhesion function and It has a major function of this integrin in activation of epithelium of retina. There is a vital role of integrin/basement membrane interaction in the RPE with the effect of light.

Recommendation

The effect various types of light (low -high energy type red-blue light on the integrin expression of the retina are evaluated. Also the effect of light on whole eye wall thickness even the cornea, lens, sclera and choroid layers should be considered.

REFERENCES

1. Remtulla, S. and Hallett, P. E. (1985) 'A schematic eye for the mouse, and comparisons with the rat.', *Vision research*, 25(1), pp. 21–31. Available at: <http://www.ncbi.nlm.nih.gov/pubmed/3984214> (Accessed: 13 July 2019).
2. Lyckman, alvin,w.Horng (2008) 'Gene expression patterns in visual cortex during the critical period: synaptic stabilization and reversal by visual deprivation.', *Proceedings of the National Academy of Sciences of the United States of America*, 105(27), pp. 9409–14. doi: 10.1073/pnas.0710172105.
3. Douglas, R. H. and Jeffery, G. (2014) 'The spectral transmission of ocular media suggests ultraviolet sensitivity is widespread among mammals', *Proceedings of the Royal Society B: Biological Sciences*. doi: 10.1098/rspb.2013.2995.
4. Hynes, RO. (2002). Integrins: Bidirectional, allosteric signaling machines. *Cell* 110: 673–687
5. Anderson, D.H., Guerin, C.J., Matsumoto, P., feffer, B, A. (1990). Identification and localization of beta-1 receptor form integrin family in mailman retinal pigmented epithelial , cell. *Invest. Ophthalmol. vis.sci*.31,81-93
6. Meitinger, D., Hunt, D.M., Shih, D.T., Fox, j.c., Hunt, R.C. (2001). Vitreous induced modulation of integrin in retinal pigment epithelial cell :effect of fibroblast growth factor -2. *Exp. Eye Res.* 73,681-692.
7. Fikova, E. (1972). Effect of Light and Visual Deprivation on the Retina. *expermentalneurology*,. 35, 450-457.
8. Santos, A.M. (2012). Sortilin participates in light-dependent photoreceptor degeneration in vivo. *PLoS One* 7, e36243
9. Yang, L. P., Zhu, X. A. & Tso, M. O. (2007). Role of NF-kappaB and MAPKs in light induced photoreceptor apoptosis. *Invest Ophthalmol Vis Sci* 48, 4766–76.
10. Noell, W.K., Walker, V.S., Kang, B.S., Berman, S., (1966). Retinal damage by light in rats. *Invest. Ophthalmol.* 5 (5), 450–473
11. Organisciak, D. T.; Darrow, R. A.; Barsalou, L.; Darrow, R. M.; Lininger, L. A. (1999). Lightinduced damage in the retina: differential effects of dimethylthiourea on photoreceptor survival, apoptosis and DNA oxidation. *PhotochemPhotobiol* 70:261-268.
12. Reme, C. E.; Grimm, C.; Hafezi, F.; Wenzel, A.; Williams, T. P. (2000). Apoptosis in the Retina: The Silent Death of Vision. *News PhysiolSci* 15:120-124;.
13. Grimm, C. (2001). Rhodopsin mediated blue light damage to the rat retina: effect of photo reversal of bleaching. *Invest Ophthalmol Vis Sci* 42, 497–505
14. Krigel, A., M. Berdugo, E. Picard, R. Levy-Boukars, I. Jaadane, L. Jonet, M. Dernigoghossian, C. Andrieu-Soler, A. Torriglia and F. Behar. (2016). Light-Induced retinal Damage Using Different light , protocols and rat strain Revels led phototoxisty, *neuroscience Source* of Pages 12
15. ImeneJaadane, Pierre Boulenguez, Sabine Chahory, Samuel Carré, Michèle Savoldelli, Laurent Jonet, Francine Behar-Cohen, Christophe Martinsons, Alicia Torriglia 2015, Retinal damage induced by commercial light emitting Diodes (LED), *free radical biology and medicine*
16. Crag, B. G. (1969). Structural changes in naive retinal synapses detectable within minutes of first exposure to daylight. *Brain Res.* 15: 79-96.





Ali Abdul sattar et al.

17. Osteen, W. K., and K. V. Anderson. (1971). Photically evoked responses in the visual system of rats exposed to continuous light. *Exp. Neurol.* 30: 525-534.
18. Izawa, H., Inoue, Y., Ohno, Y., Ojino, K., Tsuruma, K., Shimazawa, M., Hara, H., 2015. Protective effects of antiplacental growth factor antibody against light-induced retinal damage in mice. *Invest. Ophthalmol. Vis. Sci.* 56 (11), 6914–6924.
19. Narimatsu, T., Ozawa, Y., Miyake, S., Kubota, S., Hirasawa, M., Nagai, N., Shimmura, S., Tsubota, K., (2013). Disruption of cell-cell junctions and induction of pathological cytokines in the retinal pigment epithelium of light-exposed mice. *Invest. Ophthalmol. Vis. Sci.* 54 (7), 4555–4562.
20. Bai, S., Sheline, C.R., Zhou, Y., Sheline, C.T. (2013). A reduced zinc diet or zinc transporter 3 knockout attenuate light induced zinc accumulation and retinal degeneration. *Exp. Eye Res.* 108, 59–67.
21. Chen, J., Simon, M.I., Matthes, M.T., Yasumura, D., LaVail, M.M. (1999). Increased susceptibility to light damage in an arrestin knockout mouse model of Oguchi disease (stationary night blindness). *Invest. Ophthalmol. Vis. Sci.* 40 (12), 2978–2982.
22. Polosa, A., Bessaklia, H., Lachapelle, P., (2016). Strain differences in light-induced retinopathy. *PLoS One* 11 (6), e0158082
23. Nakamura M, Yako T, Kuse Y, Inoue Y, Anri Nishinaka, Nakamura S, M Shimazawa, H Har. (2018). Exposure to excessive blue LED light damages retinal pigment epithelium and photoreceptors of pigmented mice . *Experimental Eye Research* 177. 1-11
24. Basinger, S., Hoffman, R. and Matthes, M. (2017). Photoreceptor shedding is initiated by light in the frog retina. (4269), 1074-1076. *194Science*.
25. Tso, M.O. (1973). Photomaculopathy in rhesus monkey. A light and electron microscopic study. *Investig. Ophthalmol.* , 12, 17–34.
26. Jaadane, I.; Boulenguez, P.; Chahory, S.; Carre, S.; Savoldelli, M.; Jonet, L.; Behar-Cohen, F.; Martinsons, C.; Torriglia, A. 2015, Retinal damage induced by commercial light emitting diodes (LEDs). *Free Radic. Biol. Med.*, 84, 373–384.
27. Reme, C. E., Weller, M., Szczesny, P., Munz, K., Hafezi, F., Reinboth, J. J. and Clausen, M. (1995). Light-induced apoptosis in the rat retina in vivo: Morphological features, threshold and time course. In *Retinal degeneration*, Pp. 19–25. Plenum Press: New York, London.
28. Emeline F. Nandrot, Monika Anand, Mousumi Sircar, and Silvia C. Finnemann .(2006). Novel role for v5-integrin in retinal adhesion and its diurnal peak , *Am J Physiol Cell Physiol* 290: C1256–C1262.
29. Brem.R.B., Robens.S.G., Wilson.D.J., O'Rourke,L.M., Mixon.R.N., Robertson.J.E., Planck,S.R., Rosenbaum,J.T., 1994. Immunolocalization of integrin in human retina. *invest.ophthalmol.vis.sci.*35,3466-3474.
30. Benedicto I, Lehmann G L., M Ginsberg., D J Nolan, R Bareja, O Elemento, Z Salfati, N M. Alam, GT. Prusky, P Llanos, S Y. Rabbany, A Maminishkis, S S. Miller, S Rafii & E Rodriguez-Boulan. (2017). epithelium basement membrane and barrier function by angiocrine factors. *Nature Communications*, volume 8, Article number: 15374

Table 1. Descriptive statistics for retina thickness in different groups according to dark and light cycle

Groups	Mean μm	Standard deviation	Standard error	Min.	Max.	p-value
Control	116.86	6.67	2.11	105.46	125.71	0.012
Dark	139.02	11.31	2.53	122.26	160.98	
Light	133.22	11.89	2.66	113.34	158.44	
Inverse	124.35	33.07	8.54	10.22	147.76	





Ali Abdul sattar et al.

Table 2. Multiple comparison between different groups regarding retina thickness according to dark and light cycle

Comparison	p-value
Control/ dark	0.003
Control/ light	0.026
Control/ inverse	0.324
Dark/ light	0.325
Dark/inverse	0.023
Light/inverse	0.165

Table 3. Descriptive statistics for rods and cons thickness in micrometers μm for different groups according to dark and light cycle

Groups	Mean	Standard deviation	Standard error	Min.	Max.	p-value
Control	43.46	8.63	2.73	28.94	53.94	0.001
Dark	80.33	16.8	5.06	64.61	117.07	
Light	76.1	34.57	10.93	43.87	144.67	
Inverse	52.32	16.27	5.14	29.64	78.21	

Table 4. Multiple comparison between different groups regarding rods and cons thickness according to dark and light cycle

Comparison	p-value
Control/ dark	<0.001
Control/ light	0.001
Control/ inverse	0.356
Dark/ light	0.651
Dark/inverse	0.005
Light/ inverse	0.017

Table 5. Descriptive statistics for bipolar cell layer thickness in different groups according to dark and light cycle

Groups	Mean μm	Standard deviation	Standard error	Min.	Max.	p-value
Control	70.71	16.67	4.81	49.24	96.91	0.006
Dark	97.21	30.6	8.17	54.09	157.0	
Light	94.57	16.44	4.74	69.22	134.67	
Inverse	74.95	18.71	5.4	49.52	114.80	





Ali Abdul sattar et al.

Table 6. Multiple comparison between different groups regarding bipolar cells thickness according to dark and light cycle

Comparison	p-value
Control/ dark	0.004
Control/ light	0.01
Control/ inverse	0.637
Dark/ light	0.761
Dark/inverse	0.013
Light/inverse	0.033

Table 7: Descriptive statistics for integrin score in different groups according to dark and light cycle

Groups	Mean μ m	Standard deviation	Standard error	Min.	Max.	p-value
Control	0.197	0.03	0.01	0.13	0.24	0.001
Dark	0.158	0.05	0.014	0.11	0.26	
Light	0.295	0.13	0.04	0.15	0.64	
Inverse	0.196	0.05	0.016	0.11	0.28	

Table 8 Multiple comparison between different groups revealed that light group differed significantly from all the other groups while there were no significant differences between dark, inverse and control groups.

Comparison	p-value
Control/ dark	0.232
Control/ light	0.004
Control/ inverse	0.086
Dark/ light	<0.001
Dark/inverse	0.238
Light/ inverse	0.004

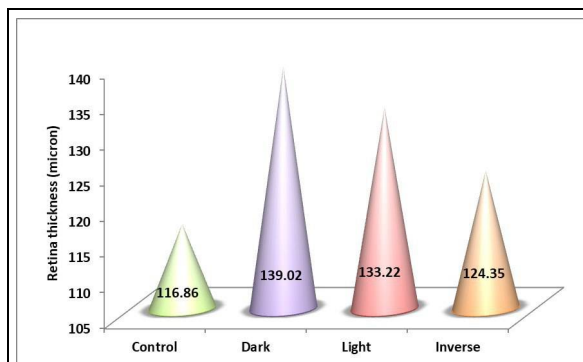


Figure 1. Mean retina thickness in micrometers for different groups of animals

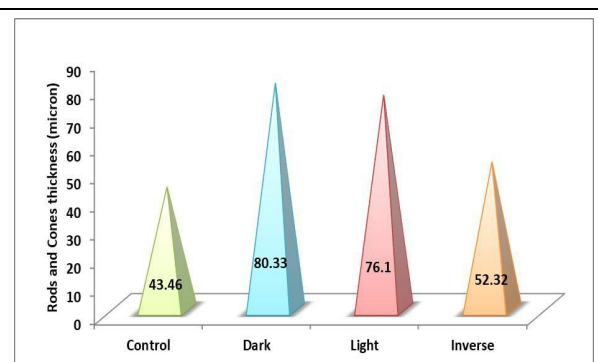


Figure 2. Mean rods and cons thickness in micrometers for different groups of animals





Ali Abdul sattar et al.

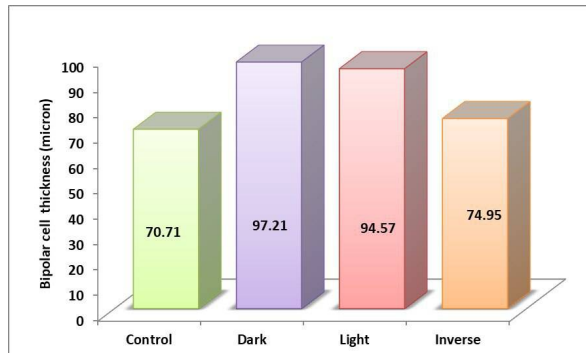


Figure 3. Mean bipolar cells layer thickness in different groups of animals

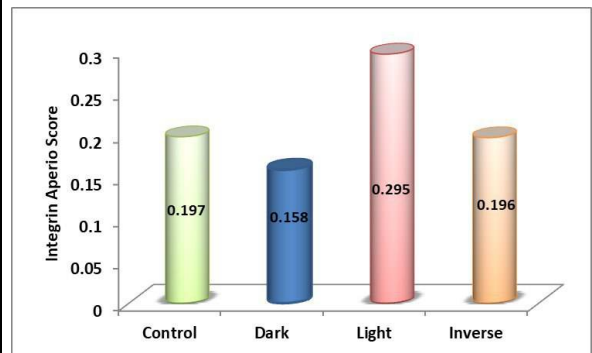


Figure 4. Mean integrin Aperio score in different groups of animals

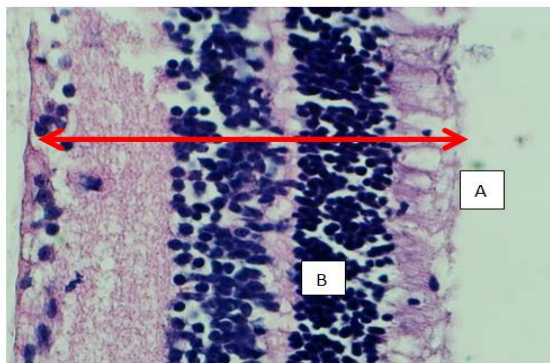


Figure 5. Cross section in retina of light group mice which reveals the thickness of the whole retina (\leftrightarrow) measured by image j software program with the photoreceptor layer (A), and bipolar layer (B) thickness. [H&E stain, 40X].

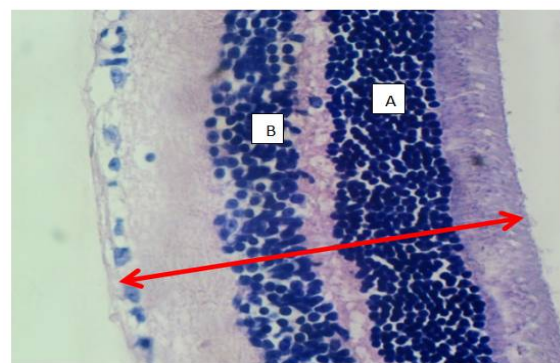


Figure 6. Cross section in retina of dark group mice which reveals the thickness of the whole retina (\leftrightarrow) measured by image j software program with the photoreceptor layer (A), and bipolar layer (B) thickness. [H&E stain, 40X].

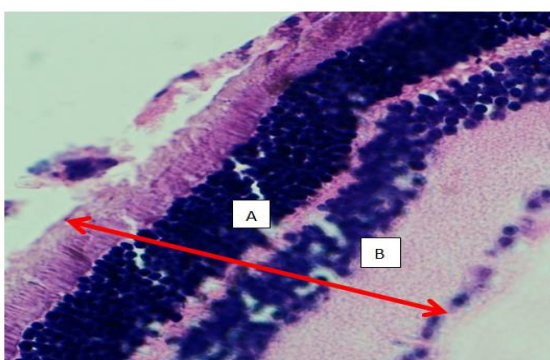


Figure 7. cross section in retina of reverse group which reveals the thickness of the whole retina (\leftrightarrow) measured by image j software program with the photoreceptor layer (A), and bipolar layer (B) thickness. [H&E stain, 40X].

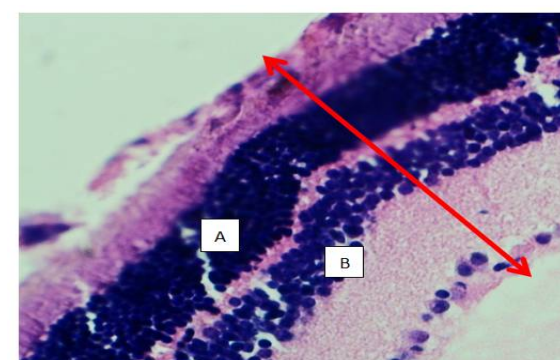


Figure 8. Cross section in retina of control group which reveals the thickness of the whole retina (\leftrightarrow) measured by image j software program with the photoreceptor layer (A), and bipolar layer (B) thickness. [H&E stain, 40X].





Ali Abdul sattar *et al.*

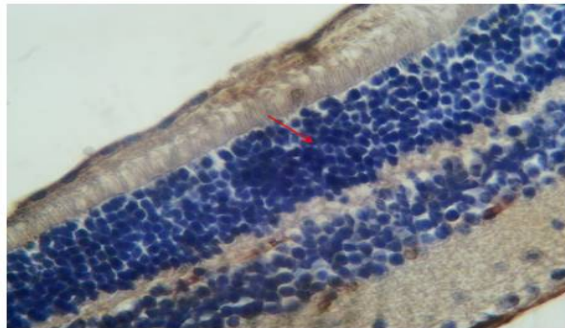


Figure 9. A-cross section in retina in light group animals which show high marked expression of integrin beta 1 at retina (→) stained by IHC technique, 40X].

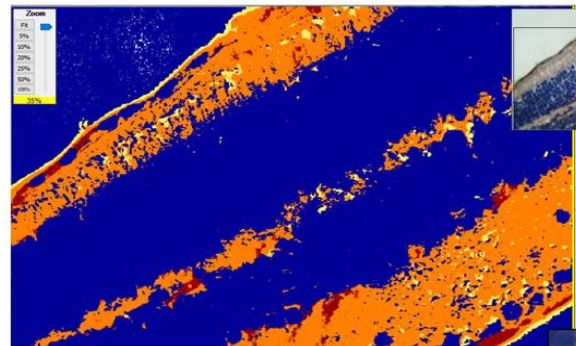


Figure 10. Thesction in retina in light group animals which show high marked expression of integrin beta 1 at retina and analyzed by aprio image J soft ware program, brown color = strong positive, orange = positive, yellow = weak positive, blue = negative.

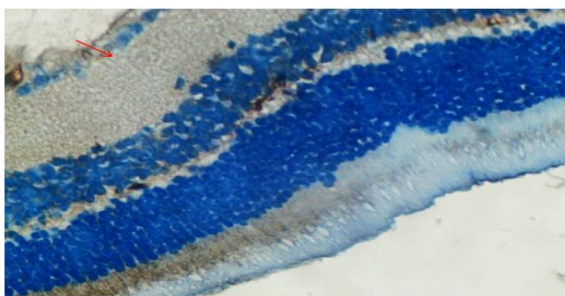


Figure 11. A-cross section in retina in dark group animals which reveal very weak expression of integrin beta 1 at retina (→) stained by IHC technique for integrin beta 1 is protein, 40X].

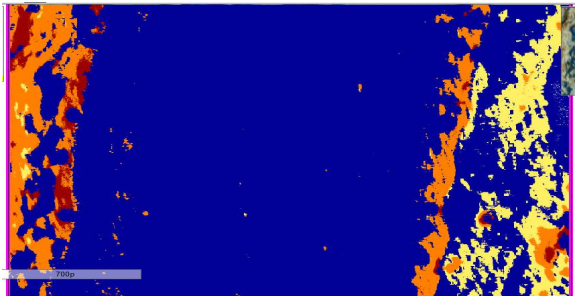


Figure 12. The section in retina in dark group animals which reveal very weak expression of integrin beta 1 at retina and is analyzed by aprio image J software program, brown color = strong positive, orange = positive, yellow = weak positive, blue = negative .

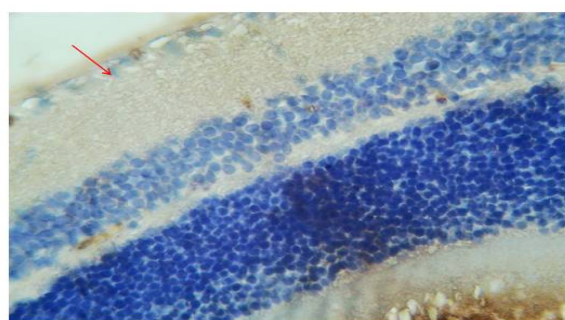


Figure 13. Cross section in retina of reverse group animals which they reveal low expression of integrin in comparison to control group at retina (→) stained by IHC technique for integrin beta 1 is protein, 40X].

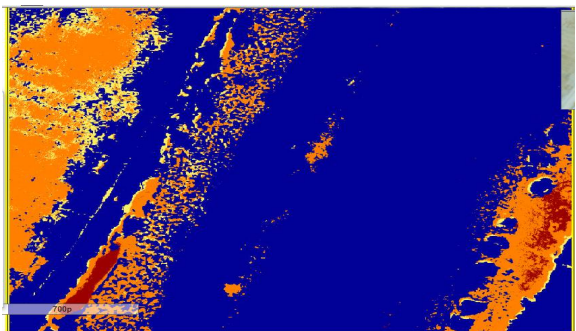


Figure 14. The section in retina of reverse group animals which they reveal low expression of integrin in comparison to control group and analyzed by aprio image J software program, brown color = strong positive, orange = positive, yellow = weak positive, blue = negative .





Ali Abdul sattar et al.

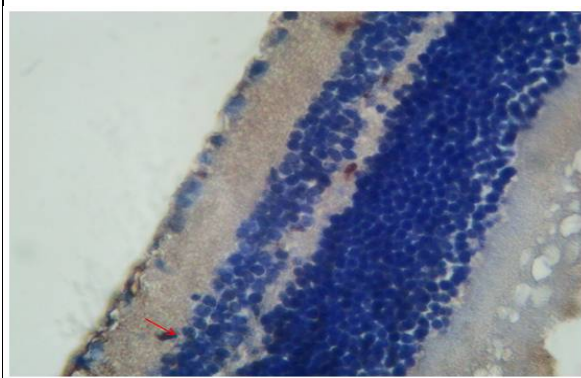


Figure 15. cross section in retina in control group animals which reveal high expression of integrin beta 1 in comparison to dark & reverse group, at retina (→) stained by IHC technique for integrin beta 1 is protein, 40X].

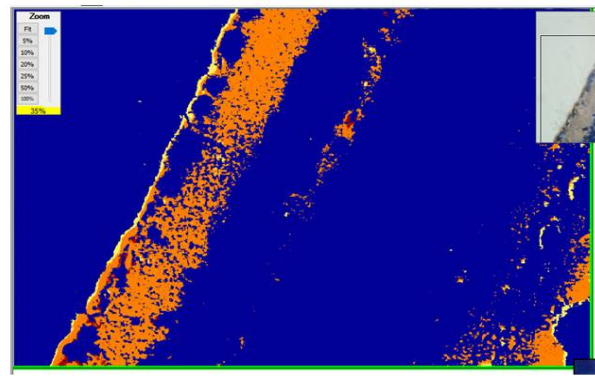


Figure 16. The section in retina in control group animals which reveal high expression of integrin beta 1 in comparison to dark & reverse group, and analyzed by aprio image J soft ware program, brown color = strong positive ,orange = positive ,yellow =weak positive, blue = negative .





RESEARCH ARTICLE

Air Quality and Respiratory Health Surrounding Adnama Mining Resources, Inc. (AMRI), Bryg. Urbiztondo, Claver, Surigao Del Norte

Elmer R. Causing*, Edwin C. Escobal and Edilmar P. Masuhay

Surigao State College of Technology, Mainit, Surigao del Norte, Philippines.

Received: 01 Aug 2019

Revised: 03 Oct 2019

Accepted: 06 Nov 2019

*Address for Correspondence

Elmer R. Causing

Surigao State College of Technology,
Mainit, Surigao del Norte, Philippines.



This is an Open Access Journal / article distributed under the terms of the **Creative Commons Attribution License** (CC BY-NC-ND 3.0) which permits unrestricted use, distribution, and reproduction in any medium, provided the original work is properly cited. All rights reserved.

ABSTRACT

Adnama Mining Resources, Inc. (AMRI) started its Self-Monitoring Report (SMR) in 2012 to monitor the concentration of Total Suspended Particulates (TSP), in compliance with the DAO 2003-27 of the Environmental Management Bureau (EMB) – Department of Environment and Natural Resources (DENR). Starting in 2017, the EMB-DENR requires all mining companies to shift from quarterly monitoring to monthly monitoring of ambient air quality. TSP are some of the causes of respiratory health diseases. TSP pose the greatest health risk to preadolescent children and in preterm delivery. Both the data from the AMRI Ambient Air Monitoring and AMRI Morbidity Report were analyzed using nonparametric correlation analysis. Descriptive statistics were used to obtain data from the demographics, level of awareness and perceived impact of the residents. Despite the nonlinear relationship between the TSP concentration and cases of respiratory illnesses, the concentration of TSP significantly affected the incidence of respiratory illnesses in the area, even though the TSP concentration are below the maximum limit set by EMB-DENR. The residents of AMRI are very aware about TSP and the risk associated with it. They are also very knowledgeable about the operations and practices conducted by AMRI to mitigate TSP level. The residents generally agree that the air quality have change since before the mining operation that it was caused by AMRI. Further correlation test on other mining companies are recommended to further establish the correlation between TSP level and cases of respiratory illnesses and to determine if the threshold set by the EMB-DENR is still valid.

Keywords: Air Quality Assessment, Respiratory Illnesses, Adnama Mining Resources, Inc. (AMRI), Total Suspended Particulates (TSP), Level of Awareness..

INTRODUCTION

The Oriental Synergy Mining Corporation (OSMC) started the Kalamazoo Nickel Mining Project in 2007 in Urbiztondo, Claver, Surigao del Norte and conducted the operation of its quarterly Self-Monitoring Report (SMR)

17867



**Elmer R. Causing *et al.***

which includes quarterly air sampling activity from 2008 to 1st Quarter 2017 and monthly air sampling starting in April 2017 for the concentration of TSP in compliance with the EMB Memorandum Circular (MC) No. 2003 – 08. The EMB MC 2003-08 was issued to adopt the Procedural and Reference Manual for DAO 2003-27 (August 2003 Edition). The MC requires each firm to track their own compliance and permit the government to conduct review and monitor each firm's compliance with the existing laws. The DENR Standard for TSP on a 24-hour averaging time is 230 $\mu\text{g}/\text{Ncm}$ (Section 12, Article 1, Chapter of RA 8749 of the Philippine Clean Air Act of 1999) using High Volume – Gravimetric, USEPA 40 CFR, Part 50, Appendix B (DAO 2000-81). Non-compliance shall be penalized and a fine shall be imposed to the violating firm. Total Suspended Particulates (TSP) is defined as any material, other than uncombined water which exists in a finely divided form as a liquid or solid (DAO 2000-81). TSP are 100 micrometers or less in diameter. They come from natural and human-made sources. The smaller components of TSP (PM_{10} and $\text{PM}_{2.5}$) are associated with health effects ranging from respiratory irritation to some forms of cancer. TSP is small enough to be inhaled; however, the larger particles (10-100 μm) are filtered out in the nasal cavity and are often relatively harmless (MFE 2015).

In 2014, 92% of the world population was living in places where WHO air quality guideline standards were not met. Outdoor air pollution in both cities and rural areas was estimated to have caused 3 million deaths worldwide in 2012 (WHO World Health Statistics 2017). Each 10 $\mu\text{g}/\text{m}^3$ elevation in fine particulate air pollution was associated with approximately a 4%, 6% and 8% increased risk of all-cause, cardiopulmonary and lung cancer mortality respectively (Pope 2002). In the Philippines, the leading cause of morbidity was attributed to air pollution (DOH Philippines 2014). According to Ware *et al.* (1986), rates of bronchitis and a composite of lower respiratory illness of preadolescent children were significantly associated with average particulate concentrations. Furthermore, the analyses of lifetime residents showed that these outcomes were significantly associated with measures of lifetime mean TSP Concentration ($\mu\text{g}/\text{Ncm}$). TSP also contributes to excess risk of preterm delivery (Xu *et al.* 2010). PM_{10} were also observed to have effects on the occurrence of asthma symptom episodes, and to a lesser extent on cough and PEF among children (Weinmayr *et al.* 2010).

The research shall attempt to conduct analyses on the correlation between the amount of TSP and its effect on the respiratory health of the residents in the surrounding community. The study aims to determine the association between the TSP concentration and respiratory health incidence. The level of awareness of the residents of Brgy. Urbizondo and their perceived impact will show whether the observed changes in the air quality in the area will align with the actual data on air quality based on the Self-Monitoring Report.

OBJECTIVES**General Objective**

This study aims to determine the association / relationship between ambient air quality and cases on respiratory illnesses surrounding AMRI. Specific Objectives Assess the air-quality around AMRI based on the data from its Self-Monitoring Report.

1. Determine significant relationship between the air quality around AMRI and cases on respiratory illness in the area.
2. Determine the level of awareness of the community regarding the climate condition and AMRI operations and programs.
3. Determine the perceived impacts of AMRI operations to respiratory illnesses of the community.





Elmer R. Causing et al.

Significance of the Study

The result of the study shall serve as a foundation for future assessments on the ambient air quality on mining areas, and shall serve as a guideline for the following:

- a. Flora conditions surrounding mining sites as affected by the ambient air quality.
- b. Fauna conditions surrounding the mining sites as affected by the ambient air quality.
- c. Range of the Total Suspended Particulates (TSP) from the site and its effect per unit distance.
- d. Further research and assessment of the other mining corporations.

METHODOLOGY

Location of the Study

The research was done at Brgy. Urbiztondo, Claver, Surigao del Norte.

Sample Survey

The data on the ambient air quality and respiratory health situation was sourced from AMRI while data on demographics was taken from the Local Socio-Economic Profile (LSEP) 2018 of Brgy. Urbiztondo, Claver, Surigao del Norte. The population of Brgy. Urbiztondo, Claver, Surigao del Norte was 749 as of January 2018. The computed sample size is 254, with 95% level of confidence. The research used Stratified Random Sampling on each Purok and Systematic Random Sample within Purok

RESULTS AND DISCUSSION

Facilities Used

The research used a survey questionnaire to determine the perception and level of awareness/ knowledge of the community regarding mining, TSP and AMRI.

Actual Survey

Using the Stratified Random Sampling, the actual interview was conducted per Purok, determining the number of participants per Purok based on the proportion to the number of Household in the entire Barangay. The Systematic Random Sampling was implemented within a purok. One person per household (preferably household head) was interviewed.

Data analysis

The level of awareness was computed using the following scale Table 3. The level of awareness was measured from the respondents' perception regarding the following areas:

- A. Climate Conditions
- B. AMRI Operations
- C. AMRI Mitigation Practices
- D. Perceived Impact on the Community



**Elmer R. Causing et al.**

The study used descriptive statistics to determine the mean, standard deviation and frequency on the demographics and the level of awareness among the respondents. Inferential analysis was used to establish the relationship between the TSP concentration and incidence of respiratory illnesses. The study sourced the data on TSP Concentration ($\mu\text{g}/\text{Ncm}$) from AMRI Ambient Air Monitoring 2012- 2017, while the data on Respiratory Illnesses was based on AMRI Morbidity Record 2012-2017. The annual mean was computed and compared against the standard set forth in DAO 2000-81. The ambient air quality in the area have remained compliant with the DENR standard of 230 $\mu\text{g}/\text{Ncm}$. The general trend of TSP level is undulated and is very close to the baseline level (Figure 3). The annual mean of TSP Concentration is very low. This signifies that there are little changes in the TSP concentration on the course of six years. The trend of respiratory illnesses incidence in the area is undulated. There were drastic changes in the first three years but have since slowed down (Figure 4).

Figure 4 shows a nonlinear relationship between TSP Concentration and respiratory illnesses incidence of AMRI Workers. Spearman's nonparametric correlation test shows a moderately significant correlation. This signify an association in the TSP concentration and respiratory illnesses incidence and imply that the TSP level could be an indicator for the incidence of respiratory illnesses. The data shows that 71.70 % of the respondents are female. This could be due to the husband being at work during the interview. The youngest of the participants is 18 while the oldest is 94 while the mean of age is 41.35. It is also shown that 70.90 % of the respondent are not presently working at AMRI and 94.5% do not have another household member working at AMRI. 9.44 % of the respondents are residents in the barangay for eight years and have experienced the difference in the air quality before and after AMRI. The level of awareness about Total Suspended Particulates (TSP) is very high. This indicate that the residents of Brgy. Urbiztondo are well-informed about the presence of TSP and the harm that it causes (Figure 8). The residents have very high knowledge on all the AMRI operations. This suggest an effective information drive on the part of AMRI (Figure 9). The residents of Brgy. Urbiztondo believe that the climate conditions have change since that the start of mining operations. They believe that AMRI is the main reason for this change. They think that the control measures conducted by AMRI to mitigate TSP is enough, but they believe that AMRI should still intensify their efforts on their mitigation operation (Figure 11).

CONCLUSION AND RECOMMENDATIONS

The air quality surrounding AMRI have not significantly change over the last six (6) years based on the Self-Monitoring Report (SMR) and the company have remained compliant with the DENR standards. There is, however, a significant relationship between mean TSP concentration and Respiratory Illnesses Incidence in the area. This shows that despite the TSP concentration being below the threshold, it still has an effect on the human respiratory health, suggesting that the current limit set the law may be outdated and requires revision. The community have very high level of awareness regarding the air quality and AMRI operations and programs, and their mitigation practices which indicates knowledgeable, well-informed society. The communities have very positive view on the AMRI operations, stating that the mitigation practices conducted was enough, yet they asserted that AMRI still should intensify their efforts in the programs.

REFERENCES

1. DENR Department Administrative Order No. 2000-81. Implementing Rules and Regulations for RA 8749. Retrieved from policy.denr.gov.ph/2000/ENV_DAO_2000-81.pdf
2. DENR Department Administrative Order No. 2003-27 (Series of 2003). Amending DAO 26, DAO 29 and DAO 2001-81 among others on the Preparation and Submission of Self-Monitoring Report (SMR). Retrieved from policy.denr.gov.ph/b2003/dao2003-27.pdf
3. Memorandum Circular No. 2003-008 (2003). Procedural and Reference Manual for DAO 2003-27 (Self-Monitoring Report (SMR) System. Environmental Management Bureau, Department of Environment and Natural





Elmer R. Causing et al.

4. Resources. <http://pepp.emb.gov.ph/wp-content/uploads/2016/06/SMR-DAO-2003-27.pdf>
5. Republic Act No. 8749 (1999). Philippine Clean Air Act of 1999. Retrieved from <http://www.emb.gov.ph/wp-content/uploads/2015/09/RA-8749.pdf>
6. National Air Quality Status Report 2010-2011. (2012). Environmental Management Bureau, Department of Environment and Natural Resources. Retrieved from <http://air.emb.gov.ph/wp-content/uploads/2016/04/DenrAirQualityStatReport10-11.pdf>
7. Field Health Service Information System 2014, Epidemiology Bureau, Department of Health, Philippines (2014). <https://www.doh.gov.ph/morbidity>
8. World Health Statistics (2017). Monitoring health for the SDGs. World Health Organization. ISBN 978-92-4-156548-6. Retrieved from <http://apps.who.int/iris/bitstream/10665/255336/1/9789241565486-eng.pdf>
9. Pope, C. A. III, Burnett, R. T., Thune, M. J., et al. (2002). Lung cancer, cardiopulmonary mortality, and long-term exposure to fine particulate air pollution. *JAMA*. 2002;287(9):1132-1141 (DOI:10.1001/JAMA. 287.9.1132)
10. Kontos, A. S., Fassois, S. D., Deli, M. F. (1999). Short-term effects of Air Pollution on Childhood Respiratory Illness in Piraeus, Greece, 1987-1992: Nonparametric Stochastic Dynamic Analysis. *Environmental Research Section A* 81, 275-296
11. Ware, J. H., Ferris, B. G. Jr., Dockery, D. W., Spengler, J. D., Stram, D. O., Speizer, F. E. (1986). Effects of ambient sulfur oxides and suspended particles on respiratory health of preadolescent children. *American Review of Respiratory Disease*. ISSN: 0003-0805. Volume 133. Issue. Pages 834-842.
12. Weinmayr, G., Romeo, E., De Sario, M., Weiland, S. K., and Forastiere, F. (2010). Short-term effects of PM₁₀ and NO₂ on Respiratory Health among Children with Asthma or Asthma-like Symptoms: A Systematic Review and Meta-Analysis. *Environmental Health Perspectives* 118(4):449-57. DOI: 10.1289/ehp. 0900844
13. Hu, H., Ha, S., Roth, J., Kearney, G., Talbott, E. O., Xu, X. (2014). Ambient air pollution and hypertensive disorders of pregnancy. *Atmospheric Environment*. Volume 97, Pages 336-345. <https://doi.org/10.1016/j.atmosenv.2014.08.027>
14. Local Socio-Economic Profile (2018). Brgy Urbiztondo, Claver, Surigao del Norte.
15. Oriental Synergy Mining Corp. (2008). Urbiztondo Nickel Laterite Mining Project Environmental Impact Statement (EIS)

Table 1. No. of Households per Purok

Purok	No. of Households*	Sample size
1	173	59
2	146	50
3	160	54
4	98	33
5	67	23
6	105	36
Total	749	254

*LSEP 2018, Brgy. Urbiztondo, Claver

Table 2. Scoring & Quantification of Data

Rate	Description
4.01 – 5.00	Very high
3.01 – 4.00	High
2.01 – 3.00	Moderate
1.01 – 2.00	Low
1.00	Very Low





Elmer R. Causing et al.

Table 3. Mean TSP Concentration (µg/Ncm) and Standard Deviation

	Baseline 2007	2012	2013	2014	2015	2016	2017	Mean	STD
Q1			191.09	161.10	157.85	55.19	74.50		
Q2			226.31	215.29	92.52	224.28	193.88		
Q3	121.03	206.49	153.01	218.81	213.96	101.83	213.71		
Q4		212.89	144.40	184.82	104.35	125.33			
Annual Mean		209.69	178.7025	195.005	142.17	126.6575	160.6967	168.82	31.65
						Coefficient of Variation		0.1875	

Table 4. Quarterly TSP Concentration (µg/Ncm) and Respiratory Illnesses Incidence

Quarter	TSP	Respiratory Illnesses Incidence
2012 Q3	206.49	99
2012 Q4	212.89	62
2013 Q1	191.09	77
2013 Q2	226.31	164
2013 Q3	153.01	95
2013 Q4	144.40	63
2014 Q1	161.10	41
2014 Q2	215.29	84
2014 Q3	218.81	42
2014 Q4	184.82	11
2015 Q1	157.85	63
2015 Q2	92.52	75
2015 Q3	213.96	129
2015 Q4	104.35	38
2016 Q1	55.19	19
2016 Q2	224.28	135
2016 Q3	101.83	78
2016 Q4	125.33	154
2017 Q1	74.50	33
2017 Q2	193.88	79
2017 Q3	213.71	174

Source: AMRI Ambient Air Monitoring, AMRI Morbidity Record

Table 5. Test of significance using Spearman’s rho

	Respiratory Illnesses
Correlation Coefficient	0.516*
Sig. (2-tailed)	0.017

* Correlation is significant at the 0.05 level (2-tailed).





Elmer R. Causing et al.

Table 6.a. No. of respondents who are presently working in AMRI

Response	n	Percent (%)
1.) Yes	74	29.10
2.) No	180	70.90
Total	254	100.00

Table 7.b. Have another household member working at AMRI

	n	Percent (%)
1.) Yes	14	5.50
2.) No	240	94.50
Total	254	100.00

Table 8. Level of awareness/ knowledge about TSP/SPM/dust generation/dust emission.

Questions	Mean	Std. Dev.	Description
1.) How aware are you about Particulate Matter (PM)?	4.86	0.46	Very high
2.) Are you aware that PM could cause/ worsen respiratory illness?	4.89	0.42	Very high
3.) Are you aware that PM can come from mining areas?	4.81	0.52	Very high
4.) Are you aware that PM can be mitigated?	4.45	0.96	Very high
5.) Are you aware of other sources of PM?	4.40	1.06	Very high
mean of means	4.67	0.68	Very high

Table 9. Level of awareness/ knowledge on AMRI operations

Questions	Mean	Std. Dev.	Description
1.) How aware are you about AMRI?	4.97	0.22	Very high
2.) How aware are you about the following AMRI operations:			
2.a) Road sweeping	4.91	0.39	Very high
2.b) Desilting	4.83	0.52	Very high
2.c) Tree planting	4.90	0.39	Very high
2.d) Water spraying	4.67	0.86	Very high
2.e) Coastal clean-up	4.77	0.70	Very high
2.f) Mangrove planting	4.89	0.48	Very high
2.g) In-house air and water quality monitoring	4.31	1.26	Very high
2.h) Nursery seedling production	4.94	0.29	Very high
mean of means	4.25	0.57	Very high





Elmer R. Causing et al.

Table 10. Level of awareness / knowledge on AMRI mitigation practices

Questions	Mean	Std. Dev.	Description
1.) Are you aware that AMRI is held responsible for controlling PM in the area?	4.67	0.75	Very high
2.) Are you aware that AMRI is regularly conducting control measures for PM?	4.22	1.15	Very high
3.) Are you aware that AMRI is regularly monitoring the Air Quality in the area?	3.77	1.42	Very high
4.) Are you aware that AMRI is not allowed to exceed the PM threshold?	3.92	1.28	Very high
5.) Are you aware that AMRI will be penalize if they exceed the threshold?	4.43	1.10	Very high
mean of means	4.20	1.14	Very high

Table 11. Perceived impact on the community

Questions	Mean	Std. Dev.	Description
1.) Do you think the climate conditions have changed over the last eleven years?	4.39	1.09	Very high
2.) Do you think AMRI caused the change of climate conditions?	3.23	1.40	High
3.) Do you think AMRI operations have positive effect on the community?	4.30	1.06	Very high
4.) Do you think the control measures conducted by AMRI are enough?	3.68	1.25	High
5.) Do you think AMRI should intensify their efforts on their mitigation operation?	4.65	0.88	Very high
Mean of means	4.05 or 4	1.14	High





RESEARCH ARTICLE

Effect of Application of Combined Organic and Inorganic Fertilizers on the Yield Characteristics of Sigue-sigue Corn Variety (*Zea mays* L.)

Erma Catipan Taer^{1,2*}, E.R.M.Maglinte², M.B.Humandos², J.G.Abellano² and J.O.P.Villarino²

¹Pongtud, 8425 Alegria, Surigao del Norte, Philippines.

²Surigao State College of Technology, Mainit, Surigao del Norte, Philippines.

Received: 02 Sep 2019

Revised: 06 Oct 2019

Accepted: 09 Nov 2019

*Address for Correspondence

Erma Catipan Taer

Pongtud, 8425 Alegria,

Surigao del Norte, Philippines.

Email: ermataer@gmail.com



This is an Open Access Journal / article distributed under the terms of the **Creative Commons Attribution License** (CC BY-NC-ND 3.0) which permits unrestricted use, distribution, and reproduction in any medium, provided the original work is properly cited. All rights reserved.

ABSTRACT

Improving the yield of Sigue-sigue OPV corn planted by local farmers in the province of Surigao del Norte, the right combination of organic and inorganic fertilizers was being assessed. The study was conducted at SSCT-Mainit Campus using Vermicompost (VC) and chicken dung (CD) as organic and 14-14-14 fertilizer as inorganic fertilizer (IF). Experiment treatment was, T1 Control, T2 (0.50 kg VC + 0.50 kg CD), T3 (0.50 kg VC + 0.010 kg IF), and T4 0.050 kg 14-14-14 inorganic fertilizer alone (IFA) in four replications. Data gathered were analyzed by one way ANOVA in randomized complete block design. The results showed significantly higher in corn height ($P < 0.05$) noticed on the three treatments (IFA, VC + IF, and VC + CD) over the control treatment. The corn under the combined organic VC + CD produced the highest ear height (EH) compared to combined organic + inorganic and inorganic alone treatments. However, the combined VC + IF significantly higher values on parameters of kernel counts per ears (KPE) and weight of grain yield (GY) among the parameters tested ($P < 0.05$). Of all the parameters tested, the number of ears per plant (EPP) was not significantly altered by all treatment of fertilizer combinations. Therefore it was concluded that the right combinations were the application of 0.50 kg of vermicompost + 0.010 kg of 14-14-14 fertilizer per hill of corn. A further experiment should be performed to include the effect of different organic and inorganic fertilizers on the soil properties and growth and yield of Sigue-sigue corn.

Keywords: OPV, Vermicompost, Chicken dung, Yield performance, Inorganic fertilizer.



**Erma Catipan Taer et al.**

INTRODUCTION

In the Philippines being an agriculture country is quite behind in producing satisfactory crop yields due to many constraints, among those, depleted soil nutrients caused by several factors like the unreasonable application of intensive farming practices and the misuse of chemicals used in farming. Worldwide, there is increasing desire in the utilization of organic fertilizers due to degradation in the soil fertility because constant use of synthetic fertilizers generates possibility polluting consequences due to chemicals in the surroundings (Das, Singh, Ram, and Prasad, 1991). Vermicompost is an excellent soil supplement made up of dissolved compost. Chemical examinations of the castings were performed (Ruz-Jerez, Ball, and Tillman, 1992; Parkin and Berry, 1994) and discovered that it carries five times the nitrogen content, seven times the potash content and 1.5 times more calcium content in 15 cm of good topsoil. It is described that phosphorous gone through worms digestive tract is transformed into the plant's available structure (Reinecke, Viljoen, and Saayman, 1992). The use of chicken dung as an organic fertilizer is crucial in upgrading soil fertility and crop production (Dikinya and Mufwanzala, 2010). Chicken dung is favored amongst other livestock wastes because of its high availability of macro-nutrients (Warman, 1986; Duncan, 2005). Moreover, organic manure is also being endorsed by several environmentalists worldwide to conserve the sustainability of agricultural productions. But utilizing only organic fertilizers may be disadvantageous because organic fertilizer produces a slow-release action of giving nutrients to the soil to be availed and utilized by plants for their growth and development for a longer period (Pascual, Jarwar, and Nitural, 2013).

Meanwhile, Sigue-sigue (*Zea mays*) is an open-pollinated corn variety mostly planted by smallholder farmers in the province of Surigao del Norte. In 2018, a total of 7,771.9 metric tons harvested corn grains out of 2,511.4 hectares of land area planted with corn nationwide (PSA 2019). As to percentage distribution of corn production by region in 2018, Caraga Region - XIII only contributed 1.75% out of 52.66% in the entire Mindanao area (PSA 2019). The fact is substantial that the Caraga region is much behind in terms of corn production. Purposely this experiment was conducted to determine the yield characteristics of Sigue-sigue corn under different organic and inorganic fertilizer combinations.

MATERIALS AND METHODS

Location of the Study

The experiment was carried out at the college agronomy field area of SurigaodelNorte State College of Technology – Mainit Campus at Magpayang, Mainit, Surigao del Norte, Philippines. Mainit is located on 9° 32' North, 125° 31' East (9.5378, 125.5225) and 47.9 meters (157.2 feet) above sea level. The experiment was a single factor having four treatments replicated four times in a randomized complete block design (RCBD). Treatment compositions are the following; T1 – Control (C) no fertilizer, T2 – 0.50 kg vermicompost (VC) + 0.50 kg chicken (CD) dung per hill, T3 – 0.50 kg vermicompost (VC) + 10 g 14-14-14 inorganic fertilizer (IF), and T4 – 0.050 kg 14-14-14 inorganic fertilizer alone (IFA alone) per hill. The experimental area measured 200 square meters to hold four plots as experimental replication blocks measuring 50 square meters including canals as alleyways.

Soil Samples

Soil samples from the experimental area were gathered using the zigzag method having a total of 15 samples. The soil sample was mixed thoroughly, air-dried for two weeks, then pulverized and sieved to get a kilogram sample and pack by a polyethylene bag and submitted for analyses of N, P, K, organic matter content and soil pH. The inorganic fertilizer used was 14-14-14 complete commercial fertilizer from known agriculture farm supply, while organic fertilizers were vermicompost (VC) and chicken dung (CD). The VC was taken from the college vermicompost production project while the CD was collected from the college poultry micro-project area. The application of

17876



**Erma Catipan Taer et al.**

fertilizer varies according to the fertilizer type (organic and inorganic). For the organic fertilizers, the application was done by basal at one week before planting in which by the specified amount the fertilizer was placed under the soils where corn is going to be planted. While the inorganic fertilizer was applied along sides of the plant (sidedress) at seven days after planting and a follow-up application was done at 45 days after planting approximately before corn silking. The amount of fertilizers per hill were dependent to treatments, 0 fertilizer for control, 0.50kg VC + 0.50kg CD, 0.50kg + 10g IF, and 0.05 kg IF alone. After a thorough area of land preparation, the Sigue-sigucorn seeds were planted at a distance of 25 cm within rows and 75 cm between rows (Yusuff, Ahmed, Yahaya, and Majid, 2007), having three seeds per hill in 4-5 cm depth. Before planting the seeds were pre-germinated for 24 hours to ensure uniform and 100% germinations. Exactly two weeks after planting the newly emerged corn was thinned uniformly to one plant per hill. Other management practices were done as per the recommendation made for the crop at each location.

Data Gathering

Data were collected on major phenological, growth, yield and yield-related traits described by (Kinfe et al., 2017), as follows; The plant height (PH) of corn was measured at 50 days after planting (time of silking in maize) wherein five randomly obtained plants from harvestable row was measured from base of the plant to the point where the tassel starts branching and the average value was recorded. Ears per plant (EPP) was recorded as the total number of ears harvested from a plot divided by the total number of plants in a plot at harvest, unfilled ears were not counted. Ear height (EH) from five randomly selected plants from harvestable row was measured from the base of the plant to the uppermost useful ear bearing node and the average value was recorded. Meanwhile, kernels per ear (KPE) were recorded from five randomly selected and hand-harvested ears from every treatment per plot. Ears were dehusked and kernels were counted and recorded. Kernels from uniform rows per ear were separately counted from kernels in partial and non-uniform rows. Grain yield (GY) data on grain yield at harvest were obtained from plants in the net rows

RESULTS

Data of PH, EPP, EH, KPE, and GY were subjected to analyses of variance in a randomized complete block design (RCBD) and are presented in (Table 1). Statistical analysis of variance for the PH of corn under different organic and inorganic fertilizers and their combinations showed significant differences at the 5% probability level. Table 1 showed that the application IFA, the combined VC + IF, and the combined VC + CD are equally recorded higher (201.13, 201.09, and 200.11) plant height respectively over the control which was no fertilizer applied to have (110.31). The application of combined organic and inorganic fertilizers and inorganic alone failed to show any significant differences in the number of EPP ($P = 0.37$) however, a highly significant difference was noted on the effect of EH ($P < 0.001$). The combined VC + CD yielded the highest ear height among the tested fertilizer combinations (31.75) in (Table 1). Moreover, the combined VC + IF and IFA were statistically tied having (26.50 and 23.25) EH values respectively as next higher, while the lowest value in control (16.58) since no fertilizer was applied. On the other hand, kernel count per ears (KPE) in this study was obtained from uniform rows in every ear, while kernel from partial and non-uniform rows was excluded. The result showed significantly higher counts of kernel per ears in the combined organic and inorganic fertilizer (VC + IF) ($P < 0.001$) compared to the combined organic (VC + CD) and IFA. Kernels per ears count were; 496.00, 450.00, 426.50, and 374.50 for T3 (VC + IF), T4 (IFA), T2 (VC + CD), and T1 (Control) respectively. Grain yield as outcome of different plant growth and development processes starting from the vegetative phase, going to the reproductive stage, and ending with the grain-filling stage of corn in this trial was of similar values pattern with KPE count ($P < 0.001$), indicating significant differences between VC + IF (10.70), IFA (7.56), VC + CD (7.45) and control (3.89).



**Erma Catipan Taer et al.**

DISCUSSION

Materchera and Salagae, (2002) stated that higher plant height could be attained with the application of chicken dung and cattle manure. Taller plant, optimum stem girth, greener leaves, and highest corn fodder yield were recorded with the application of 120 kg nitrogen ha⁻¹ with the combinations of 3000 kg/hectare farmyard manure (Oad, Buriro, and Agha, 2004). The present result revealed that the effect of combined VC + CD, VC + IF gave comparable IF alone results in terms of the height of corn at the silking stage. Previous studies of the effects of organic fertilizers confirmed substantial reductions in sweet corn growth and yield under both organic Dufault, Hester, and Ward, (2008) and integrated cropping systems (Yusuff, Ahmed, Yahaya, and Majid, 2007). Nonetheless, we found corn under combined organic VC + CD recorded highest EH of the corn plant at 31.75 ± 1.50 than the combined organic and inorganic VC + IF with 26.50 ± 3.10 and IF alone at 23.25 ± 2.98 while control have the lowest EH of 16.58 ± 1.49 because they were not applied with fertilizer. The favorable higher EH in VC + CD combinations may be explained by the amount of macro and micronutrients that they have.

The vermicompost and chicken dung that we utilized in this trial were not tested chemically but several kinds of literature proved their worth. According to Prabha, Nagalakshmi, and Priya, (2015), vermicompost has a higher content of macro and micronutrients like nitrogen, phosphorus, potassium, calcium, sodium, magnesium and micronutrients namely iron, copper, zinc and manganese which play the important aspect in waste management. While in the study of Li, Liu, and Shan, (2009), indicating that the contents of N, P, Zn, Cu, were higher in chicken and pig manures than in cattle and sheep manures, but K contents were similar. Moreover, previous studies use of organic fertilizers, both alone or in combination with inorganic fertilizers, can increase ear quality and grain nutrient content of sweet corn further than with alone inorganic fertilization and that the nutritional quality of vermicompost-treated crops is superior (Akinrinde and Lawal, 2006). Furthermore, Boateng, Zickermann, and Kornahrens, (2006) study revealed that poultry wastes is an effective fertilizer and can appropriately substitute for synthetic fertilizer in the forest areas of Ghana. Poultry manure application harvested higher values for plant height, leaf area index and biomass. The four tons poultry manure per hectare rate harvested corn grain yield of 2.07 tons per hectare which was statistically equal from that of the inorganic fertilizer rate (2.29 tons per hectare) and 6 tons poultry manure per hectare (2.60 tons per hectare), while the 6 tons poultry manure per hectare was not statistically different from the 8 ton poultry manure per hectare rate.

The performance of Sique-siguecorn in terms of kernel count (KPE) and grain yield (GY) was positively enhanced by the application of combined organic and inorganic (0.50 kg VC + 0.010 g CF). The observation was similar in Amujoyegbe, Opabode, and Olayinka, (2007), grain yield was highest in sorghum (3.55 kg per ha) and corn (2.89 kg per ha) under inorganic fertilizer and poultry manure followed by inorganic fertilizer treatment for corn (2.33 kg/ha) and poultry manure treatment for sorghum (3.37 kg per ha). The appropriate application of inorganic and organic fertilizer combinations reduced soil bulk density, enhanced soil moisture, soil fertility, growth of corn and output and promoted corn grain quality (Rong et al., 2001). It is recommended that the appropriate application rate of inorganic and organic fertilizer combinations ranging from 25 % to 50 % organic + 75 % to 50 % inorganic should be supplied for maize fodder production. The present result revealed that 0.50 kg of vermicompost combined with 0.010 kg of 14-14-14 complete fertilizer per hill surpassed the yield performance of Sique-siguecorn under 0.050 kg of 14-14-14 complete fertilizer alone per hill. It is therefore recommended that the application of combined 0.50 kg of vermicompost and 0.010 g of complete 14-14-14 fertilizer for better yield performance of Sique-siguecorn in SSCT-Mainit and nearby area conditions.

The above studies reveal that both organic and inorganic fertilizers have their roles to play the yield characteristics of Sique-sigueOPV corn variety. But for better yield, the combination of both organic and inorganic fertilizer is better than that of combined organic + organic or inorganic fertilizer alone. As recommendations, a further trial will be



**Erma Catipan Taer et al.**

conducted to include the effect of combined organic and inorganic fertilizer on the soil properties, growth and yield performances of Sigue-sigüecorn.

ACKNOWLEDGEMENTS

This work was supported by Surigao State College of Technology headed by the college president DR. GREGORIO Z. GAMBOA JR, vice president for research development and extension headed by DR. GIDEON A. EBARABAL and research director Prof. Teresita Senados.

REFERENCES

1. Das, M., Singh, B. P., Ram, M., & Prasad, R. N. (1991). Response of maize (*Zea mays*) to phosphorus-enriched manures grown in P-deficient alfisols on terraced land in Meghalaya. *Indian Journal of Agricultural Sciences*, 61(6), 383-388.
2. Ruz-Jerez, B. E., Ball, P. R., & Tillman, R. W. (1992). Laboratory assessment of nutrient release from a pasture soil receiving grass or clover residues, in the presence or absence of *Lumbricus rubellus* or *Eisenia fetida*. *Soil Biology and Biochemistry*, 24(12), 1529-1534.
3. Parkin, T. B., & Berry, E. C. (1994). Nitrogen transformations associated with earthworm casts. *Soil Biology and Biochemistry*, 26(9), 1233-1238.
4. Reinecke, A. J., Viljoen, S. A., & Saayman, R. J. (1992). The suitability of *Eudriluseugeniae*, *Perionyx excavatus* and *Eisenia fetida* (Oligochaeta) for vermicomposting in southern Africa in terms of their temperature requirements. *Soil Biology and Biochemistry*, 24(12), 1295-1307.
5. Dikinya, O., & Mufwanzala, N. (2010). Chicken manure-enhanced soil fertility and productivity: Effects of application rates. *Journal of Soil Science and Environmental Management*, 1(3), 46-54.
6. Warman, P. R. (1986). The effect of fertilizer, chicken manure and dairy manure on Timothy yield, tissue composition and soil fertility. *Agricultural Wastes*, 18(4), 289-298.
7. Duncan, J. (2005). Composting chicken manure. WSU Cooperative Extension, King County Master Gardener and Cooperative Extension Livestock Advisor.
8. Pascual, P. R., Jarwar, A. D., & Nital, P. S. (2013). Fertilizer, fermented activators, and EM utilization in pechay (*Brassica pekinensis* L.) production. *Pakistan Journal of Agriculture, Agricultural Engineering and Veterinary Sciences*, 29(1), 56-69.
9. PSA (2019). Selected Statistics on Agriculture. Philippines Statistics Authority. Retrieved from <https://psa.gov.ph/content/selected-statistics-agriculture>
10. Yusuff, M. T. M., Ahmed, O. H., Yahaya, W. A. W., & Majid, N. M. A. (2007). Effect of organic and inorganic fertilizers on nitrogen and potassium uptake and yield of sweet corn grown on an acid soil. *Am. J. Agric. Biol. Sci*, 2, 118-122.
11. Kinf, H., Tsehaye, Y., Redda, A., Welegebriel, R., Yalaw, D., Gebrelbanos, W., Seid, H. (2017). Evaluating Adaptability and Yield Performance of Open Pollinated Maize Varieties in North Western Tigray. *Advances in Crop Science and Technology*, 05(06). <https://doi.org/10.4172/2329-8863.1000316>
12. Materechera, S. A., & Salagae, A. M. (2002). Use of partially-decomposed cattle and chicken manure amended with wood-ash in two South African arable soils with contrasting texture: effect on nutrient uptake, early growth, and dry matter yield of maize. *Communications in soil science and plant analysis*, 33(1-2), 179-201.
13. Oad, F. C., Buriro, U. A., & Agha, S. K. (2004). Effect of organic and inorganic fertilizer application on maize fodder production. *Asian J. Plant Sci*, 3(3), 375-377.
14. Dufault, R. J., Hester, A., & Ward, B. (2008). Influence of organic and synthetic fertility on nitrate runoff and leaching, soil fertility, and sweet corn yield and quality. *Communications in soil science and plant analysis*, 39(11-12), 1858-1874.





Erma Catipan Taer et al.

15. Prabha, L. M., Nagalakshmi, N., & Priya, S. M. (2015). Analysis of nutrient contents in vermicompost. *European Journal of Molecular Biology and Biochemistry*, 2, 42-48.
16. Li, S. T., Liu, R. L., & Shan, H. (2009). Nutrient contents in main animal manures in China. *Journal of Agro-Environment Science*, 1, 179-184.
17. Akinrinde, E. A., & Lawal, A. B. (2006). Influence of various sources of nutrients on growth attributes, nutrition and biomass production of sweet corn (*Zea mays* L. *Saccharum*). *J BiolSci*, 6, 854-860.
18. Boateng, S. A., Zickermann, J., & Kornahrens, M. (2006). Poultry manure effect on growth and yield of maize. *West African Journal of Applied Ecology*, 9(1).
19. Amujoyegbe, B. J., Opabode, J. T., & Olayinka, A. (2007). Effect of organic and inorganic fertilizer on yield and chlorophyll content of maize (*Zea mays* L.) and sorghum *Sorghum bicolor* (L.) Moench. *African Journal of Biotechnology*, 6(16).
20. Rong, X., Jiang, J., Zhu, H., LIU, Q., ZHANG, F., LIU, J., & YUE, Z. (2001). Effects of application of inorganic fertilizer in combination with organic fertilizer to red upland soil. *Journal-Hunan Agricultural University*, 27(6), 453-456.

Table 1. Corn yield characteristics parameters under combined organic and inorganic and inorganic alone fertilizers

Treatment	Replication				MEAN ± SD
	Rep. I	Rep. II	Rep. III	Rep. IV	
PLANT HEIGHT					
Control	100.00	109.40	120.34	111.50	110.31 ± 8.34 ^b
0.50kg VC + 0.50kg CD	198.90	200.01	199.43	202.10	200.11 ± 1.40 ^a
0.50kg VC + 10g IF	200.10	200.43	200.43	203.43	201.09 ± 1.56 ^a
0.050kg IF alone	200.00	201.02	199.90	203.60	201.13 ± 1.72 ^a
COB PER PLANT					
Control	1	2	2	1	1.50 ± 0.57 ^{ns}
0.50kg VC + 0.50kg CD	2	2	2	2	2.00 ± 0.50 ^{ns}
0.50kg VC + 10g IF	2	1	3	2	2.00 ± 0.81 ^{ns}
0.050kg IF alone	3	2	2	2	2.25 ± 0.00 ^{ns}
EAR HEIGHT					
Control	17.5	14.5	16.5	17.8	16.58 ± 1.49 ^a
0.50kg VC + 0.50kg CD	30	33	33	31	31.75 ± 1.50 ^c
0.50kg VC + 10g IF	24	25	26	31	26.50 ± 3.10 ^b
0.050kg IF alone	20	24	22	27	23.25 ± 2.98 ^b
KERNELS PER COB					
Control	392.0	364.0	364.0	378.0	374.50 ± 13.40 ^a
0.50kg VC + 0.50kg CD	420.0	406.0	432.0	448.0	426.50 ± 17.84 ^b
0.50kg VC + 10g IF	464.0	480.0	512.0	528.0	496.00 ± 29.21 ^c
0.050kg IF alone	434.0	406.0	465.0	495.0	450.00 ± 38.47 ^b
GRAIN YIELD					
Control	3.80	3.75	3.81	4.20	3.89 ± 0.20 ^a
0.50kg VC + 0.50kg CD	6.2	6.5	7.5	9.6	7.45 ± 1.53 ^b
0.50kg VC + 10g IF	10.25	10.50	10.70	11.35	10.70 ± 0.47 ^c
0.050kg IF alone	5.35	9.4	8.25	7.25	7.56 ± 1.71 ^b

Mean and SD column of the same superscript are not significantly different at 5% probability





Screening of Hepatitis B and C Virus Infections among Surgery Patients; Detremining the Significance of Pre-Operative Investigations as a Preventive Measure

Muhamamd Rahim^{1*}, Mehtab Rahim² and Fareed Ahmed³

¹Associate Professor, Surgery Department, Muhammad Medical College, Mirpurkhas, Pakistan.

²Gynaecologist, Bhurgri Hospital, Matli, Pakistan.

³House officer, Indus Medical College, Tando Muhamamd Khan, Pakistan.

Received: 16 Sep 2019

Revised: 19 Oct 2019

Accepted: 22 Nov 2019

* Address for Correspondence

Muhamamd Rahim

Associate Professor,
Surgery Department,
Muhammad Medical College,
Mirpurkhas, Pakistan.
Email: m_raheem76@yahoo.com



This is an Open Access Journal / article distributed under the terms of the **Creative Commons Attribution License** (CC BY-NC-ND 3.0) which permits unrestricted use, distribution, and reproduction in any medium, provided the original work is properly cited. All rights reserved.

ABSTRACT

Pre-operative screening of Hepatitis B and C is not very common in the medical setting of Pakistan. This major public health issue is increasing rapidly resulting in numerous chronic conditions specifically involving liver and under severe cases it may also lead to primary hepatocellular carcinoma. The aim of this study was to determine the seroprevalence of hepatitis B and C viral infections among the pre-surgical patients presented to the tertiary care hospital of Matli, Pakistan. A descriptive unicentre study was conducted at Bhurgri Hospital, Matli-Pakistan over a sample of 6108 patients presented for elective or emergency surgical procedures. The study continued from October 2014 to November 2018. The inclusion was made after attaining written informed consent from each patient. Patient demographic and clinical characteristics, hepatitis B surface antigen (HBsAg) and hepatitis C antibody (Anti-HCV) through immunochromatographic (ICT) methods. The recorded data was analyzed using SPSS Version 22. According to our findings, out of 6108 patients presented to the study setting 187(3.06%) had HBV while 504(8.25%) were having HCV infection. Majority patients were from 20-29 years age group majority patients. Moreover, increased prevalence of both the viral infections was observed among the patients from early and late adulthood. HBV and HCV infections were frequently present among the study population as identified through pre-operative screening. Indicating the necessity to add the screening of these measures before surgical procedures in order to avoid all sorts of complications during, before or after surgery and to execute appropriate management and treatment strategies.



**Muhamamd Rahim et al.**

Keywords: Hepatitis B, Hepatitis C, Pre-surgical Screening, Hepatitis B Surface Antigen (HbsAg), Hepatitis C Antibody (Anti-HCV).

INTRODUCTION

HBV and HCV are the leading viral infections affecting liver and globally resulting in significant morbidity and mortality (1,2). Both these viral infections are significantly hazardous and has affected massive population. It is estimated that approximately 300-400 million carriers of hepatitis are present worldwide (3). According to the statistics provided by several studies, infections caused by these viruses are leading towards increased death rate i.e. 1.34 million deaths in 2015 were reported due to HBV and HCV(4). Of which 720 000 deaths are due to hepatitis leading to liver cirrhosis and 470000 deaths due to hepatocellular carcinoma (4).

It is reported that Pakistan has 2nd highest prevalence of hepatitis C5, although internationally much of the disease rate has been controlled with implementation of universal hepatitis vaccination program (6) but locally in Pakistan, this disease burden can only be controlled with awareness session and campaigns to highlight the importance of vaccination, efficient and individualized therapy regimen is required in order to control the primary disease and to prevent associated liver complications as well (7). Both these viral infections are contagious, mainly transmitted by parents. It may result from transfusion or contaminated surgical supplies mainly infected needles (8). As the virus easily transfuses and can also be transmitted through broken skin, the exposure to infected blood or any other body fluids is the major source of transmitting infection (9). Due to which the health care providers are always at risk of developing this viral infection. The lack of awareness, timely diagnosis, management and precautions have intensified the overall disease risk (9). Globally in developed countries, the standard laboratory examination involves pre-operative screening of HBV and HCV infection prior to all sorts of elective or emergency surgical procedures. Through this study, we aimed to find out the prevalence of HBsAg and Anti-HCV among the patients admitted for surgery, through pre-operative screening in order to control the transmission and take precautionary measures and to highlight the significance of assessing these viral measures before any complex surgery.

METHODOLOGY

This descriptive unicentre study was conducted at Bhurgri Hospital, Matli-Pakistan. A total of 6108 patients presented to the study setting for various surgical procedures either elective or emergency were included in the study. The study continued for a period of 49 months, from October 2014 to November 2018. All conducts were made in accordance with the ethical guidelines and written informed consent were taken from each patient before inclusion in the study. After attaining the demographic history, all patients were screened for HBsAg and anti HCV through immunochromatographic (ICT) methods. Patients with already known hepatitis history were also screened for confirmation. The recorded data was analyzed using SPSS Version 22. Frequencies and percentages were used for data display.

RESULTS

The demographic and clinical parameters were assessed when the patient first showed up for elective or emergency surgery. Majority patients 2835(46.41%) were in between 20-29 years of age. Out of all, HbsAg was positive among 187(3.06%) patients and HCV in 504(8.25%) patients. The prevalence of both hepatitis viral infection was frequent among patients aged 20-40 years i.e. 44.9%-HBV, 31.74%-HCV and 50.6%-both, while patients ≤19 years displayed least number of incidences of the two infections.





Muhamamd Rahim et al.

DISCUSSION

The incidence rate of Hepatitis varies across the world among different countries. Based on the epidemiological data provided by WHO, Australia and Canada are having <1% prevalence of HCV followed by United states of America (USA) and Europe i.e. 1% (10). Moving towards the developing countries, the peak frequency >2% is observed in Africa and South-East Asia (10). The incidence rate of HBV and HCV has escalated in Pakistan in the past few years (11), being a country with numerous contradictory factors including economic crisis, declining health facilities, illiteracy, rising poverty, social, ethical, and cultural issues etc (7).

A study revealed the prevalence of HBV and HCV among the local Pakistani population was 10% and 5-10% respectively (12). Moreover, the frequency of this endemic condition may vary within a country as well. Based on the data of a comparative study including different areas of Pakistan, the frequency of HBV and HCV was greater among the rural population as compared to urban (13). In our study the frequency of Hepatitis-C positive amongst admitted patients was 504(8.25%) and Hepatitis-B was 187(3.06%) i.e. HBV was less common in comparison to HCV in our studied population (Table 1). It was observed that both HBV and HCV are highly prevalent in the age group between 20-40 years, while prevalence of HBV and HCV infections is least in the age group <20 (Figure 1). Based on the evidence provided by the previous literature the hepatitis risk increases with age therefore the disease incidences are more common among older age group as compared to the younger counterparts (11,14). Mahesh et al., reported that 7.1% incidences were present among patients aged 20 to 30 years while it increased to 21.4% for the older patients of 40 to 50 years (11). Our findings supported the presence of these viral infections more frequently among patients in late 20's, in contrast Talpur et al in his study revealed the occurrence of HBV and HCV more frequent among patients above the age of 40 years (14).

According to WHO, around 12 million Pakistani's are suffering from HBV and HCV (4). Among the major contributing factors for viral transmission, contamination either through needles or blood products with infectants are most prominent. The staff and physicians working in such contaminated healthcare setting are at high risk of developing the infection. Therefore, it is highly recommended that pre-operative screening must be carried out for each patient admitted for surgery so that the healthcare providers are better aware of the silent conditions that might cause medical harm to the individual patient, caregivers and the healthcare provider as well and precautions could be taken accordingly.

CONCLUSION

The high frequency of HBV and HCV in the studied population indicated the need for inclusion of pre-operative screening of these viral infections among the patients presented to the primary & tertiary care hospital for surgical procedures. As it is a significant occupational hazard for all the health care professionals including surgeons, anesthetics, associated health care team and staff. Moreover, patients and healthcare providers must be provided with adequate knowledge regarding the health hazards of the endemic condition and the hospital management staff must dispose off all the used infected materials properly following the biosafety protocols.

Conflicts of Interest

The authors have no conflicts of interest.

Sources of Funding

None.





Muhamamd Rahim *et al.*

ACKNOWLEDGEMENTS

The authors wish to acknowledge the support of Medical Affairs department of Getz Pharma for providing technical support in terms of manuscript editing and formatting.

REFERENCES

1. Frambo AA, Atashili J, Fon PN, Ndumbe PM. Prevalence of HBsAg and knowledge about hepatitis B in pregnancy in the Buea Health District, Cameroon: a cross-sectional study. BMC research notes. 2014;7(1):394-400.
2. Sharavanan TK, Premalatha E, Dinakaran N. Seroprevalence of hepatitis B surface antigen among rural pregnant women attending a tertiary care hospital. Blood Transfusion. 2014;10:1-9.
3. World Health Organization. Global Hepatitis Report 2017. Geneva: World Health Organization; 2017. Licence: CC BY-NC-SA.;3.
4. World health Organization. Prevention and control of hepatitis. Available at <http://www.emro.who.int/pak/programmes/prevention-a-control-of-hepatitis.html>
5. World health Organization. Pakistan tackles high rates of hepatitis from many angles. [Updated 11 July 2017]. Available at: <https://www.who.int/news-room/feature-stories/detail/pakistan-tackles-high-rates-of-hepatitis-from-many-angles>
6. Nwokediuko S. Seroprevalence of Hepatitis C virus antibody in public servants of Enugu state of Nigeria. Journal of College of Medicine. 2010; 15(1): 40-43.
7. Akhtar H, Badshah Y, Akhtar S, Hassan F, Faisal M, Qadri I. Prevalence of hepatitis B and hepatitis C Virus infections among male to female (MFT) transgenders in Rawalpindi (Pakistan). Advancements in Life Sciences. 2018;5(2):46-55.
8. Padilla FJB, Elizondo GV, Todd AV, et al. Gonzalez E G, Gonzelez J A G, Garza H J M. Hepatitis C virus infection in health-care settings: Medical and ethical implications. Annals of Hepatology. 2010; 9: 132-140.
9. Yenesew MA, Fekadu GA. Occupational exposure to blood and body fluids among health care professionals in Bahir Dar town, Northwest Ethiopia. Safety and health at work. 2014;5(1):17-22.
10. ul Huda W, Jameel N, Fasih U, Rehman A, Shaikh A. Prevalence of Hepatitis B and C in Urban Patients Undergoing Cataract Surgery. Pakistan Journal of Ophthalmology. 2013;29(3):147
11. Lohano MK, Su L, Narsani AK, Jawed M, Naveed H. Frequency of Hepatitis B surface antigen (HBsAg) and Hepatitis C antibody (HCVAb) seropositivity among preoperative eye surgery patients. British Journal of Medical Practitioners. 2016;9(2):5-9.
12. Tahir MA, Cheema A, Tareen S. Frequency of Hepatitis-B and C in patients undergoing cataract surgery in a tertiary care Centre. Pakistan journal of medical sciences. 2015;31(4):895
13. Naeem SS, Siddiqui EU, Kazi AN, Khan S, Abdullah FE, Adhi I. Prevalence of Hepatitis 'B'and Hepatitis 'C'among preoperative cataract patients in Karachi. BMC research notes. 2012;5(1):492.
14. Talpur A, Ansari A, Awan M, Ghumro A. Prevalence of hepatitis B and C in surgical patients. Pak J Surg. 2006;22(3):150-153.





Muhamamd Rahim et al.

Table 1. Demographic and clinical characteristics of the study population

Variables	(n=6108)
Age Groups (Years)	
≤19	694(11.36)
20-29	2835(46.41)
30-39	1127(18.45)
≥40	1452(23.77)
HbsAg Positive	187(3.06)
HCV Positive	504(8.25)
Mixed Positive	83(1.36)

**Values are given as n(%)*

**HbsAg-Hepatitis B Surface Antigen; HCV- Hepatitis C Virus*

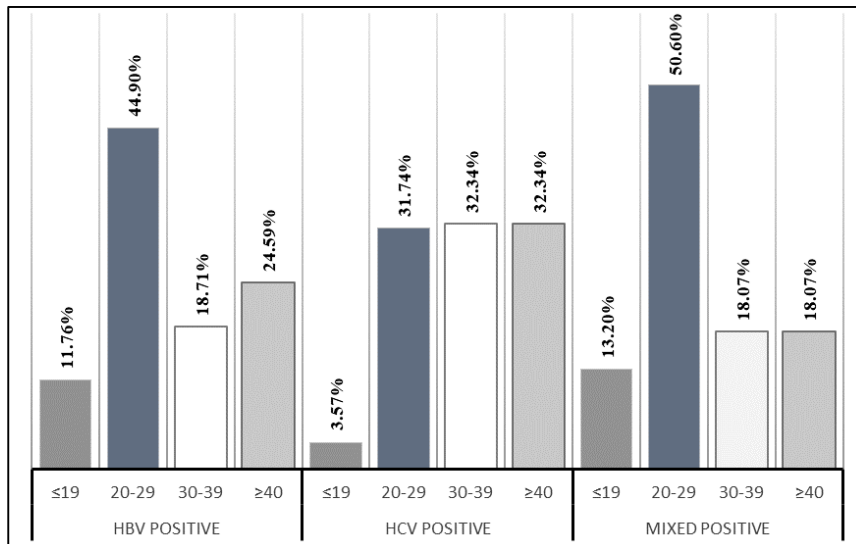


Figure 1. Prevalence of HBV and HCV in different age groups





Anatomical and Some Morphometrical Features of Small Intestine in Adult Local Sheep (*Ovis ares*) in Iraq

Israa G. Hussein* and Ahmed S. AL-A'araji

Department of Anatomy, Embryology and Histology, Collage of Veterinary Medicine, Baghdad University, Iraq.

Received: 15 Sep 2019

Revised: 17 Oct 2019

Accepted: 22 Nov 2019

*Address for Correspondence

Israa G. Hussein

Department of Anatomy,
Embryology and Histology,
Collage of Veterinary Medicine,
Baghdad University, Iraq.
Email: israa.ghassan@yahoo.com



This is an Open Access Journal / article distributed under the terms of the **Creative Commons Attribution License** (CC BY-NC-ND 3.0) which permits unrestricted use, distribution, and reproduction in any medium, provided the original work is properly cited. All rights reserved.

ABSTRACT

This study was conducted on 10 samples of small intestine in adult local sheep in Iraq. General gross description of intestine was done in situ immediately after animal slaughter whereas further study like morphometrical parameters related to the weight and length were completed in laboratory. The result proved that the intestine was pale pink to gray in color composed of three segments duodenum; the first part that start after the end of abomasum, jejunum; the middle and longest part and ileum; the terminal and shortest segment with no clear anatomical demarcation lines separated between them. These segments were situated at the right half of abdomen attached to the right abdominal wall and related to the dorsal aspect of abdominal cavity. The result showed that the small intestine was nourished with blood through two main Sources: celiac trunk and cranial mesenteric trunk; both of them were branched from common trunk named celiac - mesenteric which arise from aorta.

Keywords: Small intestine, Anatomical, morphometrical, sheep.

INTRODUCTION

Food is the fundamental requirement that the animal body demands for growth and maintenance the life through nutrients absorption (1). It is impossible to use the food in its original form without changed by organs of digestive system that make it effortless absorbed in blood stream (2). Small ruminants such as sheep consider a significant provenance to output milk and meat even in inimical surroundings as well as hard situations and diseases resistant, so these animals have a great ability to create supplemental income especially in pauper rustic areas (3, 4). The intestine do fundamental function in the digestion and absorption of different nutrients that animals consumed.



**Israa G. Hussein and Ahmed S. AL-A'araji**

Small intestine is the first site concerned with breakdown of enzyme, in addition to absorption of carbohydrates, fatty acid, and amino acids (5). There is rarity of literatures on macroscopic and microscopic structure of this part of digestive tract excepting some researches has been achieved in some ruminants which is insufficient to established a good and obvious data base about the intestine (6). The current work was intended to investigate the anatomical and some morphometrical features of small intestine in adult local sheep.

PROCEDURE AND PARAMETERS

To achieve the objectives of this study, 10 samples of small intestine were used. All animals from which that the anatomical samples were took were weight before slaughter. The all parts of small intestine were observed, described in situ, photographed and collected instantly after animal slaying, then they transmitted to laboratory in ice containers that make ability to fulfillment other aims of the study. Blood supply was done by injected of a mixture composed of three parts latex and two-part ammonium hydroxide colored with carmine stain in the common carotid artery.

RESULTS AND DISCUSSION

The present work revealed that the small intestine in adult local sheep was pale pink to gray in color ,composed of highly vascularized three segments which (in order) duodenum; the first part that start after the end of abomasum at pyloric region, jejunum; the middle and longest part and ileum; the terminal and shortest segment which attached to other group of organs called large intestine (fig.1,2). It is important to mentioned that there are no anatomical demarcation lines to isolated these parts one from other (fig.2,3). This findings were conformable with (7) in his study on ruminants digestive system. All these segments were situated at the right half of abdomen attached to the right abdominal wall, largely covered with ribs, rumen and other digestive organs and related to the dorsal aspect of abdominal cavity (fig.4). An exact match between the results of this study and the results of that reported by (8) in her study on indigenous Gazelle .The morphometric measurements of the three segments of small intestine are in table (1& 2).

The duodenum was pale pink in color composed of five parts: Cranial portion, cranial duodenal flexure, Descending portion, caudal duodenal flexure, ascending duodenum and Duodeno jejunal flexure. It originated with cranial portion at the level of 9th – 10th rib near the pyloric region of true stomach (abomasum). The passageway of duodenum give it ability to grasp the pancreas between its two limbs (ascending and descending parts) (fig. 3). In the present work, the gross anatomical results on duodenum were compatible to a large extent with the results of many previous researches in different domestic animals (9,10,11,12). After about 17 cm from the pylorus and exactly after the Cranial duodenal flexure (*Flexura duodeni cranialis*) a straight duct opened in the start of descending part of duodenum to pass about 1 centimeter within the wall of duodenum as intra duodenal part or (intramural part) then it opened finally into the lumen with one or common papillae slightly to the left side (fig.5,6). This distance between end of abomasum and the papillae of duct was shorter than distance in study of (13) on intestine of goat who reported that the bile duct opened 26.5 to 30 cm away from the pylorus. The results of (14) proved that there were two papillae in first part of the duodenum (papilla duodeni major and papilla duodeni minor) in donkey's study.

Both papillae were located near to each other with a distance less than 1 cm and very near to the ostium pyloricus. The jejunum was the second and longest segment of small intestine composed of high number of short series u-shaped mesenteric loops which act to prolonged it. The prevailing direction that these loops pass was is ventrally, caudally then dorsally toward the ileum and large intestine within the abdominal cavity. It starts after the end of duodenum at the duodeno- jejunal flexure and terminate at the junction with the ileum. The end of this segment of small intestine and start the next part is remarkable by an obvious fold called (ileo cecal fold) and by thickening of the wall of the ileum (fig.1,2,3,4). Similar findings were reported in (2017) by Maruti in his study on sheep and goat.



**Israa G. Hussein and Ahmed S. AL-A'araji**

The present work shows that the length of mesentery supported jejunum (meso-jejunum) is much higher than that attached to the previous segment duodenum (meso duodenum), so the jejunum is appeared greatly mobile than duodenum (fig.7). These results were parallel to what mentioned by (15,16). The ileum was the last segment of small intestine appeared as straight short tubular organ connected to the jejunum shortly caudal to the head of cecum and directed toward the caudal end of the body. In fresh samples its appeared as light pink in color in the first two thirds while grey in color in the third third . The ileum is Intermediate the position between spiral loops of ascending colon with centrifugal ansa from one side and the cecum with ileo cecal fold from other. the start of this organ which can be also recognized through an anatomical structure consist of peritoneal layer called ileo cecal fold. The upper border of this fold is fixed to the ileum, contrary to its mesenteric attachment side while its lower part reach to the ileo cecal junction. Ileum ends at the other part of the digestive tract called large intestine, exactly at the cecum to open at the ileoceco- colic orifice (fig.1,2). A great similarity was present in the study of (17) in goat and study of (18) in goat and sheep in which they mentioned that the ileum was the terminal segment of the small intestine. It passed cranially which was nearly straight and short and joined to large intestine on the ventromedial surface of the cecocolic junction. In the same context, (19) referred to the ileum in his study on deer and mentioned that it was attached to the caecum by the ileocecal fold which is opened into the large intestine through the ileal ostium.

The small intestine were nourished with blood through two main Sources: celiac trunk and cranial mesenteric trunk ; both of them were branched from common trunk named celiaco - mesenteric which arise from aorta in abdominal region (fig.8). This result was dissimilar to the result of (20) in his study on Barbados Black Belly sheep in which he found the cranial mesenteric artery originated separately from the ventral aspect of the abdominal aorta caudal to the origin of the celiac artery. In the present study the duodenum supplied with blood through the gastro-duodenal trunk which give rise to cranial pancreatico- duodenal artery that directed caudally to supply caudal and middle part of duodenum to unite finally with caudal pancreatico- duodenal artery that originated from cranial mesenteric artery(fig.8). The blood vessels supplied the jejunum were branched directly from cranial mesenteric artery called (jejunal branches) which passed dorsally to jejunum and parallel to the centrifugal ansa (fig.9). The cecal branch arise also from cranial mesenteric artery to direct toward the end of cecum to nourished it by many small branches along the cecal course. Tiny obvious arteries arise from terminal portion of cecal artery supplying the first part of ileum (fig.10). The cecal artery have another branch directed dorsally named ileo-colic branch which nourished the last part of ileum near ileoceco colic orifice by two small arteries; as well as the ileo colic artery supplied the initial part of colon (fig.11). Current findings as well as those obtained by (21) in goat ascertained that the jejunal arteries were detached from the cranial aspect of the cranial mesenteric artery along its whole length. In addition to that the current investigation, corresponding with those of (21) in goat, (22) in ruminants and (23) in buffalo, in which they clarified that the cecal artery gave off cecal and antimesenteric ileal branches and continued as the antimesenteric ileal artery.

CONCLUSIONS

No obvious differences in anatomical form between domestic sheep and other ruminants. Morphological modifications of small intestine was desired in the sheep to performance its physiological role.

REFERENCES

1. Tarquinio, D.; Motil, K. ; Hou, W. L. and Percy, A.K. (2012). Growth failure in Rett syndrome: Specific growth references. *Neurology* 79:1653-1661.
2. Nancy ,D.B (2010) the digestive system . university of maine . sckool of social work . Pp:1-9.
3. Gatenby RM, Trail JCM. Small ruminant breed productivity Africa. International Livestock Centre for Africa, (1982); Addis Ababa, Ethiopia.





Israa G. Hussein and Ahmed S. AL-A'araji

4. Huda Shadhan Awadha Eman Fasiat Abdall Hassan. Detection of cholecystokinin and glucagon like peptide in small intestine of Awassi sheep. AL-Qadisiyah Journal of Vet. Med. Sci. Vol. 16 No. 1 2017.
5. AL-A'araji, A.S. and AL-Kafagy, S.M. (2016). A comparative anatomical, histological and histochemical study of small intestine in Kestrel (*Falco tinniculus*) and white eared bulbul (*Picnonotic leucotis*) according to their food type. The Iraqi Journal of Veterinary Medicine, 40(2):36-41.
6. Damron, S. W. (2003) . Introduction to Animal Science.2nd. editions. Prentic Hall Co. U.S.A. p: 95-111.
7. Parish, J. (2011). Ruminant Digestive Anatomy and Function. Beef Production Strategies.
8. Al-Mansor, N.A.S. (2018). Anatomical and Histological Study of Small Intestine in Adult Male Indigenous Gazelle (*Gazella subgutturosa*). MSc. Thesis . Anatomy and Histology department . collage of Veterinary Medicine. Baghdad University.
9. Perez, W. and Vazquez, N. (2012). Gross anatomy of the gastrointestinal tract in the Brown Brocket deer (*Mazama gouazoubira*). J. Morphol. Sci., vol. 29, no. 3, Pp: 148-150.
10. Christiane, S.; Elise, R. and Reto, N. (2013). Gastrointestinal endoscopy in the cat: Equipment, techniques and normal findings. Journal of Feline Medicine and Surgery. 15, 977–991.
11. Gerard, T. (2014). Principles of Anatomy & Physiology. USA: Wiley. P: 913.
12. Charly, P.; Minh, H.; Roman, H. and Vladimir, J. (2015). Veterinary Clinics of North America Exotic Animal Practice, 18(3):369-400.
13. Ajay, P. and Chandra, G. (2000) "Gross anatomical studies on intestine of goat" Ind. J. Vet. Anat.12 (1): 23-26
14. Jerbi, H.; Rejeb, A.; Erdogan, S. and Perez, W. (2014). Anatomical and morphometric study of gastrointestinal tract of donkey (*Equus africanus asinus*). J. Morphol. Sci., vol. 31, no. 1, p. 18-22.
15. MARUTI, G.M. (2017). COMPARATIVE GROSS ANATOMICAL AND HISTOMORPHOLOGICAL STUDIES ON SMALL INTESTINE IN SHEEP (*Ovis aries*) AND GOAT (*Capra hircus*). MSc. Thesis. VETERINARY ANATOMY AND HISTOLOGY DEPARTMENT. KRANTISINH NANA PATIL COLLEGE OF VETERINARY SCIENCE. MAHARASHTRA ANIMAL AND FISHERY SCIENCES UNIVERSITY, NAGPUR.
16. Bragulla, H. (1991). Die Hinfallige Hufkapsel (*Capsula unguale decidua*) of Pferde-fetus und neugeborenen Fohlens. Anat. Histol. Embryol.; 20: 66-74.
17. Constantinescu, G.M. (2002). Clinical Anatomy for Small Animal I. Ames: Iowa State Press.
18. Pachpande, A. M.; Dhande, P. L.; Lambate, S. B. ; Ghule, P. M. ; Yadav, G. B and Gaikwad, S. A. (2011) "Gross anatomical and Biometrical observation on small intestine of goat" Ind. J. Vet. Anat. 23 (2): 49-55.
19. Perez, W.; Erdogan, S. and Ungerfeld, R. (2014). Anatomical Study of the Gastrointestinal Tract in Free-living Axis Deer (*Axis axis*). Blackwell Verlag GmbH, Anat. Histol. Embryol
20. MOHAMED, R. (2017). Anatomical studies on the cranial and caudal mesenteric arteries of the Barbados Black Belly sheep. J. Morphol. Sci., vol. 34, no. 2, p. 93-97.
21. YOUSSEF, A. (1991). Some anatomical studies on the coeliac, cranial mesenteric and caudal mesenteric arteries of goat. Msc. Thesis. Benha: Faculty of Veterinary Medicine, Zagazig University.
22. WILKENS, H. and MUNSTER, W. (1981). The circulatory system. In NICKEL, A., SCHUMER, R. and SEIFERLE, E. The anatomy of the domestic animals. Hamburg: Wright Verlag Paul Parey, p. 159-268. vol. 3. Ciccocioppo, R; Sabatino, A. D; Parroni, R; Muz, P; Alò, S. D; Ventura, T; Pistoia, M. A; Cifone, M. G. and Corazza, G. R. (2015). Increased enterocyte apoptosis and Fas-Fas Ligand System in celiac disease. Am. J. Clin. Pathol; 115: 494-503.
23. Machado, M.R.F.; MIGLINO, M.A.; DIDIO, L.J.A.; HONSHO, D. and BORGES, E.M.C. (2002) The arterial supply of buffalo intestines (*Bubalus Bubalis*). Buffalo Journal, vol. 18, n. 2, p. 249-256.





Israa G. Hussein and Ahmed S. AL-A`araji

Table 1: Shows the weight of animal's body involved in this study, whole weight of small intestine, weight of each segment and the ratio of small intestine weight to body weight

Parameters	Range	Mean ± SE
Total Weight of animal's body	20- 29 Kg	23 ± 2.4
Weight of duodenum	22-39 gr	31 ± 4.2
Weight of jejunum	462-857 gr	674 ± 114
Weight of ileum	19- 28 gr	24 ± 2.5
Total weight of small intestine	503 - 924 gr	729 ± 121
Ratio of small intestine weight to body weight	2.515% - 4.045%	3.149 ± 0.5

Table 2. Shows the total length of small intestine, length of duodenum, jejunum, ileum, and the ratio of length each segment to the total length of intestine.

Parameter	Range	Mean ± SE
length of duodenum	52 – 61 cm	57 ± 2.6
length of jejunum	1143 – 1164 cm	1155 ± 6.1
length of ileum	29 – 36 cm	33 ± 2.0
Total length of small intestine	1224 – 1261 cm	1242 ± 10.7
Ratio of duodenal length to small intestine length	4.248 – 4.837 %	4.583 ± 0.2
Ratio of jejunal length to small intestine length	92.307 % - 93. 382 %	92.763 ± 0.3
Ratio of ileal length to small intestine length	2.369 – 2.868 %	2.654 ± 0.1



Fig. 1. The small intestine in adult local sheep appeared pale pink to gray in color composed of three segments: duodenum, jejunum and ileum



Fig. 2. Gross section in small intestine of adult local sheep. Jejunum the middle and longest part. Ileum the terminal portion which attached to cecum.





Israa G. Hussein and Ahmed S. AL-A`araji



Fig.3. Course of duodenum with its parts.1: abomasum 2: Cranial portion 3: Cranial duodenal flexure 4: Descending portion 5: Caudal duodenal flexure 6: Ascending duodenum 7: Duodeno- jejunal flexure. 8: jejunum

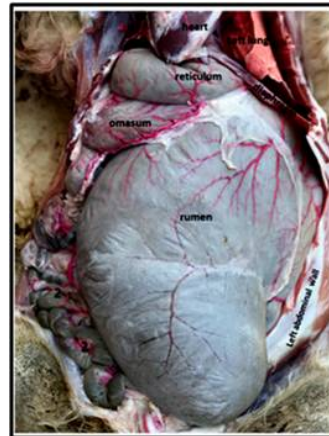


Fig.4. Position of the small intestine in abdominal cavity which attached to the right abdominal wall. The jejunum and small segment of duodenum are the only parts of the intestine that are exposed when the abdominal cavity opened in midline.



Fig. 5. Common bile and pancreatic duct which opened in duodenum at the cranial duodenal flexure. 1. duodenum, 2. Cranial duodenal flexure e, 3. Descending portion of duodenum.



Fig. 6. Papillae of common bile and pancreatic duct inside the duodenum. 1. Intramural part, 2. Entrance of duct 3. Papillae of duct.





Israa G. Hussein and Ahmed S. AL-A'araji



Fig.7.Meso-jejunum which appeared longer than meso-duodenum in order to give jejunum exceptional level of mobility. 1: duodenum 2. meso-duodenum 3: jejunum 4. Meso-jejunum



Fig. 8: Blood supply branching of small intestine. 1: abdominal aorta 2: celiaco – mesenteric trunk 3: celiac trunk 4: cranial mesenteric artery 5: splenic artery 6: hepato-gastric trunk 7: left gastric artery 8: hepatic artery 9: cystic artery 10: gall bladder 11: gastro-duodenal trunk 12: right gastric epiploic artery 13:cranial pancreatico-duodenal artery 14: caudal pancreatico-duodenal artery 15:right gastric artery



Fig. 9. Branching of cranial mesenteric artery in supplying jejunum with blood.1: cranial mesenteric artery 2: jejunal branches 3:centrifugal ansa



Fig.10. Branching of cecal artery.1: ileal branches 2: cranial mesenteric artery 3: cecal artery 4: ileo-colic artery 5: ileal arteries 6:colic artery



Fig. 11: Cecal artery and its branches to supplying the ileum. 1. Cecal artery, 2. Ileal arteries or (branches), 3. Ileo-ceco-colic orifice.





Eco-Friendly Modification of Severe Tropical Cyclone: Vedic Vigyan Based Social Welfare Technology

Deepak Bhattacharya

Sri Radha Krishna, Kedar Gouri Road, Bhubaneswar, Odisha, India.

Received: 14 Aug 2019

Revised: 17 Oct 2019

Accepted: 25 Nov 2019

*Address for Correspondence

Deepak Bhattacharya

Sri Radha Krishna,
Kedar Gouri Road, Bhubaneswar,
Odisha, India.
Email: oddisilab1@dataone.in



This is an Open Access Journal / article distributed under the terms of the **Creative Commons Attribution License** (CC BY-NC-ND 3.0) which permits unrestricted use, distribution, and reproduction in any medium, provided the original work is properly cited. All rights reserved.

ABSTRACT

Depressions and deep depressions harbringes bounty. Tropical cyclones have a tendency to intensify and inflict wanton loss. India suffers incessantly. She has the means, and has no method to down-regulate killer / destructive cyclones. An economic, feasible, eco-friendly theory is discussed. It uses thermal power plant fly ash and or activated charcoal as seed, dropped in form top at designate locations. Cloud feeder channels be the best sites. Aim is to disrupt (i) principal energy input mechanism (ii)electrostatic mechanism (iii)stochastic pathway and make the system non-synchronous, specially the front.

Keywords: Cyclones; Fly ash; Feeder channel; Down regulation; Up-regulation.

INTRODUCTION

Very severe cyclones are geography specific. The india Meteorology Department (IMD) classifies various sea sourced cyclonic systems as in Table-1(1). In 2006, India had 16 Cyclones and depressions of synoptic scale, of which 14 had crossed the Odisha coast line (2). In 2013, India had 10 cyclones over north Indian Ocean, 1deep depression over the Arabian Sea, 1 land depression and 8 cyclones over Bay of Bengal i.e., BoB (3). The Brahmani-Mahanadi delta (Odisha) receives excess rainfall agro-meteorologically bracketed between July-Sep. Further, annually, 3-15 depressions and 1-2 severe cyclones cross Odisha's coastline shedding 231BillionM³ rain/yr., between 1stJuly–30thSep., of which, run-off to the sea is of the order 200 Billion M³/yr. Spring tide ingress is between 50-100Kms., inland, with short inter-tidal zones (0.25-1mt amplitudue). Storm assisted tidal bores ranging between 2-20m high are also experienced (4). Hydrologically, large number of drainages with large cross sections are naturally warranted to drain such large volume spurt flow. Hence Odisha is the ideal candidate for the caption studies. Fig.-1 is the satellite image in the visible range of the Brahmani-Mahanadi delta; exposed in non rainy season (from Google Earth, with thanks). The focus domain is a maze of drains and channels of various cross sections; remnants included. All being dry. We have compared the same with other large delta(s) viz., Amazon; Mississippi; Rhine; Danube; Leena; Ob; Yellow; Mekong;

17893



**Deepak Bhattacharya**

Padma (Ganga-Brahmaputra combined); Indus; Congo. We confirm, that geographically and geomorphologically excepting the Padma delta, non of the afore mentioned deltas/command areas have anything alike. Therefore, if severe cyclones and above categories could be down-regulated to <4 close isobars pre ingression into this region, then copious rain water could be stored in these channels with lot much good for the sub-populations on the ground.

Seasonally, the drainages fall dry during the 8months long no-rainy season. Figure-1 is exposed in dry period. To the informed beholder it conjures an impression of riparian country (Odra desa, in Prakrit-Sanskrit lingua). The frequency of cyclone land fall in this domain is so regular that the native coastal people have indigenous cyclone resistant rural house building know-how (5). This coastal domain and most locations in the north-east India have an annual average rain fall of the order 1500mm. Some of the plateaus (Koraput; Kandhamal; Similipal; Jharkhand; Sikkim; Meghalaya) have an annual average rain fall of the order 1800mm (6). A sever cyclone can (additionally) unload anything between 20-40 BillionM3 of water in a span of 24hours spread over a 400Km2 rectangular catchment zone in the inter-valleys of these plateaus. Wind velocity bring in another set of (insurmountable) problems for the afflicted natives and the administrations. This apart, the eastern shore board of India is also the focus region for Govt. of India's flag ship research program termed 'STORM (IMD-STORM, 2012) (7). Storms are very intense cyclones of small cross section (meso scale). Bhattacharya (8) and again Bhattacharya & Misra (9) have pioneered a study as to how sever cyclones and intense storms (micro-bursts) cause acute problems for the pregnant, the heart & lung disease patients and for the geriatric group. Bhattacharya (10) has discussed the nexus between such atypical meteorology & malaria in the BoB rim. Bhattacharya, et.al.,(11) have reported that the same geography also experiences Tornados (twisters of micro scale) which makes our domain special on pan global basis.

Therefore, there is a need for killer/destructive cyclone down-regulation technology. It will lead to standardization of storm down regulation technology, by & by Following Bhattacharya (2003) (12); 2006 (13), Alamaro et.al., 2006 (14, 15), had proposed a ultra expensive and cumbersome technique of upward spraying of sea water by 'compressible free jets' from ships located around a cyclone with a aim to induce *enthalpy* all around the periphery becauseing a down regulation which was later found to be untenable (followed Bhattacharya on *datum*). As run up to this treaties Bhattacharya a native of the Super Cyclone (10-1999, Odisa, India) effected zone had as usual gone out to study the same and survived miraculously (supporting information). He has discussed the correlation between geo-spatial & meteorological aspects and the mechanics of the Super Cyclone using principles of fluid mechanics (16) and also discussed the causative factors of high gyration in the tropical cyclones germinating in the Bay of Bengal (BoB)(17); the weak points of the Super Cyclone –1999's structure. Bhattacharya dealt upon the meteorological physics of weather modification in a International conference of multidisciplinary scholars (18,19), and presented the fly ash (FA) as an very effective cum economic candidate aerosol that could be used for down regulating killer cyclones by top seeding and also discussed the mechanics of down-regulation. Bhattacharya, again by a lead oral presentation at the International Conference of Asia Ocenia Geo-Science (20) presented the physics and the mechanics of 'Eco-friendly (limited) down-regulation'- using 'FA' as the aerosol/CCN. D. Rosenfield, et.al., (21) followed by discussing the history of failed theories and proposed a sideral seeding with sub-micron hygroscopic aerosols, without mentioning any candidate (aerosol) in particular

Natural Preferences

Hill/ precipe type orography as is the western ghats of the Indian peninsula and the Rocky mountain chains of the North American continent develop (compressed) fluid boundaries which deflect; thwart land fall and inland ingression. The delta valley geographies such as that of belly China; Ganga-Padma-Rupnarayan region, Brahmani-Mahanadi region, and Godavari regions of the Indian sub-continent permit land fall; on-land life and inland ingression. This is due to their unique orography. Long on-land life is the principal cause of destruction of property, precious human & veterinary life. Selenic phase and alignment intensifies (22). Therefore, geography, orography, geomorphology and also aerosols posits as vital cause factors in appreciating the causes of intensification, on-land life, down-regulation, decay deflection and path alterations. In this communication we discuss the (possible) multi-





Deepak Bhattacharya

disciplinary role of the Indian Air Force/Indian Navy, the remote sensing & met scientists can in real-time play in the attainment of such socio-strategic objectives. We are further of the view that sidereal seeding of cyclones by micronised hygroscopic material i.e. warm CCN (Rosenfield's method) will be sucked near uniformly into the lower and mid circulatory (dynamic zone) and result in quick evolution of crisp boundary phenomena; high gyration; high 'T' factor; robust stem; erect architecture; forward motion; intense cloud to ground arching; heavy load shedding; efficient recharging all over the system; synchronised front; increase in 'H' dimension (will result in stoachisation on planetary scale = disaster as in SC-10/1999) and/or even induce straight track (swift land-fall ~ reduce reaction time; viz. Andhra Cyclone 1998). The system will gain in reciprocating enthalpy and enstrophy. Its energy basket will fold rise; ability to withstand ultra high solid state bottom friction (land) will leap frog resulting in longer duration effective on land life (actual killer/destruction period). Hence our theory (which is quite different) needs detailed discussion.

Figure-2a is on a geography map. It shows schematically the Indian peninsula and the BoB rim as a pair of near complementing triangles. Hence, either can be fractralised using Sierpinski's *model*, which is a tool in (i) size function (ii) thrust function (iii) angle vector studies. The in-sea lower triangle marks the genesis domain of atmospheric weather systems of the vortical form and initial direction of incidence (March-Sep., period). The small triangle (northern BoB) marks the zone of the compressed forcings transpiring out of the stepped-down architecture of the triangular morphology (fractal effect) and as the natural preferred domain for genesis of anti-clock spirals. Figure-2b has a line (A-B) drawn from the Sikkim plateau to the Arakans (through Meghalaya plateau & Cachar plains). The term 'cachar' is phonetically pronounced as 'kachar' (muddy in local lingua). This plain name is a descriptive geographic term as alike the 'Flushing meadows' of the British Isles. Figure-2c is the schematic cross section of the geomorphology along the line A-B. The corner apex (viewer's left) being the Himalayas → Sikkim → Brahmaputra valley → Meghalaya → Kachar plains → Arakan hills. Fig.-2d shows the fractalization of monsoon's hydrodynamic thrust – in 3D as enmeshed members.

In Figure-3 is the line 2-3. It is that of the schematically drawn monsoon trough as during *cold SST* year (e.g., 2006) originating at sea (BoB), ingression through the Mahanadi-Brahmani -Rupnarayan delta-valley drainages (preferred gateway) and extending past New Delhi. At its sea end is a boxed domain that marks the locus of genesis of deep systems; sea surface touching and enlarging energy basket. Along line 2-3 are 3 transverse lines that have been drawn at 3 different geo-locations to arrive at the barotropic architecture of the cross sections at 'A-B', 'C-D', & 'E-F', of the atmospheric trough (also known as 'monsoon trough'). They indicate the depth and the width aspects which is inverse at locations away from the sea. This provides the pathway for initial ingression. And whereas, the geomorphology of the river valleys offer a similar physical architecture with altered sequence (as in cross sections A-B, C-D, & E-F) at variable elevations from MSL. In other words the physical domain or valley effect is steep in the inland regions. Whereas, the close isobars are noted only towards the sea face regions. Height gain and valley constriction combined is the principle cause of [i] heightened friction (drag due solid state bottom) [ii] systemic back pressure (iv) stationary on coastal plains (v) decay. Thus, systems fail to negotiate the central Indian high-lands (heavy ones stay put in coastal regions). If we have a technology to up-regulate such systems; drag inland and induce copious precipitation in the Sutlej-Ganga-Yamuna agro belts and specially in the rain shadow regions during monsoon viz. Budelkhand; Bidharv; Rayalseema; Chitoor; Kadapa; etc. Such type of weather modification will help bounty & family welfare.

On the other side, the Himalayan ultra high rise chain geomorphology that rises above the meteorological boundary layer (~ 900-1000mts above MSL) from Sikkim plateau is closest to the BoB. Jointly with the Arakans it locks the Bangla-Brahmaputra plains with the southern precipitous face of the Shilliong plateau jutting in the middle as alike an axle facing the BoB (23). Circular flow around it creates additional (atypical) met domain which in turn reduces back pressure in the boxed region as in Figure-3. Such compaction of fluid with reduction of domain promotes genesis of systems in series circular flow and swivel towards the eastern shore board of India while asyclic back pressure assists the spiral form. The copular thrust of the sea-atmosphere (in parts) gets locked in the valley-plains of





Deepak Bhattacharya

the NE. Their synclines (solid state boundaries) produce (fluid) boundary effect of variable dynamic orders (couple thrust dependant), which because swivel of the lines of the forcings as per the lie of the solid state boundary (Arakan-Himalayan geomorphology) in tune with Coriolis. Such sea-atmosphere couplar thrust (monsoon period) takes a supine pyramidal form and swivels (F-3 inset). Hydro dynamic compression because size reduction. Orography induces swivel towards the zone of least resistance (viz. deltas). Variable swivel permits a wider land-fall domain & subsequent events. Leaf, log & organic burnings create good CCNs which all traverse via the giant river valley and get injected into the met systems, and up-regulate (colateral data). This is the cause of the eastern shore board of the Indian sub-continent acting as upregulator of met fronts and most preferred destination domain of atmospheric weather systems i.e., sea sourced cyclones; land sourced tornados and in the shifting of the monsoon trough line (thrust dependant). Hence, severe weather event caused social & national losses will keep on occurring all along the eastern shore board of the Indian sub-continent. The western shore board of India experiences not all these primarily due orography & geomorphology inspite of being triangular. This also is the cause of aridification of west & west/central India (also either side of the triangular Arabian sea). Herein we present the basic skeleton of a hypothesis to develop a home grown technology to (i) down regulate destructive cyclones (ii) up-regulate weak ones (iii) alter ingression potential. On pan global basis, this is a 1st time work. It is backed by two decades of on-foot, field work; a decade of academic co-relating and preparatory run-up.

Super Cyclone 1999:

OBSERVATIONS AND DISCUSSION

Fig.-4a is that of the Super Cyclone of 1999, at location landfall (NOAA, 2003) (24). It may be co-read with T-1. Fig.-4b is the outline of that system along with the inter-hemispheric long FC which is of planetary scale. It describes the yo-yo cum wave type form (zenithal view). Fig.-4c schematically incorporates the overall wind cum moisture flow and marks out few typical aspects that are associated with destructive cyclones. It is our own developed between 1990-2000. Around the eye is the CZ (core zone). Around it is another moderately high circulatory wind zone extending laterally beyond the circulatories having destructive force. It too is circular being hooded by depleted cloud marked as CH (cloud hood). Thereafter, is the down-draft zone marked by clear sky; as different from gravity waves (see R-29). The CH is the outer rim of the circulatories (depleted). It is bereft of rain and is a collinear cum supplementary mechanism. In other words, in frictionless or in near frictionless conditions, objects/particles having similar mass will develop in-field copulations having uni-directional flow i.e., fields of static inertia will gradually become dynamic (enlarge; viz. mid pacific systems). Such copulation will be interactive and have size; mass; & therm based stratifications. The CZ & the CH are a complementing couple.

The oval ring represents the field in which strong, laminar, cool surface breeze that was noted (wind vane based) to be flowing in the direction of the CZ alias 'surface in-flows' (SIF). The tip of the oval is the farthest point from 'E'. It is co-incident with the direction of inclination of the system; the 'F', and the track. SIF is a thin, compressed fluid bed having centripetal flow marked by arrows. Deep systems float on SIF fluid beds which also supplements the radiator component of the system, apart being the source for updraft. If solid state friction from geomorphology be high then SIF will be weak & inconsistent. Stronger and consistent the SIF, erect be the central column; high be the wind velocity in the CZ with a more synergic 'F', respectively. Our experience is that if the SIF has 10knots speed (a) consistent over a terrestrial field of 100kms (b) for >3hrs (c) it means the system is intensifying beyond 7 close isobars (d) displacement (b) gain in length dimension (c) height dimension per unit of time i.e., @3hrs. There is a direct relationship between the length dimension of the oval architecture & the number of close isobars. Longer be the cross section of the field of the SIF (G-D axis) stable; long duration in sea life; withstand longer period of solid state bottom friction (on ground longer life). Systems develop destructive potential if all the conditions are *in-situ*. Thus the SC-1999 could have a near stationary on ground life of >24hrs. In Fig.-4c, position PC in the FC is the locus of 'parcel cloud' racing towards position TC → CO along a curved pathway alias the FC. These are pre tor type cloud masses. Beyond position CO until the principle energy injection point (EIP at B1) the FC is compact with tor/ribbed





Deepak Bhattacharya

type cloud having large length dimension as compared to breadth. It is also the zone of very high Reynolds up-till the EIP. This is non tweak zone. Any fiddeling herein imparts killer potential. The FC is also the prime energy feeder and the EIP (energy injection point; B1 in Fig.4c) is its delivery point. The FC is inclined in a screw cum spiral path bounded on either side by electrostatic conditions which causes crisp boundary phenomena. It is signature of synergy. In other words, a synergic 'F' will induce higher rotational speed and crisp boundaries (reciprocal). In free atmosphere the FC also acts as a balancing boom for the rotating screw. FC's length & central column's erectness are also reciprocal. Region KS denotes 'clear sky', and coincides as high pressure zone; high column thrust & high speed cool down draft (another of the aberrations i.e., non gravity high speed cascade not free fall, is system efficiency dependant). Fig.-4c can also be generated as a real-time projection from primary met-data obtained from field systems (remote or Doppler).

The Theory (Down Regulation / Up-Regulation)

In this section we first discuss the hypothesis (Theory) via (i) 'Schematic Description' then discuss (ii) down regulation (iii) up-regulation (iv) infliction of swerve. All this portends harnessing of nature i.e., critical technology.

Schematic Description

In Fig.6, the system is traversing from the viewer's left towards the right. It shows a transport aircraft (say Antonov; Hercules), dropping FA (fly ash) over the designate PC region in the FC (F-4c). We recommend non propeller type aero-vehicles that can drop with the tail wind; avoid widening of the sprayed field; least mix of turbine fuel (bad CCN); rapid descend; formation of hydripiles. Due the sever cyclonic aberration though bumpy the interior of the FC are quite dense (not rarified as in normal atmospheric conditions). Therefore, wide bodied propeller aircrafts can carry voluminous cargo and be stable platform within the FC. The FA has to be sealed with dry nitrogen gas in thin film, high density, brittle poly/latex bags that will balloon at about 700-800hPa in the low pressure field and burst spew. The nitrogen gas will defer the onset of arching by a 'time window' and will allow the crew to take (drilled) evasive actions from the archings because cloud-to-cloud arching is very intense and cover very large swaths in tropical weather system (particularly in the eastern shore board of India). Sealing the FA with variably pressurised (unlike hydrosonde balloon) relatively heavier & yet inert nitrogen gas will allow the 'packed-load' variable rates of downward trajectory, explode at various levels of the column i.e. variable depth charge effect; limited scatter. Explosion can also be assisted by pyrophorics.

By adopting the depth charge system our variable objectives can be served depending upon the atypicalites of the individual systems (no two systems are identical). Meso systems will form in the hind (of the synoptic system) and rain down heavily when seeded in the PC region of the FC. The otherwise firm electro-static side borders will lyse when seeding be done at the outer edges of the FC between location TC & CO. The system will then tend to swerve away from its natural path. Also experience down regulation. In Fig-6, to the viewer's right i.e., the front 'F' is the aircraft quite a bit afar from the eye and in fact is also away afar from the 'F'. It is in the mode of down-regulation and or effecting a swerve. To the viewer's left i.e., to the rear 'R' of the system the aircraft is shown (due to 2 dimensional graph) relatively closer to the Eye. It is conducting seeding operations in the mode of up-regulation. We have been schematically demonstrating such seeding operation in numerous forums for various regulation objectives, since 2000.

Caution

There will be a natural tendency for such seed material to reach the SIP/F when the seeding is done affront the F or if done anywhere near to the CZ resulting in up-regulation, attainment of killer potential. Seeding affront the F will up-





Deepak Bhattacharya

regulate. Using propeller aircrafts shall fail hydropile formation and tend to jinx outcome results. Hydropile formation is vital for down-regulation. Scattering for up-regulation.

Cyclone Down-regulation

Any weather systems cause clouds which because shade and rain. Wind awakens. Rain is romance. Our theory includes the ability to kill any weather system if it be more-desirable from human and agro-met perspectives. However, we herein intend (only) limitedly down-regulating the efficiency of fluid flow i.e., energy uptake at 'F'. This will lead to desired weakening of any killer system. The crux point of our hypothesis is that a weather system sans an F (front) will lack inland driver potential. Rain is more needed in the interiors. Front energizing and de-energizing technology is warranted. It is critical technology (25). Cyclones belong to the spiral group of weather systems. Spirals cover wider domain and also have expand-shrink property (due to border less conditions). Shrinking phase is associated with compaction, energisation; prominent electrostatic boundaries, gain in mass, carrying capacity, up-loading, less friction & warm-moist-homogenous bottom. Expanding is associated with bottom friction/drag, loss of mass; load shedding; gravity waves and decay. They harbinger bounty, provide relief from the scorching-humid conditions. From the perspective of physics, cyclones/tornadoes are thermodynamic-weather systems that even out fronts (anomalies) resulting in barocline equilibrium.

We propose to top seed the feeder channel in the central region of the FC at locus marked PC (Fig.-4c). PC denotes 'parcel clouds', the parcels are semi-convective, in non-conjugated state having wide breath dimension, in rapid forward motion. TC→CO denotes 'tor & compressed', respectively. At locations between TC→CO the PC develop lamination, become elongated (pre tor form), is in accentuated dynamic state with ultra-absolute Reynolds (another part of the aberration). The FC of a super/ultra cyclone is planetary in scale. In planetary scale natural phenomena, Reynolds is low (collinear data). Pre to energy injection point (EIP; i.e., B1-Fig.4c) the PCs i.e., saturated fluid mass gets ribbed due to compression + speed alias maximum mass in minimum space (yet another aberration in nature). From location to location the cloud masses undergo alterations in shape, size, compaction & displacement rates; do not cause rain; deliver the full laden energy at EIP. Heavy rain (load shedding) at EIP i.e., the 'F' happens due to confluence of near tangential flows and intense cloud to ground arching happens due to energy saturation i.e., quenching failure (supporting info).

In the BoB the PC region normally ranges between the south →east (meridionally). The TC→CO region is to the north-east & north and the EIP is to north-west & west of any system in relation to the geographical grid, see Fig-4a & 4c. Such systems make land fall on the Odisha beaches. Systems that will barge into Bangladesh will have its EIP consistently to the east during the in-sea intensification period and swivel to the N 300-200kms off shore. BoB system that will barge into Bengal (India) will have its EIP consistently to the NE during the in-sea intensification period. In the Arabian sea there is a clock wise arc shift by an order of 60^o-90^os. Only then will the system fjord the Konkan or else have landfall between Alibag-Marakan coast (mahar-india). This is due to the spiral architecture and coriolis. And, Arabian sea system that will barge into the Marakan coasts will have its EIP consistently to the N during the in-sea intensification period. System that will barge into the N African coasts will have its EIP consistently to the N by NW. The Indus valley providing the good CCNs (mostly drawn from the Kashmir valley and partly from the Karakoram foothills).

Our seed material is *activated charcoal* (AC), and or *fly ash* (FA). Either have a surface area ~2000 mt²/gm, a mesh size ~ 150-200micro meters. It is to be packed in pressurized polypropylene / latex bags in desiccated nitrogen, dropping @ ½ - 1 MT one drop, per location. AC initially is hydrophobic for 60-90 seconds (post-burst), → alter ion balance, → weaken side boundaries, → subsequently become hydrophilic (rain zone), → act as CCN (initially as Bosons), → jump start rain drop formation (large sized), → abruptly alter (shrink) the breadth dimension of the FC due conversion of cloud to water, → will reduce mass, → abrupt energy depletion (H₂O will trap heat) at reduced height, → (thereafter) act as Fermion type compounds i.e., biphasic character, → trigger ultra heavy cloud to sea arching, →

17898





Deepak Bhattacharya

heightened ion deregulation, → more energy depletion, → result in near creation of a neo axis of vertical turbulence (meso scale), → draw away energy to the rear\sides from the highly energized & radio opaque axial core & the EIP, → peripheral boundary layer failure, → induce up draft & down draft of micro/meso scale, → (H₂O) aspect gravity, → form super sized droplets in sea location, → act as a hydro pile (hydroglast opposite of pyroglast) → act as pier against the horizontal flows & dynamic wind balance, → break velocity, → disrupt energy stochasticisation & inertia, →alter bulk mass modulus & the lines of the hydrostatic thrust, → because internal concoction/wobble, → non synergic 'F', → weakening of crisp boundary conditions. Independent eddies will break out of the FC i.e., (alike) evolution of Karnam vortex street effect (26). Enthalpy is vertical; TC is horizontal. Such tangency is contra indicated for synergic obliquity. All this will cause back pressure in the energy feed pathways leading to loss of inertia inside the FC, → genesis of gravity wave phenomena, → systemic internal deregulation, → dissipation of eye, etc., i.e., down regulation. Top seeding will induce *enthalpy* of high magnitude in a limited region within the system apart the central column, which is in contrast to the natural scheme of an efficient mono EIP with a mono axle (core lumen) - the highway of enstrophy. Creation of at-sea hydropile & hydroglasts (ultra cloud bursts) is the objective of our mechanics. Inducing poly nodes of enthalpy is the crux physics of our said mechanics. For systems that have dual feeders such theory holds good, as well.

FA seed particulates are non symmetrical. As the particulate absorbs moisture shear cracking and poly splitting will happen. This will result in the formation of more number of large droplets more swiftly as compared to pure CCNs (atomized particles have to go thorough collation mechanics of longer duration, will also tend to sail further – more lateral shift). Condensation and collation are associated with lapse rate. Interestingly, the lapse rate is nil\low with higher T-factor (as there is a meteo inversion). Greater the T factor lower is the lapse rate (inverse relationship). When black-&-gray bodied hygroscopic particulates (FA; chimney soot) are used, condensation phenomena is by-passed and collation jump starts. These candidates have dry dispersion and also wet dispersion property. Advantage. In crass numerical terms the objective is non decaying, limited down regulation maintaining the 'T' factor around No.5 at about 300-200 kms., off shore, through to land-fall then again up-regulate and maneuver the system to sail inland skirting the geomorphic barriers to serve rain fed cum subsistence agriculture, soil \ ground toxin(s) removal & water bodies & water table charging & polluted drainage flushing (viz-Yamuna), etc. Systems normally undergo (significant) change in a period range of 3-6hrs. And, in the BoB, historically, systems auto intensify between the range 75-150kms off shore (continental shelf + warm SST + good CCN loaded land-breeze flowing over warm, moist, green flora - regions). Thus it is a small window of time & space and shall necessitate overlapping sorties. The seeding therefore has to be 'abrupt dropping' (bolus) backed by 24 x 7 Doppler imaging & real time co-ordination. Doppler will yield the genesis, locus of the hydropiles and life periods cum yield of the individual hydroglasts.

Up-regulating Sea Based Depressions

Every system experiences *enstrophy* from top. This causes the typical screw type up-draft cum the radio opaque central column with a lumen (akine to the colimela as in zancus pyrum, Fig - 7) and the eye 'E' in any system. Within 'E' the locus of the lowest barometric low is between the mid-centre and the top (not base), point of least resistance cum least drag (with an occluded lumen). When the twine aspects combine at the top of the column the lumen gets to be clear = 'E'. To the IR the 'E' is cold while the CH and the lumen wall is warm. The lumen i.e., the 'E' acts as the vent as in a thermodynamic black body. This is also a sort of inversion cum anomaly. Hence, energy as heat (embedded in depleted-to-desiccated clouds) is able to escape due the thermal gradient at great elevation (another aberration). This is the principal pathway of enstrophy. Thus the system does not explode even with sever piston effect generated by the compressing field (centripetal conditions). Note: a met-front is a anomaly alike a shear tear in a fabric. A cyclone (spiro-conico vertical anomaly) is alike a needle-thimble device that attempts rapid equilibrium. Failure results in a repeat system; else fair weather (supporting observation). Yet again, the pressure zones; the cool wind; the warm wind and the moisture entrapped energy flow along lines that are oblique to one another. Obliquity is a high point. It is hetero directional in and around the evolving system and core oriented in fully evolved systems; above 800hPa barometer field it is stratified. Either are dynamic, synoptic & planetary scale, respectively. Such is not





Deepak Bhattacharya

normal in nature, especially in fair weather, in meso scale, et.al. Aberration indeed. During germination stage of a tropical cyclonic weather systems the lines of the forcings of the component sub-systems assume a synergistically oblique-to-each-other i.e., angled variously. Within the boundary layer. Synergy in flow direction-& speed gradually builds up – a tendency towards Newton's 1st Law. And, the angle of the curvature of the earth coupled with the geostrophic rotation (spin) provides a two dimensional platform for the curved pathways and obliquity. Spirals span more space, time & offset force/thrust hence conserves energy inefficiently. Spiro helicals do best which a tropical cyclone is. From work done perspective they are also inefficient. Work done potential of screw type (spiro-helical) weather systems arise out of ultra high mass in frictionless-borderless conditions. Spiro-helical sustains the architecture and thus the system. Gradually intensifying electrostatic borders butts & bounds the spiro-helical architecture. Such borders sustain the dimensions (L-H-W-D) of the spiro-helical perimeter. Decay being marked by gravity waves i.e., free fall (27). Swift waning of electrostatic borders thence is a high point during decay. Whence synergy among the variably oblique flows occurs the central core pressure 'falls alike a bomb' (28) with 'crisp boundary phenomena' (borders). Synergy among the oblique flows is buoyancy dependant. Buoyancy is astronomical gravity dependant, geography upregulated (see ref 22).

Astronomical gravity is highest when the full moon be at perigee in syzygy and sun in the same hemisphere (e.g., Odisha Super cyclone 1999). Warm sea is the ideal geography. Such astronomical gravity and geography are the 2 uncinates. Spiro-helical form and the dynamic oblique flows are reciprocal. Central low because centripetal condition(s) and inclines the pathways of ultra load mass (towards core) which compacts and enhances obliquity in phase alike a cascade along the horizontal cross section of synoptic scale (aberration). All with macro domain variability. Synergistic obliquity helps intensification in stages. Ultra high mass and compaction necessitates flow rate (speed\displacement) for even VSCS are low RPM members. Mass, speed, compaction necessitates an exhaust route for excess energy escape i.e., enstrophy mechanism ('E formation' - real time signature-1). The 'E' i.e., the enstrophy pathway is the chimney aspect in the form of a central column with a lumen (Eye). If the geotroph be non-globular and or if there be no spin of the platform the spiro-helical architecture cannot form (circular can). If there be no central column then large H dimension with ultra load cannot sustain (non starters). It there be no high speed circulatory displacement then low RPM system cannot be in compressible fluid beds. For energy conservation in Newtonian fluids in frictionless-borderless conditions the spiro-helical is the preferred form. Intensifying synergy of the oblique flows and enhancing SIF frontal field (B2,fig 4c) be the indices. Intensification is conservation dependant. Energy conservation has to be made relatively more efficient to up-regulate depressions.

Fig-7 is the X-Ray (radiographic) image of the zancus pyrum shell (sankha). We can see the spiraling bands in an upward angulation. This is the colimela (central column). We have produced it from Rath & Naik's (29) as it explains our case best and derived inspiration from such natural being. The pyrum gives us the Fibonacci fractals, which we have also co-related with system intensification steps, apart from deriving the understanding that a system needs 3 dimensions (ref 25). And, in on-land weather systems retaining the depth dimension (including self priming) is the crux. The colimela provides the axel for the horizontal and the vertical depth dimension to any centripetal gaseous system which translates as compressed mass i.e., carrying capacity. In friction-less, boundary-less conditions stochastic pathways seek uniform, acute angles of the curvature which results in efficiency (the phone 'intensification' is ascribed description). That can happen when there be an interactive central column with a lumen. The horizontal: height depth ratio is another signature of system's intensification possibilities, etc. The range of such ratio being between 1: 2.5 to 1:1.6 (towards Fibonacci). All the aforesaid be for synoptic systems. Whereas, meso-scale members are associated with heterogeneous flow pathways of the stochastic processes. They do not have mono colimela, often poly, mostly incomplete. In case completion then becomes a 'Tornado'. The kinetics and the mechanics of the synoptic-&-meso systems are very different. Meso system up-regulation is herein dealt below separately at sub section 5 and traverse path swerving at sub section 6, respectively (read with ref 25). An efficient EIP at B1 auto mandates high rotational speed, which means the at ground force of the wind will be destructive for agriculture and horticulture (also for river traffic). Moreover, even high rotational speed has thus far not been related to ingress potential. It only results in compaction (gyre i.e., wind velocity) and destructive force. Whereas, our





Deepak Bhattacharya

objective is harbinger precipitation sustained over large similar/identical agro-met domains with ground wind conditions of around a T3 system. By studying Doppler images we have noted that the flow pathways in severe systems have 3 principal set of curves viz., 10° , 20° & 30° s (supporting information). Greater obliquity (10°) is associated with intensity and on ground destruction, while 30° with moderate systemic efficiency and salubrious conditions post pass. It seems in nature efficiency is 'not a member in haste'. Therefore, the real-time for any weak/inefficient system is its wide curvature and/or non-synergistic obliqueness of the associated stochastic process pathways. Inflicting/instilling acuteness in such lines will result in efficiency = greater ingress potential and longer life.

In order to up-regulate a weak system (say upregulating from 2 close isobar to between 4 – to – 7 close isobars) and thereby enhance its rain bearing and causing capacity and ingress potential the seeding has to be done gradually over extended period (week+ long), over extended zones within the SIF region between position B2→B1, with an theoretically permissible arc shift of 45° on the imaginary oval parabolic SIF arc (Fig.4c). Flying with the tail wind will scatter yet not disperse nor make the seed particulates flow along undesirable/unintended lengths (each particulate having numerous candidate CCNs), Seeding being at the lowest possible elevations within the boundary layer. Therefore, the SIF affront the F (B1) will result in systemic conservation of energy more from the direction of the seed/CCN input. The most prominent observable aspect will then be an up-regulation (gain in H dimension) with lessened cloud-to-ionosphere arching and enhanced cloud-to-ground & inter-cloud arching; swift condensation; throw down and loss of elevation of cloud parcels = gusts (next cycle).

We know that in the BoB numerous systems of category 1-3 (Table-1) germinate that experience in-sea conjugation → lack of driver potential and decay between 200-300kms off-shore; also dissipate (only cloudy condition – as in June 2014). Gravity waves are associated with system decay (see refs to the ref.27) and also with slack front potential. By such observation, correlation, understanding and know-how thereof, systems forming in the north Arabian Sea can also be made to up-regulate post landfall and ingress into east African arid regions or into the Indo-Pak arid-desert regions and shed the ferried load; monsoon period specially (30). Similarly, the BoB systems post ingress onto Maikal ranges & Chota Nagpur plateau can be up-regulated to traverse deep into the indo-Gangetic plains. Again, such systems can be adjunct by attracting inflows from the Assam valley (via Purnea-Jalpaiguri axis). The unified stream can further be up-regulated at about east-of-Lucknow with an objective of carrying rainable load uptill India's National Capital region. Systems can be made to drive in from Bhubaneswar-towards-Raipur, and again from Alibag-towards-Nagpur. The two seed variants (FA & AC) comes out to us as biphasic candidates for dual use technology.

Up-regulating Meso members

In meso scale thunderstorms the up-draft is the SIF with short apron and low adiabatic condition. Normally is associated with significant precipitation. Cloud cover span is significant of the Okta; limited period. However, rain fail occurs primarily because the SIF is bereft of good CCNs and/or RH. Even surface level seeding will stoke such systems. Meso scale systems have high lapse rate because SIF is robust and poly directional feed. Therefore condensation is prominent pre to collation (as compared to synoptic systems). Rain helps in reducing/interdicting hail events. Therefore AC (even chimney soot) will be better seed-feed(s) compared to FA (i.e., particles viz., anthracite smoke (from ground as bootom seeding) in place of FA particulates. More condensation means more throw-down. Keeping it balanced and on designate track will be case specific. This shall help in inter-crops.

Swerving a Cyclone

Synoptic scale systems that are heading in the direction of excess rainfall or towards repeat landfall or towards outer sea can be made to swerve in the desired direction by seeding in that particular angle within the SIF field (non-hill geomorphology). The locations in the FC between position CO→FP (B1; Fig-4c) is the most robust part of the FC with



**Deepak Bhattacharya**

firm boundaries i.e., the fluid herein indicate almost unilateral in flow behavior (cannot be fiddled with). Seeding done between positions CO→FP will co-linearise the EIP with line G→D (as in a balanced yo-yo in play motion, Fig.-4b). This will up-regulate synergy within the system and between the various pathways of energy input and their conservation (including rotational speed) i.e., an efficient 'F'. This is particularly relevant when systems having crossed the shore line and need to fjord towards inland viz., Yamuna plains via the indo-gangetic monsoon trough.

Bottom Seeding - Surface Level Operation – Heritage Aspects

Modern period surface level operations with an aim to cause rainfall was first tried by IMD station-in-charge Vishakhapatnam. He had used incendiaries (Diwali crackers & rockets) during monsoon period in the hinter regions of N Andhra 2005-07. It had resulted in copious rain fall. Farm, irrigation & piciculture sectors had much benefited. The IMD took dim view of his pioneering efforts and had shifted him (31). However, Bottom seeding is well known in indo Hindu Vedic practices as "parjaan yagna" (rain becausing drill). We have dealt with such aspect as a chapter in our seminal book "Indian Ancient Sciences" (32). We stand inspired. A separate communication shall be presented on indo native heritage i.e., Vedic Vigyaan (plural sciences) for weather modification.

DISCUSSION

It is interesting to note, that following our efforts in this direction a concise cum popular *lingua* write up was hoisted by the Manila (Philippines) Cyclone warning centre (www, 2000) (33) and then again by Queensland Geo-Engineering (34,35). It is co-incident, that, since then no killer cyclone has made land fall on the Chinese main land ever since the hoisting of our work. We have been given an impression that in such case, our model has been implemented by the Chinese (for public good). Thin film water bodies (36) also provide conditions for such drills. Such weather modification technology should be for (i) family welfare (ii) employment generation (iii) socio-economic welfare with the family at heart (iv) a laid back life style and not for prosperity of 1% of the sub population (37). Down regulating any system also translates into fuel and time saving by the international air, maritime transport sectors and above all thwarts disturbances even in unconnected distant lands. These natural events also inflict incalculable loss to finance and insurance service sectors. All such disturbances inflict more deleterious effect on the developing economies. Down-regulating a destructive cyclonic storm and or upregulating a weak one are urgent emerging needs. They constitute critical technology.

The averments herein may be correlated with the fact that if coal (lignite\anthracite i.e., high ash content fossil fuel) based thermal power plants are located on the coast and specially if they be in the system's natural ingression path ways (e.g., Mahanadi; Godavari; Rupnarayan; Padma), north east Bihar then there will a up-regulation effect. Because, among the large industries only coal smoke produce the highest amount of rain causing good CCNs. If set up in rain shadow regions they will reduce high floods and top soil loss. Petro-chem units in east Assam will also reduce wasteful rain episodes in the NE. If, petrochemical industries are set up on the shore line in killer cyclone ingression regions, it will lead to down regulation. Because, this type of industries produce the highest amount of rain failing (bad) CCNs. Paradip & Haldia based petrochemicals will down regulate killer cyclones along with economic bounty. On the other hand, high ash content (Lignite) coal based power plants located in Chittoor; Kadapa; Rayalseema; Telengana; Chattisgarh; Vidharva; Marathwada; Budelkhand; Saurashtra; Rajasthan; will be of much help to the agro-met of such rain deficient domains and to the hail storm effected Sutlej-Ganga plains.

CONCLUSION

Vis-à-vis sea sourced cyclones, FA sourced form power plants and AC from cinder deposits posit as best candidate pair for inducing weather modification including up-regulating and down-regulating any system and inflicting swerve in rain bearing systems. Location 'feeder channel' posits as best locus for seeding operations in killer



**Deepak Bhattacharya**

cyclones. Vis-à-vis land based tornados. Synoptic & meso systems can be down-regulated and also upregulated. Synoptic systems needs to be clawed away from the rear for down regulation. Synoptic and Meso systems can be upregulated from the front and sides. However, tornados need to be toppled by spraying of chilled micronised water i.e., wetting (separate communication). Vis-à-vis our caption, principles of fluid mechanics appear attractive. Our understanding (for working out a socially relevant Technology) for down regulation and up-regulation aspects has arisen out of our two decade long comparative study of the effect of the geography and orography also tradition & cultural practices (separate communication).

ACKNOWLEDGEMENTS

Author most gratefully acknowledges the life-saving support that the rural people of coastal Odisha have provided with unconditionally and most willing ranging over more than a decade as he went out time and time to the field to observe what happens when a severe cyclone rages. This effort is dedicated to them. During the same period Susmita Bhattacharya to malign me in public that this author is involved in various anti-social & one Pradip Bhattacharya conspired against my wife (who was ailing) in a criminal manner. They wanted property usurpation. My wife demised of shock & attack. Police called the bluffs. Human Rights Commission case. Hence, presentation further delayed.

REFERENCES

1. Dastidar, S. K. (Sr. Meteorologist), 2000. India Meteorology Society, Bhubaneswar (personal communication).
2. IMD., 2006. Annual Monsoon Report, did not report the fact that 14 of the systems crossed over Odisha, N. Rajivan (Ed.). That year only 1 system had traversed through the Godavari (system) ingression pathway and that state was given record relief and grant materials. Orissa was visited by 14 systems one after another (same period) with repeat high floods; was not given such assistance. Due absence of "critical technology" severe weather events are used as politico-economic tool in India. Therefore, there is need for "critical technology" for intervention.
3. IMD., 2014. National Workshop on Enhanced and Unique Cyclonic Activity during 2013, New Delhi, 24-25th July-2014. (ii) inspite of all this Odisha is the only state that has not been provided with a Doppler radar; consistently all appeals turned down during last 60yrs.
4. Bhattacharya, Deepak., Irrigation Heritage Of India : Select Matter, *Journal of The Institution Of Engineers India*, Vol.,92, 2011a,pp.28-37.
5. Bhattacharya, Deepak., Effects of Very Severe Tropical Cyclone : Select Short Perspectives, *Journal of the Institution of Engineers-India*, Kolkata, 18thApr.2010, AR-178, 91 : 26-32.
6. Panigrahi, D.K, Mohanty, P. K. Mohanty, Acharya, M. & Senapati P. C., Optimal Utilisation Of Natural Resources For Agricultural Sustainability In Rainfed Hill Plateaus Of Orissa, *Agricultural Water Management*, Vol., 97 (7), 2010, 1006 – 1016.
7. IMD - 'Project STORM', 2012. is funded by Dept. of Earth Sciences, Govt. of India through numerous academic and field agencies in the state of Jharkhand & Bengal & Assam (Odisha has possibly been kept out; possibly because she has too many varieties of micro & meso scale severe weather events (apart highest number of depressions) ranging over more number of calendar months, annually).
8. Bhattacharya., Deepak. Atmospheric Low Pressure & Human Health : Medical Meteorology, *Vayu Mandal*, Journal of The Indian Meteorological Society, Vol.32 (3&4), 2006a, pp.58-61.
9. Bhattacharya., Deepak, & Misra, B.K., Medical Meteorology India: Select Aspects, *International Journal of Clinical Case Reports*, Vol.,3, No.2, 2013, pp. 7-16. doi: 10.5376/ijccr.2013.03.0002
10. Bhattacharya Deepak, 2016. Indian Monsoon Climate and Malaria: Medical Meteorology, *Journal of Malaria Control & Elimination*, Volume 5, Issue 2, pp.2-6. Doi: 10.4172/2470-6965.1000141
11. Bhattacharya, Deepak., Panigrahi, D.K., Naik, P. C., Orissa Tornadoes: Select Discussions, *The International Journal Of Meteorology*, Vol.,36.No.358, 2011, pp.47-50.





Deepak Bhattacharya

12. Bhattacharya, Deepak., Few Aspects of Super Cyclone; XXIV-IIG, & International Conference, NEHU, 03-2003.
13. Bhattacharya, Deepak., Mechanical Aspects of Tropical Cyclones, Technology for Disaster Mitigation – TECHDIM - 2006, National Engineering Conference, JITM., DST., sponsored, 27-28 /01/2006.
14. Alamaro, Moshe, et.al., Simulation of hurricane response to suppression of warm rain by sub-micron aerosols, *Journal of Weather Modification*, Vol., 38, 2007, p.82.
15. <http://www.atmos-chem-phys.net/7/3411/2007/acp-7-3411-2007.pdf> & http://alamaro.home.comcast.net/~alamaro/hurricane_modification_page.htm.
16. Bhattacharya, Deepak., *Proceedings of TROPMET 2006*, Pune, Maharashtra (India), India Met., Society, Vol. I, 2006. pp. a81-83.
17. Bhattacharya Deepak , The Orography of Orissa & Andhra Act as Hydraulic Devices *vis-à-vis* Monsoon Drafts: A Theory, *National Workshop on Mesoscale Modeling of Atmospheric Process*, DST, Andhra Uni., 29-31 Jan, 2007.
18. Bhattacharya, Deepak., Inducing Modification in a Severe Cyclonic Storm : A Theory, International Workshop on Weather Modification, JNTU, Hyderabad, 18-20th Jan. 2007, (submitted Feb-Mar 2006)..
19. Bhattacharya Deepak, 2008. Effects of Very Severe Tropical Cyclone–Select Short Perspectives – Infrastructure Meteorology, *Journal of the Institution of Engineers-India*, Vol. AR- 178, No. 91, pp.26-32.
20. Bhattacharya, Deepak., Eco-friendly, Modification of Severe Tropical Cyclone : A Theory, 4th Asia-Pacific Geo-Science International Conference, Bangkok, Illustrated Abstract, Submitted in 04-2006, IWG11-A0001.
21. Rosenfield, D. et.al., Atmospheric Chemistry & Physics, Vol.7, 2007, pp. 3411- 24.
22. Bhattacharya Deepak, 2016. The Super Cyclone of 1999 and Lunar Alignment Effect, *International Jor of Earth Science & Engineering*, Volume 09, No.6, pp. 2338-47.
23. Deepak Bhattacharya, Geography; Geomorphology & Geology as Coupled Factors in Shillong & Sikkim Plateau Hydrological Cycles, *International Journal of Earth Sciences & Engineering*, Volume 07, Oct-2014, No. 04, pp.1681-89.
24. NOAA., 2003. OUT REACH, E. mail, Ann Bradford, Dt. 21-03-2003.
25. Bhattacharya Deepak, 2015. Artificially Initiating Meso Scale Systems & Up-regulation (Principles & Fluid Mechanics); *International Journal of Earth Science Engineering*, Vol.8, No.1, pp.144-47
26. Yuan, S. W., Foundation of Fluid Mechanics, Prentice Hall, 1964. New Delhi.
27. Kumar, K.N. & T. K. Ram Kumar, 2008. 'Characteristics Of Inertia-Gravity Waves Over Gadanki During The Passage of A Deep Depression Over The Bay Of Bengal', *Geophysical Resh Letters*, VOL. 35, L13804, 5 pp. doi:10.1029/2008GL033937.
28. Mr. Sikka, Ex-Director IMD, was the original concept giver. He used to talk about the abrupt evolution of the eye as alike "fall of a bomb". Quoted with regards (name not known).
29. Rath, S.K. & Naik, P.C., Fibonacci Structure In Conch Shell, *Current Science*, Vol.4,2005, pp.555-57.
30. Vide my e.mail to IMS president AVM Ajit Tyagi 'How india can help arresting the eastward expansion of the Thar desert and the associated aridification pre to desertification' "Weather modification heritage of India – Indian Ancient Science" ISBN 978-3-8443-2437-2, lap Lambert, Germany, 2010,pp.225-46
31. Mr. J V M Naidu - IMD officer, VSKP, Cyclone warning centre. IMD was unhappy & unrewading 2007.
32. Bhattacharya Deepak, Indian Ancient Sciences, 2009, Lap Lambert, Berlin, ISBN 978-3-8443-2437-2.
33. www. 2000. <http://www.typhoon2000.ph/info.htm> (6th from the bottom).
34. Bhattacharya, Deepak., 2011, Inducing Modification in a Severe Cyclonic Storm: Super cyclone (SC) of 1999, Queensland's Chemtrails and Geo-engineering Abominations on Thursday, September 15, 2011.
35. Face-book, 2012. www.facebook.com/pages/Queenslands.../189021377793533?sk.
36. Bhattacharya Deepak, 2017. Large Volume Holding of Water At Surface Is Potent Anti-Dote to Pollution & Health Hazards, Air & Water Borne Disease, Vol.6,134.
37. Bhattacharya Deepak, Lesser Known Aspects of Global Warming and Energy Priorities, Photon, The Journal of Energy and Environmental Science, Vol. 127 (2013), pp. 224-239. Republican-D Trump's election-policy team said to have referenced & relied upon pre-to-US election 2015.





Deepak Bhattacharya

Table 1. IMD's Classification of sea sourced weather events.

Category	Nomenclature	Wind Speed (knots)	Close Isobars
1	Low Pressure	<17	1
2	Depression	17-27	2
3	Deep Depression	28-33	3
4	Cyclone	34-47	4-7
5	Severe Cyclone	48-63	8-10
6	Very Severe Cyclone	64-119	11-39
7	Super Cyclone	>120	>40

For Land Tornadoes, the IMD is yet to finalise. India has either types. Ref.11.

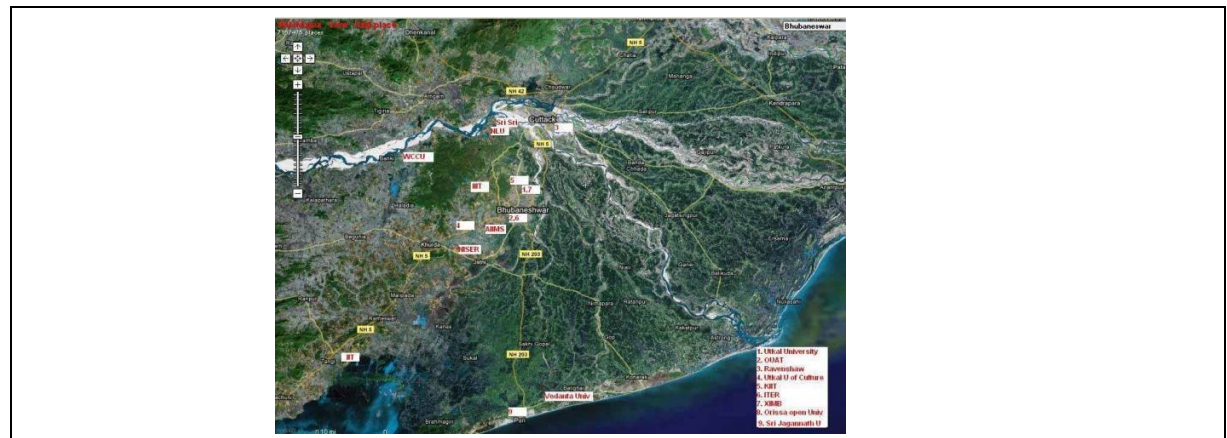


Fig. 1. Is the satellite image, downloaded from Google earth with thanks. It shows the Mahanadi Delta in the visible range.

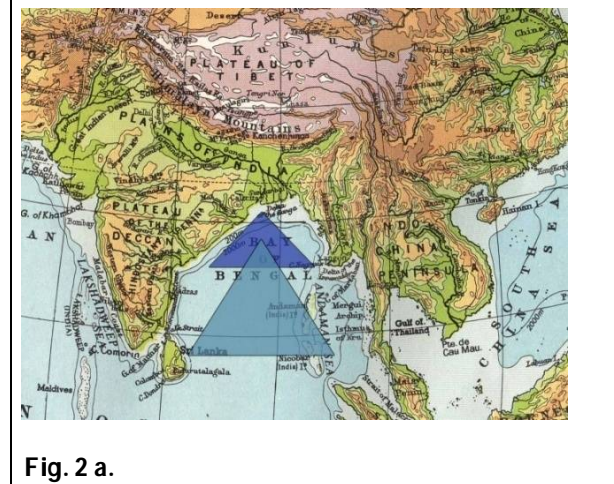


Fig. 2 a.

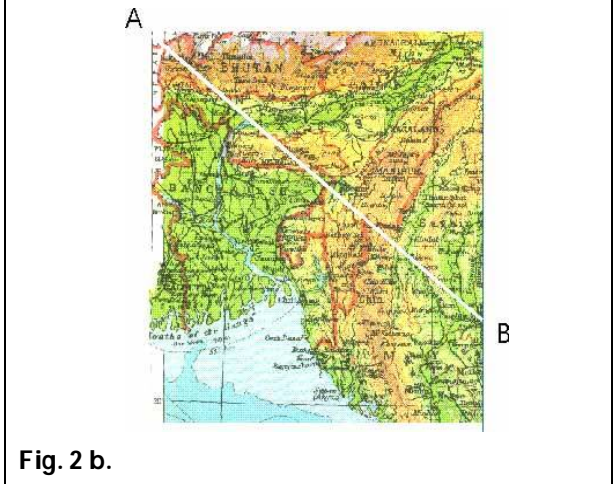


Fig. 2 b.





Deepak Bhattacharya

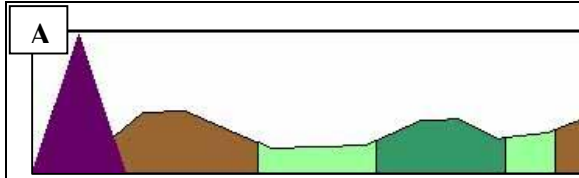


Fig. 2 c.

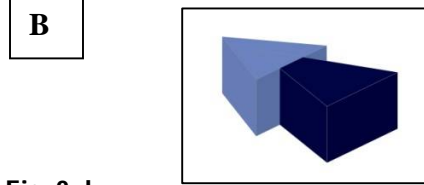


Fig. 2 d

Fig. 2 series: explained in detail in the following para. ✪✪ Fig-2d in particular shows effect of the triangular architecture of the BoB in the initiation and propulsion of the horizontal component of the sea-atmosphere couple during monsoon in the BoB. It is alike Serisprinsky's fractals. Orography & Pacific factor jointly swivel/vectors the horizontal component of the thrust.

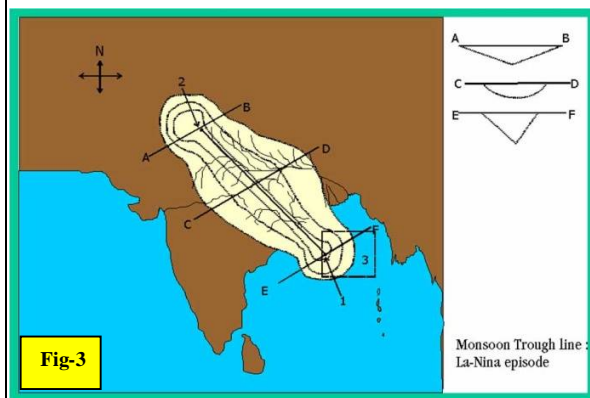


Fig-3

Fig.-3. Shows the ideal trough of the Indian monsoon with schematic cross sections of the atmospheric trough and the valley pathways and angle of the hydro-dynamic thrust of the ocean-atmosphere couple. The 3D box represents system height & direction

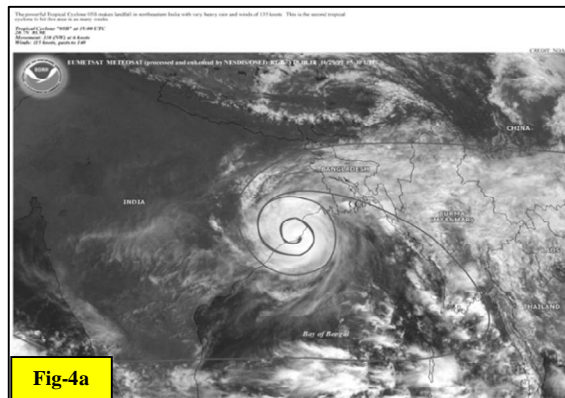


Fig-4a

Fig. 4a is that of the Sc-1999, at time land fall. Outline has been provided indicating the electrostatic boundaries of the cloud/moisture feeder channel (Curtsey NOAA; ref 24).

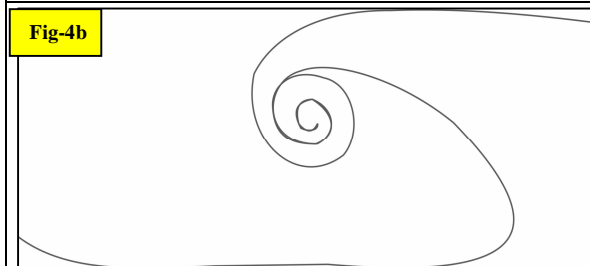


Fig-4b

Fig.4b : Shows the yo-yo form. Energy conservation is around the Eye. Energy conservation in borderless frictionless conditions happens via a curved path. Parabola due geotropic spin effect.

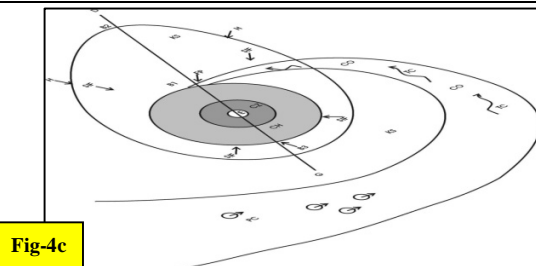


Fig-4c

Fig.. 4c . Shows the architecture and the field of wind and moisture flow, the cloud feeder channel FC, the oval SIF zone, the CH & the core zone. It is schematic, zenithal view. Indicates the various positions. Also indicates location for seeding to up-regulate intensity cum carrying capacity and to inflict greater ingestion potential (selectively) into the systems. See text. Fig.4c has been in public domain since 2000-02. FC is curved, inter-continental\inter hemispheric in scale & inclined; balancing boom. Electrostatic boundary.





Deepak Bhattacharya

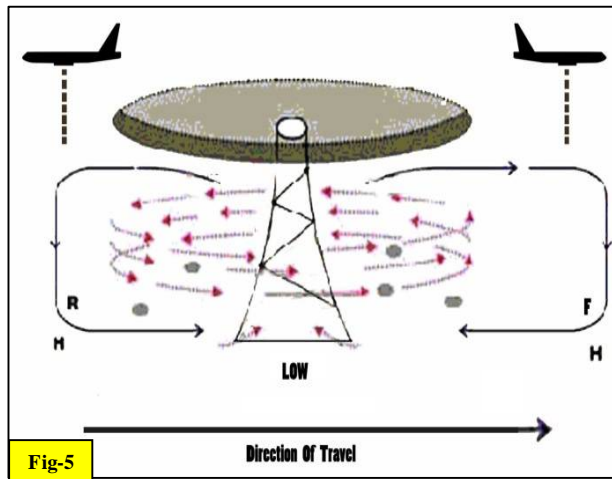


Fig-5

Fig. 5.Schematic representation of top seeding operations using AC or FA. R = rear; F=Front; H=High pressure. For system down regulation. Seeding in the rear = down regulates. It has to be in the FC region i.e., afar from the core region. It has to be in front of the F. The seed material will sail-in and get injected via the SIF. The system will also tend to move in that direction.



Fig.6. X-Ray image of the zancus pyrum, Blowing side is at bottom. Note, tapering spiral central column-Colimela. Image loaned from Rath & Naik (ref.28).





Study the Plasma Parameters due to the Different Energies for Laser Produced Lead Oxide Plasma

Ruaa K. Hassan^{1*} and Mohanad A. Aswad²

¹Department Affairs of Student Accommodation, University of Baghdad, Iraq

²Department of Physics, College of Science, University of Baghdad, Iraq

Received: 05 Sep 2019

Revised: 09 Oct 2019

Accepted: 11 Nov 2019

*Address for Correspondence

Ruaa K. Hassan

Department Affairs of Student Accommodation,

University of Baghdad, Iraq.

Email: Ruaawissam 258@gmail.com



This is an Open Access Journal / article distributed under the terms of the **Creative Commons Attribution License** (CC BY-NC-ND 3.0) which permits unrestricted use, distribution, and reproduction in any medium, provided the original work is properly cited. All rights reserved.

ABSTRACT

In this work, the parameters of plasma (electron temperature (T_e), electron density n_e , plasma frequency (f_p), Debye length (λ_D) and Debye number (N_D)) have been studied using the spectrometer that collect the spectrum of Laser produce PbO plasma at different energies. The results of electron temperature for PbO range 0.75-1.12 eV also the electron density 2.94×10^{18} – 7.03×10^{18} cm⁻³ have been measured under vacuum reaching 2.5×10^{-2} mbar. Optical properties of PbO were determined through the optical transmission method using ultraviolet visible spectrophotometer within the range 190 – 1100 nm.

Keywords: Laser Induced Plasma Spectroscopic (LIPS), Optical Emission Spectroscopic (OES), Spectroscopy diagnostic, *Lead oxide* (PbO).

INTRODUCTION

Laser-produced plasmas from interactions with solid targets are a promising candidate for many fundamental and applied researches. The characteristics of these plasmas depend upon many parameters characterizing the features of the target: properties of the ambient medium, laser wavelength, pulse duration etc., (1). The ablation process using long pulse duration lasers (> 1 ns) is divided into three stages. In the first stage, the laser light interacts with the solid resulting in rapid ionization of the target surface into plasma on a time scale short compared with the pulse duration. In the second stage, the laser light is efficiently absorbed by the plasma which expands isothermally. In the third stage, after the end of the laser pulse, the resultant plasma plume expands quasi-adiabatically in a medium, which can include vacuum or a background gas, with or without applied fields (2). Sample types can be wide ranging because optical absorption processes initiate LIBS sampling, thus, allowing analysis of solids, liquids, and gases (3). Once the energy from the laser pulse heats, ablates, atomizes, and ionizes the sample material, a plasma is formed. *Lead oxide* is an important element and orange hygroscopic solid mineral that occurs naturally as *Pericles* and is a source of magnesium. It has a formula of PbO and consists of a lattice of PbO²⁺ ions and O²⁻ ions held together

17908





Ruaa K. Hassan and Mohanad A. Aswad

by ionic bonding. Lead hydroxide can be reversed by heating it to separate moisture (4). In the case of lines corresponding to $6s^27p$ levels of PbO, data of relative transition probabilities are almost absent from the literature; this was the reason for this work, which presents the transition probabilities for ten lines corresponding to level Pb from measurements of emission lines intensities in a plasma generated by focusing a laser beam on a sample of PbO under vacuum. The results are compared with our theoretical values using the Coulomb approximation (5). The light of the plasma is then spectrally resolved and detected by a spectrograph and a detector. Both quantitative and qualitative information, such as elemental composition, can be deduced from the resulting plasma spectrum. Emission line properties such as widths, shapes, and shifts can provide information on plasma temperature and electron density (6). Plasma temperature is an important thermodynamic property due to its ability to describe and predict other plasma characteristics such as the relative populations of energy levels and the speed distribution of particles. The method used in this laboratory experiment is the ratio method using two lines of Hydrogen, which assumes that local thermodynamic equilibrium (LTE) is met within the plasma. Under Vacuum with pressure tell to 2.5×10^{-2} mbar, it has been shown through approximations that LTE is usually met after a couple hundred nanoseconds after plasma formation using LIBS with irradiances greater than 10^8 W/cm². The ratio method is a common way of reporting plasma temperature can be calculated through the intensity ratio of a pair of spectral lines of atom or ion of same ionization stage[7]. In LTE, The plasma temperature is calculated from the equation (7):

$$T = \frac{(E_2 - E_1)}{k \ln \left(\frac{I_1 \lambda_1 A_2 g_2}{I_2 \lambda_2 A_1 g_1} \right)} \dots \dots \dots (1)$$

Electron density (n_e) describes the number of free electrons per unit volume. There are several credible techniques used to determine electron density, including plasma spectroscopy, microwave and laser interferometry, and Thomson scattering. The determination of electron density by linear Stark broadening of spectral lines, as used in this lab, is a well-established technique. Line broadening in LIBS plasmas is caused primarily by Doppler width and the Stark effect. Doppler width is dependent only on the temperature and atomic mass of the emitting species; this type of broadening is disregarded in this experiment as the Doppler width of the hydrogen line used is usually between 0.04 nm and 0.07 nm. The Stark effect is considered a type of pressure broadening that involves interactions of radiators and neighboring particles. In plasmas, these interactions are caused by collisions of ions and to lesser extent electrons. The Stark effect is mainly responsible for the line broadening of the hydrogen line used in this experiment (6,8).

Saha-Boltzmann equation utilizes spectral lines of the same element and successive ionization stages. the Saha-Boltzmann equation is given as(7):

$$n_e = \frac{I_1}{I_2} 6.04 \times 10^{21} (T)^{3/2} e^{\frac{(E_1 - E_2 - X_z)}{kT}} \text{ (cm}^{-3}\text{)} \dots \dots \dots (2)$$

Where

$$I_2^* = \frac{I_2 \lambda_2}{g_2 A_2} \dots \dots \dots (3)$$

X_z is the ionization energy of the species in ionization stage z in eV, T_z is the line intensity for transition from upper level-2 to lower level-1, λ_2 is the corresponding wavelength of transition from level-2 to level-1, g_2 is the statistical weight of transition from level-2, A_2 is the transition probability from level-2 to level-1 and T_e is the electron temperature. The subscript z denotes the ionization stage of the species for the referred. While the plasma frequency is calculate from the equation:

$$f_p \approx 8.98 \sqrt{n_e} \text{ (Hz)} \dots \dots \dots (4)$$





Ruaa K. Hassan and Mohanad A. Aswad

This frequency, depending only on the plasma density, is one of the fundamental parameters of plasma. Because of the smallness of m , the plasma frequency is usually very high (9). The response of charged particles to reduce the effect of local electric fields is called *Debye shielding* and the shielding gives the plasma its quasi-neutrality characteristic. a distance λ_D , called the *Debye length* and defined as (10)

$$\lambda_D = \left(\frac{\epsilon_0 k T_e}{n_e e^2} \right)^{1/2} = 743 * (T_e / n_e)^{1/2} \dots\dots\dots (5)$$

where λ_D : is the Debye length (cm) ,L: is the system dimension(cm) , n_e : is the density of the electron (m^{-3}) , T_e : is the electron Temperature (K) , e : is the electron charge (C) and N_D also known as the number of particles in the Debye sphere which is dependent on electron density and electron temperature this Second condition for plasma existence $N_D \gg 1$ as follows (12)

$$N_D = \frac{4\pi}{3} n_e \lambda_D^3 \dots\dots\dots (6)$$

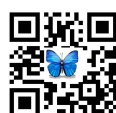
EXPERIMENTAL SETUP

The diameter of laser spot can be changed by changing the distance between the laser lens and the target. Pulse duration (9 ns) with 6 Hz repetition rate frequency. The exactly distance during the measurements for system accuracy and precision. In this work a lens of 10 cm focal length has been used. A shorter focal length lens can produce a small beam waist, and therefore, stronger breakdown, but it also has a smaller depth of focus, Figure 1 shows a schematic diagram for the LIBS setup (1).

The spectrometer analysis was done using the light emitted from sample bombarded by the pulse laser. The spectrometer with short response time from Ocean Optics (HR 4000 CG-UV-NIR) was used in the setup to analyze emitted light. The light produced by the ablated plasma was collected by the optical fiber which was set at angle of about 45 degree to axes of the laser beam to avoid splashing and then guided to the entrance slit of the spectrometer. The spectrometer has a high resolution depending on grating used in it, and responds to a wavelength between 200-900 nm with 3648 pixels. Nd: YAG laser at 1064 nm is tightly focused on the target to produce plasma plume. In order to insure exposing a fresh surface after every train of shots the target surface was rotated manually. The spectrum of plasma with different value of laser energies varied from 300mJ to 800 mJ collect the Spectra of PbO, each spectrum was obtained over a 300-800nm wavelength range. Finally the results were analyzed and compared with National Institute of Standards and Technology data (NIST) (13) and evaluate the plasma parameters.

RESULTS AND DISCUSSION

Figure (2) show the emission spectra of laser induced PbO target plasma which confined in Vacuum in the spectral range (300-800) nm with different pulsed laser energy E=(300,400,500,600,700,800) mJ. The optical emission spectra of PbO target plasma which confined in vacuum were recorded using (OES) technique. Figure (3) show the emission of the PbO plasma plume with different energies. Table (1) display the calculated electron density (n_e), electron temperature (T_e), plasma frequency (f_p), Debye length (λ_D), and Debye number (N_D) for PbO target at different laser pulse energies. All calculated plasma parameters (λ_D , f_p and N_D) were satisfied the criteria for the plasma. It shows that f_p decrease with laser energy because it is proportional with n_e , while λ_D and N_D increase with it such as in (Nek. M. Shaikhand et-al.) (14).





Ruaa K. Hassan and Mohanad A. Aswad

The variation of (T_e) and (n_e) was determining the Ratio Method using two lines of Lead (Pb I in this part) for PbO is shown in Figures (4) for different laser energies. The higher calculated values of electron temperature T_e (Eq.1) in the vacuum is attributed to the high kinetic energy of free electrons in the plasma comparing with more collisions present in other media caused energy transfer to species by numerous ways and presence of secondary charged particles. It can be seen that the electron temperatures shows in fig.5, a slow linear increase as the laser peak energy increased; which is due to the absorption of laser photon by the plasma, and at the same time the plasma is relatively transparent to the laser beam. Electron density is an important parameter that is used to describe a plasma environment and is also crucial for establishing thermodynamic equilibrium. The electron density (n_e) in the plasma can be measured from the emission coefficient and intensity of spectral lines using the Saha- Boltzmann equation. Figure (6) show electron densities of laser induced plasma for PbO component target in the vacuum, at different laser peak energies, respectively. It can be seen that the electron density varies directly with varying laser peak energy. It can be noticed at a given laser energy that the value of electron density vacuum is proportional with laser energy. This results agree with (M. HANIF and et-al) (4)

Figure (7) show plasma frequency in Vacuum laser induced plasma for PbO Component target. From the figure it is seen that the plasma frequency increase with the increase of the laser peak power as shown in Table (1). Figure (8) Illustrates Debye shielding length of PbO component target plasma, induced by Nd:YAG laser irradiation in Vacuum media as a function of laser peak energy. From this figure, its appeared that for a given laser energy the Debye length in Vacuum is higher Value at low energy, because Debye length depends on plasma temperature and plasma density (varies directly with $\sqrt{T_e}$ and inversely with $\sqrt{n_e}$). Since the value of electron temperature is larger Vacuum, then the Debye length is greater at low energy. Number of particles in Debye sphere (N_D) are calculated using Eq.(6). It showed from figure (9) that for a given laser energy the Debye sphere N_D in Vacuum, The higher values of N_D at low energy due to that it's dependent on n_e and T_e , because of the values of T_e in Vacuum is high, and the values of n_e are smaller leads to increase N_D values in Vacuum.

CONCLUSIONS

A Q-switched Nd:YAG laser at its fundamental wavelength (1064 nm) was used to study the laser produced *Lead oxide* plasma. The emission spectrum of the plasma reveals transitions of neutral atoms and singly ionized lead ions. The spectral lines intensities of the laser induced plasma emission exhibited a strong dependence on the ambient conditions. It is found that the intensities at different laser peak powers increase with increasing laser peak power and then decreases when the power continues to increase. Plasma parameters such as electron temperature, electron density, Debye length, number of particles in Debye sphere and plasma frequency are found to be strongly effective by the laser energy. The results showed variations of the electron temperature and the electron number density with the laser energy indicate that both increase with increasing in laser energy. The electron temperature calculated for the 1064 nm that the values of T_e , n_e and f_p were increased in case of laser induced plasma in vacuum environment while the values of λ_D and N_D were decreased in laser induced plasma vacuum environment.

REFERENCES

1. A. A. I. Khalil, "Spectroscopic studies of UV *Lead oxide* plasmas produced by single and double-pulse laser excitation," *Laser Phys.*, vol. 23, no. 1, 2013.
2. N. M. Shaikh, Y. Tao, R. A. Burdt, S. Yuspeh, N. Amin, and M. S. Tillack, "Spectroscopic Studies of Tin Plasma Using Laser Induced Breakdown Spectroscopy," *J. Phys. Conf. Ser.*, vol. 244, no. PART 4, pp. 2–5, 2010.
3. M. L. Najarian and R. C. Chinni, "Temperature and electron density determination on Laser-Induced Breakdown Spectroscopy (LIBS) plasmas: A physical chemistry experiment," *J. Chem. Educ.*, vol. 90, no. 2, pp. 244–247, 2013.
4. M. Hanif, M. Salik, and M. A. Baig, "Spectroscopic studies of the laser produced lead plasma," *Plasma Sci. Technol.*, vol. 13, no. 2, 2011.





Ruaa K. Hassan and Mohanad A. Aswad

5. C.Colón, A.Alonso-Medina, and C.Herrán-Martínez, "Spectroscopic study of a laser-produced lead plasma: experimental atomic transition probabilities for Pb III lines," *J. Phys. B At. Mol. Opt. Phys.*, vol. 32, no. 15, pp. 3887–3897, 1999.
6. David A. Cremers, *Handbook of Laser-Induced Breakdown Spectroscopy*, 2nd Editio. USA, 2013.
7. S. Z. H. R. and J. A. Kashif Chaudhary, "Laser-Induced Plasma and its Applications," *RFID Technol. Secur. Vulnerabilities, Countermeas.*, 2016.
8. S. S. Harilal, C. V. Bindhu, R. C. Issac, V. P. N. Nampoori, and C. P. G. Vallabhan, "Electron density and temperature measurements in a laser produced carbon plasma," *J. Appl. Phys.*, vol. 82, no. 5, pp. 2140–2146, 1997.
9. M. C. Chen and E. C. Chen, *Introduction To Plasma Physics And Controlled Fusion*, vol. 1. Los Angeles, 1983.
10. A. M. El Sherbini, "Measurement of Plasma Parameters in Laser-Induced Breakdown Spectroscopy Using Si-Lines," *World J. Nano Sci. Eng.*, vol. 2, pp. 206–212, 2012.
11. BORIS M. SMIRNOV, *Physics of Ionized Gases*, vol. 16, no. 1. 2001.
12. Suresh Chandra, *textbook of plasma physics*, 1ed ed. india, 2010.
13. version 5., "National Institute of Standards and Technology (NIST) Atomic spectra database," 2017. .
14. N. M. Shaikh, M. S. Kalhoro, A. Hussain, and M. A. Baig, "Spectroscopic study of a lead plasma produced by the 1064 nm, 532nm and 355 nm of a Nd:YAG laser," *Spectrochim. Acta - Part B At. Spectrosc.*, vol. 88, pp. 198–202, 2013.

Table 1. Plasma parameters for PbO in Vacuum with different laser energy

Laser energy (mJ)	Te (eV)	ne (cm ⁻³)	f _p (Hz)	λ _D (cm)	N _d
800	1.22	7.03E+18	2.4E+13	2.9E-05	7.0E+05
700	1.15	4.47E+18	1.9E+13	3.5E-05	8.0E+05
600	1.12	3.68E+18	1.7E+13	3.8E-05	8.5E+05
500	1.10	3.10E+18	1.6E+13	4.1E-05	9.0E+05
400	1.05	2.17E+18	1.3E+13	4.8E-05	1.0E+06
300	0.85	2.94E+17	4.9E+12	1.2E-04	2.0E+06

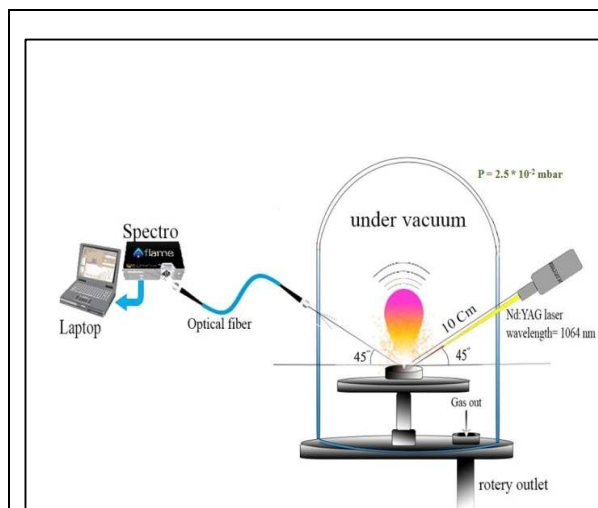


Figure 1. Laser Induced Plasma Spectroscopy (LIPS) System configuration

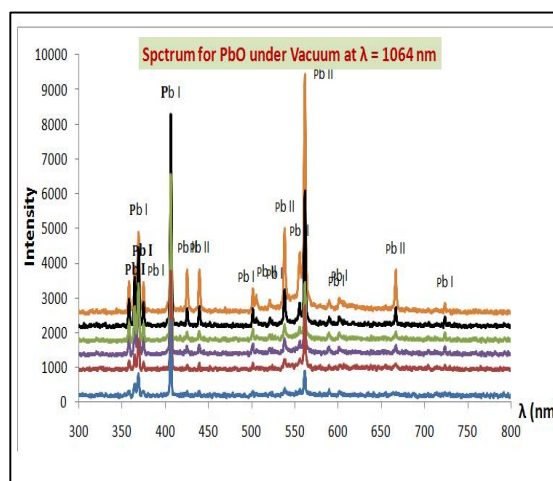


Figure 2. Emission spectra of laser induced PbO target in Vacuum with different laser energies





Ruaa K. Hassan and Mohanad A. Aswad

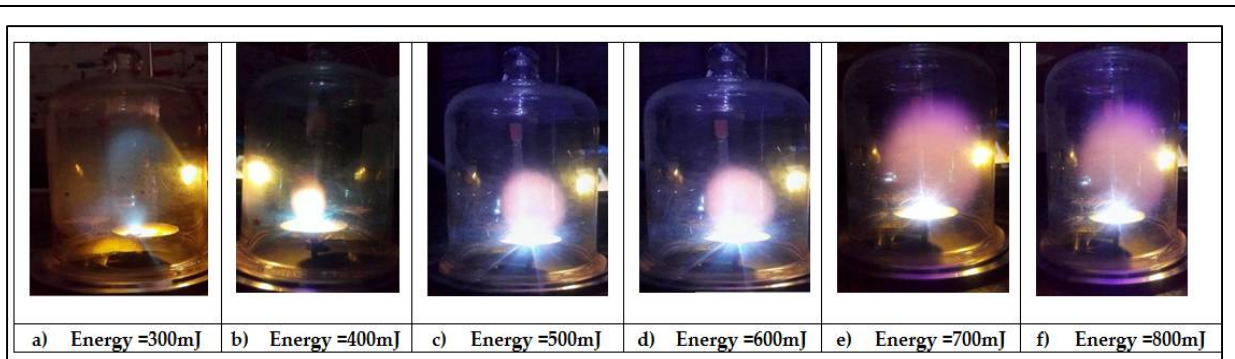


Figure 3. plume plasma PbOtarget in Vacuum with different laser energies

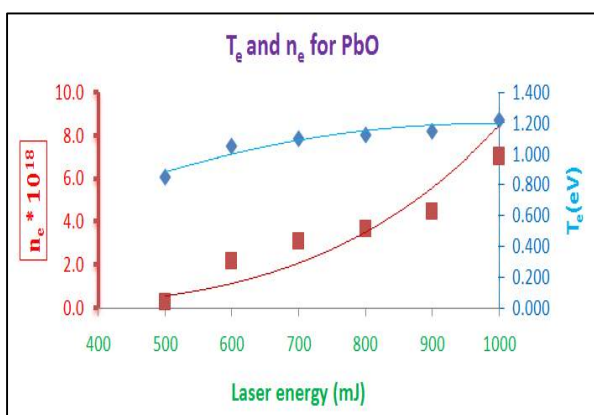


Figure 4. The variation of (T_e) and (n_e) versus the laser energy for PbO in Vacuum

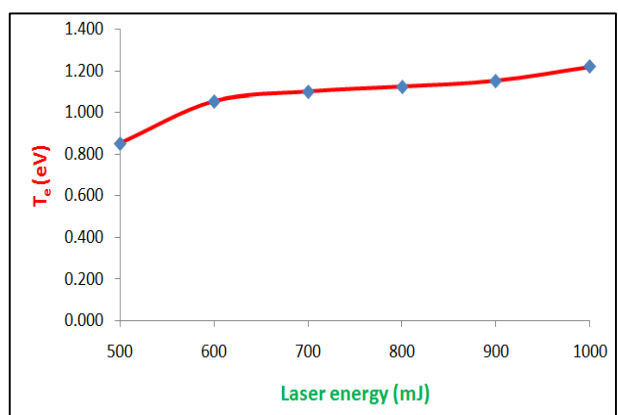


Figure5. Electron temperatures for PbO in Vacuum different laser energies

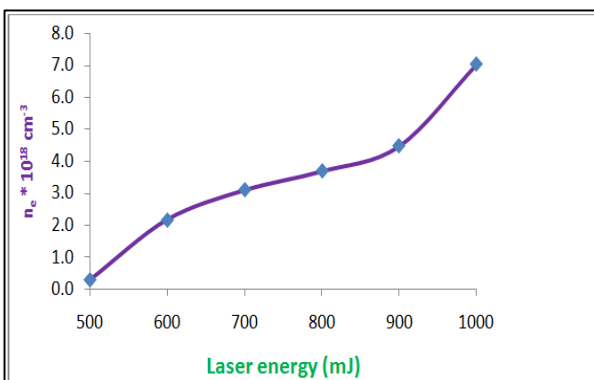


Figure 6. electron densities for PbO in vacuum different laser energies

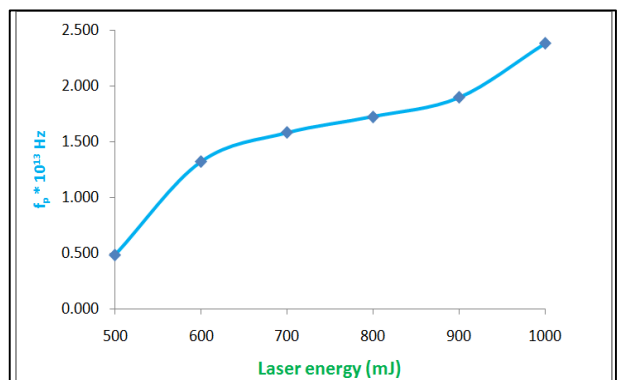


Figure 7. plasma frequency vs. Laser peak energy of laser induced PbO target plasma





Ruaa K. Hassan and Mohanad A. Aswad

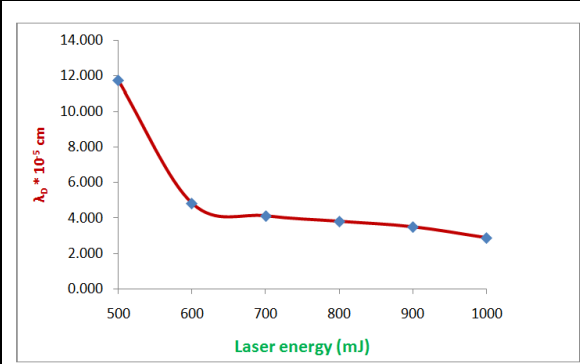


Figure 8. Debye length for PbO in Vacuum different laser energies

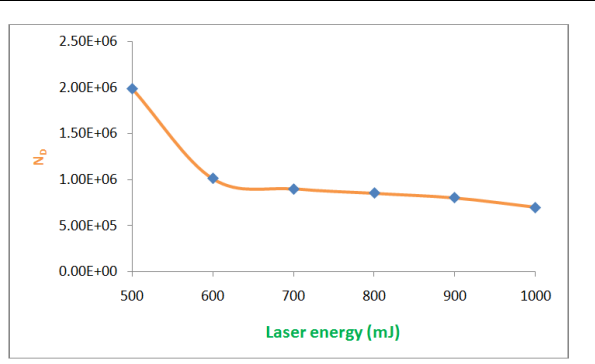


Figure 9. Debye number for PbO in vacuum different laser energies





Human Breast Milk: A Review on Milk Constitution and Development of Milk Microflora

Krupal Patel¹, Margi Patel¹, Jatin Patel¹, Gopalkumar Raol¹, Nirav Bhavsar¹, Viral Surati¹ Yogesh Gopani¹, Ishita Joshi¹, Rupesh Jha¹, Anju Kunjadia² and Yati Vaidya^{1*}

¹Department of Microbiology, Shri A. N. Patel P. G. Institute of Science and Research, Charotar Education Society, Anand, Gujarat, India.

²Center for Interdisciplinary Studies in Science and Technology (CISST), Sardar Patel University, Vallabh Vidyanagar, Gujarat, India.

Received: 17 Sep 2019

Revised: 20 Oct 2019

Accepted: 24 Nov 2019

* Address for Correspondence

Yati Vaidya

Department of Microbiology,
Shri A. N. Patel P. G. Institute of Science and Research,
Charotar Education Society, Anand,
Gujarat, India.

Email: daveyati@gmail.com



This is an Open Access Journal / article distributed under the terms of the **Creative Commons Attribution License** (CC BY-NC-ND 3.0) which permits unrestricted use, distribution, and reproduction in any medium, provided the original work is properly cited. All rights reserved.

ABSTRACT

Human milk is a vital source of nutrient as well as continuous source of bacteria to newborn. Microbes those that are present in milk aid to initiation and development of infant gut microflora. These bacteria play an important role in reduction of incidences and severity of infection to the child. Breast milk protects the newborn against infectious diseases, as it consists of different antimicrobial compounds, immunoglobulin, immune component cells and bacteriocins secreted by probiotic bacteria, which all together stimulate the growth of the beneficial bacteria in neonate gut. In the present review effort has been made to understand transfer microbial diversity in healthy breast milk to her infants. The review reveals that breast milk is a source of more life then we envision.

Keywords: Human milk, Milk component, milk microbiota.

INTRODUCTION

The human microbiome project was taken up via National Institutes of Health in the year 1991 with a goal to conduct survey of microbes present within the body and those resting on human body part and provide vital role for prediction of human health status. However, one of the key systems ignored, was the human milk microbiome. Human milk is an intricate biological fluid which fulfills nutritional supplies of new born baby, helps in the development of infant immune system and provide defense against pathogens (Morrow and Rangel 2004).



**Krupal Patel et al.**

Breastfeeding confers protection against gastrointestinal infections, respiratory infections, allergic diseases and it is also associated with a reduced long term risk of diseases such as inflammatory bowel disease (IBD), obesity or diabetes as reviewed by the American Academy of Pediatrics (Duijts et al. 2010). The protective role of human milk seems to be the consequence of a synergistic action of the wide range of health-promoting components such as carbohydrates, nucleotides, fatty acids, immunoglobulins, cytokines, immune cells, lysozyme, lactoferrin and other immunomodulatory factors (Boehm and Moro 2008). Recent studies articulate the presence of not only the environmental bacteria but also the symbiotic and probiotic bacteria in the milk which are transmitted through milk to the infant and hence contribute in constructing gut microflora of infant (Martín et al. 2009). Daily consumption of breast milk by an infant is 800 ml/day, this in fact contributes to transport of 1×10^5 to 1×10^7 bacteria each day leading to their colonization in gut and finally built up gut microflora (Heikkilä and Saris 2003).

Human milk is an intricate biological fluid which fulfills supplies of new born baby and helps in the development of infant immune system and provide defense against pathogens. As the neonate are born with immature immune system, they are more prone to get infected. In such situation breast feeding can help in building up the immune system of infant as it contains fatty acids IgA oligosaccharides lactoferrin lysozyme antioxidants and cytokines molecules bearing immune protective role. Human milk micro biota play vital roles in the neonates gut they decrease occurrence and severity of infections involve in production of antimicrobial compound and improve intestinal barrier role by enhancing mucine formation and decreasing intestinal permeability (Olivares et al. 2015). Researcher recognize neonates and infants as begins immunologically immature and at increased risk for infection with common infections like otitis media, upper respiratory tract infections etc. By immunological properties innate immunity is play a role in human milk. The innate immune system is defense system against infection of pathogenic microorganisms. As examples of this local innate immunity is the way collectively act on the epithelial surface of the lung alveoli to bind microbes leading to aggregation, opsonisation and increased clearance of microorganisms by alveolar macrophages. Innate immunity includes substances that function as prebiotics, free fatty acids, monoglycerides, antimicrobial peptides and human milk glycans which binds diarrheal pathogens.

Composition of lactating mother Milk

Human breast milk is a complex fluid with a common composition, i.e. 1.0% protein, 3.8% fat, 7% lactose and 87% water. The 50% fat and 40% lactose are providing a total energy of the milk (Figure 1) (Guo 2014). Conversely, the human breast milk component is dynamic and changes over time, this change is vital for the growing child. Such as, during each breastfeeding, the colostrum which has thinner texture expressed along with a higher content of lactose, that fulfills an infant's thirst, and following foremilk, is creamy with a considerable higher amount of fat for the infant's needs. These type of variations during breastfeeding are due to maternal diet, maternal health, environmental exposure and age of infant. During early lactation, the amount of protein in human milk ranges from 1.4–1.6 g/100 mL, then after three to four months of breastfeeding 0.8–1.0 g/100 mL and after six months 0.7–0.8 g/100 mL (Guo 2014; Jackson et al. 2004). The amount of fat is strongly depending on maternal diet and is also affected in weight gain for the period of pregnancy. Unusually, it has been seen that a human milk should has adequate amount of essential nutrients which vital for infant's growth and development but unfortunately mother own nutrition is inadequate. Even though the mean concentrations of protein, potassium sodium, and chloride in colostrum and premature milk are essential to transfer in adequate amount to preterm infants, this vital nutrition is transfer from breast milk to preterm infants (Koletzko et al. 2014; Gross et al. 1981).

In contrast to fat and protein, lactose is fairly constant in mature milk means after 21 days postpartum. The constant amount of lactose is essential for maintaining a steady osmotic pressure in breast milk. In addition, lactose also assists the absorption of calcium and other minerals. In human milk, various carbohydrate-based bioactive substances, like oligosaccharides, are also attached to lactose. But if the small intestine does not secrete sufficient amount of a lactase enzyme for digestion of lactose complex then lactose intolerance and



**Krupal Patel et al.**

malabsorption syndromes may be developed. However, lactase deficiency malabsorption and disease are very rare especially in breastfed infant.

Protein in Human Milk

There are mainly two classes of protein are found in breast milk i.e. whey and Casein. The core whey proteins presents are lactoferrin, secretory IgA and alpha-lactalbumin. further proteins which includes are casein, lipase, lysozyme, amylase, bifidus factor and folate-binding protein, antichymotrypsin and alpha1-antitrypsin, and haptocorrin (Guo 2014). The whey/casein ratio in breast milk is varying from 70/30 to 80/20 during early lactation period and then drop to 50/50 in late lactation period (Lönnerdal 2003). This ratio is considerably higher than the milk from other mammals. In cow's milk, only 18% whey proteins are found. According to type of milk i.e. from colostrums to mature milk, 80% to 50% of protein in human milk is whey protein because it remains in liquid form in digestive system whereas casein make clumps (Guo 2014). In past, infant formulas were contained high amount of casein which makes them heavier to digest by infants in compared to human milk. The overall amino acid profile of breast milk is fluctuating according to the stage of lactation. The most abundant free amino acid mainly glutamine, is found to 20 times higher in mature milk compared to colostrum (Zhang et al. 2013). Glutamine is play key role in citric acid cycle by giving ketoglutaric acid, which perhaps act as a neurotransmitter in the brain, and providing energy to intestinal cells (Agostoni et al. 2000).

Fats in Human Breast Milk

Fats are the essential components of human milk which delivering energy to infants and also assist the development of central nervous system. Furthermore, in the breast milk fat is main compounds which give it taste and aroma. Mainly, fat are presents in ranges from 3.5% to 4.5% in human milk during lactation periods. Human milk have two crucial fatty acids, 15% linoleic acid and 0.35% alpha-linolenic acid which converted into arachidonic acid (AA) and eicosapentaenoic acid (EPA) respectively, afterward further converted to docosahexaenoic acid (DHA) (Guo 2014). AA, EPA and DHA are significant for vision, development of immune function, cognitive, regulating growth, inflammatory responses, cell differentiation and development of active synapses in newborns. It is found that long chain polyunsaturated fatty acids are transmitted from pregnant mother to fetus during third trimester via placenta, and also from breast milk to infants via breastfeeding (Herrera 2002). Notably, the synthesis of AA and DHA from linoleic acid (18:2 ω 6) and alpha-linolenic acid (18:3 ω 3) is limited in the fetus and neonate due to the premature enzyme activity. Thus, the required amounts of AA and DHA must come from the mother during pregnancy, or as breast milk after birth. One study has showed that the fat content and the percentage of all polyunsaturated fatty acids in breast milk increase significantly between the sixth week and sixth month of lactation (Joardar et al. 2006). There is evidence that slowly turning-over maternal body pools of AA are the major source of milk AA (Szabó et al. 2010). The AA concentration in breast milk is dose-dependently associated with the consumption of AA-rich foods in lactating mothers (Del Prado et al. 2001). Breast milk EPA and DHA concentrations are also closely linked to maternal dietary EPA and DHA intake (Weseler et al. 2008). Human milk from lactating women consuming vegan or vegetarian diets has <0.1% DHA, compared to mean levels of 0.2%–0.4% DHA in the United States and 0.8% DHA in China, where DHA intakes from fish or other sources are high (Makrides et al. 1996). It is suggested that intakes of ~300 mg of DHA per day are necessary to achieve human milk levels of 0.3%–0.35% of DHA (Fleith and Clandinin 2005). However, the effects of human milk fatty acids on neurodevelopment is complex, particularly because neurodevelopment is assessed after the period of the first six month of exclusive human milk feeding. In premature birth, the transmission of these fatty acids is interrupted from the placenta to the fetus during the critical last trimester. Studies also showed that decreased postnatal docosahexaenoic and arachidonic acid blood levels in premature infants are associated with neonatal morbidities (Innis 2014). Thus, after birth, the preterm infant is dependent on an adequate diet for sufficient fatty acid levels. Adding DHA and AA to preterm-infant formulas led to initial beneficial effects on visual acuity, visual attention and cognitive development compared with infant receiving no supplementation (Martin et al. 2011).



**Krupal Patel et al.****Vitamins, Minerals and Other Bioactive Components in Breast Milk**

Human breast milk contains adequate amounts of most vitamins to support normal infant growth, except for vitamins D and K. Infants who are exclusively breastfeeding receive below the minimum recommended intake of vitamin D, and much lower than the recommended dietary intake. These infants are at the risk for vitamin D deficiency, inadequate bone mineralization and conditions such as rickets. However, the overall risk of vitamin D deficiency in breastfed infants is also correlated with overall sun exposure with increasing risk in climates with a lower sun index. Maternal supplementation with 400–2000 IU (International Unit) of vitamin D/day can increase the levels of vitamin D in breast milk, but only a higher dose (2000 IU) achieves satisfactory levels of 25-OH-D in the infant (Guo 2014). Normal vitamin D stores present at birth are depleted within eight weeks. Sunlight exposure and vitamin D supplementation are recommended for breastfed infant. Formula-fed infants often have higher serum concentration of vitamin D metabolites than breastfed-infants. Vitamin K is essential to the protein involved in blood coagulation. However, only limited amounts of vitamin K is transferred from the placenta to fetus. Thus, a newborn infant often has an extremely low concentration of vitamin K, and is at risk of developing hemorrhagic disease. After birth, vitamin K supplementation is recommended. In human breast milk, minerals contribute to a variety of physiological functions, forming essential parts of many enzymes and are of biological important to molecules and structures. The contents of minerals are comparable between human milk and bovine milk. Over the decades, many other bioactive components have been identified in human milk, including hormones, growth factors and immunological factors.

Somatic cell count

Milk consists of somatic cell that are 75% leukocytes, neutrophils, erythrocytes, macrophages, lymphocytes and 25% epithelial cells (Vaidya et al. 2017). During intra-mammary infection a significant increase in total SCC is observed where mostly epithelial cell and white cell are present in large number. It also observed that the cell count increases whenever the mammary glands are injured. The white blood cell plays a fundamental role in the immune system. They are considered as a defending element which fights against infection and are actively involved in the repair of damaged tissue. During inflammation a considerable number of neutrophils is reported in the milk accounting for more than 90% of the total SCC (Olivares et al. 2015). Alteration in neutrophil count is also dependent on the lactational stages and breast health in addition to the prevalence of pathogens. During attack of pathogens, the number of leukocytes increases specially neutrophils; their number also depends on lactational stages and breast health (Cabrera-Rubio et al. 2012). Recent studies illustrate that increase in number of leukocytes and macrophage is directly associated with breast infection and that their number decreases significantly upon recovery (Riskin et al. 2012).

Transferring of mother gut microflora to her infant

The occurrence of microflora in the various human body parts makes dynamic and interconnected network (Costello et al. 2009). Probability exists that the neonate's mouth or mother skin may contribute in the development of breast milk microflora to some extent (Figure 2). Beside this physiological and hormonal alteration occurring during pregnancy and after pregnancy increased gut permeability which in turn transfer of gut microflora to the mammary gland. Dendritic cells and macrophages also play an important role in the migration of microbes to the mammary gland (Fernández et al. 2013). These bacteria are transferred from maternal community to breast milk via entero-mammary pathway (Figure 2). Along with above apparent mechanisms, the retrograde flux between the mother's skin microbes and infant's oral microbes may also help in the development of the human milk microbiome (Makino et al. 2011; Albesharat et al. 2011). Some microbiota of the new-born's oral cavity might contaminate breast milk during feeding due to milk flow back again into the milk ducts of the breast (Ramsay et al. 2004). Still, this retrograde flux does not clarify why colostrum consist the microflora which characterizes breast milk (Martín et al. 2004).



**Krupal Patel et al.**

Though the human salivary microbiota is fully explored, *Streptococcus* species present dominantly in both adults (Aas et al. 2005; Nasidze et al. 2009) and in infants (Bearfield et al. 2002; Li et al. 1997). Streptococci are also predominantly found in breast milk (Jiménez et al. 2008) which reveals that salivary microbiota significantly affect the breast milk microbiome. Some of the common skin microflora like *Corynebacterium*, *Staphylococcus*, and *Propionibacterium* (Gao et al. 2007), are also found in human milk. But it should be highlighted that the prevalence of this group of microorganisms also occurred in the mucosal layer of the genitourinary tract and gastrointestinal tracts. Streptococci and Staphylococci have gained attention about their role of initial colonization in infant gastrointestinal tract (Martín et al. 2012).

Remarkably, the studies reveal that abundance of *Staphylococcus epidermidis* was significantly different between the feces of healthy breast-fed newborns to formula-fed newborns (Balmer and Wharton 1989; Lundequist et al. 1985) this shows that such microbes are already present in mammary glands. Regardless of sharing of few phylum, the prevalence of microbiota in breast milk and breast skin microbiome are significantly different to each other (Hunt et al. 2011a) e.g. bacterial belongs to the *Bifidobacterium* genus are strictly anaerobic so they can't grow on breast skin. Similarly, *Bifidobacterium longum* DNA was shared by breast milk, maternal and infant's feces (Grönlund et al. 2007). Jost et al. reported that anaerobic genera, like *Bacteroides*, members of the *Clostridia* class *Bifidobacterium* and *Parabacteroides* was shared among human milk, maternal and neonatal feces using pyrosequencing approach (Jost et al. 2014). Disadvantage of metagenomics studies is that it doesn't give data in regarding of the viability of the identified microbes also strain level can't be obtain identification. Therefore, without confirming the occurrence of these microbes by culture dependent method, it remains indistinct whether human milk is a resource of viable gut-incorporated anaerobes or dead cells (Jost et al. 2014). However, transmission of lactobacilli, bifidobacteria and other bacterial strain from the mother gut to the infant gut (Kulagina et al. 2010), from the mother gut to human milk (Abrahamsson et al. 2009), from human milk to the infant gut (Martín et al. 2012) has also been confirmed using bacterial strain specific study. Such studies support the hypothesis which stated that microbes might be vertically transmitted from lactating women to their infant through breastfeeding.

CONCLUSIONS

Breast milk is the best nutrition for infant growth and development, and is also rich in antibodies that provide the first source of adaptive immunity in a newborn's intestinal tract. In preterm or low birth weight newborns, a mother's own milk is the first choice for preterm infants; when it is unavailable, donor breast milk is considered as the next best choice. With improved understanding of the impact of breast milk microbiota, it may be possible to manipulate these microbial communities to improve the health and development of mothers and their neonates.

REFERENCES

1. Aas, J. A., B. J. Paster, L. N. Stokes, I. Olsen, and F. E. Dewhirst. (2005) Defining the normal bacterial flora of the oral cavity. *J. Clin. Microbiol* 43 (11):5721-5732.
2. Abrahamsson, T. R., G. Sinkiewicz, T. Jakobsson, M. Fredrikson, and B. Björkstén (2009) Probiotic lactobacilli in breast milk and infant stool in relation to oral intake during the first year of life. *J Pediatr Gastroenterol Nutr* 49 (3):349-354.
3. Agostoni, C., B. Carratù, C. Boniglia, A. M. Lammardo, E. Riva, and E. Sanzini (2000) Free glutamine and glutamic acid increase in human milk through a three-month lactation period. *J Pediatr Gastroenterol Nutr* 31 (5):508-512.
4. Albesharat, R., M. A. Ehrmann, M. Korakli, S. Yazaji, and R. F. Vogel (2011) Phenotypic and genotypic analyses of lactic acid bacteria in local fermented food, breast milk and faeces of mothers and their babies. *Syst Appl Microbiol* 34 (2):148-155.



**Krupal Patel et al.**

5. Balmer, S., and B. Wharton (1989) Diet and faecal flora in the newborn: breast milk and infant formula. *Arch Dis Child* 64 (12):1672-1677.
6. Bearfield, C., E. S. Davenport, V. Sivapathasundaram, and R. P. Allaker (2002) Possible association between amniotic fluid microorganism infection and microflora in the mouth. *BJOG: An Int J Gynaecol Obstet* 109 (5):527-533.
7. Boehm, G. n., and G. Moro (2008) Structural and functional aspects of prebiotics used in infant nutrition. *J Nutr* 138 (9):1818S-1828S.
8. Cabrera-Rubio, R., M. C. Collado, K. Laitinen, S. Salminen, E. Isolauri, and A. Mira (2012) The human milk microbiome changes over lactation and is shaped by maternal weight and mode of delivery. *Am J Clin Nutr* 96 (3):544-551.
9. Costello, E. K., C. L. Lauber, M. Hamady, N. Fierer, J. I. Gordon, and R. Knight (2009) Bacterial community variation in human body habitats across space and time. *Sci*. 326 (5960):1694-1697.
10. Del Prado, M., S. Villalpando, A. Elizondo, M. Rodríguez, H. Demmelmair, and B. Koletzko (2001) Contribution of dietary and newly formed arachidonic acid to human milk lipids in women eating a low-fat diet. *Am J Clin Nutr* 74 (2):242-247.
11. Duijts, L., V. W. Jaddoe, A. Hofman, and H. A. Moll (2010) Prolonged and exclusive breastfeeding reduces the risk of infectious diseases in infancy. *Pediatrics* 126 (1):e18-e25.
12. Fernández, L., S. Langa, V. Martín, A. Maldonado, E. Jiménez, R. Martín, and J. M. Rodríguez. (2013) The human milk microbiota: origin and potential roles in health and disease. *Pharmacol Res* 69 (1):1-10.
13. Fleith, M., and M. Clandinin (2005) Dietary PUFA for preterm and term infants: review of clinical studies. *Crit. Rev. Food Sci. Nutr* 45 (3):205-229.
14. Gao, Z., C.-h. Tseng, Z. Pei, and M. J. Blaser (2007) Molecular analysis of human forearm superficial skin bacterial biota. *Proc Natl Acad Sci U S A* 104 (8):2927-2932.
15. Grönlund, M. M., M. Gueimonde, K. Laitinen, G. Kociubinski, T. Grönroos, S. Salminen, and E. Isolauri (2007) Maternal breast milk and intestinal bifidobacteria guide the compositional development of the Bifidobacterium microbiota in infants at risk of allergic disease. *Clin Exp Allergy* 37 (12):1764-1772.
16. Gross, S. J., J. Geller, and R. Tomarelli (1981) Composition of breast milk from mothers of preterm infants. *Pediatrics* 68 (4):490-493.
17. Guo, M (2014) Human milk biochemistry and infant formula manufacturing technology: Elsevier.
18. Heikkilä, M. P., and P. Saris (2003) Inhibition of *Staphylococcus aureus* by the commensal bacteria of human milk. *J Appl Microbiol* 95 (3):471-478.
19. Herrera, E (2002) Implications of dietary fatty acids during pregnancy on placental, fetal and postnatal development—a review. *Placenta* 23:S9-S19.
20. Innis, S. M (2014) Impact of maternal diet on human milk composition and neurological development of infants. *Am J Clin Nutr* 99 (3):734S-741S.
21. Jackson, J. G., D. B. Janszen, B. Lonnerdal, E. L. Lien, K. P. Pramuk, and C. F. Kuhlman (2004) A multinational study of α -lactalbumin concentrations in human milk. *J Nutr Biochem* 15 (9):517-521.
22. Jiménez, E., L. Fernández, S. Delgado, N. García, M. Albújar, A. Gómez, and J. Rodríguez (2008) Assessment of the bacterial diversity of human colostrum by cultural-based techniques. Analysis of the *staphylococcal* and *enterococcal* populations. *Res Microbiol* 159 (9-10):595-601.
23. Joardar, A., A. K. Sen, and S. Das (2006) Docosahexaenoic acid facilitates cell maturation and β -adrenergic transmission in astrocytes. *J Lipid Res* 47 (3):571-581.
24. Jost, T., C. Lacroix, C. P. Braegger, F. Rochat, and C. Chassard (2014) Vertical mother–neonate transfer of maternal gut bacteria via breastfeeding. *Environ. Microbiol* 16 (9):2891-2904.
25. Koletzko, B., B. Poindexter, and R. Uauy (2014) Nutritional care of preterm infants: scientific basis and practical guidelines: Karger Medical and Scientific Publishers.
26. Kulagina, E., A. Shkoporov, L. Kafarskaia, E. Khokhlova, N. Volodin, E. Donskikh, O. Korshunova, and B. Efimov (2010) Molecular genetic study of species and strain variability in bifidobacteria population in intestinal microflora of breast-fed infants and their mothers. *B Exp Biol Med* 150 (1):61-64.



**Krupal Patel et al.**

27. Li, Y., E. Teague, Z. Zhuang, and P. Caufield (1997) Screening for the spaP gene of Streptococcus mutans in preterm infants. Paper read at J Dent. Res.
28. Lönnerdal, B (2003) Nutritional and physiologic significance of human milk proteins. Am J Clin Nutr 77 (6):1537S-1543S.
29. Lundequist, B., C. Nord, and J. Winberg (1985) The composition of the faecal microflora in breastfed and bottle fed infants from birth to eight weeks. Acta Pædiatrica 74 (1):45-51.
30. Makino, H., A. Kushiro, E. Ishikawa, D. Muylaert, H. Kubota, T. Sakai, K. Oishi, R. Martin, K. B. Amor, and R. Oozeer (2011) Transmission of intestinal Bifidobacterium longum subsp. longum strains from mother to infant, determined by multilocus sequencing typing and amplified fragment length polymorphism. Appl. Environ. Microbiol. 77 (19):6788-6793.
31. Makrides, M., M. Neumann, and R. A. Gibson (1996) Effect of maternal docosahexaenoic acid (DHA) supplementation on breast milk composition. Eur. J. Clin. Nutr 50 (6):352-357.
32. Martin, C. R., D. A. DaSilva, J. E. Cluette-Brown, C. DiMonda, A. Hamill, A. O. Bhutta, E. Coronel, M. Wilschanski, A. J. Stephens, and D. F. Driscoll (2011) Decreased postnatal docosahexaenoic and arachidonic acid blood levels in premature infants are associated with neonatal morbidities. J. Pediatr 159 (5):743-749. e742.
33. Martín, R., E. Jiménez, H. Heilig, L. Fernández, M. L. Marín, E. G. Zoetendal, and J. M. Rodríguez (2009) Isolation of bifidobacteria from breast milk and assessment of the bifidobacterial population by PCR-denaturing gradient gel electrophoresis and quantitative real-time PCR. Appl. Environ. Microbiol. 75 (4):965-969.
34. Martín, R. o., S. Langa, C. Reviriego, E. Jiménez, M. a. L. Marín, M. Olivares, J. Boza, J. Jiménez, L. Fernández, and J. Xaus (2004) The commensal microflora of human milk: new perspectives for food bacteriotherapy and probiotics. Trends Food Sci Tech. 15 (3-4):121-127.
35. Martín, V., A. Maldonado-Barragán, L. Moles, M. Rodríguez-Baños, R. d. Campo, L. Fernández, J. M. Rodríguez, and E. Jiménez (2012) Sharing of bacterial strains between breast milk and infant feces. J Hum Lact. 28 (1):36-44.
36. Morrow, A. L., and J. M. Rangel (2004) Human milk protection against infectious diarrhea: implications for prevention and clinical care. Paper read at Seminars in pediatric infectious diseases.
37. Nasidze, I., J. Li, D. Quinque, K. Tang, and M. Stoneking (2009) Global diversity in the human salivary microbiome. Genome res. 19 (4):636-643.
38. Olivares, M., S. Albrecht, G. De Palma, M. D. Ferrer, G. Castillejo, H. A. Schols, and Y. Sanz (2015) Human milk composition differs in healthy mothers and mothers with celiac disease. Eur J Nutr 54 (1):119-128.
39. Ramsay, D. T., J. C. Kent, R. A. Owens, and P. E. Hartmann (2004) Ultrasound imaging of milk ejection in the breast of lactating women. Pediatrics 113 (2):361-367.
40. Riskin, A., M. Almog, R. Peri, K. Halasz, I. Srugo, and A. Kessel (2012) Changes in immunomodulatory constituents of human milk in response to active infection in the nursing infant. Pediatr. Res 71 (2):220.
41. Szabó, É., G. Boehm, C. Beermann, M. Weyermann, H. Brenner, D. Rothenbacher, and T. Decsi (2010) Fatty acid profile comparisons in human milk sampled from the same mothers at the sixth week and the sixth month of lactation. JPediatr Gastroenterol Nutr 50 (3):316-320.
42. Vaidya, Y., S. Patel, C. Joshi, D. Nauriyal, and A. Kunjadia (2017) Somatic Cell Count: A Human Breast Wellbeing Indicator. Eur. J. Breast Health 13 (2):88.
43. Weseler, A. R., C. E. Dirix, M. J. Bruins, and G. Hornstra (2008) Dietary arachidonic acid dose-dependently increases the arachidonic acid concentration in human milk. J Nutr 138 (11):2190-2197.
44. Zhang, Z., A. S. Adelman, D. Rai, J. Boettcher, and B. Lönnerdal (2013) Amino acid profiles in term and preterm human milk through lactation: a systematic review. Nutrients 5 (12):4800-4821.





Krupal Patel *et al.*

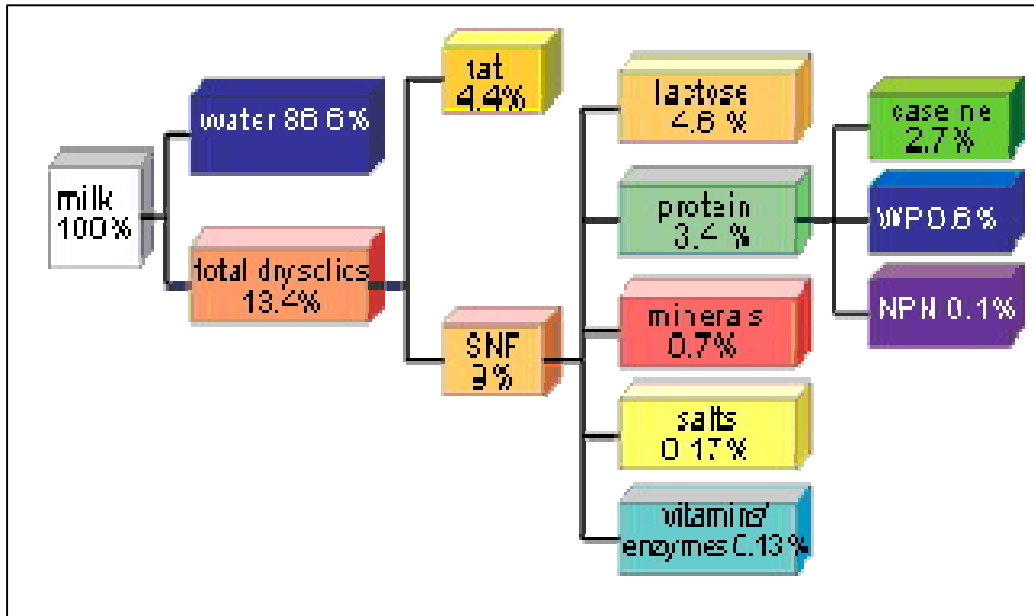


Figure 1. Human Milk Composition

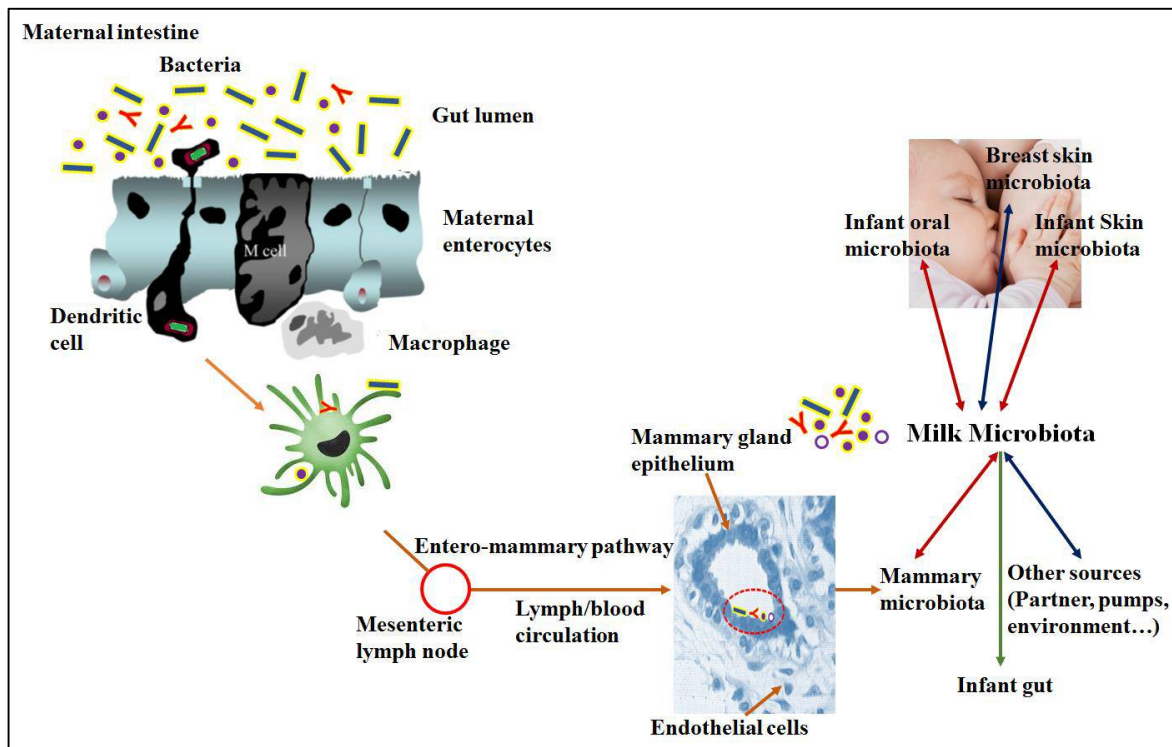


Figure 2. Origin of microflora in human breast milk (Fernández *et al.* 2013)





Development and Validation of a Forced Degradation UPLC Method for the Simultaneous Determination of Eplerenone & Torsemide in Bulk and Pharmaceutical Dosage Form

S.Sangeetha^{1*}, S.Alexandar² and B. Jaykar²

¹Lecturer, Department of Pharmaceutical Chemistry, Vinayaka Missions College of Pharmacy, Vinayaka Mission's Research Foundation (Deemed to be University), Salem, TamilNadu, India.

²Department of Pharmaceutical Chemistry, Vinayaka Missions College of Pharmacy, Vinayaka Mission's Research Foundation (Deemed to be University), Salem, TamilNadu, India.

Received: 15 Sep 2019

Revised: 18 Oct 2019

Accepted: 20 Nov 2019

*Address for Correspondence

S.Sangeetha

Lecturer,

Department of Pharmaceutical Chemistry,

Vinayaka Missions College of Pharmacy,

Vinayaka Mission's Research Foundation (Deemed to be University),

Salem, TamilNadu, India.

Email: sangeethakarathi2010@gmail.com



This is an Open Access Journal / article distributed under the terms of the **Creative Commons Attribution License** (CC BY-NC-ND 3.0) which permits unrestricted use, distribution, and reproduction in any medium, provided the original work is properly cited. All rights reserved.

ABSTRACT

A effective method with simple, precise was developed for Eplerenone & Torsemide by using Forced degradation UPLC method. The column used was C-₁₈ BEH _ 1.7 μm x 2.1 x 50 mm in ambient temperature. Flow rate was 0.8 ml/min; wavelength of 278nm, mobile phase used was acetonitrile: Buffer (60:40). Buffer used 0.01 N Disodium hydrogen phosphate with pH 3.5 adjusted by OPA. Run time 4 min. The percentage purity and RT of Eplerenone & Torsemide was found to be 99.86, 99.30 and 1.280 & 2.153 respectively. The validation parameters was carried out, linearity of Eplerenone was found to be (5 μgm/ml to 40 μgm/ml) R²= 0.998 and Torsemide was found to be (2.0 μgm/ml to 16.1 μgm/ml) R²= 0.999. Intermediate precision, Robustness, LOD LOQ was within the limit as per ICH guidelines. Recovery studies taken place in 80%,100% and 120. Forced Degradation was carried out in three conditions acidic, basic and peroxide condition, degradation takes at basic and peroxide. As per literature review there is no method developed for Eplerenone & Torsemide in Forced degradation UPLC method. So we made attempt to develop the Eplerenone & Torsemide in UPLC method.

Keywords: UPLC, Eplerenone, Torsemide, ICH guide lines, forced degradation.

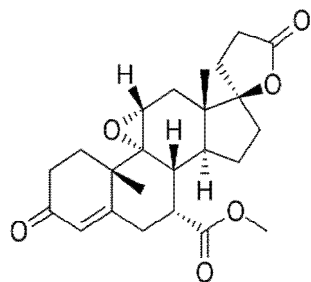




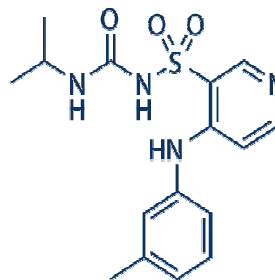
Sangeetha et al.

INTRODUCTION

Eplerenone ($7\alpha, 11\alpha, 17\alpha$)-9,11-epoxy-17-hydroxy-3-oxo-pregn-4-ene-7,21dicarboxylic acid, γ -lactone, 7-methyl ester (1). It is a steroidal antimineralocorticoid of the spiro lactone group that is used as an adjunct in the management of chronic heart failure and high blood pressure. Torasemide is an N-sulfonylurea obtained by formal condensation of [(3-methylphenyl) amino] pyridine-3-sulfonic acid with the free amino group of N-isopropylurea. Torasemide, also known as torsemide, is a medication used to treat high blood pressure and fluid overload due to heart failure, kidney disease, and liver disease (2). The FDA and ICH guidances state the requirement of stability testing data to understand how the quality of a drug substance and drug product changes with time under the influence of various environmental factor (4,5).The drug was subjected to acid, base, oxidation, which enabled separation and detection of degradation products from basic and oxidation stress (6) .Ultra Performance Liquid Chromatography (UPLC) system is an innovative product that brought revolution in high performance liquid chromatography by outperforming conventional high performance liquid chromatography (HPLC). There is, however, no work reported on combination of these two drugs. In the present communication, we propose fast, simple and accurate spectrophotometric method for simultaneous estimation of both the drugs in tablet dosage form.



Structure of Eplerenone



Structure of Torsemide

MATERIALS AND METHOD

HPLC Water- Milli-Q grade, Acetonitrile- Fisher scientific, Methanol- Fisher scientific, Potassium di hydrogen phosphate- Merck, Ortho phosphoric acid- Sigma, Hydrochloric acid- Merck. These solvents were throughout method development and validation. Eplerenone & Torsemide are gift sample from Mylan Pharmaceuticals Hosur.

Instrumentations

The UPLC method development and validation was done using Waters Acquity UPLC BEH Column. The dissolution apparatus Distek , UV-Visible spectrophotometer -Perkin elimer, Analytical balance-Sartorius.

ASSAY

Test Solution Preparation

Preparation of stock

10 tablets were weighed and powered. Powered tablets transferred equivalent to about 25mg of Eplerenone and 5 mg of Torsemide into 50 mL volumetric flask. Add about 10mL of mobile phase and sonicate for 15min. Dilute to volume with diluent and mix well.



**Sangeetha et al.****Preparation of standard**

Pipette out 10 mL of the above stock solution into a 100 mL volumetric flask. Dilute to volume with diluent and mix well and to get final Concentration of about 100 µg/mL. Filter the above solution through 0.45 µm PVDF membrane filter.

Chromatographic condition

In the present study column used C₁₈ BEH - 1.7 µm x 2.1 x 50 mm in ambient temperature. Flow rate was 0.8 ml/min, wavelength of 278 nm, mobile phase used was Acetonitrile Buffer (60:40). Buffer used 0.01 N Disodium hydrogen phosphate with pH 3.5 adjusted by ortho phosphoric acid. Run time 4 min. The retention time was found to be 1.280 & 2.153 for Eplerenone & Torsemide.

VALIDATION PARAMETER

- System Suitability
- Specificity
- Linearity and Range
- Precision
- Ruggedness
- Accuracy
- Robustness
- Limit of Detection and Limit of Quantitation
- Solution stability

System Suitability

System suitability was performed by injecting 5 replicate of injections Eplerenone & Torsemide. Eplerenone & Torsemide was diluted by mobile phase to the final concentration of 2.5 µg/ml and 5 µg/ml respectively. It was performed to determine the resolution, theoretical plates, tailing factor, repeatability of retention time etc. All parameters are within the range as per the ICH guidelines.

Specificity

Specificity is the ability to assess unequivocally the analyte in the presence of components which may be expected to be present. It was performed to identify the any impurity may present, it was done by using standard, sample, placebo dilutions of both Eplerenone & Torsemide

Calibration Curve (Linearity)

Linearity of Eplerenone was found to be (5 µg/ml to 40 µg/ml), 25.1 mg of Eplerenone was taken which is diluted to 50 ml from that 0.2 ml to 1.6 ml was taken and make up to 100 ml. Torsemide was found to be (2 µg/ml to 16 µg/ml), 25.1 mg of Torsemide was taken and diluted with mobile phase to 50 ml from that 0.2 ml to 1.6 ml was taken which is diluted to 100 ml. % RSD of both Eplerenone and Torsemide was found to be 0.998 and 0.999 respectively. Tab 02, Fig 02, 03.



**Sangeetha et al.****Precision**

Intermediate precision was carried in both Eplerenone & Torsemide, Precision of Eplerenone standard dilution was (50µgm/ml) and sample dilution was (20 µgm/ml) ,Torsemide standard dilution (10 µgm/ml) and sample dilution was (20 µgm/ml) to determine repeatability of method development. With the same solution precision was carried out next day also. % RSD was with in the limit as per ICH guidelines. Tab 03

Accuracy

Eplerenone & Torsemide accuracy was study done in 80%, 100% and 120%. Recovery and percentage purity of Eplerenone & Torsemide was found in the range of 24.6 mg to 24.9 mg., 99.30% to 99.46% and 9.93 to 9.97 mg, 99.64 % to 99.92 % respectively. Tab 04

Robustness

Robustness study was done by changing the pH, wavelength, flow rate in both the drug. % RSD was with in the limit as per ICH guidelines. Tab

LOD and LOQ

Limit of detection was carried out in Eplerenone & Torsemide the value are found to be 3.24and 3.63 respectively. Limit of quantification was carried out in Eplerenone & Torsemide the value are found to be 11.66 and 10.74 respectively.

Forced Degradation Study**Acid Degradation Study (2N HCL)**

The sample solution of Eplerenone & Torsemide 50µgm/ml and 50µgm/ml respectively are expose to acidic condition for 30 minutes but there is no degradation takes place.

Base Degradation Study (2N NaOH)

The sample solution of Eplerenone & Torsemide 25 µgm/ml and 50µgm/ml respectively are expose to basic condition for 30 minutes there was degradation takes place, Extra peak were obtained and changes in RT.

Peroxide Degradation Study (2N H₂O₂)

The sample solution of Eplerenone & Torsemide 2.5µgm/ml and 5µgm/ml respectively are expose to a peroxide condition for 30 minutes there was degradation takes place, extra peak were obtained.

UV degradation study

The sample solution of Eplerenone & Torsemide 2.5µgm/ml and 5µgm/ml respectively are expose to a UV light for 7 days there was no degradation takes place.





Sangeetha et al.

Thermal degradation study

The sample solution of Eplerenone & Torsemide 2.5µgm/ml and 5µgm/ml respectively are expose to a thermal condition for 100°C for 12 hours there no was degradation takes place, extra peak were not obtained.

CONCLUSION

The present study was method development and validation of Eplerenone & Torsemide by uplc method with forced degradation study. Since no method was developed in UPLC, RT of Eplerenone & Torsemide was found to be 2.133 and 1.697 respectively. In forced degradation study both Eplerenone & Torsemide degraded by basic and peroxide condition. Analytical method validation plays a fundamental role in pharmaceutical industry for releasing the commercial batch and long term stability data. So this study is useful for routine pharmaceutical analysis.

REFERENCES

1. <http://www.drugbank.ca/drugs/DB00214>
2. <http://www.drugbank.ca/drugs/DB00700>
3. Development of forced degradation and stability indicating studies of drugs—A reviewpanel Blessy M.Ruchi D.Patel Prajesh N.PrajapatiY.K.AgrawalVolume 4, Issue 3, June 2014, Pages 159-165 JPA
4. Vanita P. Rode, Madhukar R. Tajne A Validated Stability-Indicating High-Performance Thin-Layer Chromatographic Method for the Analysis of Pitavastatin in Bulk Drug and Tablet Fomulation. Asian Journal of Pharmaceutical Analysis, 2018, 8(1), 49-52.
5. ICH guidelines, Q1A (R2): Stability Testing of New Drug Substances and Products (revision 2), International Conference on Harmonization. Available from: [http://www.fda.gov/downloads/Regulatory Information/Guidances/ucm128204.pdf](http://www.fda.gov/downloads/Regulatory%20Information/Guidances/ucm128204.pdf)

Tab.1: Assay of Torsemide and Eplerenone

Commercial Formulation	Drug	Standard area	Sample Area	Label Claim (mg)	Amount Present (mg)	% Purity
Eptus T	Torsemide	544639	547922	10mg	9.92mg	99.30
	Eplerenone	1482033	1483321	25mg	24.93mg	99.86

Tab. 2. Linearity and Range Linearity of Torsemide and Eplerenone

S.no	Torsemide		Eplerenone	
	Conc (mcg/mL)	Mean area	Conc (mcg/mL)	Mean area
1	2.0	73594	5	205245
2	4.1	190761	10	513787
3	6.1	313636	15	868529
4	8.1	427636	20	1167646
5	10.2	554826	25	1505764
6	12.1	668135	30	1816299
7	14.1	781150	35	2127674
8	16.1	904648	40	2459021





Sangeetha et al.

Tab. 3. Intermediate precision of Torsemide and Eplerenone

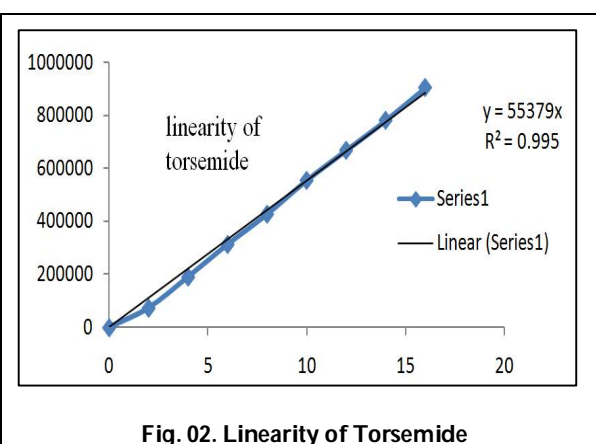
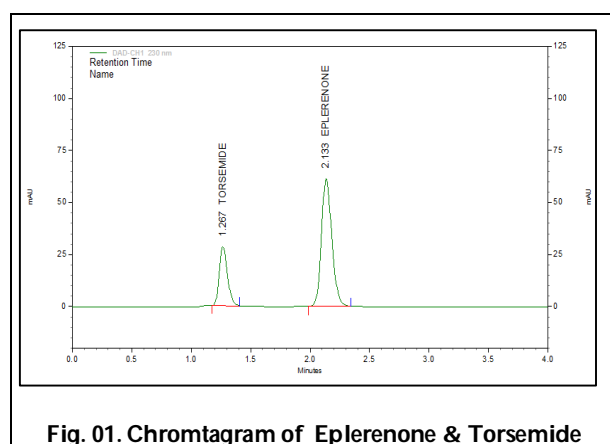
Analyst 1	Torsemide			Eplerenone		
	mg/tab	Area	%Assay	Mg/tab	Area	%Assay
1	9.92	554193	99.25	24.87	1364168	99.51
2	9.89	554610	98.99	24.93	1361928	99.75
3	9.92	553552	99.21	25.02	1364915	100.11
4	9.93	554610	99.39	24.97	1368279	99.89
5	9.97	554610	99.76	25.06	1369571	100.25
6	9.92	554610	99.29	25.09	1369456	100.40
Mean	9.31	554610	99.31	24.99	1366386	99.99
%RSD		0.15			0.15	

Tab. 4. Accuracy of Eplerenone & Torsemide

% Conc	Torsemide				Eplerenone			
	mg/tab	AREA		%Assay	mg/tab	AREA		%Assay
		STD	SAMPLE			STD	SAMPLE	
80%	9.93	536614	431782	99.32	24.86	1463369	1160283	99.46
100%	9.97	536614	542260	99.46	24.95	1463369	1456623	99.84
120%	9.98	536614	650292	99.49	24.85	1463369	1737111	99.30

Tab. 5. Robustness of Torsemide and Eplerenone

S.no	Torsemide				Eplerenone			
	Std area	Sample area	Assay	%RSD	Std area	Sample area	assay	%RSD
Flow rate (0.6 ml)	698038	704247	99.69	0.48	1885720	1896656	99.62	0.80
Flow rate (0.8 ml)	544639	547922	99.21	0.19	1482033	1487395	99.99	0.19
Flow rate (1.0ml)	473267	477298	99.63	0.14	1277374	1268440	99.93	0.13
Wavelength 228nm	662714	669369	99.87	0.23	1406182	1412332	100.5	0.98
Wavelength 230nm	571633	575226	99.50	0.16	1568288	1562015	99.74	0.92
Wavelength 232nm	503841	508570	99.81	0.79	1755648	1747959	99.70	0.80





Sangeetha et al.

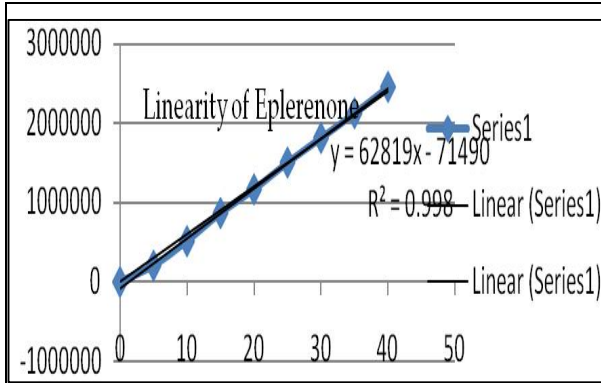


Fig. 03. Linearity of Eplerenone

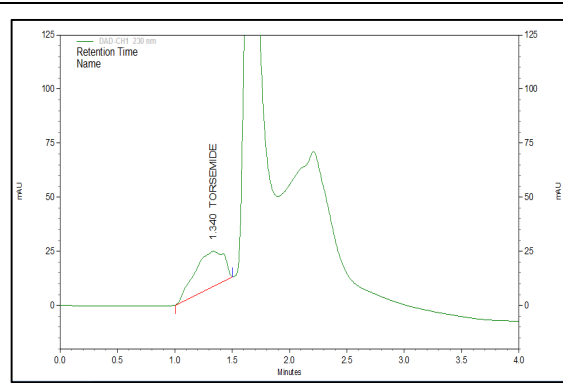


Fig. 04. Base Degradation Chromatogram

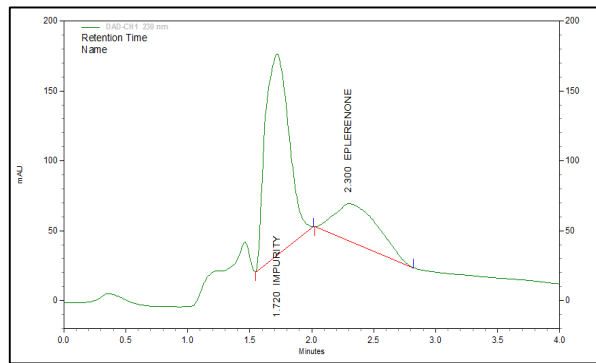


Fig. 05. Peroxide Degradation Chromatogram





Expression of Recombinant *Toxocara canis* Excretory Secretory Antigen (Tes-26) In *Escherichia coli*

A.Nandini¹, Anju Varghese^{1*}, C. Angeline Felicia Bora¹, Lanchalung Malangmei¹, C. K. Deepa¹, K. G. Ajith Kumar¹, Reghu Ravindran¹, A. Muhasin Asaf², Lijo John³, Prashant S. Kurbet¹, B. M. Amrutha¹, R. K. Pradeep¹ and M. Nimisha¹

¹Department of Veterinary Parasitology, College of Veterinary and Animal Sciences, Pookode, Wayanad, Kerala, India

²Department of Animal Genetics and Breeding, College of Veterinary and Animal Sciences, Pookode, Wayanad, Kerala, India

³Department of Veterinary Biochemistry, College of Veterinary and Animal Sciences, Pookode, Wayanad, Kerala, India.

Received: 22 May 2019

Revised: 25 Jun 2019

Accepted: 28 July 2019

* Address for Correspondence

Anju Varghese

Assistant Professor,

Department of Veterinary Parasitology,

College of Veterinary and Animal Sciences,

Pookode, Wayanad, Kerala, India

Email: dranjuvarghese@gmail.com



This is an Open Access Journal / article distributed under the terms of the **Creative Commons Attribution License** (CC BY-NC-ND 3.0) which permits unrestricted use, distribution, and reproduction in any medium, provided the original work is properly cited. All rights reserved.

ABSTRACT

The gene encoding the excretory-secretory antigen TES-26 of canine ascarid worm *Toxocara canis* was cloned into pDrive (T/A) cloning vector and transformed into competent *E. coli* DH5 α cells. After sequence confirmation, it was sub-cloned in a prokaryotic expression vector (pPROEXHT-b) and the recombinant proteins were expressed in the *E. coli* DH5 α cells. Routine serological tests like ELISA for diagnosis of toxocarosis uses total TES antigens (*Toxocara* excretory secretory antigen) derived from *in vitro* larvae culture. However, with the use of native TES-antigen the specificity was often low chiefly in tropical countries. Therefore, prokaryotic expression systems such as *E. coli* produce non-glycosylated proteins; the use of such proteins in seroassays would reduce the possibility of cross-reactivity. The present study produced highly specific recombinant TES-26 antigen suitable for the diagnosis of toxocarosis in humans and adult dogs.

Key words: *T. canis*, recombinant TES-26, *E. coli* DH5 α cells, expression vector (pPROEXHT-b).



**Nandini et al.**

INTRODUCTION

Toxocara canis is the etiological agent for toxocarosis in dogs and other canids and its distribution is widespread (Glickman and Schantz, 1981; Lewis and Maizels, 1993; Despommier, 2003). Close relationship between human and dogs is associated with a number of zoonotic diseases, among which *T. canis* in particular poses a serious public health concern worldwide (Khante *et al.*, 2009). *T. canis* is considered as one of the main enteropathogens of dogs, especially in newly whelped or neonates (Blagburn *et al.*, 1996). Adult dogs act as reservoir host for *T. canis* and source of infection to new born puppies and puppies play an important role in spreading the infection to humans (Cruz *et al.*, 2008). In adult dogs the infection is characterized by encapsulated 2nd stage larvae (L2). However, in pregnant female dogs these larvae can get activated and cross the placental barrier to infect the neonates (Akao and Ohta, 2007). Infected dog excrete thousands of eggs in the environment that are potential source for human infection. Infection in humans is through accidental ingestion of soil contaminated with embryonated eggs (Daryani *et al.*, 2008)

During the somatic migration of infective larvae through the organs, the larvae shed huge quantity of immunogenic glycoproteins known as *Toxocara* excretory-secretory (TES) antigens. The shedding of prodigious amounts of TES antigens is believed to be a strategy of the larvae to escape the immune attack of the host (Gems and Maizels, 1996). Diagnosis by identification of the larvae in the tissues is rarely done. Antibody detection is the more common means of confirmation of toxocarosis. Routine serological tests like IgG based ELISA kits have been developed based on *Toxocara* excretory-secretory (TES) products obtained from the *in vitro* culture of *T. canis* L2 larvae (Smith and Rahman, 2006). However, with the use of native TES-antigen the specificity was often low, chiefly in tropical countries, where co-infections with other helminthes are common (Schoenardie *et al.*, 2013). Therefore, compared to native TES-antigen, the use of recombinant antigens has increased sensitivity and specificity of the assay. Several researchers have cloned, expressed, and developed EIAs based on recombinant antigens of the assay (Fong *et al.*, 2003; Fong *et al.*, 2004; Norhaida *et al.*, 2008; Mohamad *et al.*, 2009). TES-26 glycoproteins of *T. canis* larvae are closely related mucins which form the major constituents of the larval surface coat and ES antigens. In the present study, *T. canis* recombinant TES-26 was expressed in *E. coli*.

MATERIALS AND METHODS

Collection of adult *T. canis* worms

The adult worms recovered from naturally infected pups by piperazine treatment. Female worms were separated and eggs were retrieved from the gravid uteri. The eggs were incubated in tap water containing 0.2% formalin at 28°C for three weeks for embryonation to L2 larvae. The embryonated eggs with L2 larvae were treated with equal volume of 4% sodium hypochlorite for 30 min at 37°, washed with water and deshelled manually in a small glass tissue homogenizer for the release of larvae. Live larvae were separated from un-embryonated eggs and dead larvae by Baermann method.

Isolation of total RNA of *Toxocara canis* and cDNA synthesis

Total RNA from *Toxocara canis* larvae L2 was extracted using Trizol reagent. L2 larvae (n= 10,000) was triturated in one mL of Trizol reagent using mortar and pestle. Worm lysate was incubated for five min at room temperature (RT) to permit the complete dissociation of nucleoprotein complexes and 0.2 mL of chloroform per one mL of Trizol was added and shook vigorously for 15 sec and incubated at RT for two to three min. The sample was centrifuged at 12000 x g for 15 min at 4° C and aqueous phase was transferred to a fresh micro-centrifuge tube. RNA was precipitated by addition of isopropyl alcohol (0.5 mL per mL of Trizol reagent), followed by incubation of the samples at 4° C for 30 min and centrifuged at 12000 x g for 20 min at 4° C. The supernatant was discarded and pellet washed with 70 per cent ethanol. Finally, RNA pellet was centrifuged at 7500 x g for five min at 4° C, air dried and



**Nandini et al.**

resuspended in RNase free water. Total RNA was quantified and stored at -80° C until its use. The cDNA was synthesized from total RNA using oligo (dT) primer and MMLV reverse transcriptase enzyme (MBI Fermentas, USA) in a standard reverse transcription reaction. *T. canis* TES-26 cDNAs were PCR amplified with gene specific primers (Table 1).

Cloning and expression of recombinant TES-26

The TES-26 PCR fragment was ligated into pDrive (T/A) cloning vector and transformed into competent *E. coli* DH5 α cells and TES-26 genes cloned in TA cloning vector after sequence confirmation were sub-cloned in a prokaryotic expression vector (pPROEXHT-b) and the recombinant proteins were expressed in the *E. coli* DH5 α . The genes were cloned in frame at NcoI and Hind III restriction sites of the expression vector for expression of a fusion protein with a 6x histidine tag. Recombinant TES-26 was expressed in *E. coli* grown at 37° C for 8–9 h in LB broth supplemented with 1mM IPTG. The cultures after optimum growth were pelleted at 6000 rpm and analyzed in 12% SDS-polyacrylamide (SDS-PAGE) gels (Laemmli, 1970) stained with Coomassie blue (Fig 2). Recombinant TES-26 was purified by Ni-NTA affinity chromatography with 6M guanidine hydrochloride as protein denaturants in Tris-phosphate buffer, pH 8.0, supplemented with 5 mM imidazole and was resolved in 12% SDS-PAGE.

RESULTS

The PCR product obtained from cDNA got amplified at 793 bp, TES-26 (Fig.1). The PCR products of respective cDNAs was cloned in TA cloning vector and custom sequenced for determining the authenticity of the gene sequences and nucleotide variations, if any. Nucleotide sequence analysis of the TES-26 gene of *T. canis*, our isolate revealed 99 per cent homology TES-26 (accession no: U29761.1). Recombinant TES-26 expression in *E. coli* was achieved at 37° C for 8-9 h post induction with IPTG at the concentration of 1mM and this protein showed expression at 33kDa when resolved in 12% SDS-PAGE (Fig 2). Purified TES-26 by Ni-NTA affinity chromatography resolved at 33kDa in SDS-PAGE (Fig 3).

DISCUSSION

Since toxocarosis in adult dogs and humans is characterized by encysted L2 larvae, Detection of larvae by biopsy and PCR techniques are not available. ELISA as serological assay is the test of choice to diagnose *Toxocara* infection in human and canines (Bachmeyer *et al.*, 2003). Most of the commercial toxocarosis seroassay kits use total TES antigens derived from *in vitro* larva culture. These antigens are heterogeneous in their composition, and this may increase the risk of cross-reaction with non-*Toxocara* helminth antibodies (Fong *et al.* 2003). Although the sensitivity of larval ES antigens is fairly high, cross-reactions with other parasites have compromised their specificity (Mohamad *et al.* 2009). One of the main explanations for cross-reactivity among helminth protein antigens is the occurrence of common carbohydrate (glycosyl) moieties in their peptides. Therefore, compared to native TES-antigen, the use of recombinant antigens has increased sensitivity and specificity of the assay. Several investigators have reported recombinant antigens that are potentially useful for the sero-diagnosis of toxocariasis in humans, namely TES-30 (Yamasaki *et al.*, 1998; 2000; Norhaida, *et al.*, 2008) and TES-120 (Fong *et al.*, 2003; Fong and Lau, 2004). By knowing the importance of recombinant antigens in the diagnosis of *T. canis* infection in humans, the present study was also aimed at characterization of the larvae (L2) of *T. canis* excretory secretory protein (TES-26). Complementary DNA from larvae was successfully amplified by RT-PCR and both proteins were successfully expressed in pPROEXHT vector.

ACKNOWLEDGEMENTS

This work was supported financially by Kerala Veterinary Animal Sciences University





Nandini et al.

REFERENCES

1. Akao, N. and Ohta, N. Toxocariasis in Japan. *Parasitol. Int.* 2007; 56: 87-93.
2. Bachmeyer, C., Lamarque, G. and Morariu, R. Visceral larva migrans mimicking lymphoma. *Chest.* 2003; 123: 1296-1297.
3. Blagburn, B.L., Lindsay, D.S., Vaughan, J.L., Rippey, N.S., Wright, J.C., Lynn, R.C., Kelch, W.J., Ritchie, G.C. and Hepler, D.I. Prevalence of canine parasites based on faecal flotation. *Comp. Contin. Educ. Vet. Pract.* 1996; 18: 483-509.
4. Cruz, A.T., Franklin, G.Y. and Kaplan, S.L. Toxocariasis causing eosinophilic ascites. *Pediat. Infect. Dis. J.* 2008; 27: 563-564.
5. Daryani, A., Sharif, M., Amouei, A. and Gholami, S. Prevalence of *Toxocara canis* in stray dogs, Northern Iran. *Pak. J. Biol. Sci.* 2009; 12: 1031-1035.
6. Despommier, D. Toxocariasis: clinical aspects, epidemiology, medical ecology and molecular aspects. *Clin. Microbiol. Rev.* 2003; 16: 265-272.
7. Fong, M.Y. and Lau, Y.L. Recombinant expression of the larval excretory secretory antigen TES-120 of *Toxocara canis* in the methylotrophic yeast *Pichia pastoris*. *Parasitol. Res.* 2004; 92: 173-176.
8. Fong, M.Y., Lau, Y.L., Init, I., Jamaiah, I., Khairul, A. and Rahman, N. Recombinant expression of *Toxocara canis* excretory secretory antigen TES-120 in *Escherichia coli*. *Southeast Asian J. Trop. Med. Pub. Hlth.* 2003; 34: 723-726.
9. Gems, D. and Maizels, R.M. An abundantly expressed mucin-like protein from *Toxocara canis* infective larvae: the precursor of the larval surface coat glycoproteins. *Proc. Natl. Acad. Sci. USA.* 1996; 93: 1665-1670.
10. Glickman, L.T. and Schantz, P.M. Epidemiology and pathogenesis of zoonotic toxocariasis. *Epidemiologic. reviews.* 1981; 3: 230-250.
11. Khante, G., Khan, L., Bodkhe, A., Suryawanshi, P., Majed, M., Suradkar, U. and Gaikwad, S. Epidemiological survey of gastro-intestinal parasites of non-descript dogs in Nagpur City. *Vet. Wld.* 2009; 2: 22-23.
12. Laemmli, U. K. Cleavage of structural protein during the assembly of head of bacteriophage T4. *Nature.* 1970; 227: 680-685.
13. Lewis, J.W. and Maizels, R.M. *Toxocara* and toxocariasis. Clinical, epidemiological and molecular perspectives. *Inst. Biol. London.* 1993. 169.
14. Mohamad, S., Norhaida, C.A. and Noordin, R. Development and evaluation of a sensitive and specific assay for diagnosis of human toxocariasis by use of three recombinant antigens (TES-26, TES-30USM, and TES-120). *J. Clin Microbiol.* 2009; 47: 1712-1717.
15. Norhaida, A., Suharni, M., Sharmini, L., Tuda, J. and Rahman, N. rTES-30 USM : Cloning via assembly PCR, expression and evaluation of usefulness in the detection of toxocariasis. *Ann. Trop. Med. Parasitol.* 2008; 102: 151-160.
16. Schoenardie, E.R., Scaini, C.J., Brod, C.S., Pepo, M.S., Villelo, M.M., Mc Bride, A.J., Borsuk, S. and Berne, M. E. Seroprevalence of *Toxocara* infection in children from southern Brazil. *J. Parasitol.* 2013; 99: 537-539.
17. Smith, H. and Noordin, R., Diagnostic limitations and future trends in the serodiagnosis of human toxocariasis. *Toxocara: the enigmatic parasite*, 2006; 89-112.

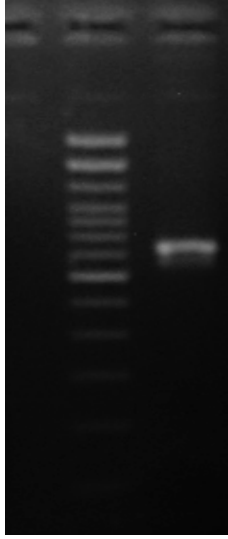
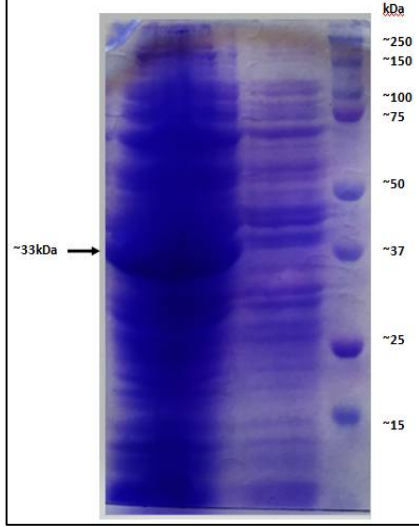
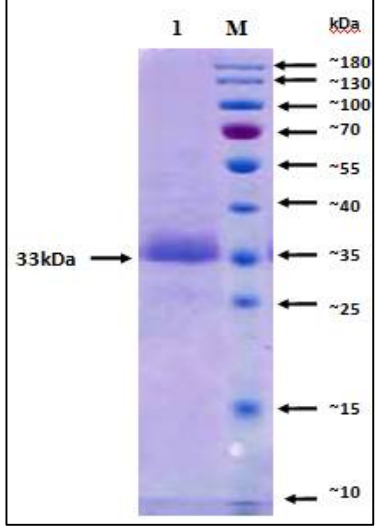
Table 1. Primers used for PCR amplification of *T. canis* TES-26 cDNA

Primer name	Primer sequence	Accession No.
TcTES-26 For	5'-CAGTGTATGGACAGTGCCTCA-3'	U29761.1
TcTES-26 Rev	5'-TTAGGCCTGCGATCGATA-3'	





Nandini et al.

		
<p>Fig. 1. PCR amplification of TES - 26 gene of <i>Toxocara canis</i></p> <p>Lane M : 100 bp plus DNA ladder Lane 1 : TES- 26 PCR product</p>	<p>Fig. 2. SDS-PAGE of the IPTG induced recombinant TES - 26</p> <p>Lane M : Protein molecular weight marker, Lane 1 :Un-induced control</p>	<p>Fig. 3. SDS-PAGE showing purified <i>T.canis</i> recombinant TES-26</p> <p>Lane M: Protein molecular weight marker, Lane 1: Ni-NTA affinity purified recombinant TES-26</p>





UV Spectrophotometric Method for the Determination of Dissolution Profile of Eluxadoline

S.Alexandar*, S.Sangeetha, M. Kumar and B.S.Venkateshwaralu

Department of Pharmaceutical Chemistry, Vinayaka Missions College of Pharmacy, Vinayaka Missions Research Foundation (Deemed to be University), Salem, TamilNadu, India.

Received: 14 Sep 2019

Revised: 17 Oct 2019

Accepted: 20 Nov 2019

*Address for Correspondence

S.Alexandar

Assistant Professor,

Department of Pharmaceutical Chemistry,

Vinayaka Missions College of Pharmacy,

Vinayaka Missions Research Foundation (Deemed to be University),

Salem, TamilNadu, India

Email: dranjuvarghese@gmail.com



This is an Open Access Journal / article distributed under the terms of the **Creative Commons Attribution License** (CC BY-NC-ND 3.0) which permits unrestricted use, distribution, and reproduction in any medium, provided the original work is properly cited. All rights reserved.

ABSTRACT

In recent years, more emphasis has been placed on dissolution testing by the pharmaceutical industry and regulatory authorities. Dissolution tests are used to assess lot-to-lot quality of a drug product in the development of new formulations and in the assurance of product quality and performance after certain changes, such as in the formulation and the manufacturing process. Our present study aims to develop dissolution profile for Eluxadoline tablets by UV spectrophotometry and validate as per ICH guidelines. The optimized method uses pH 6.8 phosphate buffer as a dissolution medium, and detection wavelength of 240 nm. The developed method resulted in Eluxadoline exhibiting linearity in the range 10 – 60 µg/ml. The method was validated according to ICH guidelines which include accuracy, precision, linearity, and analytical range.

Keywords: Eluxadoline, Dissolution, UV Spectrophotometry.

INTRODUCTION

A suitable in vitro dissolution method serves as a valuable quality control tool to assess batch to batch release performance and to assure the physiological availability of the drug. The in vitro dissolution test is also used to guide formulation development and to monitor manufacturing process. As a regulatory test, it is used to approve minor changes in formulation, and to assess the scale-up of the bio-batch to the production batch. Our present study aims to develop dissolution profile for Eluxadoline tablets by UV spectrophotometry and validate as per ICH guidelines (1). Eluxadoline is a mixed mu-opioid receptor agonist, kappa-opioid receptor agonist, and a-delta opioid receptor



**Alexandar et al.**

antagonist indicated for use in diarrhea-predominant irritable bowel syndrome. Chemical Formula is $C_{32}H_{35}N_5O_5$ (2). To our knowledge one method was developed for the estimation of Eluxadoline by HPLC (3). There is no validated UV Method for dissolution of Eluxadoline. This dissolution method validation will give a chance to apply for quality control labs. Quality control labs can adapt out validated analytical dissolution method in their quality control analysis procedures.

MATERIALS

All reagents used in this study full fill the minimum requirement set by Pharmacopeia. The analytical reagents were purchased from reliable resources; these chemicals and materials include the following, Methanol, Potassium di hydrogen Phosphate, Sodium hydroxide and Eluxadoline (Gift sample from Aurobindo Pharma Ltd)

Instruments

The instrumentations that were used during our research include the followings: Weighing balance (Sartorius), pH meter (Pulse Instrument), Dissolution tester (Lab India), UV-Visible Spectrophotometer (Shimadzu 1601).

Dissolution method development

A suitable in vitro dissolution method serves as a valuable quality control tool to assess batch to batch release performance and to assure the physiological availability of the drug. The in vitro dissolution test is also used to guide formulation development and to monitor manufacturing process. As a regulatory test, it is used to approve minor changes in formulation, changes in the site of manufacturing and also to assess the scale-up of the bio-batch to the production batch.

Dissolution method development for Eluxadoline

Dissolution studies of 100 mg of standard Eluxadoline in water and in buffer solution of pH 1.2, 6.8 and 7.2 were carried out over a period of 60 min. At pH 6.8 more than 85 % of the drugs dissolved at 50 rpm within 60 min. Hence pH 6.8, selected for further studies. Six tablets were weighed and Dissolution studies conducted using USP Apparatus 2 (paddle method) with six replicates at 37 ± 0.5 °C. A pH 6.8 Phosphate buffer was the dissolution medium (900 mL), and the paddle rotation speed was 50 rpm. In all experiments, 2-mL sample aliquots were withdrawn at predetermined time intervals (5, 10, 20, 30, 45, and 60 min) and replaced with an equal volume of fresh medium to maintain a constant total volume. After the filtration of the dissolution samples using 0.44- μ m membrane filters, the concentrations of Eluxadoline were determined simultaneously by the proposed spectrophotometric method.

Preparation of standard solutions

Accurately weighed 100 mg of Eluxadoline was transferred to a clean dry 100 ml calibrated volumetric flask and dissolved in pH 6.8 Phosphate buffer. It was shaken for few minutes and the solution was diluted to 100 ml with same. From this various dilution were prepared to get final concentration.

Validation of UV-spectrophotometric method

**Alexandar et al.****Accuracy**

The accuracy of proposed method was justified by carrying out recovery studies in known quantities of pure Eluxadoline. It was thoroughly mixed with definite amount of preanalyzed formulation sample and drug content of the mixture was determined by the proposed method. Accurately weighed formulation sample equivalent to 100mg of Eluxadoline was mixed with 50%, 100%, and 150% of pure drug Eluxadoline.

Precision

The precision was determined by studying the intermediate precision and repeatability. The percentage relative standard deviation (%RSD) was calculated

Repeatability

To check the degree of repeatability of the methods, suitable sample solutions were prepared and statistical evaluation was carried out. Repeatability was performed for six times with tablets formulation.

Linearity and Range**Development of calibration curve for valsartan**

A stock solution (1mg/ml) of Eluxadoline was prepared by dissolving 100 mg the drug in 100 ml of the phosphate buffer of pH 6.8. From the stock solution, a range of 10 to 60 µg/ml was prepared from the stock solution. The Eluxadoline (60 µg/ml) was scanned from 200 to 400 nm in an UV visible spectrophotometer and the spectrum was recorded. From the spectra, the detection wavelength (240 nm) was identified. At this wavelength, the absorbance of all the dilutions was measured. Standard curves between the concentration and the absorbance were plotted and the slope (k) and the intercept (B) values were calculated.

RESULTS AND DISCUSSION***In vitro* dissolution studies of Eluxadoline**

The dissolution data's of Eluxadoline tablets at various times are given in (Table 1) and they are plotted in (Figure 2). Dissolution data for all the experiments were highly reproducible and hence only the average values were plotted.

Validation**Linearity**

It was observed that the optimized were linear within a specific concentration and range of the drug. The calibration curve was plotted between the response factor and concentration of the standard solution. The linearity range for Eluxadoline was found to be 10 to 60 µg/ml and (Table 2 and Figure 2). The correlation coefficient was found to be 0.995, which meet the method validation acceptance criteria and hence the method is said to be linear in the range.

UV Spectra for the Linearity of Eluxadoline



Alexandar et al.

Accuracy

The accuracy of the optimized methods was determined by relative and absolute recovery Experiments and the results are given in (Table 3). The percentage recovery values for Eluxadoline range from 101.45 % to 101.83 %. The developed method is thus accurate and reliable for the estimation of the drugs.

Precision

The precision of an analytical method is defined as the closeness in agreement between independent test results obtained under stipulated conditions, and is a measure of the extent of agreement between repeated injections of a homogenous sample. The precision of a method is usually expressed as the standard deviation or as percent relative standard deviation. precision studies are listed in (Table 4 & 5).

CONCLUSION

A simple dissolution method by UV spectrophotometry method was developed and validated for the estimation of Eluxadoline in immediate release tablets as per ICH guidelines. The optimized method uses pH 6.8 phosphate buffer as a solvent and dissolution medium, and detection wavelength of 240 nm. The developed method resulted in Eluxadoline exhibiting linearity in the range 10 – 60 µg/ml. The method was validated according to ICH guidelines which include accuracy, precision, linearity, and analytical range. Dissolution conditions were 900 ml of Phosphate buffer pH 6.8 as dissolution medium at 37±0.5 °C using USP apparatus II at a stirring rate of 50 rpm for 1 hr. Accordingly it is concluded that the developed dissolution method by UV spectrophotometry is simple, accurate, precise, linear and rugged and therefore the method can be employed for the routine dissolution analysis of Eluxadoline tablets in various pharmaceutical industries. The application of each method, as a routine analysis, should be observed considering cost, simplicity, equipment, solvents, speed, and application to large or small workloads.

REFERENCES

1. ICH-Q2A, Guideline for Industry Text on validation of analytical procedures, 1995.
2. Nelson, E., Knoechel, E.L., Hamlin, W.E. and Wagner, J.G., Journal of Pharmaceutical Sciences, 51, 509, 1962.
3. Uttam Prasad Panigrahy, A. Sunil Kumar Reddy, Research Journal of Pharmacy and Technology 8 (11) : 1469 – 1476, 2015.

Table 1. *In vitro* drug release of Eluxadoline

Time (Mins)	Unit - 1	Unit - 2	Unit - 3	Unit - 4	Unit - 5	Unit - 6	Average	% RSD
5	64.82	63.91	63.56	64.06	63.23	62.45	63.67	1.262
10	71.6	72.23	73.32	72.74	70.43	74.19	72.42	1.823
20	82.92	82.54	83.8	84.27	84.14	84.86	83.76	1.042
30	93.12	93.2	94.1	96.46	94.76	95.25	94.48	1.357
45	95.31	93.81	94.78	96.86	93.44	95.37	94.93	1.295
60	96.68	94.48	94.87	96.24	94.34	95.64	95.38	1.011





Alexandar et al.

Table 2. Calibration curve of Eluxadoline

Concentration (µg/ml)	Absorbance
10	0.4387
20	0.6710
30	0.9816
40	1.3127
50	1.7385
60	1.9728

Table 3. Accuracy (Recovery studies)

Concentration of drug added	Amount added (mg)	Amount recovered (mg)	% recovery	Mean recovery ± SD
50 %	50	50.33	101.32	101.45 ± 0.150
	50	50.39	101.58	
	50	50.36	101.46	
100 %	100	100.86	101.73	101.83 ± 0.159
	100	100.96	101.92	
	100	100.92	101.85	
150 %	150	151.43	101.91	101.81 ± 0.179
	150	151.37	101.83	
	150	151.26	101.69	

Table 4. Intermediate precision

Day 1

Time (Mins)	Unit - 1	Unit - 2	Unit - 3	Unit - 4	Unit - 5	Unit - 6	Average	SD	% RSD
5	64.82	63.91	63.56	64.06	63.23	62.45	63.67	0.80	1.262
10	71.6	72.23	73.32	72.74	70.43	74.19	72.42	1.32	1.823
20	82.92	82.54	83.8	84.27	84.14	84.86	83.76	0.87	1.042
30	91.43	92.01	93.72	94.51	94.36	94.32	93.39	1.34	1.430
45	93.82	94.03	94.57	95.86	91.24	94.67	94.03	1.54	1.639
60	95.84	95.23	93.34	95.84	96.18	92.32	94.79	1.58	1.670

Table 5. Intermediate precision

Day 2

Time (Mins)	Unit - 1	Unit - 2	Unit - 3	Unit - 4	Unit - 5	Unit - 6	Average	SD	% RSD
5	62.34	62.71	63.19	62.76	63.61	64.54	63.19	0.79	1.253
10	70.87	72.34	72.75	71.15	70.32	71.64	71.51	0.92	1.281
20	83.43	82.65	83.71	82.81	82.25	85.86	83.45	1.29	1.550
30	92.32	93.15	92.72	94.62	95.72	96.12	94.11	1.61	1.710
45	94.12	95.23	96.17	95.17	93.83	95.83	95.06	0.92	0.971
60	95.62	95.21	95.32	95.19	95.28	95.45	95.35	0.16	0.172



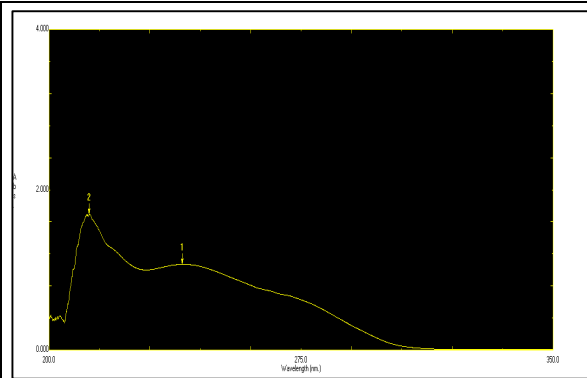


Figure 1. UV Spectrum of Eluxadoline

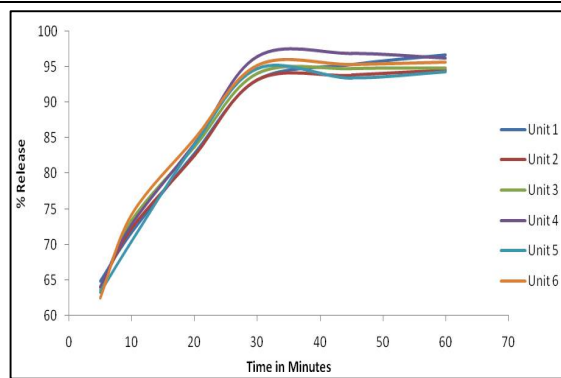


Figure 2. *In vitro* drug release profile of Eluxadoline

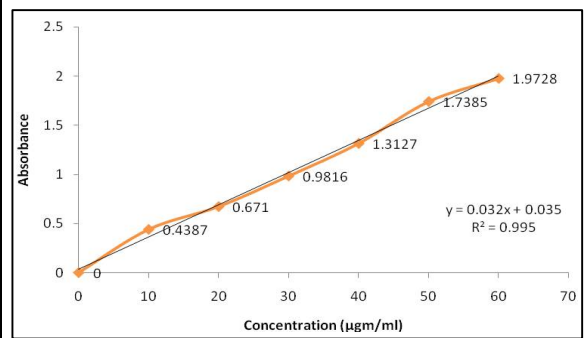


Figure 3. Calibration curve of Eluxadoline

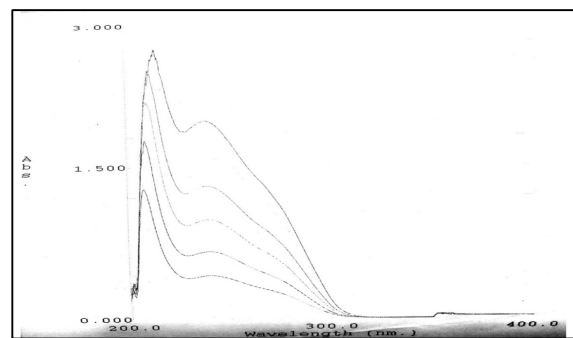


Figure 4. UV Spectra for the Linearity of Eluxadoline





***In-vitro* Analyses on the Screening for Bactericidal and Antioxidant Potential of an Ethno-Botanical Plant *Byttneria herbacea* Roxb.**

Dhannia P.Narayanan¹, V.Shanmugaiah² and S.Suresh^{1*}

¹Department of Botany (DDE), Madurai Kamaraj University, Palkalai Nagar, Madurai, TamilNadu, India.

²Department of Microbial Technology, School of Biological sciences, Madurai Kamaraj University, Palkalai Nagar, Madurai, TamilNadu, India.

Received: 16 Sep 2019

Revised: 18 Oct 2019

Accepted: 21 Nov 2019

*** Address for Correspondence**

S.Suresh

Department of Botany (DDE),
Madurai Kamaraj University,
Palkalai Nagar, Madurai,
TamilNadu, India.

Email: sureshplant@gmail.com



This is an Open Access Journal / article distributed under the terms of the **Creative Commons Attribution License** (CC BY-NC-ND 3.0) which permits unrestricted use, distribution, and reproduction in any medium, provided the original work is properly cited. All rights reserved.

ABSTRACT

Byttneria herbacea Roxb. is an ethnomedicinal plant using by various tribal communities in peninsular India. This study was mainly focused on the investigation on the phytochemical constituents, antioxidant and antibacterial activities of *Byttneria herbacea* Roxb. Qualitative analysis of phytochemistry showed the presence of flavanoids, steroids, coumarins, tannins, cardiac glycosides and phenolic compounds. Antioxidant properties were assessed by using 2, 2-diphenyl -1-picrylhydrazyl-hydrate (DPPH) radical scavenging assay and hydrogen peroxide scavenging assay. An effective free radical scavenging activity was observed in both DPPH and H₂O₂ assays which were more than the standard ascorbic acid. Antibacterial activity of different extracts (hexane, petroleum ether, ethyl acetate, chloroform, acetone, methanol, ethanol and water) were evaluated by agar well diffusion method against gram-positive (*Streptococcus epidermis*, *Staphylococcus aureus* and *Bacillus cereus*) and gram-negative bacteria (*Escherichia coli*, *Salmonella typhi*, *Klebsiella pneumonia*, *Proteus sp.* and *Serratia marcescens*). The plant has exhibited strong antibacterial activity against all the tested bacteria.

Keywords: Antibacterial activity, *Byttneria herbaceae*, MIC, antioxidant activity.

INTRODUCTION

Medicinal plants are considered as rich resource of medicine for curing various ailments and 80% of people in developing countries depend on traditional medicine. India is rich in medicinal plants and about 90% of them are collected from the forest. Several ethnic groups have been projected to use over 7,500 plant species in total



**Dhannia et al.**

(Anthropological survey of India, 1994) (1). The isolation and characterization of bioactive molecules from medicinal plants have resulted in the introduction of new drugs with higher medicinal values. *Byttneria herbacea* (Malvaceae) is a branched (sometimes unbranched) procumbent spreading herb with a perennial, woody root stocks of 4-10 cm long. The plant is distributed in peninsular India, especially found in Idukki and Palakkad districts of Kerala. Wildlife Institute of India, Dehradun's Envis Bulletin (Envis Bulletin 2008) (2) has recognized *B. herbacea* is an endemic species to the Indian Peninsular region. *Byttneria herbacea* is an important ethno botanical plant used by the tribal communities for the treatment of ailments such as dysentery, impaction, to get relief against asthma to promote retention of placenta, to treat leprosy, for treatment of limb fracture, leucorrhoea and inflammation. Achanakmar-Amankantak Biosphere Reserve (AABR), Central India tribal communities use the plant root powder for leucorrhoea and seminal weakness (Tiwari, Sikarwar, & Dubey, 2014) (3). *B. herbacea* was reported by Parrotta (2001) (4) as a Peninsular India healing plant, National Medicinal Plant Board (2012) has registered *B. herbacea* as medicinal plant of India. The medicinal use of root paste of *Byttneria herbacea* on the wound was reported by Mallik, Panda, & Padhy, 2012^[5] filed that the oral *B. herbacea* root paste is taken to get relief from body pain, while recently *B. herbacea* root used against swelling was noted by Suthari, Sreeramulu & Omkar, 2014 (6). The paste of whole plant is used in fracture of limbs and its local name reported as *Samarkai* (Prusti and Behara, 2007)(7). Reports related to the antibacterial activity, phyto constituents and pharmacological activities of *B. herbacea*, still appears to be insufficient. However, to our knowledge, no studies have been reported on antibacterial activities of the plant *Byttneria herbacea* Roxb. against a series of human pathogens. Therefore, this study investigated the antibacterial and antioxidant potentiality of the plant.

MATERIALS AND METHODS

Plant collection and identification

The fresh whole plant *Byttneria herbacea* was collected from Marayur, Idukki district, Kerala, India during the monsoon season on June (5500 ft above mean sea level (MSL)). The plant material was recognized and authenticated by Botanical Survey of India (BSI), Southern Regional Centre, Coimbatore with the number BSI/SRC/5/23/2019/Tech-145.

Preparation of Extracts

The collected plant material was cleaned with water, cut into tiny bits and dried and finely powdered at room temperature. 10g fine powder was soaked separately in 100ml of different solvents (petroleum ether, hexane, chloroform, ethyl acetate, ethanol, methanol, acetone, and water) with occasional stirring. After 72 hrs filtered through No.1 Whatman filter paper to attain a clear filtrate (Harborne, 1973 (8)). The filtrates obtained kept for evaporation and the extracts were weighed and stored in refrigerator for further use.

Determination of antibacterial activity

Bacterial strains used

The bacteria used in this study included three gram-positive bacteria (*Streptococcus epidermis* MTCC10623, *Staphylococcus aureus* MTCC3160 and *Bacillus cereus* MTCC430) and five gram-negative bacteria (*Escherichia coli* MTCC443, *Salmonella typhi* MTCC733, *Klebsiella pneumonia* MTCC3384, *Proteus sp.* MTCC1771 and *Serratia marcescens* MTCC4822). All the strains procured from the Microbial Type Culture and Collection, Mumbai, India.



**Dhannia et al.****Culture media**

Stock cultures were maintained at 4° C on Luria Broth agar (LB agar). Active cultures of strains for experiments were prepared by transferring a loopful of cells from the stock cultures to test tubes of nutrient broth that were incubated without agitation for 24hrs at 37 ° C. Muller-Hinton (Himedia, Mumbai, India) were used for susceptibility testing.

Antibacterial susceptibility testing

The modified agar well diffusion method of Kavanagh F (1972) (9) was employed. By pouring 20ml of sterile M.H. agar the culture plates were made ready and each inoculum suspension was swabbed onto the agar surface. A sterile cork borer (8 mm) has been used for extracting holes in each plate. These plates were marked and 100µl of each plant extracts (at concentration of 10mg/ml) was aseptically added into the well. Simultaneously tetracycline, a broad spectrum antibiotic was used as a positive control at a concentration of 1mg/ml. sterile water was used as the dilution medium for the positive control. The tests were carried out by triplicate. Then the plates were incubated for 24h at 37°C during which the activity was manifested by the presence of zone of inhibition surrounding the well. The activity was denoted as mean of diameter of the inhibition zones (mm).

Minimal inhibitory concentration (MIC) evaluation

The MIC of plant extracts were evaluated by the same modified agar well diffusion method. The different concentrations of the tested extracts (10µg, 20µg,30 µg ,40µg,50 µg ,60µg,70 µg, 80µg,90 µg and 100µg), diluted with DMSO were introduced into the well. The test plates were incubated under the same condition of as the screening stage. The lowest concentration of the extract showing clear zone of inhibition was taken as MIC

Phytochemical screening of the plant extract

The phytochemical analysis by qualitative methods exhibited the information on the presence or absence of different groups of secondary metabolites. The extracts under investigation (petroleum ether, hexane, chloroform, ethyl acetate, acetone, methanol, ethanol and water extracts) were subjected to various phytochemical tests (Table-3) for the presence of steroids, alkaloids, flavanoids, saponins, coumarins, tannins, terpenoids, glycosides, quinones, and phenolic compounds described by Zohra, Meriem, Samira & Muneer, 2012 (10), and Joseph, Kumbhare, & Kale, 2013 (11).

Antioxidant potentiality**DPPH scavenging activity**

The DPPH free radical scavenging assay was carried out for the evaluation of the antioxidant activity. This assay measures the free radical scavenging efficiency of the studied extract. DPPH is a molecule containing a stable free radical (Brand-Williams, Cuvelier and Berset, 1995) (12). The free DPPH radical reduces its purple color in the presence of an antioxidant, which can donate an electron to DPPH and the absorbance change is measured at $\lambda=517\text{nm}$ (Chew, Goh, and Lim, 2009) (13). The activity of the plant extract against radicals was examined based on the scavenging effect of the stable DPPH free radical activity. The different concentrations of extract dissolved in methanol were mixed with DPPH in 96 well plate and kept in dark for incubation for 30 minutes. The standard used was ascorbic acid and methanolic solution of DPPH free radical was used as a negative control. The percentage of radical scavenging activity was calculated by using the following equation,

$$\% \text{ of DPPH radical scavenging activity} = (A_{\text{control}} - A_{\text{sample}} / A_{\text{control}}) \times 100$$





Dhannia et al.

Where, A_{control} is absorbance of blank, A_{sample} is absorbance of the antioxidant at plant extract, A calibration curve was plotted with % of DPPH scavenged versus concentration of standard antioxidant (ascorbic acid).

Hydrogen peroxide scavenging assay

The ability of the ethanol extract of *Byttneria herbacea* to scavenge hydrogen peroxide was conducted by the method described by Olivier (2017) (14). Twenty millimolars (20mM) of hydrogen peroxide solution was prepared from phosphate buffer saline (PBS) with a pH of 7.4. The plant extract (1mg) was dissolved in 1ml methanol and different concentrations (20µg, 40µg, 60µg, 80µg, 100µg, and 120 µg.) are taken from that. A volume of 20µl hydrogen peroxide in PBS was mixed with plant extracts of different volume (20µl, 40µl, 60µl, 80 µl, 100 µl and 120µl) in methanol to get 2ml solution. About 300µl of mixed solutions were taken in the 96 well plate and measured the absorbance at 230 nm after 10 min incubation. The blank solution contained methanol and hydrogen peroxide and ascorbic acid used as control. The inhibition percentage was calculated by using the following formula.

$$\% \text{ of H}_2\text{O}_2 \text{ inhibition} = (A_{\text{sample}} \div A_{\text{control}}) \times 100$$

Where A_{sample} and A_{control} are absorbance of sample and control, respectively.

Data analysis

All values are expressed as mean \pm standard deviation. The antibacterial activity data were analyzed using one way analysis of variance (ANOVA) to check the significant differences among all columns against control. The P value 0.05 was considered as significant. The statistical analysis was performed using Microsoft Excel.

RESULTS AND DISCUSSION

The antibacterial potential of eight different solvent extracts of the plant species *Byttneria herbacea* was tested against three gram positive and five gram negative bacteria. The plant showed antibacterial activity to all the tested gram positive and gram negative bacteria (Table1). All the tested extracts were potentially effective in suppressing the growth of the tested bacterial strains. The gram positive bacteria *S.aureus* and *B.cereus* were more sensitive with a mean quantity of zone of inhibition 16mm to the extract (acetone) than other bacteria. Meanwhile, the bacteria *K.pneumoniae* was less sensitive with the inhibition zone ≤ 10 mm diameter to the tested plant extracts. The plant extracts were strongly active against the bacteria *S.typhi* and *E.coli* followed by *S.epidermis*, *Proteus* spp., and *S.marcescens*. Among the different extracts tested, acetone, ethanol and methanol extracts exhibited higher degree of antimicrobial activity followed by ethyl acetate, chloroform, water and hexane. Petroleum ether extract exhibited least activity with inhibition zone seems to be less than 10mm to all the tested bacterial strains. Among that bacteria tested, *S.typhi* and *S.epidermis* did not show any inhibition against petroleum ether extract. Similarly, *Proteus* sp. also could not inhibited by aqueous extract of the tested plant. The antibiotic tetracycline was so active against the tested pathogens with zone of inhibition diameter of more than 20mm except the bacteria *S.marcescens* which exhibited 15.67 ± 2.08 mm diameter zone. The results of ANOVA analysis indicates that the plant extracts are significant (0.05) in their antibacterial activity against the eight tested bacteria.

Parekh & Chanda (2006) (15) similarly reported the gram-positive bacteria were more susceptible than gram-negative bacteria. The gram-positive bacteria that were most prone was *B. cereus*, while *K. pneumoniae* was found to be most prone gram-negative bacteria. Among those investigated, the most resistant bacteria were *P.aeruginosa* and *A.fecalis*. The species *Terminalia chebula* extract of seed displayed the largest zone of inhibition, with 27 mm diameter against *B. cereus*. In fact, this plant extract (both aqueous and ethanolic) could inhibit all the bacterial strains investigated. 16 of the 50 aqueous extracts showed activity against any of the gram-positive bacteria, while only 10 extracts showed



**Dhannia et al.**

activity against any of the gram-negative bacteria. The plant extracts inhibited the gram-positive microorganisms better than that of gram negative microorganisms. This is consistent with prior reports that plant extracts against gram-positive bacteria are more effective than gram-negative bacteria. (Rabe & Van Staden, 1997) (16).

The results of the MIC values were in accordance with the antibacterial study. Among the various concentrations, of the different extracts tested for the MIC of plant extracts against bacterial strains, acetone extract showed least MIC value, 10 µg/ml to the strains of *S.aureus* and *B.cereus*. Next to this, ethanol extract had MIC of 20 µg/ml against the same strains, which were more susceptible to the antibacterial result. Whereas, ethyl acetate extract and acetone extract also exhibited the similar MIC, 20 µg/ml against *E.coli*, likewise, aqueous extract to *S.epidermis*. The activity was moderate in the case of ethyl acetate extract against *S.aureus* (100 µg/ml), whereas, the antibacterial activity was not significant in case of petroleum ether extract on *S.epidermis* and *K.pneumoniae* and water extract against *Proteus* sp. It can be inferred from the MIC values (Table 2) that *B.herbaeae* showed significant activity on different pathogens that cause human infections and diseases and the ethanol is the better solvent for extraction of the tested plant.

Shai, Chauke, Magano, Mogale & Eloff, 2013 (17) recorded higher average MIC values (1.1 and 0.7 mg/mL against Gram-negative and positive bacteria, respectively) Mudzengi, Murwira, Tivapasi, Murungweni, Burumu & Halimani, 2017 (18) also reported acetone extracts of leaves of *C.mopane*. Similarly, tannins from ethanolic extraction of the root of *D. cinerea* produced higher bacterial toxicity activity with MIC values of 5.5 mg/ mL against *S. aureus* and 5 mg/mL against *E. coli* (Banso & Adeyemo, 2007) (19) in comparison to methanol extraction in the present study. Efficacy of plants can be affected by many factors. For instance, differences in combinations of secondary metabolites such as phenolic compounds, tannins, alkaloids and steroids in different plant species determine their phytochemical uniqueness. These metabolites are also stored in varying proportions in various parts of an individual plant. Hence, higher concentrations would be expected in leaves than the bark, as leaves are responsible for phytochemical production (Banso & Adeyemo, 2007) (19). Differences in solvents used for extraction as well as geographical location could also have contributed to observed variations. Heterogeneity in the composition of compounds in the plant extracts can also lower their antibacterial activity, resulting in the plant extracts possessing little of the lower active ingredient. This could explain lower activity of the plant extracts compared to the controls such as gentamicin and ampicillin. Additionally, active compounds might exhibit higher activity in their pure form. Unlike conventional pharmaceutical products that are generally made from synthetic materials using reproducible production methods and processes, traditional medicinal products are made from plant based materials that may have been contaminated and deteriorated. (Lino & Deogracious, 2006) (20). this insight is important for the research and development of the most appropriate methods of extraction of active ingredients in any plant species.

Phytochemical analysis

The studies on the extracts of *B.herbaeae* revealed a wild array of phytoprofiles with reference to the solvents. Among the ten tested secondary metabolites like steroids, alkaloids, flavanoids, saponins, coumarins, tannins, terpenoids, glycosides, quinones and phenolic compounds, the phytochemical, coumarins were the most common and predominantly observed in six of the eight extracts, such as hexane, petroleum ether, chloroform, ethyl acetate, ethanol, and methanol. Flavanoids and tannins were comes next which showed their presence in the five of the eight tested solvent extracts. On the other hand, four extracts contained the presence of alkaloids and terpenoids and only three extracts revealed the occurrence of steroids, saponins, and glycosides among the eight extracts. But all the ten extracts were showed the presence of phenolic compounds whereas, the compound quinone was observed by none of the tested extracts. Out of eight solvent extracts (hexane, petroleum ether, chloroform, acetone, ethyl acetate, ethanol, methanol and water), ethanol extract showed more number of compounds (6/10) such as steroids, flavanoids, coumarins, tannins, glycosides and phenolic compounds. But the compounds like alkaloids, saponins, terpenoids, and quinones were absent in ethanol extract. The recovery of secondary metabolites from plant extracts



**Dhannia et al.**

depends on the solvent used for extraction and Sultana, Anwar & Ashraf, 2009) [21] has documented about the polar solvents and ethanol, a good solvent to extract phytochemicals. The difference in the presence of active compounds could be the reason for the differences in antibacterial activity of various solvent extracts. The exact active ingredients of this extract are yet to be identified.

Antioxidant activity

The DPPH radical and H₂O₂ scavenging capacities of *B. herbaceae* methanol extract were done in comparison with that of ascorbic acid as standard (Fig-1 and 2). The *B. herbaceae* extract of whole plant, exhibited the greater radical scavenging activity in both DPPH and H₂O₂ assays that of the standard ascorbic acid. Antioxidant activity analysed using DPPH and H₂O₂ scavenging assay is expressed in terms of IC₅₀ value, the inhibition concentration at which 50% of DPPH radicals and H₂O₂ are scavenged. Lower IC₅₀ indicates the stronger antioxidant potentiality. In this study *B. herbaceae* showed less IC₅₀ value in both DPPH and H₂O₂ radical scavenging assays (3.78 µg/ml and 4.81 µg/ml) when compared to the standard (5.39 µg/ml and 5.34 µg/ml). This observation suggested that significant number of oxidants in the extract especially, phenolic compounds, which has been reported, to be responsible for antioxidant activity in plants by Irshad, Zafaryab, Man Singh & Rizvi, 2012 (22) and confirmed their presence in all the extracts of the tested plant. Similarly, the studies in the plant, *Portulaca oleracea* by Lim & Quah (2007) (23) and *Phyllanthus amarus* by Lim & Murtijaya (2007) (24) also supported the findings of this study of on the significance of phenolic compounds in antioxidant activity.

The antioxidant activity of aqueous extracts of leaves, stem and roots of *Byttneria herbaceae* by nitric oxide, catalase and superoxide dismutase tests methods was reported by Somkuwar, Utpal, Dongre, Chaudhary, & Alka, (2014) (25). To our knowledge, this report is the first report of antioxidant activity of *B. herbaceae* by DPPH and H₂O₂ methods. So far, there are no prior reports in the literature about the phytochemicals in *B. herbaceae* as antioxidants. The present study has reported the strong antibacterial, antioxidant activities and phytoprofile of the plant *B. herbaceae*. The plant extract exhibited significant antioxidant and free radical scavenging activities might be useful in preventing various oxidative stresses. Our results therefore put forward a scientific basis for the traditional uses of this medicinal plant *B. herbaceae*. To our knowledge, this is the prime report on the antibacterial efficiency of crude extracts of *Byttneria herbaceae* on an array of bacteria. Furthermore, biological tests are needed for to reveal active compounds of this plant. In future, therapeutic formulation could be developed with this fascinating plant *B. herbaceae*.

ACKNOWLEDGEMENTS

The authors are thankful to the Department of Microbiology, SBS, Madurai Kamaraj University, Madurai, Tamilnadu, India for providing the facilities

REFERENCES

1. Singh KS. Editor. The schedule tribes, The people of India, National series; Anthropological Survey of India, Delhi, Oxford University Press 1994; 3.
2. Kumar P, GS Rawat. Chotanagpur plateau: Relict habitats and endemic plants. In: Rawat GS. Editor. Special Habitats and Threatened Plants of India. Environment Information System (ENVIS) Bulletin: Wildlife and Protected Areas, Wildlife Institute of India, Dehradun, India 2008 ; 11(1), pp167-173
3. Tiwari AP, Sikarwar RLS, Dubey PC. Documentation of ethno medicinal knowledge among the tribes of Achanakmar-Amarkantak Biosphere Reserve, Central India. Indian J Nat Prod Resour 2014; 5(4):345-350.



**Dhannia et al.**

4. Parotta JA. Healing plants of Peninsular India, USDA. Forest service International Institute of Tropical Forestry, Puerto Rico, USA, CABI publishing 2001.
5. Mallik B K, Panda T, Padhy, R.N. Traditional herbal practices of the ethnic people of Kalahandi district of Odisha. Asian Pac J Trop Biomed 2012; 2, 988-994.
6. Suthari S, Sreeramulu N, Omkar K. The climbing plants of Northern Telangana in India and their ethno medicinal and economic uses. Indian J Plant Sciences 2014; 3 (1):86-100.
7. Prusti AB, Behera KK. Ethno botanical exploration of Malkangiri district of Orissa, India. Ethno botanical leaflets, 2007; 11:122-140.
8. Harborne J B. Phytochemical methods, London Chapman and Hill, Ltd. 1973 ;Pp.49-188
9. Kavanagh F. Analytical Microbiology. In: Kavanagh F. (ed). Vol. 11, Academic Press, New York & London, 1972.
10. Zohra SF, Meriem B, Samira S., Muneer AM. Phytochemical screening and identification of some compounds from mallow. J Nat Prod Plant Retours 2012; 2:512-516.
11. Joseph BS, Kumbhare PH., Kale MC. Preliminary phytochemical screening of selected medicinal plants. Int Res J of Science and Engineering2013; 1:55-62.
12. Brand-Williams W, Cuvelier ME, Berset C. Use of a free radical method to evaluate antioxidant activity. Labels Was Technol 1995; 28:25–30. doi: 10.1016/S0023-6438(95)80008-5.
13. Chew YL, Goh JK, Lim YY. Assessment of in vitro antioxidant capacity and polyphenolic composition of selected medicinal herbs from Leguminosae family in Peninsular Malaysia. Food Chem 2009; 119: 373-378.
14. Olivier MT, Muganza FM, LJ Shai, SS Gololo, LD Nemitavhanani. Phytochemical screening, antioxidant and antibacterial activities of ethanol extracts of *Asparagus suaveolens* aerial parts. S Afr J Bot 2017; 108: 41-46.
15. Parekh J, Chanda S. Screening of aqueous and alcoholic extracts of some Indian medicinal plants for antibacterial activity. Indian J Pharm Sci 2006; 68 (6):835-838.
16. Rabe T, Staden VJ. Antibacterial activity of South African plants used for medicinal purposes. J Ethnopharmacol1997 ; 56: 81-87.
17. Shai LJ, Cake MA, Magano SR, Mogale AM, Eloff JN. Antibacterial activity of sixteen plant species from Phalaborwa, Limpopo Province, South Africa J Med Plants Res 2013; 7:1899–1906.
18. Mudzengi CP, Murwira A, Tivapasi M, Murungweni C, Burumu JV, Halimani T. Antibacterial activity of aqueous and methanol extracts of selected species used in livestock health management. Pharm Biol2017; 55: 1, 1054–1060.
19. Bansa A, Adeyemo SO. Evaluation of antibacterial properties of *Dichrostachys cinerea*. Afr J Biotechnol 2007; 6:1785–1787.
20. Lino A, Deogracious O. The in-vitro antibacterial activity of *Annona senegalensis*, *Securidacca longipendiculata* and *Steganotaenia araliacea* Ugandan medicinal plants. Afr. Health Sci2006; 6:31–35.
21. Sultana B, Anwar F, Ashraf M. Effect of extraction solvent/technique on the antioxidant activity of selected medicinal plant extracts. Molecules. 2009; 14:2167-2180
22. Irshad M, Zafaryab, Man Singh, Rizvi MA. Comparative analysis of the antioxidant activity of *Cassia fistula* extracts. Int J Med Chem 2012; Article ID 157125, 6pages.
23. Lim YY, Quah EPL. Antioxidant properties of different cultivars of *Portulaca oleracea*. Food chem 2007; 103:734-740.
24. Lim YY, Murtijaya J. Antioxidant properties of *Phyllanthus amarus* extracts as affected by different drying methods. LWT-Food sci and technol 2007; 40, 1664-1669.
25. Somkuwar SR, Utpal J Dongre2, RR Chaudhary, Alka Chaturvedi. *In-vitro screening* of an Antioxidant Potential of *Byttneria herbacea* Roxb. Int J Curr Microbiol App Sci 2014;3(8) 622-629





Dhannia et al.

Table 1. Antibacterial activity (in terms of inhibition zone in mm) of *Byttneria herbacea* against human pathogens

Test organism	Inhibition zone (mm)								Control
	Hexane	Petroleum ether	Chloroform	Acetone	Ethyl acetate	Ethanol	Methanol	Water	
<i>Escherichia coli</i>	5.00 ±0.00	3.67 ±0.58	12.00 ±0.00	14.00±0.0	14.00 ±0.0	13.33±1.1	12.00 ±0.00	12.00 ±0.00	28.00±0.25
<i>Salmonella typhi</i>	14.0 ±1.73	4.67 ±0.58	9.00 ±0.00	12.00±1.00	12.67 ±1.15	12.00±0.00	12.00 ±0.00	12.00 ±0.00	25.00 ±0.52
<i>Streptococcus epidermis</i>	8.3 ±1.53	-	9.00 ±0.00	10.00±0.00	6.67 ±0.58	12.33±0.58	12.33 ±1.15	14.0 ±1.73	24.33 ±0.40
<i>Klebsiella pneumonia</i>	2.00 ±0.00	-	8.00 ±0.00	6.00±0.00	4.67±0.58	10.00±0.00	4.00 ±0.00	10.00 ±0.00	21.00 ±0.00
<i>Staphylococcus aureus</i>	6.00 ±0.00	3.67 ± 0.58	6.33± 0.56	16.00±0.0	3.00 ±0.00	10.00±0.00	4.67±0.58	7.00 ±0.00	20.33± 0.58
<i>Bacillus cereus</i>	5.00 ±0.00	7.00 ± 0.00	5.67 ± 0.58	16.00±0.0	5.00±0.00	14.00±0.0	6.00±0.00	4.00 ±0.00	25.67 ±0.58
<i>Proteus sp.</i>	5.00 ±0.00	6.00 ± 0.0	7.00 ± 0.00	11.00±0.00	12.00±0.00	7.00±0.00	12.00±0.00	-	25.33±0.58
<i>Serratia marcescens</i>	7.00±0.58	3.33 ± 0.58	5.68± 0.58	9.00±0.00	12.33±0.58	8.00±0.00	7.00±0.00	7.00± 0.17	15.67± 2.08

±: mean standard deviation of three replicates

Table 2. Minimum inhibitory concentrations (µg/ml) of *Byttneria herbacea* plant extracts

Test microorganism	Minimum inhibitory concentrations (MIC) in µg/ml							
	Hexane	Petroleum ether	Chloroform	Acetone	Ethyl acetate	Ethanol	Methanol	Water
<i>Escherichia coli</i>	70	80	30	20	20	30	30	30
<i>Salmonella typhi</i>	30	60	70	50	30	60	30	30
<i>Streptococcus epidermis</i>	40	-	70	50	70	40	40	20
<i>Klebsiella pneumonia</i>	80	-	80	60	80	40	50	50
<i>Staphylococcus aureus</i>	60	80	80	10	100	20	70	40
<i>Bacillus aureus</i>	70	70	80	10	80	20	60	60
<i>Proteus sp.</i>	80	70	60	60	30	40	40	-
<i>Serratia marcescens</i>	40	80	70	40	40	40	60	30

-: no activity

Table 3. Preliminary Phytochemical Analysis of Different Solvent Extracts of *Byttneria herbacea*.

Solvents	Steroids	Alkaloids	Flavonoids	Saponins	Coumarins	Tannins	Terpenoids	Glycosides	Quinones	Phenolic compounds*
Hexane	-	-	+	-	+	+	+	-	-	+
Petroleum	-	-	+	-	+	+	+	-	-	+





Dhannia et al.

ether										
Chloroform	+	-	-	+	+	-	+	-	-	+
Acetone	-	+	+	-	-	-	+	+	-	+
Ethyl acetate	+	+	-	-	+	+	-	-	-	+
Ethanol**	+	-	+	-	+	+	-	+	-	+
Methanol	-	+	-	+	+	+	-	-	-	+
Water	-	+	+	+	-	-	-	+	-	+

+ Presence of compound;-absence of compound; *present in all extracts; **showed more number of compounds

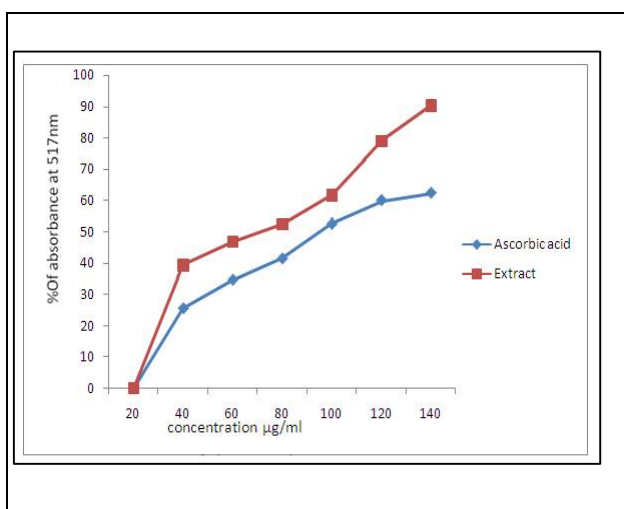


Fig.1.Scavenging activities (%) on DPPH by *B. herbaceae* extract.

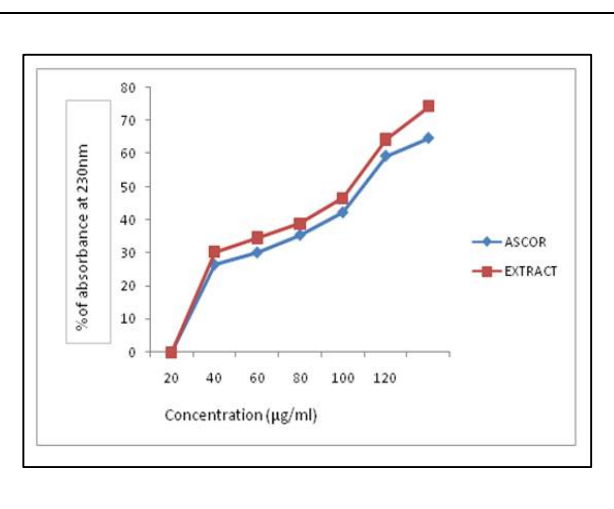


Fig.2.Scavenging activities (%) on H₂O₂ of *B. herbaceae* extract.





Influence of Post-Hatch Feeding on Broiler Performance

Abdul Muneer Kandangal

Assistant Professor, Department of Poultry Sciences, College of Veterinary and Animal Sciences, Pookode, Wayanad, Kerala, India.

Received: 14 Sep 2019

Revised: 17 Oct 2019

Accepted: 22 Nov 2019

*Address for Correspondence

Abdul Muneer Kandangal

Assistant Professor,
Department of Poultry Sciences,
College of Veterinary and Animal Sciences,
Pookode, Wayanad, Kerala, India.
Email: drmuneeerpoultry@gmail.com



This is an Open Access Journal / article distributed under the terms of the **Creative Commons Attribution License** (CC BY-NC-ND 3.0) which permits unrestricted use, distribution, and reproduction in any medium, provided the original work is properly cited. All rights reserved.

ABSTRACT

The present study was carried to assess the influence of post hatch nutrition on broiler performance. A total of 252 day old broiler chicks were allotted to seven treatment group with three replicates each and they are fed with different type of neonatal nutrients solutions within six hours of post hatch life to seventh day of age. The growth performance and feed efficiency were assessed at first week and sixth week of age. This study revealed that different neonatal feeding solutions and fasted group showed significant difference ($P < 0.05$) on body weight at first week and sixth week of age. However, feed efficiency of the broiler fed with neonatal feeding solutions only had numerical improvement over fasted group. Among the different neonatal feeding solutions used as post hatch feeding for broilers, the group fed with equal quantity of glucose and protein source showed better result in respect of body weight, feed efficiency. In conclusion starvation over a post hatch period of 24 hours will retard the growth of broilers and it indicate the early post hatch feeding results in considerable performance benefits.

Keywords: Post hatch feeding; neonatal nutrient solution; body weight gain; feed efficiency.

INTRODUCTION

The advent of genetic improvement, growth rate of embryo supersedes the nutrient availability in the egg, necessitating supplementing additional nutrients to the chicks. Unlike the mammalian embryo, the avian embryo has a finite amount of energy and nutrients for growth and development. More over in commercial practice, chicks hatched from eggs are retained within the hatchery for a period of 24 hours and removed from the hatchery only when majority of the eggs have hatched. Transportation of chicks and their placement in farms would take another 12 to 24 hours. As a result, the chicks are starved for minimum 24 - 48 hours resulting subsequent poor performance. Earlier it was considered that the egg contents are sufficient to support the growth of embryo during incubation as

17950





Abdul Muneer Kandangal

well as providing nutritional support after hatching until the chicks has access to feed in the farm. Further, there is rethinking on earlier concept that the yolk providing nutritional support to chicks until access to feed after placement. Experimental results and recent studies indicated that the growth rate of broiler chicks is greatly influenced by health status of chicks at neonate, and use of neonatal nutrient resulted in increased body weight, better feed consumption and improved uniformity of chicks and poults. It is now realized that yolk provides proteins (antibodies) and structural lipids early in life and it should be allowed to support immune activity rather than nutritional support (Dibner, 1998).

Early access to feed and water after hatching is important for subsequent broiler performance (Moran, 1990). Minimizing the holding time after hatch and early access to feed and water are therefore desirable targets. It may be hypothesized that administration of nutrients immediately after hatch will stimulate the gastrointestinal tract earlier than that of birds with delayed access to feed and water. Thus, the remedial measures on the nutritional needs to hatching chicks can be addressed as neonatal nutrient supplementation. Considering, the above facts, the present study have been attempted with following objectives

1. To assess the beneficial effect of feeding immediately after hatch out preferably within six hours.
2. Influence of glucose and protein solutions as early feeding on growth performance of broilers.

MATERIALS AND METHODS

The experiment was designed and carried out at the Poultry Research Farm, Department of Poultry Science, Veterinary College and Research Institute, Namakkal. The commercial day - old broiler chicks were procured from a commercial hatchery at Namakkal.

Experimental design

Two hundred and fifty-two commercial broiler chicks were purchased and utilized for this experiment. The commercial day-old broiler chicks were weighed, wing banded and randomly allotted to seven treatment groups with three replicates in each treatment comprising twelve chicks per replicate. The chicks were reared in cages with standard management conditions throughout the experimental period (6 weeks). All the chicks were vaccinated as per the vaccination schedule.

Preparation of Experimental solutions

The protein concentrate was prepared by adding 25 g of Soya protein concentrate (S1) in 100 ml of distilled water and 50g DL-Glucose in normal saline (G1) were used as protein and carbohydrate sources, respectively. All the chicks were fed with isocaloric and isonitrogenous diet throughout the experimental period. The broiler starter and finisher diet were formulated and prepared according to the standards prescribed in Bureau of Indian Standard (IS: 1374; 1992). The broiler starter and finisher diets were fed *ad libitum* to the birds from 1 to 28 and 29 to 42 days of age respectively. The protein nutrient solution (S1) and Glucose solution (G1) were force fed to the birds using syringes without wasting the solutions within 6 hours after hatch out and daily it was given up-to 7 days of its age. The standardized soya protein concentrates and glucose for the study were obtained from Shakthi Soya Division, Pollachi and Hi-Media, Mumbai, respectively. Apart from that, daily feed intake (g), weekly body weight gain (g) was recorded. The weekly feed conversion ratio was calculated with available data from this experiment.



**Abdul Muneer Kandagal**

RESULTS AND DISCUSSION

The Mean \pm SEcumulative, body weight gain, feed intake and feed conversion ratio were presented in Table 2.

Body Weight Gain

The present study results indicated that body weight gain first week of its age had significantly ($P < 0.005$) differ among the treatment groups. Like that the cumulative body weight gain obtained at 42nd day also had shown significant ($p < 0.05$) results between the groups. The chicks fed with 50 per cent protein plus 50 per cent glucose solution as carbohydrate sources (T5) as neonatal feed had numerically higher body weight at the end of sixth week (1950.79 g) followed by chicks fed with 100 per cent protein source (T4) (1946.67 g), 30 per cent carbohydrate plus 70 per cent protein sources (T7) (1943.85 g), 100 per cent carbohydrate source (T3) (1929.53 g), normal diet (Control - T1) (1914.85 g) and 70 per cent carbohydrate plus 30 per cent protein sources (T6) (1884.89 g) when compared to chicks fasted for 24 hours after placement (T2) (1798.55 g). The comparison of means suggested that the chicks received different neonatal feeding solutions including control group showed significantly higher body weight when compared to chicks fasted for 24 hours.

Cumulative feed intake

The mean feed intake (g) of broilers up to 6 weeks of age as influenced by feeding of different neonatal feeding solutions is furnished in Table 2. From the table it was understood that the cumulative feed consumption of broilers received different neonatal feeding solutions viz. in groups T1, T2, T3, T4, T5, T6, and T7 were 3373.75, 3341.69, 3363.25, 3512.89, 3512.84, 3425.70, and 3508.29 g respectively. The average feed consumption of birds at sixth week of age in group T4 and T5 was maximum followed by T7, T6, T1, T3 and T2 respectively. Further, the average feed consumption of birds from groups T1, T2 and T3 were almost comparable. The statistical analysis of the study revealed no significant difference in feedconsumption due to feeding of different neonatal feeding solutions although numerical differences were observed.

Feed conversion ratio

The results of this study revealed that the mean cumulative feed efficiency in groups T1, T2, T3, T4, T5, T6 and T7 were 1.81, 1.91, 1.79, 1.85, 1.85, 1.87, and 1.85 respectively. The fasted group (T2) of birds showed poor feed efficiency (1.92) when compared to other treatment groups including control group. The chicks in group T3 fed with 100 per cent carbohydrate source had better feed efficiency when compared to other treatment groups including control group.

CONCLUSION

It was concluded that, the chicks which not received protein and glucose solution with in six hours shown lesser body weight gain during the experimental period. The cumulative body weight gain was better in all other groups. However, the feed intake and feed conversion efficiency were did not differ significantly between the groups.

REFERENCES

1. B.I.S., 1992. Requirement for chicken feeds. I.S.1374 -1992, Marak Bhavan, New Delhi.
2. Delgado, L.C., A.N. Clare and M.T. Marites, 2003. Project on Livestock Industrialization, Trade and Social - Health-Environment Impacts in Developing Countries, FAO, Rome.





Abdul Muneer Kandangal

3. Dibner J.J., C.D. Knight and F.J. Ivey.1998a. The feeding of neonatal poultry. *World Poultry*.14: 36 – 40.
4. Moran, E.T., 1990. Effects of egg weight, glucose administration of hatch and delay access to feed and water on the poult at 2 weeks of age. *Poult Sci.*, 69: 1718 -1723.

Table 1. Treatment group and experimental diet of broilers

Treatment	Experimental diet
T ₁	Feeding started within 6 hours with basal feed (control)
T ₂	Feeding started after 24 hours with basal feed
T ₃	Feeding started within 6 hours with glucose solution only (2 ml daily) and basal feed
T ₄	Feeding started within 6 hours with protein solution only (2 ml daily) and basal feed
T ₅	Feeding started within 6 hours with 1 ml protein solution and 1 ml glucose solution only (2 ml daily) and basal feed
T ₆	Feeding started within 6 hours with 1.4 ml glucose solution and 0.6 ml protein solution (2 ml daily) and basal feed
T ₇	Feeding started within 6 hours with 0.6 ml glucose solution and 1.4 ml protein solution (2 ml daily) and basal feed

Table 2 Mean ± SE Body weight, Feed Intake and Feed Conversion Ratio of broiler birds during experimental period

Parameters	T ₁	T ₂	T ₃	T ₄	T ₅	T ₆	T ₇	P value
Body weight (g)								
Day old Body weight (g)	39.6 ± 0.85	39.2 ± 1.12	40.2 ± 1.19	40.6 ± 0.95	39.8 ± 1.15	40.4 ± 0.75	40.3 ± 1.23	0.080
Body weight at 7 th day(g)	153.38 ^a ± 3.02	145.75 ^b ± 3.66	153.13 ^a ± 4.37	155.43 ^a ± 3.57	155.64 ^a ± 3.54	154.19 ^a ± 3.16	156.43 ^a ± 4.17	0.041
Cumulative body weight at 42 nd day (kg)	1914.85 ^a ± 60.02	1798.55 ^b ± 69.72	1929.53 ^a ± 78.51	1946.67 ^a ± 68.92	1950.79 ^a ± 69.84	1884.89 ^a ± 77.74	1943.85 ^a ± 78.84	0.05
Feed Intake (g)								
Feed Intake up to 7 th day(g)	121.35 ± 8.92	109.38 ± 3.85	124.23 ± 4.44	123.51 ± 6.41	127.82 ± 0.58	121.58 ± 3.15	126.51 ± 1.42	0.061
Cumulative Feed Intake at 42 nd day (kg)	3373.75 ± 132.60	3341.69 ± 84.38	3363.25 ± 19.65	3512.89 ± 63.03	3512.84 ± 23.23	3425.7 ± 28.44	3508.29 ± 12.31	0.073
Feed Conversion Ratio								
FCR at 7 th day(g)	1.17 ± 0.03	1.14 ± 0.03	1.2 ± 0.02	1.17 ± 0.03	1.21 ± 0.02	1.17 ± 0.03	1.19 ± 0.01	0.065
Cumulative FCR at 42 nd day (kg)	1.81 ± 0.01	1.91 ± 0.05	1.79 ± 0.02	1.85 ± 0.02	1.85 ± 0.04	1.87 ± 0.04	1.85 ± 0.02	0.075

^{a,b}Mean ± SE values with superscript in the same row are significantly at P < 0.05

